UNIVERSITY OF TRENTO - Italy

International PhD Program in Biomolecular Sciences
Centre for Integrative Biology
29th Cycle

ETV7 CAN TRIGGER BREAST CANCER CHEMORESISTANCE

Tutor

Alberto INGA

CIBIO, University of Trento

Advisor

Yari CIRIBILLI

CIBIO, University of Trento

Ph.D. Thesis of

Federica ALESSANDRINI

CIBIO, University of Trento

Academic Year 2015-2016

Declaration of authorship

I Federica Alessandrini confirm that this is my own work and the use of all material from other sources has been properly and fully acknowledged.

INDEX

LISTS OF FIGURES

LIST OF TABLES

ABBREVIATIONS

TNBC Triple Negative Breast Cancer
ETS E26-Transformation-Specific
PNT Pointed
EMT Epithelial to Mesenchymal Transition
ABC ATP-binding cassette
TNF-α Tumor Necrosis Factor alfa
TGF-β Transforming Growth factor beta
MDM2 Mouse double minute 2 homolog
ER Estrogen Receptor
RE Response Element
5-FU 5-Fluorouracil
NFκB nuclear factor kappa-light-chain-enhancer of activated B cells
EGFR Epithelial Growth Factor Receptor
ChIP Chromatin Immuno-Precipitation

1. ABSTRACT

Chemotherapy still represents the most common and sometimes the only possible therapeutic option for advanced breast cancer. Its efficacy is profoundly threatened by intrinsic or acquired chemoresistance, which, in some cases, can be unexpectedly promoted by the chemotherapeutic drugs used. ETV7, a poorly characterized ETS factor with no established roles in breast cancer so far, is reported here to be activated at the transcriptional level by chemotherapy and be able to promote breast cancer cells chemoresistance. This project proposes a novel drug resistance circuitry in breast cancer cells, specifically to Doxorubicin, governed by the ETV7 repressive action on DNAJC15, a gene whose low expression was previously associated with drug resistance in breast and ovarian cancer. Moreover, the impact of ETV7 in causing drug resistance is proved here to extend also to another type of drug, 5-Fluorouracil (5-FU), a chemotherapeutic agent commonly used in combination with Doxorubicin for breast cancer treatment. In this case, additional novel ETV7 targets (DPYD and DPEP1) were established and can represent important mediators for ETV7-mediated resistance to 5-FU. Additional relevant data, relative to biological implications for ETV7 in breast cancer progression, is provided here by the ETV7 ChIP-seq analysis, which reveals the first reported *in vivo* mapping of ETV7 occupancy. Through ChIP-seq novel ETV7 direct targets have been identified, some of them yet unexplored in breast cancer; notably, their expression revealed to be capable of predicting breast cancer patients outcome. Furthermore, a possible control exerted by ETV7 on the TGF-β pathway, discovered by enrichment analysis on ChIP-seq ETV7 targets, suggests a different and opposing role for ETV7 activation in either advanced stage cancers or normal and early stage breast cancers.

Taken collectively, the results from this project propose an important key role for ETV7 in triggering breast cancer multi-drug resistance phenotype in response to chemotherapy, by controlling the expression of specific targets.

2. INTRODUCTION

2.1 BREAST CANCER

2.1.1 Subtypes

Breast cancer still represents the most frequently diagnosed type of cancer worldwide and the second leading cause of cancer death among women (Jemal, Bray and Ferlay, 2011; American Cancer Society, 2016). It is a very heterogenous disease in terms of genetics and phenotype features, relative to different subtypes (inter-tumor heterogeneity) or different cancer cells present inside cancer (intra-tumor heterogeneity) (Skibinski and Kuperwasser, 2015). Subtype classification is meant to simplify heterogenity and direct therapeutic decision. In the clinics, the most common type of classification relies on histo-pathological features: expression of estrogen and progesterone receptors (since mammary epithelium where breast cancer usually originates depends on estrogens), HER2 (also known as EGFR2) amplification or the absence of the three receptors (generally known as triple negative group). Another type of classification, called the molecular classification, is based on microarray-based technology and next generation sequencing gene expression, mutation and chromosomal aberration data and allows a better stratification of patients in terms of prognosis and a deeper understanding of molecular mechanisms and mutations characterizing each subtype. For example, molecular characterization of the pathologic group triple negative, showed that some subtypes of triple negative breast cancer could be successfully treated with immunotherapy (Anders *et al.*, 2016). According to molecular classification, there are at least six different breast cancer subtypes: Luminal A, Luminal B, HER2-enriched, Claudin-low, Basal-like and a Normal Breast-like group (Perou *et al.*, 2000; Prat and Perou, 2011). Each subtype is characterized by different mutational spectra, and specifically Basal-like subtype displays a high number of somatic mutation, with p53 being the most frequent mutated gene (Skibinski and Kuperwasser, 2015).

In 2009 Parker and co-workers proposed a 50-gene panel called PAM50 (Predictive Analysis of Microarrays (Nanostring Technologies Inc., Seattle, Washington) based on the expression analysis of 50 classifier genes and 5 controls, for standardizing the classification of the aforementioned breast cancer subtypes, that was validated also for formalin-fixed-paraffin-embedded (FFPE) samples (Parker *et al.*, 2009). More recently, different groups, using RNA

extracted from patient-derived biopsies, have tried to identify gene signatures, whose expression levels could generate more precise prognosis for breast cancer patients; for instance, Mammaprint (a 70-gene microarray test, Agendia, Irvine, CA and Amsterdam, The Netherlands) (Veer *et al.*, 2002), Oncotype DX (a 21-gene RT-qPCR based assay, Genomic Health, Inc., San Francisco, CA) (Paik *et al.*, 2004) and 76-gene Rotterdam set (a 76-gene microarray test, Veridex, LLC, Johnson & Johnson, Warren, NJ) (Foekens *et al.*, 2006). The presence of such high number of classification systems underlines the extremely heterogenous nature of breast cancer and its complex biology and the importance of identifying novel markers to improve patients' prognosis and treatment.

2.1.2 p53's role in breast cancer

p53, known as the "guardian of the genome", is a key factor for normal breast cancer development and for the control of breast cancer progression (Walerych *et al.*, 2012). Being activated by various stressor stimuli, such as DNA damage, oncogenes activation, hypoxia, oxidative stress, and telomeres erosion, p53 can control the DNA repair, growth arrest, apoptosis, senescence and metabolic homeostasis (Levine and Oren, 2009). p53 protein stability is tightly regulated by MDM2, which ubiquitinates p53 targeting it for proteasomal degradation. Upon p53 activating stimuli MDM2-p53 interaction is prevented by serine phosphorylations in the p53 N-terminal domain. Inhibition of MDM2 binding to p53 can be also directly achieved by the pharmacological treatment with the MDM2 antagonists, such as Nutlin-3a, resulting in inhibition of proliferation of cancer cells bearing wild type p53. Once activated p53 protein can rapidly accumulate into the nucleus where it can carry out most of its properties that rely on its funtions as transcription factor. The DNA binding of p53 to its target sequences is an accurately regulated process, influenced by p53 post translational modifications and by the conformation of p53 response elements (RE), which are usually composed of two decamers, called half sites, divided by a spacer typically with a length ranging from 0 to 13 bases. The canonical consensus sequence recognized by the p53 is 5' - RRRCWWGYYY n RRRCWWGYYY – 3' (R:purine, Y:pyrimidine; W:A/T, n:spacer) (Menendez, Inga and Resnick, 2009).

The importance of p53 relatively for breast cancer is strongly supported by the high risk of developing breast cancer in patients affected by the Li-Fraumeni syndrome, a genetic disorder characterized by a germline p53 mutation at heterozygous level (Walerych *et al.*, 2012). Another important relevance is given by the high rate of p53 mutations in breast cancer,

which can be responsible for transforming p53 into a “rebel angel”, a driving factor in breast carcinogenesis (Walerych *et al.*, 2012).

2.1.3 Chemotherapy and Chemoresistance

Chemotherapy is still representing the basic standard treatment for breast cancer, particularly if locally advanced, non-responding to endocrine therapy and in the case of metastatic dissemination. Chemotherapy serves as the only treatment option when surgery cannot be done, or, alternatively, is used to reduce tumor burden before surgery (neoadjuvant) or after surgery (adjuvant), and it also proved very efficacious in boosting immunotherapy.

Chemotherapy relies on different groups of cytotoxic drugs: anthracyclines (Doxorubicin, Epirubicin, Mitoxantrone), taxanes (Paclitaxel, Docetaxel) alkylating agents (Cyclophosphamide), fluoropyrimidines (Capecitabine, 5-Fluorouracil), antimetabolites (Methotrexate), vinca alkaloids (Vinolerbine, Vinblastine, Vincristine), and platinum compounds (Carboplatin, Cisplatin). Anthracyclines are mostly used in adjuvant setting and among them, Doxorubicin, which acts by inhibiting topoisomerase 2, causing DNA damage and subsequently cancer cell death, by potently inducing p53 (Yardley, 2013). Similarly to Doxorubicin, also the fluoroquinolone Etoposide acts by inhibiting topoisomerase 2, leading to DNA damage (Heisig, 2009). Topoisomerase 1 is inhibited by Camptothecin, which blocks the Topoisomerase 1-DNA cleavage complex and leads again to DNA damage (Sakasai and Iwabuchi, 2015). 5-Fluorouracil (5-FU), another commonly used antineoplastic drug, is responsible for the misincorporation of fluoronucleotides into RNA and DNA, and to the inhibition of the nucleotide synthetic enzyme thymidylate synthase, causing DNA damage (Curtin, Harris and Aherne, 1991; Peters *et al.*, 2000).

Chemotherapy is still one of the most effective treatments for breast cancer but in general 50 to 70% of breast cancer patients experience a relapse within a year, usually associated to chemoresistance (Fernández-Cabezudo *et al.*, 2016; Majidinia and Yousefi, 2017). Thus there is an urgent need to better understand the mechanisms underlying drug resistance, in order to improve the effectiveness of breast cancer treatments.

Drug resistance, either intrinsic or acquired, is a complex and dynamic process and involves various mechanisms: increased drug efflux or decreased drug influx, lack of response to cytotoxicity, topoisomerase poison, spiked expression of detoxyfying proteins, suppression of

apoptosis, deregulated autophagy, alterations in DNA repair, in drug targets and in signaling pathways (Huang, Li and Ren, 2015; Pan *et al.*, 2016; Q. Chen *et al.*, 2016).

Increased drug efflux is frequently associated to the up-regulated expression of ATP-binding cassette (ABC) transporters; among them, P-glycoprotein/MDR1/ABCB1 is the most studied, and it is involved in the efflux of various types of drug (antracyclines, antimetabolites, taxanes, and vinca-alkaloids). ABC transporters are often responsible for causing resistance to totally unrelated drugs, the so called multi-drug resistance phenotype (Yardley, 2013).

Alterations in drug-metabolizing enzymes can affect both the response to the drug and the drug-related toxicity. For example, polymorphisms in the DPYD gene, encoding the dihydropyrimidine dehydrogenase (controlling the catabolism of pyrimidines), can cause 5-Fluorouracil severe toxicity in various types of cancer, including breast cancer (Gross *et al.*, 2008). At the same time, DPYD repression by EZH2 can increase drug sensitivity to 5-FU, and it is associated with better survival in colorectal as well as gastric cancer (Wu *et al.*, 2016). Conflicting evidence regarding the role of DPYD in chemoresistance is reported by Deng and colleagues, which observed an increased resistance to 5-FU upon increased expression of miR-21 and consequent downregulation of DPYD expression (Deng *et al.*, 2014). Conversely, cytochrome P450 monooxygenases, involved in the catabolism of most drugs, like several detoxifying enzymes, are often found over-expressed in resistant cancer cells and also in breast cancer stem cells (Yao *et al.*, 2000; McFadyen, Melvin and Murray, 2004; Al-Dhfyan, Alhoshani and Korashy, 2017).

Crosstalk with the microenviroment plays an important role in shaping drug resistance and in promoting epithelial to mesenchymal transition (EMT), a phenotype which confers invasive properties, de-differentiation, reduction in adhesion, increased proliferation and cancer stem cells features (Huang, Li and Ren, 2015). The presence of cancer stem cells is another important hurdle to overcome drug resistance: these cells usually display high expression levels of ABC transporters, anti-apoptotic proteins, are largly quiescent, slowly cycling, and rich of adehyde dehydrogenase, an enzyme that contributes to metabolizing cytotoxic drugs.

Drug resistance can be mediated by different pathways: increased secretion of insulin-like growth factor, p27 dysregulation, EGFR up-regulation, activation of Akt, decreased PTEN (Huang, Li and Ren, 2015). The extreme complexity of known mechanisms responsible for drug resistance renders the treatment of drug resistant breast cancers particularly challenging, and underlines the importance of discovering and targeting novel key regulators of drug resistance, possibly able to control simoultaneously multiple drug resistance pathways.

2.1.4 The role of chemotherapy in triggering breast cancer resistance

Drug resistance is governed by a complex and dynamic network of factors, therefore it is difficult to target. In order to prevent chemoresistance outbreak, acting upstream could represent a possible strategy. To reach this aim, it is essential to understand which are the mechanisms responsible for triggering chemoresistance.

These mechanisms sometimes can also be directly activated by chemotherapy. Generally, chemotherapeutic drugs generate chronic inflammation, which consequently promotes survival, cancer proliferation, angiogenesis, metastasis and chemoresistance (Vyas, Laput and Vyas, 2014). Inflammation can also play tumor suppressive roles, by promoting the recognition of early cancer progression; therefore, inflammation is generally considered a double-edged sword in oncology (Hagemann, Balkwill and Lawrence, 2008). Typically, if inflammation becomes chronic, it can promote cancer by modulating NFκB functions.

For example, Cisplatin, Paclitaxel, 5-Fluorouracil and Doxorubicin can activate the NFκB pathway, leading to the activation of pro-survival, inflammatory genes and the production of various cytokines (Vyas, Laput and Vyas, 2014). The NFκB pathway relies on a family of transcription factors, able to bind as dimers to small response element (κB sites), characterized by the consensus sequence 5′ - GGGRNWYYCC - 3′ (R: purine, Y: pyrimidine, W: A/T, N:all) (Hoffmann, Natoli and Ghosh, 2006). There are five transcription factors belonging to the NFκB family: p50, p52, p65 (RelA), c-Rel, and RelB. They are negatively regulated by IκB (Inhibitor of κB), which is responsible for their sequestration into the cytoplasm in absence of NFκB-stimulating signals. Among the secreted cytokines activated by the NFκB transcriptional activity, IL-6 plays an important role because it activates STAT3 (Signal Transducer and Activator of Transcription 3), a transcription factor itself, considered as an oncogene and able to promote multi-drug resistance and the acquisition of stem cell properties (Conze *et al.*, 2001; Vyas, Laput and Vyas, 2014; Saha *et al.*, 2016). NFκB and other pathways activated by chemotherapy (such as PARP, Poly ADP-Ribose polymerase, and MAPK, Mitogen-Activated Protein Kinase, pathways) can also induce TNF-α, which in turns keeps inflammation continuously active (Vyas, Laput and Vyas, 2014). Inflammation can be further increased in presence of mutant p53, through its control on DAB2IP, promoting NFκB activation (Minin *et al.*, 2014). DAB2IP is often hypermethylated in breast cancer, where it is responsible for the inhibition of EMT (Dote *et al.*, 2004; Xie *et al.*, 2010).

All DNA damaging drugs cause genotoxic stress, which activates MAPK (JNK in case of cisplatin and p38 upon 5-Fluorouracil), which ultimately promotes EMT. Doxorubicin also induces the production of TGF-β, which activates its related signaling, characterized by a bi-phasic role in cancer: being an oncosuppressor in normal tissue and in early stage of cancer and an oncogene in advanced stage cancer, where it can promote EMT, invasion and survival and acts on the tumor stroma promoting immunosuppression and angiogenesis (Roberts and Wakefield, 2003). TGF-β pathway effects are also largely affected by the presence of mutant p53 and oncogenic Ras, which together with TGF-β activated Smads (Small Mother Against Decapentaplegic, the effectors of TGF-β signal) are inhibiting TAp63 tumor suppressive functions leading to migration and metastasis (Adorno *et al.*, 2009). Doxorubicin can further promote drug resistance by increasing the expression of some drug efflux pumps like MRP1 in breast cancer (B. Kim *et al.*, 2015).

Chemotherapy also alters tumor stroma, favouring the development of drug resistance, which can be also mediated through exosomes signalling (Deng *et al.*, 2016; Wang *et al.*, 2016). Moreover, chemotherapy has been demonstrated to cause a stromal reaction that resulted in the production of TNF-α by endothelial and other stromal cells and therefore it can trigger survival, chemoresistance and metastatic spread of breast cancer cells through a CXCL1/2 and S100A8/9 axis (Acharyya *et al.*, 2012). Furthermore, chemotherapy can provoke damages in mitochondrial DNA, that in addition to altered mitochondrial respiration can promote drug resistance and metastasis (Roesch *et al.*, 2013; Porporato *et al.*, 2014; van Gisbergen *et al.*, 2015). In fact, genes controlling mitochondrial respiration, such as DNAJC15, have already reported roles in drug resistance (Shridhar *et al.*, 2001; Fernández-Cabezudo *et al.*, 2016).

2.1.5 Transcription factors can be crucial players in triggering breast cancer chemoresistance

To simplify the complexity of drug resistance mechanisms originated by chemotherapy treatment, it is important to discover primary triggers, linking chemotherapy to drug resistance. Transcription factors, thanks to their large spectra of regulation, could represent critical triggers activating this deleterious process. Furthermore, changes in DNA are observed very soon after drug exposure, and epigenetic factors are acquiring more and more importance in the drug resistance therapy; meaning that discovering key transcription factors involved in the epigenetic control upon chemotherapy could be a promising strategy (Yardley, 2013). Inflammation and its related pathways are important modulators of chemotherapy-

derived chemoresistance; thus it could be relevant to uncover transcription factors strongly activated by chemotherapy combined with inflammation.

2.1.6 Thesis' experimental background

This PhD project arises from a study aiming at the analysis of genes synergistically activated by the combined treatment with Doxorubicin and TNF-α, mimicking a condition often found in breast cancer patients treated with chemotherapy (as explained above), resulting in a signature of genes (Figure 1A), responsible for increased migratory potential of the breast cancer-derived MCF7 cells (Figure 1B) (Bisio *et al.*, 2014).

Among the highly synergistically activated genes, a transcription factor member of ETS family (ETV7) came to my attention given its conserved induction upon Doxorubicin and TNF-α treatment observed, not only in breast cancer MCF7 cells, but also in lung cancer cells (A549) and normal endothelial cells (HUVEC). Furthermore, this gene could represent a very promising player as a promoter for cancer cells chemoresistance, given its conserved mechanism of activation upon a wide spectra of chemotherapeutic drugs and in different cell types (see Results section, Figure1). Another supporting evidence for the choice of ETV7 could by simply represented by the relevant functions and implications of the other ETS family members in cancer, including breast cancer (see section below), and the still unexplored features of ETV7 itself.

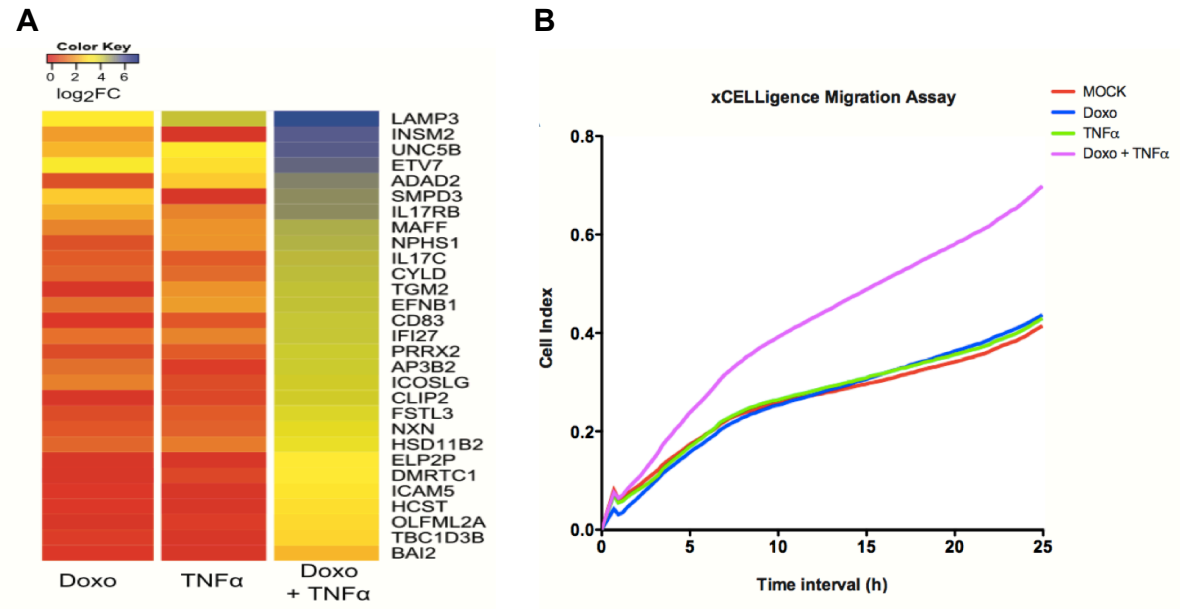

INTRODUCTION-Figure 1: A) Microarray data heatmap of top 29 synergistically up-regulated genes by Doxorubicin and TNF-α combined treatment in MCF7 cells. B) Migration analysis of MCF7 cells treated with Doxorubicin, TNF-α and combined treatment, analyzed by real-time cell migration xCELLIGENCE. (Bisio *et al.*, 2014).

2.2 ETS FAMILY ("E26-Transformation-Specific")

2.2.1 ETS complexity and common features

ETS is a large family of transcription factors (27 members) bearing important roles in various physiological biological processes, such as differentiation, development, hematopoiesis, proliferation, some more directly relevant to cancer, such as apoptosis, metastasis, tissue remodelling, and angiogenesis.

The main characteristic of ETS family proteins is represented by the DNA binding domain, called ETS domain, composed of a winged helix-turn-helix motif, binding to a purine-rich core sequence GGAA/T. Multiple ETS factors can bind the same target region, resulting in redundancy and competition in binding.

Flanking nucleotides and interaction with cofactors are key determinants for the binding specificity of each ETS member. Normally, there is less redundancy among ETS family proteins in genes containing a low affinity ETS binding site, especially in enhancer region, where adjacent or nearby binding sites for other transcription factors contribute to specificity (Hollenhorst, McIntosh and Graves, 2011). Some ETS can act as transcription activators, others as repressor and others can do both. Transcriptional activity is also controlled by the typical autoinhibition ability, obtained by regions flanking the ETS domain, and by post translational modifications, mainly phosphorylation by MAP kinases (Hagman and Grosschedl, 1992; Wasylyk, Kerckaert and Wasylyk, 1992; Wasylyk, Hagman and Gutierrez-hartmann, 1998). Another common domain in ETS family proteins is the Pointed domain (PNT) responsible for protein-protein interaction and oligomerization.

ETS family can be divided in 4 subgroups according to binding sequence specificity, and a schematic view of this subgroups is represented in Figure 2 (Wei *et al.*, 2010).

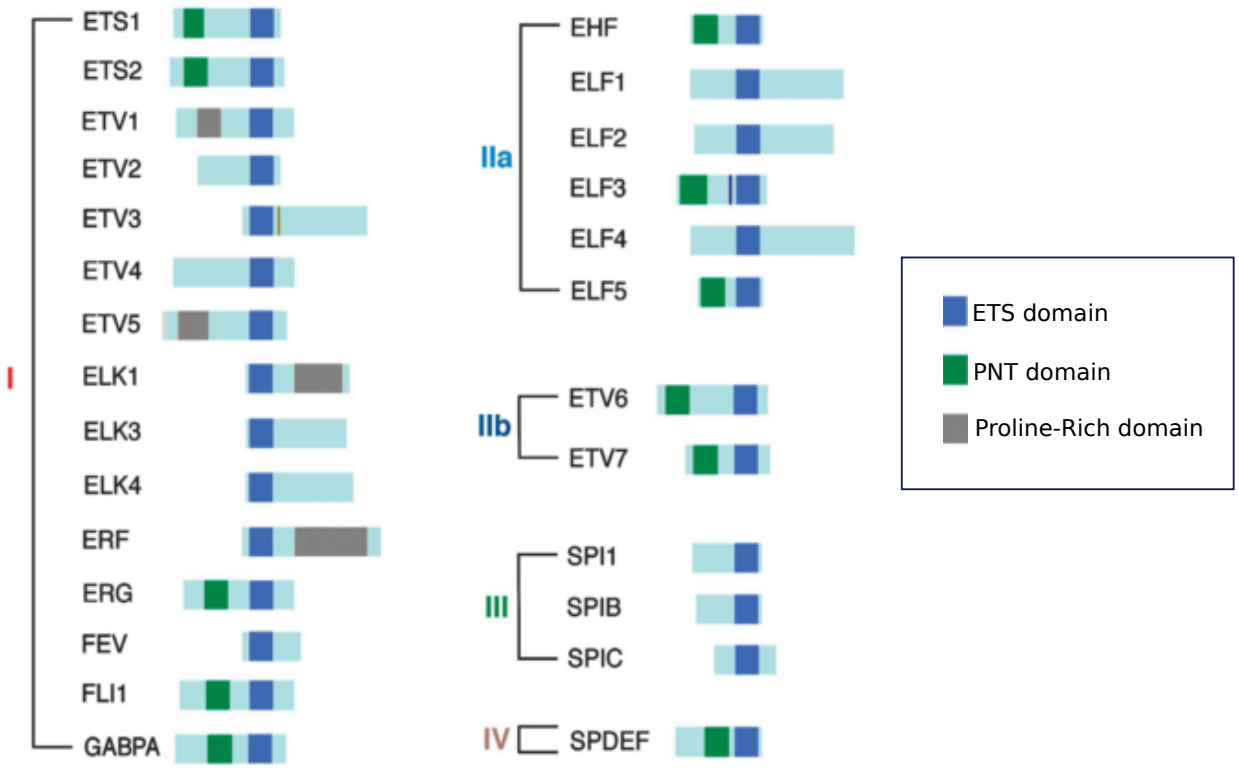

INTRODUCTION-Figure 2: Adapted from the work of Wei and colleagues (Wei *et al.*, 2010). ETS family is divided into 4 groups according to sequence binding specificity. In blue is depicted the ETS domain, in green the PNT domain, in grey the Proline-Rich domain

2.2.2 ETS role in breast cancer

The involvement of ETS in breast cancer can be seen as a complex and dynamic network of transcriptional regulation; which can be subtype-specific, time and cancer stage-dependent and sometimes even contradictory (Turner, Findlay, *et al.*, 2007).

SPDEF, a prostate-derived ETS factor with known roles in breast cancer biology, represents a great example both for the ETS family complexity and its contradictory network in breast cancer. SPDEF was found over-expressed in breast cancer tissues, where it promotes migration and invasion (Ghadersohi and Sood, 2001; Gunawardane *et al.*, 2005). Conversely, SPDEF loss was observed in invasive breast cancer, where it negatively controls breast cancer invasion by both increasing p21 expression (one of the most important protein involved in cell cycle arrest) and repressing urokinase plasminogen activator (uPA) (Feldman *et al.*, 2003; Turner, Moussa, *et al.*, 2007). Urokinase plasminogen activator is directly associated with increased invasion and poor survival, and the same ETS binding site, can be bound by another ETS factor, ETS-1, but resulting in transcriptional activation (Turner, Findlay, *et al.*, 2007). ETS-1 itself is not devoid of contradictory actions, as it is found upregulated in breast

cancer tissues and associated to metastasis by some groups (Buggy et al. 2004), but it is also reported to be downregulated with respect to normal mammary epithelia by other groups (He *et al.*, 2007). Similarly, ELF5 roles in breast cancer are conflicting and strictly dependent on the specific subtype. In ER negative breast cancers, ELF5 has a tumor suppressor role, by directly repressing SNAI2 and the EMT process (Chakrabarti *et al.*, 2012). Conversely, in luminal A breast cancers, tumor ELF5 is implicated in endocrine therapy resistance and promotes metastasis to the lung by directly cooperating with the innate immune system (Kalyuga *et al.*, 2012; Gallego-Ortega *et al.*, 2015).

Similarly to SPDEF, other ETS are important players in both prostate and breast cancer, two hormone-driven type of cancers that can be considered "more similar than different" (Risbridger *et al.*, 2010).

ESE3/EHF negatively controls EMT and stemness acquisition in prostate cancer (Cangemi *et al.*, 2008; Albino *et al.*, 2012). The stemness control exerted by ESE3/EHF was first found to involve the Lin28/let7 axis (Albino, Civenni, Dallavalle, *et al.*, 2016). Later ESE3/EHF was also decribed as regulator of STAT3 pathway either by direct repression of IL-6 promoter (Albino, Civenni, Rossi, *et al.*, 2016) or by controling the miR-424/E3 ubiquitin ligase COP1 axis responsible for STAT3 degradation (Dallavalle *et al.*, 2016). These studies suggested that a similar mechanism could possibily be present in breast cancer: IL-6 is often found up-regulated in breast cancer and directly linked to the acquisition of stemness; miR-424 is up-regulated in cancer; ubiquitin ligase COP1 positively correlates with ESE3/EHF expression; and Lin28/let7 axis is a known stemness controller in breast cancer (Albino, Civenni, Rossi, *et al.*, 2016; Dallavalle *et al.*, 2016). Another evidence, yet unpublished in scientific journal, comes from a dissertation thesis data reporting a down-regulation of EHF/ESE3 in aggressive breast cancer cells, which correlates with poor prognosis (Pferdehirt, 2015) .

Another very good example of common ETS in breast and prostate cancer, is ESE1/ELF3, the first ETS found to be linked to breast cancer (Chang *et al.*, 1997). ESE1/ELF3 can transform mammary epithelial cells and controls ERα transcriptional activity (Prescott *et al.*, 2004; Gajulapalli *et al.*, 2016). Similarly, in prostate cancer, ESE1/ELF3 regulates NFκB and EZH2, it controls tumor growth and metastasis and correlates with adverse prognosis (Kunderfranco *et al.*, 2010; Longoni *et al.*, 2013; Semenchenko *et al.*, 2016).

A comprehensive analysis of all ETS factors expression in breast cancer conducted by He and co-workers, confirmed up-regulation of some already known ETS factors involved in breast cancer biology, such as SPDEF, ELF3 and showed increased expression for a relatively novel

one, Tel2/ETV7(He *et al.*, 2007). ETV7 showed a peculiar expression in breast cancer cell lines: it was expressed at high level in 3 breast cancer cell lines (MDA-MB-468, T47D, BT474) compared to the non-transformed MCF10a taken as normal counterpart, it was slightly expressed in MDA-MB-231, and down-regulated in SkBr3, ZR75.1, and MB453 (He *et al.*, 2007). No clear-cut connection between ETV7 expression and subtypes was observable in cancer cell lines studies, but when comparing breast cancer tissue with normal mammary tissue, the increase in the former was consistently observed (He *et al.*, 2007) (Figure 3A). Later, RNA-seq experiments confirmed the upregulation of ETV7 in breast cancer, especially in the basal subtype (Piggin *et al.*, 2016) (Figure 3B). Publicly available data from the Metabric study confirmed the up-regulation of this factor in breast cancer tissues, which positively correlated with increasing with histopathological grade (Figure 3C-D).

Taking advantage from these observations and given the poorly characterized nature of this ETS factor, this project aims at better understanding the role of ETV7 in breast cancer.

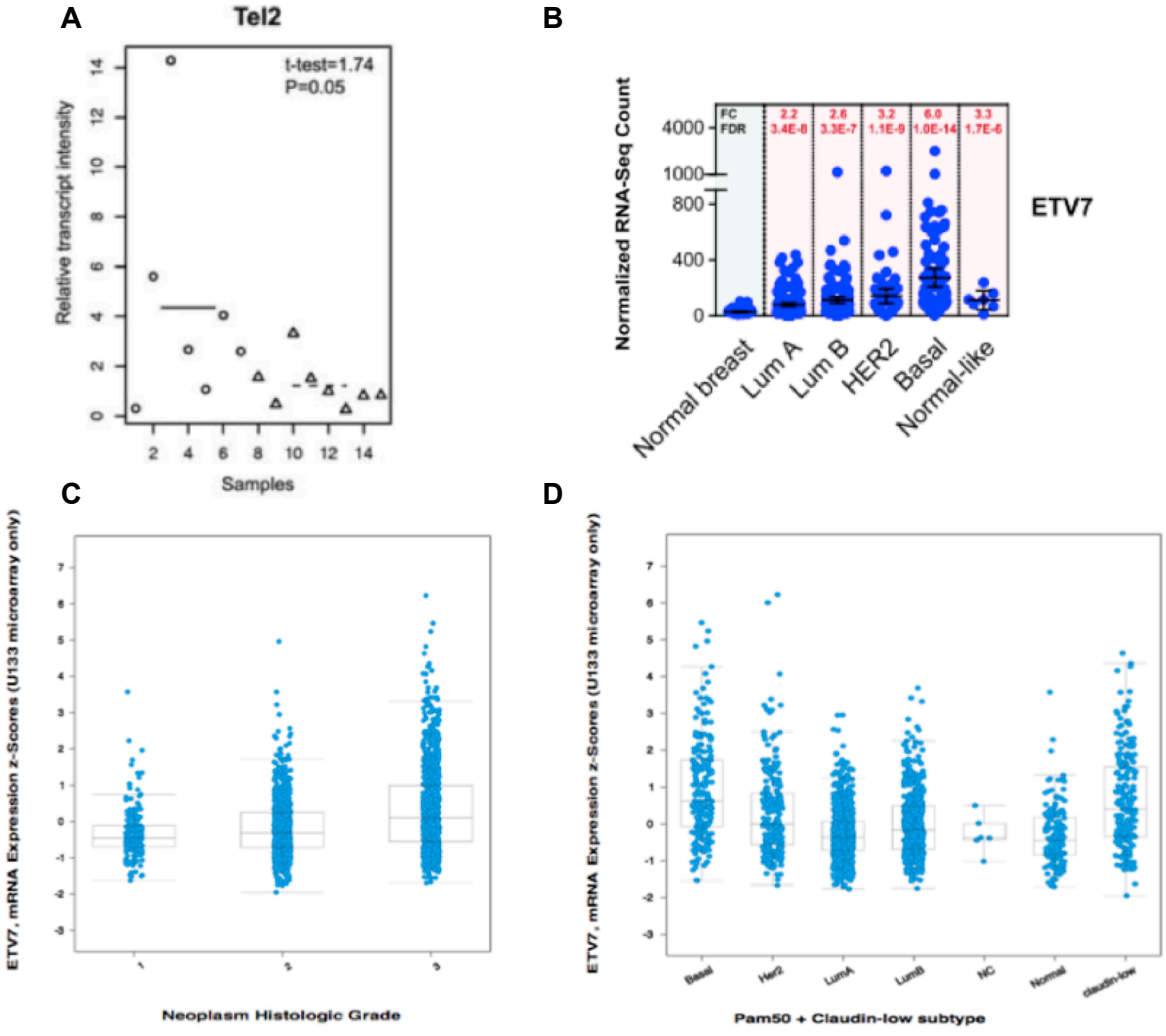

INTRODUCTION-Figure 3: A) ETV7 expression in breast cancer (depicted as circles) compared with normal mammary tissue (triangles), taken from He and collegues (He *et al.*, 2007). B) ETV7 expression in different

cancer subtypes, adapted from Piggin and co-workers (Piggin *et al.*, 2016). C-D) ETV7 expression in Metabric dataset relative to breast cancer histological grade (1 to 3, with a numeric increasing severity) (C) and breast cancer subtypes (according to molecular classification) (D).

2.3 ETV7/TEL2

2.3.1 ETV7 domain organization

ETV7 discovery was reported simultaneously by three different groups as a novel ETS member closely related to ETV6/TEL (Poirel *et al.*, 2000; Potter *et al.*, 2000; Gu *et al.*, 2001).
ETV7 is a transcriptional repressor composed of a Pointed domain (PNT) at the amino-terminal, and an ETS domain at the carboxy-terminal: these are the regions where ETV7 and ETV6 share the highest aminoacid homology (Poirel *et al.*, 2000; Potter *et al.*, 2000; Gu *et al.*, 2001). PNT domain is required for protein-protein interaction and mediates both the self-association of ETV7 with itself and with ETV6. ETS domain and PNT domain are necessary for an efficient transcriptional repression, thus suggesting that ETV7-mediated repression is an active process and requires co-repressors (Poirel *et al.*, 2000; Potter *et al.*, 2000; Gu *et al.*, 2001).
ETV6 and ETV7 are very different in their central region, ETV7 has a PEST sequence responsible for its rapid intracellular proteolysis (Gu *et al.*, 2001), whereas ETV6 contains the interaction domain with epigenetic factors such as HDAC3 (Chakrabarti and Nucifora, 1999; Lopez *et al.*, 1999). They also show different expression patterns (ETV6 is abundant and ubiquitous, ETV7 is expressed at low level and in specific tissues) (Potter *et al.*, 2000; Gu *et al.*, 2001) and display opposing biological roles: ETV7 exerts a pro-tumorigenic role and ETV6 a tumor suppressive one (Van Rompaey *et al.*, 1999; Irvin *et al.*, 2003; Kawagoe *et al.*, 2004; Cardone *et al.*, 2005).

2.3.2 ETV7 isoforms

ETV7 is present in 6 different splice isoforms (ETV7-a, b, c, d, e, f) with different expression patterns (Figure 4). All variants comprise the first exon containing the 5'UTR; ETV7-a and ETV7-b are composed of 8 exons, ETV7-a has an alternative splice variant of exon 3 (exon3a) which interrupts the open reading frame; ETV7-c doesn't have exon 2, ETV7-d is missing exon 3, ETV7-e and –f lack exon 8 but have exon 9 and ETV7-f also lacks exon 3 (Gu *et al.*, 2001).

The exon 9 present in –e and –f can gives additional unknown biological roles to these two isoforms, encoding a leucine/isoleucine-rich region.

Exons 2,3,4 are encoding the PNT domain, whereas exons 6,7,8 are required for ETS domain.

ETV7-b is the principal isoform, the most closely related to ETV6, and encodes the full-length protein of 341 aa corresponding to 39 KDa (Gu *et al.*, 2001). All biological data reported in next sections and this thesis project are referring to this isoform.

ETV7-d is the most abundant isoform in human tissues, whereas ETV7-a and -c show the lowest expression and only in specific tissues. Variants with exon 8 are mostly expressed in placenta, lung, liver, pancreas, peripheral blood leukocytes, and fetal lung, whereas isoforms –e and –f are mostly expressed in placenta, spleen, prostate, thymus, and ovary.

ETV7-b acts as a transcriptional repressor, ETV7-a slightly enhanced transcription probably by binding to a co-repressor and preventing its binding to other transcription factors and has low level associated to DNA. ETV7-c isoform is very stable, can bind to DNA but it does not affect transcription. When analyzed in western blot, all isoforms show an additional 22KDa protein, probably due to the presence of an additional ETV7 protein isoform translated from a internal translation start site located upstream of the ETS domain (Gu *et al.*, 2001).

ETV7 mutants studied *in vitro* lacking either the PNT or the ETS domain were reported to exert an inhibitory role on the ETV7 transcriptional repression and are responsible for increasing the differentiation and the growth of U937 human myeloid leukemia cells; however, *in vivo* ETV7-c isoform (missing part of PNT domain) is down-regulated during differentiation similar to ETV7-b (with an intact PNT), therefore probably the dominant negative effects of the ETV7-c seen *in vitro* is not relevant *in vivo* (Kawagoe *et al.*, 2004).

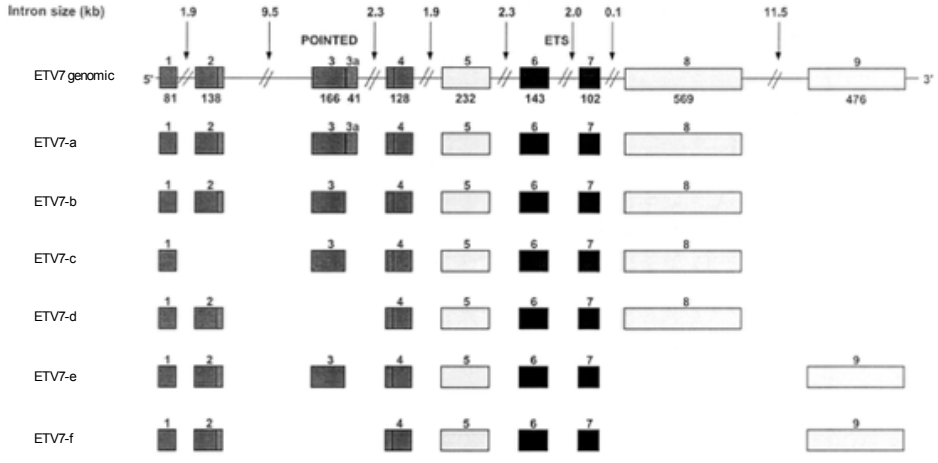

INTRODUCTION-Figure 4: Genomic organization of the *ETV7* gene and exon configuration of the six ETV7 splice isoforms. Exons are represented by boxes and introns by connecting lines; their length is reported above the introns (in kb) and below exons (in bp). Adapted from the work of Gu and colleagues (Gu *et al.*, 2001).

2.3.3 ETV7 expression regulation

ETV7 is deleted in most rodents, but found in all other vertebrates; it localizes to the nucleus and it is generally expressed at low level in tissues and cells (Potter *et al.*, 2000; Gu *et al.*, 2001; Quintana *et al.*, 2014). ETV7 mRNA is mostly found in placenta, liver, prostate, lung, ovary, spleen, thymus, hematopoietic system and in fetal lung and kidney; in cell lines in culture it is highly expressed in epithelial A431 squamous carcinoma cells and in non-epithelial U937 monocytic cells, synovial fibroblasts, and primary human chondrocytes (Potter *et al.*, 2000; Gu *et al.*, 2001). *In vitro* translation showed two in frame alternative translation start sites (at position 1 and 17) which results in two proteins with similar molecular weight (Poirel *et al.*, 2000; Gu *et al.*, 2001).

Upstream the transcriptional start site, an initiatior Inr element is found with overlapping binding sites for ETS and E2F factors and further upstream there are also other additional ETS binding sites and binding regions for NFκB, AP1, Ikaros, and transcription factors having the HLH DNA binding domain (Gu *et al.*, 2001).

A strong induction of ETV7 transcription upon Doxorubicin and TNFα combined treatment, and the associated p53 and p65 transcriptional control are reported in this thesis and the relative publication (Bisio *et al.*, 2014).

Interferon alfa is another known inducer of ETV7 expression through the JAK-STAT pathway (Park *et al.*, 2013; Rempel *et al.*, 2013; Contreras *et al.*, 2015; Ignatius Irudayam *et al.*, 2015). Relatively recently, interferon stimulated genes have gained interest in breast cancer research thanks to their predictive role in drug resistance, experimentally demonstrated for STAT1, ISG15, and IFIT1 (Weichselbaum *et al.*, 2008). This thesis project, extended those observations to ETV7. Not surprisingly, being an interferon stimulated gene, ETV7 is activated by infection, observed for Hepatitis C (Ignatius Irudayam *et al.*, 2015), HIV-1 (Rempel *et al.*, 2013); in fact ETV7 induction has been proposed in a patented assay for detecting specific RSV infection (Ginsburg *et al.*, 2014), but its role in viral infection is still unknown.

ETV7 is probably regulated by phosphorylation like most ETS factors, and contains putative phosphorylation sites for AKT, $p90^{rsk}$, Protein Kinase C, Casein Kinase 2, CDC2 Kinase, Tyrosine Kinase, and for some MAP kinases suc as ERK, JNK, and p38 (Gu *et al.*, 2001) .

One MAPK site localizes in a small region upstream the PNT domain (37 aa upstream), which is highly conserved between ETV6 and ETV7 (Potter *et al.*, 2000; Gu *et al.*, 2001).

Phosphorylation by MAPK is generally very important for ETS factors transcriptional activity (Wasylyk, Hagman and Gutierrez-hartmann, 1998). ERK-mediated phosphorylation can positively regulate trascription (as for ETS1 ans ETS2) or negatively (as for ETV6) and it can also convert a repressor into an activator of transcription (Gu *et al.*, 2001; Vivekanand and Rebay, 2012). Phosphorylation could possibly represent a relevant mechanism for ETV7 regulation, given that among all the ETS factors ETV7 ranked sixth for the presence of MAPK interaction motifs and displayed the highest affinity for p38α followed by JNK1 (Selvaraj, Kedage and Hollenhorst, 2015).

2.3.4 ETV7 consensus, targets and mechanism of repression

2.3.4A ETV7 consensus DNA binding site

ETV7 consensus sequence *in vitro* was first reported as identical to the ETV6 one (Potter *et al.*, 2000); later on more specificity was added (Gu *et al.*, 2001), and the latest one was determined by microwell-based transcription factor-DNA-binding assays (Wei *et al.*, 2010) (Figure 5). This project reports the first *in vivo* consensus sequence for ETV7.

1. ccGGAAgt
2. A/g/t-A/C/G-C-A/C-G-G-A-A-G-T-T-A/g-N
3. 

INTRODUCTION-Figure 5: ETV7 *in vitro* consensus sequences, reported in chronological order respect to their literature evidence; consensus sequences refer to the studies of Potter and co-workers (Potter et al. 2000, sequence 1), to the work of Gu and colleagues (Gu et al. 2001, sequence 2), and to the analysis of Wei and colleagues(Wei et al. 2010, sequence 3).

2.3.4B ETV7 targets

Low-throughput microarray analysis on MG-63 osteosarcoma cells ectopically transfected with an ETV7 expression vector showed only a few genes changing in a significant way, among them Thymosin β-10 was up-regulated around 3 fold, BMP-6 was down-regulated 5/10 fold, RARα was repressed 5 fold and interleukin-6 was repressed 2 fold; but no binding

analysis was performed, thus some of them the could represent also indirect targets (Gu *et al.*, 2001). Therefore, investigation and validation of ETV7 targets represents a totally unexplored research area, which can provide promising information also regarding the few ETV7 biological roles reported so far.

2.3.4C ETV7-mediated repression mechanism

ETV7 acts as a transcriptional repressor *in vitro* and the level of ETV7 expression correlates with the degree of down-regulation (Gu *et al.*, 2001). ETV7 can bind to DNA as homo-oligomers, forming cooperative and insoluble polymers (Kar and Gutierrez-Hartmann, 2013; Selvaraj, Kedage and Hollenhorst, 2015). Similarly to ETV6, both PNT and ETS domains are required for an efficacious transcriptional repression (Gu *et al.*, 2001) .

ETV7 central domain (aa 113-210) was proved to have important roles for the active repression of transcription, therefore suggesting that probably some corepressors could bind to this region (Poirel *et al.*, 2000). Also the ETV6 central region provides for the binding to many co-repressors; however, ETV7 and ETV6 are very different in their central region , thus probably they are not sharing the same interactors within this region (Cardone *et al.*, 2005). Nevertheless, some corepressors like Sin3a bind ETV6 in the Pointed domain, which is also highly conserved in ETV7 (Lopez *et al.*, 1999), therefore they could be account also as ETV7 cofactors. It could also be that ETV7 through its PNT could interact with other proteins containing SAM domain like the Polycomb group of proteins (Gu *et al.*, 2001), that are also involved in transcriptional repression. ETV7 can also block the transcriptional activity of ETS1, ETS2 and ETV6, by direct binding via its PNT domain; specifically, the isoform ETV7-a (made of only the PNT domain) was the most effective in antagonizing the repressive activity of ETS1, ETS2 and ETV6 (Vivekanand and Rebay, 2012).

2.3.5 ETV7 oncogenic role in cancer

Insights of ETV7's role as an oncogene were present already from its discovery: its genomic location at 6q21.3 was frequently rearranged in different types of cancer (Poirel *et al.*, 2000; Gu *et al.*, 2001; La Starza *et al.*, 2006) and its sequence was found within the cDNA library of various cancer tissues, such as colon cancer, adenocarcinoma, lung carcinoma, B-cell chronic

lymphocytic leukemia, adrenal adenoma, germ cell tumor, ovarian and endometrial cancer(Potter *et al.*, 2000; Gu *et al.*, 2001). More recently an increased expression of ETV7 was reported also in primary human leukemia samples, pediatric B-ALL, lung cancer, rectal cancer and in hepatocellular carcinoma (Kawagoe *et al.*, 2004; Cardone *et al.*, 2005; Matos *et al.*, 2009).

ETV7 definition as an oncogene was based on correlative data until the report of its direct involvement in cellular transformation (Kawagoe *et al.*, 2004). In particular it was demonstrated that over-expression of ETV7 can promote the Ras-driven cellular transformation by blocking the tumor suppressing action of ETV6 in NIH3T3-UCLA; for exerting this action both PNT and DNA binding domain are required (Kawagoe *et al.*, 2004). The ability of ETV7 to bind to ETV6 was already known from its discovery (Poirel *et al.*, 2000; Potter *et al.*, 2000) but the functional relevance of this binding was not known. Another effect of ETV7 binding to ETV6 is the inhibition of ETV6-mediated transcription, which was specifically reported for the ETV7/Tel2a isoform, also able to block ETS1 and ETS2 transcriptional output (Vivekanand and Rebay, 2012).

Another direct involvement of ETV7 in tumorigenesis refers to the ability of ETV7 to interact with Myc and promote lymphomagenesis (Cardone *et al.*, 2005). Bone marrow cells over-expressing ETV7 or an empty control were transplanted in a transgenic mouse model of Burkitt lymphoma (Eμ-Myc) and it was observed that ETV7 over-expressing cells were growing quicker and were developing B-cell lymphoma faster than the empty control (Cardone *et al.*, 2005). Specifically, ETV7 accelerated the lymphomagenesis by decreasing the apoptosis driven by Myc over-expression and by increasing the cell growth; both the ETS domain and the PNT domain were essential for mediating these roles (Cardone *et al.*, 2005). A common characteristic of ETV7- Eμ-Myc-derived lymphomas was the inactivation of p53 pathway by mutations or by Mdm2 over-expression and the consequent Arf protein increase, which suggests a possible negative interaction between p53 and ETV7 (Cardone *et al.*, 2005). ETV7 expression is often found up-regulated in pediatric B-ALL with increased MYC or MYCN expression, indicating that the cooperation between ETV7 and MYC is recapitulated also in clinical data (Cardone *et al.*, 2005). *In vitro* it was seen that ETV7 over-expression in bone marrow cells from Eμ-Myc transgenic mice led to increased proliferation (corresponding to increased expression of c-Myc and E2f1), decreasead apoptosis (corresponding to Bcl-2 upregulation) and immortalization (corresponding to Arf loss) (Cardone *et al.*, 2005). Decreased apoptotic levels and associated Bcl2 protein up-regulation was observed also after

ETV7 over-expression in bone marrow derived Lin- hematopoietic stem cells (Carella *et al.*, 2006). A microarray analysis in these cells showed an increased expression for pro-apoptotic genes (Trp53inp1, Stk17b, Dapk2, Bmf) and c-Kit, and down-regulation of antiproliferative genes (Btg1, Btg2, Cdkn1B, Rb1cc1) and gene associated with differentiation (cFes, Btg1, Btg2, Tgfbr2) (Carella *et al.*, 2006). ETV7 over-expression in bone marrow derived Lin- hematopoietic stem cells provided a growth advantage especially when interacting with stromal cells and it caused a myeloproliferative disease characterized by an increase in the population of early myeloid progenitor cells and a long-latency period, suggesting that ETV7 overexpression requires additional mutations for causing leukemia (Carella *et al.*, 2006). Furthermore, over-expression of ETV7 in hematopoietic cell was also indirectly stimulating T-cell lymphomagenesis (Carella *et al.*, 2006).

According to TCGA and METABRIC databases, only 1% of breast cancers present an amplification of the ETV7 region and according to TCGA only a 0.3% frequency of mutation. The low mutation frequency does not exclude ETV7's oncogenic potential, and in fact ETV7 was listed among genes that are associated with low mutation frequency but have a high normalized mutation burden in their protein interaction network, and could therefore represents important cancer driver genes (Horn *et al.*, 2015). Taken collectively, a better understanding of ETV7 role in cancer and ETV7 targets identification and validation, can represent a novel and promising research aim.

2.3.6 ETV7 role in differentiation

Other indirect data supporting the oncogenic function of ETV7 refers to its ability to block differentiation, specifically observed in monocytic differentiation driven by vitamin D3 and 12-O-tetradecanoylphorbol 13-acetate (TPA) in U937 and HL60 human myeloid leukemia cells (Kawagoe *et al.*, 2004). The ETV7 negative role on monocytic differentiation was not driven by an inhibitory binding to ETV6, and both PNT and ETS domains were essential for this function (Kawagoe *et al.*, 2004).

The role in differentiation can also be indirectly inferred from the effects of ETV7 over-expression causing the repression of the differentiation inducers retinoic acid receptor α (RARα) and Bone Morphogenetic Protein-6 (BMP-6) (Gu *et al.*, 2001). Furthermore, ETV7

expression increases during differentiation of K562 human chronic myeloid leukemia cells into megakaryocyte by TPA (Sakurai *et al.*, 2003).
By studying ETV7 physiological role in zebrafish it was discovered an important role in red blood cell differentiation: ETV7 positively regulates the Lanosterol Synthase (LSS) gene, responsible for the cholesterol synthesis, essential for normal red blood cell development (Quintana *et al.*, 2014). Given that the positive regulation on the LSS gene comes only from over-expression and silencing studies, it is still not known if ETV7 contrarily from its reported repressive role, can, in this case, activate the transcription of this gene, or by repressing negative regulators of LSS, promotes its activation indirectly. It has been postulated that ETV7 can have a differentiation role also in platelets (Schick *et al.*, 2016).

2.3.7 ETV7 tumor suppressor roles

Many data are supporting the oncogenic role of ETV7, nevertheless, in nasopharyngeal carcinoma ETV7 can directly inhibit migration and invasion of cancer cells by repressing SERPINE1 gene expression (Sang *et al.*, 2015). Similarly, a decreased expression of ETV7 was observed in 5-Fluoruracil- and cisplatin-resistant cancers (Maeda *et al.*, 2014). Indirect data on a possible tumor suppressor role of ETV7 in prostate cancer comes from the evidence of its down-regulation in the stroma of peripheral zone (more prone to develop cancer) with respect to the transitional zone (Shaikhibrahim *et al.*, 2012).
This contradictory evidences suggest a cell type- and time-dependent effect of ETV7 in cancer cells and in cancer progression, probably influenced by different ETV7 interaction partners present in different cells and at a different time, an observation that is in line with the role of other ETS factors in breast cancer.

This project reports for the first time a role for ETV7 in breast cancer, in particular in promoting drug resistance to Doxorubicin and 5-Fluorouracil. In particular, ETV7-mediated repression of the co-chaperone DNAJC15 is reported as a mechanism responsible for drug resistance.

2.4 DNAJ FAMILY

HSP40/DNAJ is a very large (49 members) and heterogenous family of Heat Shock Proteins (HSP). Its main function is co-chaperoning HSP70, but recent evidence also supports a role for DNAJ independent from HSP70, possibly acting with other chaperones (Sterrenberg, Blatch and Edkins, 2011). Chaperones are key regulators of protein homeostasis. Both in physiological and stressful conditions; they assist protein folding, stability, transport, and interactions. Co-chaperones stimulate the chaperones, regulate the client specificity and assist in the formation of multi-chaperone complexes.

DNAJ family can be divided into 3 subgroups according to the domain organization: DNAJA, DNAJB, and DNAJC. The typical feature of DNAJ family is the J-domain of 70 aa (containing a characteristic tripeptide), which is required for the stimulation of the ATPase activity of HSP70. Some DNAJ, especially members of the DNAJC subgroup, can also have functions independently from the J-domain (Sterrenberg, Blatch and Edkins, 2011).

2.4.1 DNAJ role in breast cancer

A role in breast cancer has been recognized only relatively recently for DNAJ co-chaperone protein family.

The large isoform of DNAJB6/MRJ blocks breast cancer migration, growth, metastasis and triggers a partial Mesenchimal to Epithelial transition (MET) (Mitra *et al.*, 2008, 2010; De Bock *et al.*, 2010; Menezes *et al.*, 2012) and it can be regulated by miR-632 (Mitra *et al.*, 2012). Similarly, also DNAJA3/TID can block breast cancer cells migration (Kim *et al.*, 2005). DNAJC12/JDP1 shows higher expression in ER+ breast cancer and may be involved in controlling ER signaling (De Bessa *et al.*, 2006). DNAJC12 together with DNAJC10 was found up-regulated in mammospheres derived from ER+ tumors (Kok *et al.*, 2009) DNAJC13 and DNAJB1 are listed in the breast cancer invasiveness signature, being found highly expressed in breast cancer stem cells (Liu *et al.*, 2007).

Some DNAJ proteins are important also for the tumorigenesis driven by viral infection. For example, DNAJC14/HSJ3 is required by Flaviviridae to replicate and cause hepatocellular carcinoma (Yi *et al.*, 2011). Other DNAJ, plays important role in cancer chemoresistance. DNAJB11/ERDJ3 is involved in paclitaxel resistance (Di Michele *et al.*, 2010); DNAJA1/HDJ2 in glioblastoma radiotherapy resistance (Wang *et al.*, 2006). Certainly, the DNAJ member which has the most consistent role in breast cancer chemoresistance is DNAJC15.

2.5 DNAJC15

DNAJC15 is a small protein of 147aa (around 17 KDa) belonging to the type II transmembrane co-chaperone. It has a J domain at the C-terminus (essential for chemoresistance), a non-conserved N-terminal region and a transmembrane domain, which is not a common feature for DNAJ proteins that are mostly soluble (Hatle *et al.*, 2007; Sinha and D'Silva, 2014).
Its direct evolutionary ancestor is yeast TIM14, an inner mitochondrial membrane protein, and it probably originated from gene duplication of DNAJC19, a mitochondrial co-chaperone, with whom it shares a similar C-terminal domain (Hatle *et al.*, 2007).

2.5.1 Regulation of DNAJC15 gene expression

DNAJC15 was named MCJ (Methylation Controlled J protein), because it was discovered as a highly methylated and thus repressed gene in ovarian cancer and it was induced upon 5-Aza-2-deoxycytidine treatment in those cells (Shridhar *et al.*, 2001). Frequently, methylation at one allele is combined with the deletion of the other allele, resulting in DNAJC15 loss in many ovarian cancers (Shridhar *et al.*, 2001).
Increased methylation of DNAJC15 in CpG islands, localized within the first exon and the first intron, was observed in epithelial cells compared to non-epithelial cells and was associated with reduced histone acetylation, also in the promoter region (Strathdee *et al.*, 2004). Very high level of CpG islands methylation was observed in some ovarian tumors and associated with poor prognosis (Strathdee *et al.*, 2005). Also in malignant pediatric brain tumor an extensive pattern of methylation in most of the CpG sites of the intronic CpG island was observed (Lindsey *et al.*, 2006). Conversely, in neuroblastoma DNAJC15 gene methylation localizes in the promoter region (-179 to the Transcription Start Site –TSS-) and is often found in neuroblastoma samples bearing MYCN amplification (Lau *et al.*, 2012). Similarly, in breast cancer, methylation was also reported in the proximal promoter region (Fernández-Cabezudo *et al.*, 2016).
In murine macrophages, DNAJC15 was reported to be regulated by another type of repression independent from methylation, but relying on the Ikaros transcription factor. Ikaros binds at the position of -350, -361 from TSS of DNAJC15 and it is activated by IFNγ through post-translational modifications by Casein Kinase 2 (Navasa *et al.*, 2015).
This project reports a new type of DNAJC15 repression, mediated by the ETS factor ETV7.

2.5.2 DNAJC15 biological functions and its role in drug resistance

The impact of DNAJC15 on drug resistance was very clear from its discovery: it was seen that DNAJC15 repression in ovarian cancer cells was able to induce resistance to topotecan, cisplatin and paclitaxel (Shridhar *et al.*, 2001; Witham *et al.*, 2008). Same observation was made also in breast cancer cells in response to doxorubicin (Boettcher, Kischkel and Hoheise, 2010; Sinha and D'Silva, 2014).

Later on, an increased DNAJC15 promoter methylation was also found very often in Wilm's tumor (90% cases), neuroblastoma (50% primary neuroblastoma), malignant pediatric tumors, melanoma (50%cases) and resistant breast cancer (Ehrlich *et al.*, 2002; Lindsey *et al.*, 2006; Muthusamy *et al.*, 2006; Boettcher, Kischkel and Hoheise, 2010; Lau *et al.*, 2012; Hatle *et al.*, 2013; Fernández-Cabezudo *et al.*, 2016).

It was first shown *in vitro* that DNAJC15 expression was lower in drug resistant breast cancer cell lines (MCF7/ADR, MD22) when compared with drug-sensitive cell lines (MCF7 and MDA-MB-231), and, similarly, in uterine multi drug resistant cells (MES-SA/Dx5 cell line) with respect to the sensitive cells (MES-SA) (Hatle *et al.*, 2007). In MCF7 cells, DNAJC15 silencing leads to doxorubicin and paclitaxel resistance by increasing the drug efflux (Hatle *et al.*, 2007). In details, DNAJC15 can bind to c-Jun and promotes its degradation, thus if lower level of DNAJC15 are present, c-Jun escapes the DNAJC15 control and dimerizes to activate the transcription of ABCB1, which increases the drug efflux, thereby promoting drug resistance (Hatle *et al.*, 2007). Furthermore, the autocrine IL-6 production observed in multi-drug resistant cells, was also able to decrease the expression of DNAJC15 via unknown mechanisms (Conze *et al.*, 2001; Hatle *et al.*, 2007).

DNAJC15 was first described as localized in the Golgi apparatus, oriented with its C-terminus in the Golgi lumen and bearing a cytoplasmic N-terminus (Hatle *et al.*, 2007).

Then, all the following studies, starting from Schusdziarra and collaborators, report DNAJC15 localization inside the mitochondrial inner membrane with the J domain oriented to the matrix (Schusdziarra *et al.*, 2013). It can be that DNAJC15 over-expression led to a partially artifactual Golgi localization, neverthess, its negative action on JNK pathway was confirmed also by recent studies regarding mitochondrial DNAJC15 in macrophages (Navasa *et al.*, 2015).

Inside the mitochondrial membrane, DNAJC15 can carry out various important functions: controlling the protein import into mitochondria, controlling in a negative fashion the respiratory chain complexes, and regulating the transition pore complex (Hatle *et al.*, 2013; Schusdziarra *et al.*, 2013; Sinha and D'Silva, 2014).

DNAJC15 exerts its co-chaperone role by promoting ATPase activity of mortalin, a core component of the TIM23 translocase A complex (a pre-protein import complex mostly involved in the regulation of mitochondrial DNA copy number and Nodal signalling molecules). Its homolog DNAJC19 is essential for the functioning of TIM23 translocase complex B1 and B2, which are the most important complexes for the import of proteins (Schusdziarra *et al.*, 2013; Sinha *et al.*, 2014). Therefore, DNAJC19 is essential for the protein import, whereas DNAJC15 is dispensable (Sinha, Srivastava and D'Silva, 2016). MAGMAS controls the binding of DNAJC15 to mortalin (Schusdziarra *et al.*, 2013; Sinha *et al.*, 2014). Despite the fact that there is no direct link between DNAJC15 loss, its role on protein import, and chemoresistance, it could be that its influence on mitochondria could affect the apoptotic response. Other data supporting this hypothesis comes from the fact that MAGMAS is often up-regulated in many prostate cancers and mortalin is also involved in tumorigenesis (Jubinsky *et al.*, 2005; Kaul, Deocaris and Wadhwa, 2007; Schusdziarra *et al.*, 2013).

The direct evidence connnecting DNAJC15 and apoptosis comes from a study observing that DNAJC15 over-expression can lead to mitochondrial permeability transition pore (MPTP) opening and apoptosis induction (Shridhar *et al.*, 2001). Upon high level of ROS or calcium, MPTP forms a non-specific pore leading to loss of potential, osmotic gradient and organelles disruption. Peptidyl-proline isomerase cyclophilin D (CypD) is the motor core of MPTP and is recruited to MPTP by DNAJC15, specifically by binding to its J domain (Shridhar *et al.*, 2001).

Negative regulation by DNAJC15 on the mitochondrial respiration is exerted by interacting and blocking complex I, therefore DNAJC15 loss is responsible for an increase in complex I activity, membrane potential and ATP production, which is critical in case of metabolic alterations such as fasting: DNAJC15 loss determines a rapid metabolism preventing lipid accumulation and liver steatosis (Hatle *et al.*, 2013).

Increased ROS production and apoptosis induction provide a direct link between mitochondrial DNAJC15 and chemoresistance. The negative role on respiratory complex could link also the DNAJC15 loss to drug resistance, given that most metastatic cancer cells are strongly dependent on mitochondrial respiration for their metabolism (Fernández-Cabezudo *et al.*, 2016). The inhibitory role on respiratory chain exerted by DNAJC15 was observed also in immune cells as mean of metabolic control, specifically in macrophages and in CD8+ cells,

where it controls the response to inflammatory stimuli, and for instance its expression in CD8+ cells also controls the response to influenza virus (Navasa *et al.*, 2015; Champagne *et al.*, 2016).

High expression of DNAJC15 is associated to insulin resistance, confiming a role for DNAJC15 in the control of metabolism (Do *et al.*, 2015). Moreover, insulin treatment can directly down-regulate DNAJC15 expression (Gupta and Tikoo, 2012).

Recently, a different promoter methylation in DNAJC15 was associated also to a predisposition for more aggressive cancer that has been observed in afro-american women (Conway *et al.*, 2015). Lack of DNAJC15 expression was observed to drive to multi-drug resistance also in mice (Fernández-Cabezudo *et al.*, 2016).

In breast cancer patients, the lowest expression of DNAJC15 is observable in triple negative breast cancer patients, and it represents a good predictive marker for chemotherapy response inside this subgroup (Fernández-Cabezudo *et al.*, 2016).

This PhD project uncovered a novel direct link between DNAJC15 and ETV7 which is critically important for breast cancer chemoresistance and could represent a promising target to improve therapeutic efficacy.

3. AIM OF THE THESIS

ETS factors are key regulators of many biological processes both in physiological and pathological conditions, including cancer progression. Among several ETS family members, I decided to focus my attention on ETV7. ETV7 has a very limited literature with some promising data on proposed tumor-promoting actions. Most evidence is centered on the oncogenic role of ETV7 in liquid tumors, but increased ETV7 expression is also found in various solid tumors, where its role is completely unknown. This project aims to address the role of ETV7 specifically in breast cancer. ETV7 ranked at the top of a signature of genes synergistically activated by Doxorubicin and TNF-α in breast cancer cells, a condition associated with increased cancer aggressiveness. Furthermore, the observation that many chemotherapeutic drugs are able to consistently activate ETV7 expression in different solid cancer-derived cell lines, including breast cancer, suggests a possible role for ETV7 in response to drug treatment.

For these reasons one of the main objectives in this study is represented by the analysis of ETV7-mediated drug resistance to Doxorubicin in breast cancer cells as a first step; this aspect will also be extended the resistance analysis to 5-FU often used in combination with Doxorubicin in breast cancer chemotherapy.

The lack of evidence regarding *in vivo* validated ETV7 targets and consensus sequences have been exploited in this study in order to provide the first reported ChIP-seq for this transcription factor. The results may lead to the discovery of novel direct ETV7 targets with known roles in drug response and involved in key cancer pathways; this might strongly support the oncogenic role for ETV7 in breast cancer proposed by this project, which appears remarkably promising. Moreover, this project also aims to better characterize how chemotherapeutic drugs can promote ETV7 activation at the transcriptional level, to envision possible therapeutic strategy minimizing the activation of the pathway ETV7 regulates.

Summarizing in few words, this thesis aims at the characterization of the ETV7 role in triggering breast cancer chemoresistance, focusing on the identification of novel targets regulated by the ETV7 transcriptional activity.

4. MATERIALS AND METHODS

4.1 Cell lines and culture conditions

MCF7 and U2OS cells (obtained from Interlab Cell Line Collection bank, Genoa, Italy) were cultured in DMEM supplemented with 10% FBS, 2mM L-Glutamine and 2mM of Penicillin/Streptomycin. MDA-MB-231 cells (gift from Prof. A. Provenzani, CIBIO, Trento, Italy) were cultured in DMEM supplemented with 1% Non Essential amminoacids, 10% FBS, 2mM L-Glutamine and 2mM of Penicillin/Streptomycin. A549 (from ATCC, Manassas, VA, USA) and A375M cells (gift from Dr. D. Bergamaschi, Centre for Cell Biology and Cutaneous Research, Blizard Institute, Barts and The London School of Medicine & Dentistry, UK) were grown in RPMI medium + 10% FBS, 2mM L-Glutamine and 2mM of Penicillin/Streptomycin. HUVEC cells (Human Umbilical Vein Endothelial Cells, from Interlab Cell Line Collection bank, Genoa, Italy) were cultured on 0.1% gelatin pre-coated plastics in Medium 199 (Lonza Milan, Italy) supplemented with 50 units/ ml Low Serum Growth Supplements (Life Technologies, Milan, Italy). BJ1-hTERT cells (obtained from Dr. K Lobachev, Georgia Institute of Technology, GA, USA) were grown in MEM medium supplemented with 10% FBS, 2mM L-Glutamine, 2mM of Penicillin/Streptomycin and Puromycin. CRL-4050 (HSAEC1-KT) were cultured in SABM Basal Medium (Lonza CC3119) supplemented with SAGM BulletKit medium (CC4124). Lymphocytes were obtained from the Clinical Research Unit at the National Institute of Environmental Health Sciences (NIEHS, NIH, Research Triangle Park, NC, USA); lymphocytes culture and treatment conditions are reported within Methods section in Menenedez *et al.*, 2011 (Menendez et al., 2011).

4.2 Drug Treatments

All drugs were obtained from Sigma-Aldrich, with the exception of Etoposide purchased from Enzo Life Science (Rome, Italy). Treatments were performed for 16 hours with the following concentrations: 1.5μM for Doxorubicin (0.5μM only for U2OS and BJ1-hTERT cells), 5ng/ml for TNF-α, 10μM for Nutlin-3a, 375μM for 5-Fluorouracil, 0.5μM for Camptothecin, 50μM for Etoposide. Prolonged Doxorubicin treatment was achieved treating cells with 0.5μM Doxorubicin (for MCF7 cells) and 0.8μM Doxorubicin (for MDA-MB-231) for a total of 14 days

of treatment, replacing exhausted medium with fresh one containing Doxorubicin every 3 days. Ionizing radiation dose was set at 4 Gy using Shepherd cesium irradiator (NIEHS, NC, USA) at room temperature, and cell were kept in the incubator for 6 hours after radiation. Quercetin and Genistein (purchased from Extrasynthese, Genay, Lyon, France) were used respectively at the concentration of 50μM and 30μM for 16 hours treatment.

4.3 Plasmids

The expression vectors tagged with DDK-Myc (pCMV6-Entry-Empty, pCMV6-Entry-ETV7 and pCMV6-Entry-DNAJC15) were bought from Origene (Tema Ricerca, Bologna, Italy).
To get the pCMV6-ETV7-AC-GFP expression vector where ETV7 gene is fused to AC-Green Fluorescent Protein, ETV7 coding sequence was digested (overnight at 37°C using Mlu I and Asis I enzymes) from pCMV6-Entry-ETV7 and ligated (overnight at 16°C) into the pCMV6-AC-GFP expression vector (gift from Chromosomal Stability group, NIEHS).
The pGL4.26-DNAJC15 and pGL4.26-DNAJC14 reporter plasmids were generated by cloning a portion of the promoter region of DNAJC15 (-299 to +512 from TSS) or DNAJC14 (-1335 to +8 from TSS) into the pGL4.26 backbone. DNAJC15 and DNAJC14 promoter regions were first amplified using Q5 High Fidelity DNA Polymerase (New England Biolabs, Euroclone, Milan, Italy) and primers containing Xho I and Hind III recognition sites (Eurofins Genomics, Ebersberg, Germany): DNAJC15_Fw: GCCTCGAGCAGCACAAACTCATTTGAGGG, DNAJC15_Rv: GCAAGCTTAGGCGGCCCGGAGACTCAAG,DNAJC14_Fw:GCCTCGAGAGGGTGGAGAAAGGGGACAG, DNAJC14_Rv:GCAAGCTTCCAGGGTGAGCTACGAGAG. Purified PCR product and backbone were then digested overnight using Xho I and Hind III restriction endonucleases, and ligated overnight at 16°C. Restriction analysis and direct sequencing were used to determine successful cloning (Eurofins Genomics). Plasmids used for over-expressing mutant p53 (R282Q and G279E) and relative control are pcDNA3.1 based expression plasmid and were a gift from Laboratory of Transcriptional Networks (CIBIO, University of Trento).

4.4 RNA isolation and RT-qPCR

Total RNA extraction was performed using the Illustra RNA spin Mini Kit (GE Healthcare, Milan, Italy), and RNA was reverse-transcribed into cDNA using the RevertAid First Strand

cDNA Synthesis Kit (Thermo Fisher Scientific). RT-qPCR was performed in 384 wells-plate (BioRad, Milan, Italy) with 25 ng of template cDNA, using the KAPA SYBR Fast qPCR Master Mix (Kapa Biosystems, Resnova, Ancona, Italy) and the CFX384 Detection System (BioRad). Relative fold change was calculated using the ΔΔCt method, and YWHAZ and B2M genes were used as housekeeping genes for all samples except for lymphocytes-derived cDNA, for which the 18S ribosomal RNA gene was used as housekeeping gene. Primer sequences (reported in Table 1) were designed using Primer-BLAST designing tool (https://www.ncbi.nlm.nih.gov/tools/primer-blast/), and checked for specificity by standard PCR using the KAPA2G Fast PCR Kit (Kapa Biosystems, Resnova, Ancona, Italy).

PRIMERS used for RT-qPCR	**sequence**
ETV7-Fw	CAAGATCTTCCGAGTTGTGGA
ETV7-RV	GTTCACCCGGTTCTTGTGAT
BRCA1_Fw	CTCGCTGAGACTTCCTGGAC
BRCA1_Rv	TCAACTCCAGACAGATGGGAC
ESR1_Fw	CCGGCATTCTACAGGCCAAATTCA
ESR1_Rv	AGTCTCCTTGGCAGATTCCATAGC
SKI_Fw	GGGGCTTCGACTCGGCCAAC
SKI_Rv	TCAGAGGAGACCCGGGGCAC
SMAD6_Fw	GCACCCCATCTTCGTCAACT
SMAD6_Rv	CGCTCGAAGTCGAACACCT
ID1_Fw	AATCCGAAGTTGGAACCCCC
ID1_Rv	GATCTGGATCTCACCTCGGC
FKBP1A_Fw	GGGTTGCCCAGATGAGTGT
FKBP1A_Rv	CATCGAAGACGAGAGTGGCAT
DPEP1_Fw	TGACAACCTGCTGAGGGTCTT
DPEP1_Rv	TGAGGTTGCTGGCCTGTTCC
DPYD_Fw	ACTCTGTGTTCCACTTCGGC
DPYD_Rv	TCCAGCTTCTCACAATTAAAGCA
DNAJC14-Fw	GTAGCTAGTGGGCGCTACTG
DNAJC14-Rv	GCTGCTCGCAAAACCTTGAA
DNAJC15-Fw	TGGTGTCATCGCTCCAGTTG
DNAJC15-Rv	ATGCGTAGCGACCTGCAAAT
SPDEF_Fw	GACTTCACCTGGGGCGATTC
SPDEF_Rv	TGATGAGTCCACCTCGCTGT
ELF2_Fw	TAGTCCAACAACAGCGACCTC
ELF2_Rv	AGCTGGCATCACAGTAGGGA
ABCB1_FW	TGCCTATGGAGACAACAGCC
ABCB1_RV	TGAAGGCATGTATGTTGGCCT
YWHAZ-Fw	ACTTTTGGTACTTTGTGGCTTCAA
YWHAZ-Rv	CCGCCAAGGGACAAACCAGTAT
B2M-Fw	AGGCTATCCAGCGTACTCCA
B2M-Rv	TGGATGAAACCCAGACACA

PRIMERS used for ChIP-qPCR	sequence
ETV7REChIP_Fw	AGCTCCGTGGCTGGCGTTTC
ETV7REChIP-Rv	AGGGGTTGCCTCCTGGTGGG
ETV7TATAChIP_Fw	GCTGGCCTAGAGCTTGTGAT
ETV7TATAChIP-Rv	ACAAACCAGAAGACACCGAAGA
DNAJC15ChIP_Fw	TGCGAACAGAAGTTGAGAGTGG
DNAJC15ChIp_Rv	AGTAAGCTCGGAGTCTAGCTGT
GTF2H5ChIP_Fw	GAAGCGAAGTAAGAAGTATGGCA
GTF2H5ChIP_Rv	GGCCCTACTAAGAGGCAAAGG
ACTBChIP_Fw	TCTCCCTCCTCCCTTCTTCAAT
ACTBChIP-Rv	TCGCGCCGCTGGGTTTTATA
p21REChIP_Fw	GTGGCTCTGATTGGCTTTCTG
p21REChIP_Rv	CTCCTACCATCCCCTTCCTC
p21TATAChIP_Fw	TATTGTGGGGCTTTTCTG
p21TATAChIP_Rv	CTGTTAGAATGAGCCCCCTTT
MCP1REChIP_Fw	TGTTCCCAGCACAGCCCCTAGT
MCP1REChIP_Rv	TCCCCCGCTGGGAGGTCAGT
MCP1TATAChIP_Fw	ACAGGATGCTGCATTTGCTC
MCP1TATAChIP_Rv	GCCTCTTATTGAAAGCGGGC
SKIChIP_Fw	TGGAGCCAGTGACCTCATTTC
SKIChIP_Rv	GCACAGTGTGTTGCATACAGG
SMAD6ChIP_Fw	AAAAGCAGCAGCAGCAGGAA
SMAD6ChIP_Rv	CTCAGGGCTCACTTAGCAGG
ID1ChIP_Fw	AGGCAGGCGCCACTTTC
ID1ChIP_Rv	GTCCAGGGAGATAAGGGCA
FKBP1AChIP_Fw	TCACGCTTTAAGTCCCTGGT
FKBP1AChIP_Rv	GCCAGTGAGGAGACAACTACC
DPEP1ChIP_Fw	GCCTGTAATCCCAGCACTTT
DPEP1ChIP_Rv	CCTGCCTTAACCTCCCAAGT
DPYDChIP_Fw	ACACGCCTTGTCGCTTATCT
DPYDChIP_Rv	TTTGGTGGTATGGGTGACCT

Table 1: Sequence of primers used for qPCR analysis.

4.5 Western Blot

Proteins were extracted using the RIPA buffer supplemented with Protease inhibitors and quantified by the BCA method (Pierce, Thermo Fisher Scientific). For chromatin and nuclear extraction Subcellular Protein Fractionation Kit (Thermo Fisher Scientific) was used. For cytoplasmic and nuclear extraction, protein fractions were extracted following the instructions of NE-PER kit (Thermo Fisher Scientific), and to increase the chromatin-associated proteins present in the nuclear fraction, pellets remaining from cytoplasmic extraction were directly resuspended in 1x Loading Buffer and boiled. Antibodies used for

detection were: anti-p53 (DO-1, Santa Cruz Biotechnologies, Milan, Italy), anti-RelA/p65 (C-20, Santa Cruz Biotechnologies, Milan, Italy), anti-GAPDH (6C5 Santa Cruz Biotechnologies, Milan, Italy), anti-ETV7/TEL2(F-8, sc-376137X Santa Cruz Biotechnologies), Histone H3 (ab1791, Abcam), anti-Alfa-Actinin (H-2 sc-17829, Santa Cruz Biotechnologies), anti-pSTAT3(Y705) (D3A7 XP(R), PhosphoPlus, Cell Signaling), anti-STAT3 (124H6, PhosphoPlus, Cell Signaling). ECL Select reagent (GE Healthcare) was used for detection at the UVITec Alliance LD2.

4.6 Gene Reporter Assay

Cells were seeded in 24 well-plate at a concentration of 70,000 and 45,000 for MCF7 cells and MDA-MB-231 respectively, and transfected with 250ng pGL4.26-DNAJC15 or pGL4.26-DNAJC14, along with 250ng pCMV6-Entry-Empty or pCMV6-Entry-ETV7 vectors, and 50ng pRL-SV40 for each well using Fugene HD for MCF7 (Promega, Milan, Italy) and Lipofectamine LTX for MDA-MB-231 cells (Life Technologies, Thermo Fisher Scientific, Milan, Italy). 48 hours after transfection, cells were lysed in 1X PLB buffer and luciferase activity was measured with the Dual-Luciferase Reporter Assay System (Promega) using the Infinite M200 plate reader (Tecan, Milan, Italy). Relative Light Unit (RLU) measures were determined considering the transfection efficiency values obtained by transfecting the pRL-SV40 (Promega) vector, constitutively expressing the *Renilla reniformis* luciferase cDNA.

4.7 Single cell cloning

4.7.1 Generation of CRISPR/Cas9 p53 and CRISPR/Cas9 p65 MCF7 and MDA-MB-231 cells

MCF7 and MDA-MB-231 cells were seeded in a 6-well plate respectively at a concentration of 600,000 and 300,000 respectively and transfected with 1.5 μg of CRISPR/Cas9 p53 or p65 vectors (4 different vectors each; All-in-one CRISPR/Cas9 vectors; ATUM/ex DNA 2.0) using Fugene HD for MCF7 cells and Lipofectamine LTX for MDA-MB-231 cells. 48 hours after transfection, serial dilution for single cell cloning was performed according to the Corning protocol for cell cloning in 96-well plate. Single cell clones were checked by Western Blot analysis.

4.7.2 Generation of stable pCVM6-Entry-ETV7 and -Empty MDA-MB-231 cells

MDA-MB-231 cells were seeded in a p60 dish at a concentration of 500,000 and transfected with 1 μg of pCMV6-Entry-Empty or pCMV6-Entry-ETV7 (Origene) using Lipofectamine 3000 (Life Technologies, Thermo Fisher Scientific, Milan, Italy). After 48 hours, cells were splitted and 800mg/ml of Geneticin (Life Technologies) was added. Medium was replaced with fresh and containing Geneticin each 2/3 days, for a total of 4 cycles of selection. Afterwards, single cell cloning in a 96-well plate was performed (Corning protocol) and Geneticin concentration was gradually reduced to 400 μg/ml.

4.7.3 Generation of stable pCVM6-ETV7-GFP and –GFP U2OS cells

U2OS cells were seeded in a 12-well plate (100,000 cells/well) and transfected with 1 μg of either pCMV6-ETV7-AC-GFP or pCMV6-AC-GFP using FuGene HD (Promega). 48 hours after transfection cells were transferred into a p100 dish and selection started using 800mg/ml G418. After 3 rounds of G418 selection, AC-GFP positive cells were sorted using FACS (Fluorescence Activated Cell Sorter), and seeded in a 6-well plate. Once cells reached confluence, serial dilution for single cell cloning was performed in a 96-well plate and Geneticin concentration was gradually reduced to 400 μg/ml.

4.8 Doxorubicin Efflux Analysis

MDA-MB-231 cells were seeded in a 96-well plate at a concentration of 1.5×10^4, and after 24 hours, 10 or 20 μM Doxorubicin was added for 3 hours and Doxorubicin localization was measured exploiting its intrinsic fluorescence using the 520- to 550-nm/560- to 630-nm DsRed excitation/emission filters of the Operetta High Content Imaging System (Perkin Elmer, Milan, Italy) at CIBIO High Throughput Screening Facility. The Harmony 4.1 PhenoLOGIC software was used to first determine nuclear and cytoplasmic regions using segmentation by digital phase contrast mode and then to calculate the ratio of nuclear to cyoplasmic of Doxorubicin and the total area of the Doxorubicin spot area into the cytoplasm (METHODS-Figure 1).

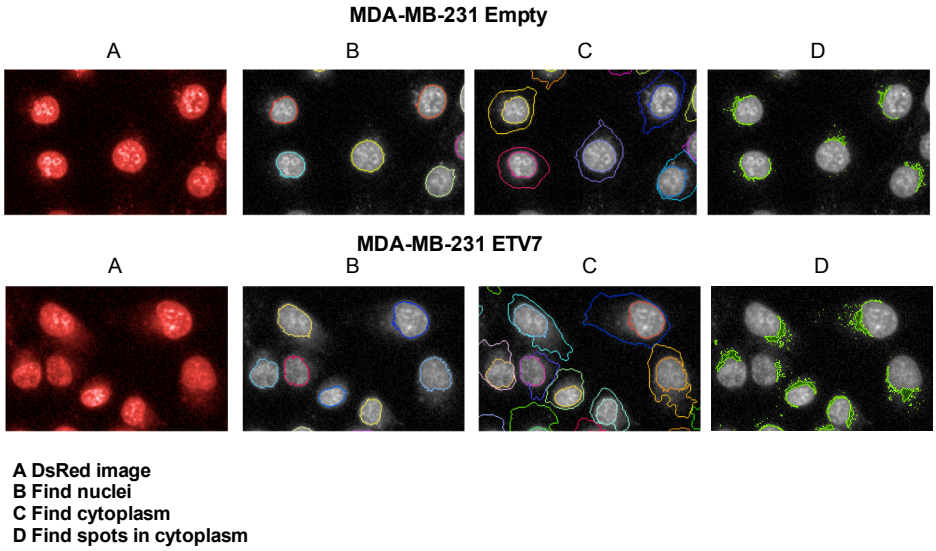

METHODS-Figure 1: Detection and analysis by Operetta Perkin Elmer of Doxorubicin intensity in nuclei and area of Doxorubicin efflux: first Doxorucibin image was taken in the DsRed acquisiton, nuclear and cytoplasmic regions were defined by dynamic light scattering acquisition and then cytoplasmic area of Doxorubicin efflux was calculated as total spots area.

4.9 Viability Assay

Cells were seeded in a 96-well plate and treated for 72 hours with increasing concentrations of Doxorubicin or 5-Fluorouracil. To avoid possible reduction effects of the added compounds with MTT reagent (Sigma-Aldrich), cells were washed with 1X PBS and 10 μl of MTT (5 mg/ml in PBS 1X) was added to 100 μl of fresh medium, and left 3 hours in incubation protected from light. Cells were then lysed using 100 μl of DMSO (Sigma-Aldrich) and reduction of MTT was measured at the Infinite M200 plate reader (Tecan). Viability was reported as a % of MTT absorbance at the indicated treatment concentration respect to the untreated control.

4.10 RSV infection

Cells were seeded in p100 dishes; medium was removed at the time of the infection and 1X PBS containing the desired RSV dilution was added and left in the incubator for 1 hour, then additional 6 ml of medium was added and cells were kept for the desidered time of infection inside the incubator.

4.11 Chromatin enriched Co-IP

Cells were seeded in p150 dishes and harvested using Farnham Buffer (supplemented with 1X PI and PMSF). Cells were then spun down at 4°C for 5 minutes at 2,000 rpm, then lysed using ChIP Lysis Buffer (supplemented with PI and PMSF), vortexed and incubated on ice for 15 minutes; the extracts were quickly sheared with the Covaris sonicator (4 minutes), spun down again at 14,000 rpm for 15 minutes at 4°C. Protein G Beads (50 μl for each sample) were coupled overnight with 5 μg of the desired antibody and 1mg of cell lysate enriched in chromatin fraction was used for immunoprecipitation (performed overnight at 4°C), keeping 1/10 for input control.
Washings were performed once using PBS-Tween20 0,02% and 4 times using RIPA buffer. Finally, beads-antibody-antigen complex was eluted in 40 μl elution + 20 μl NuPAGE LDS sample buffer, heated for 10 minutes at 70° C and supernatant was transferred to clean tubes.
4 μl of the Input and 25 μl of the IP samples were loaded on a 12% polyacrylamide gel following the standard Western Blotting procedure.

4.12 ChIP-qPCR

Cells were seeded on five p150 dishes for each treatment condition and treated for 16 hours when reaching 80% of confluence. Upon treatment completion, cells were crosslinked at room temperature for 8 minutes using 1% Formaldehyde, and afterwards quenched with 125mM Glycine for 5 minutes at room temperature. After washing dishes twice with cold PBS 1X, cells were scraped in 1ml 1X PBS + 1X protease inhibitors and centrifuged at 2,900 rpm for 10 minutes at 4°C. Lysis was performed in ice for 10 minutes using 1% SDS supplemented with 0.1mg/ml salmon sperm DNA and 1X PI, cells were centrifuged at 2,900 rpm for 10 minutes at 4°C and pellet was resuspended in 300 μl of sonication buffer (0.25% SDS, 200mM NaCl, 0.1mg/ml salmon sperm DNA and PI 1X). Sonication was performed using the Bioruptor (Diagenode, Seraing (Ougrée) - Belgium ;30sec ON/OFF for 25 cycles) and checked by running 5 μl of purified sample on a 2% TAE 1X gel (after Proteinase K and RNAse A treatment). Sonicated samples were spun down at 13,000 rpm for 10 minutes at 4°C and supernatant was used for immunoprecipitation, performed at 4°C overnight. 10% of sample were kept as Input control, 40 μl of protein G were used for each immunoprecipitation using 1 μg of each antibody. The following antibodies were used for IP: anti-p53 (DO-1, Santa Cruz Biotechnologies) anti-p65 (C-20, Santa Cruz Biotechnologies), anti-acetyl Histone H4 (06-866,

Millipore), anti-Histone H3 (trimethyl K4; ab8580, Abcam), anti-Histone H4 (acetyl K16; ab109463; Abcam), normal IgG mouse (sc-2025, Santa Cruz Biotechnologies), normal IgG rabbit (sc-2027, Santa Cruz Biotechnologies). IP samples were washed once with dilution buffer, then low salt washing buffer, and then twice with high salt washing buffer, followed by a wash with Litium Cloride, and 1X TE (pH8). De-crosslinking was performed at 65°C overnight, followed by a treatment with Proteinase K (50 μg) at 56°C for 2 hours to remove proteins, and then to remove RNA, 50 μg of RNAse was added and kept for 1 hour at 37°C. QIAquick PCR Purification Kit (Qiagen) and provided protocol was used to purify chipped DNA, eluting using 75 μl of EB Buffer pre-warmed at 65 °C. 2 μl of chipped DNA was used for subsequent qPCR analysis.

4.13 ChIP-seq

Cells were seeded in the p150 dishes (5 dishes each condition) and treated for 16 hours. A revised version of the Myers Lab ChIP-seq v011014 (Jan 2014) was used as described. Fresh Formaldehyde (Pierce™ 16% Formaldehyde (w/v) was used for crosslinking 8 minutes at room temperature. Crosslinking was blocked by adding 0.125M of 2.5M Glycine (20x) for 2 minutes; fixed cells were washed twice with PBS supplemented with 1X PI and harvested by scraping in 5 ml Farnham Buffer (+1X PI and 1X PMSF). Cells were centrifuged at 2,000 rpm for 5 minutes at 4°C and the pellet was resuspended in 1 ml Farnham buffer (+1X PI and 1X PMSF), passed through a gauge needle 10 times and centrifuged again. Pellet was resuspended in RIPA Lysis Buffer (+1X PI and 1X PMSF) and added to the AFA Fiber milliTUBEs (Covaris S-220). Sonication was performed using Covaris S-220 and the following settings: 5% Duty Cycle, 140 watts peak incident power, 200 cycle/burst, 4°C bath temperature, 8 water level, and 20 minutes processing time. Sonicated samples were centrifuged at 14,000 rpm 15 minutes at 4°C and supernatant was collected. A small aliquot (50 μl) was used for sonication control by electrophoresis (after protein and RNA removal and purification). 200 μl re-suspended protein G magnetic bead slurry was washed 3 times using 1 ml of ice cold PBS/BSA (+1X PI) and finally resuspended in 200 μl of ice cold PBS/BSA (+1X PI) containing 5 μg of primary antibody. Coupled beads were incubated overnight on a rotator at 4°C, then washed 3 times with 1 ml of ice cold PBS/BSA (+1X PI) and resuspended in 100 μl. Sonicated samples were diluted in RIPA buffer up to a 300 μl volume and coupled beads were added; 1/10 of each sonicated sample was kept for the Input. Samples were

incubated overnight on a rotator at 4°C and then beads were washed 5 times using ice cold LiCl Buffer (+1X PI), 1 time using TE 1X Buffer and finally resuspended in 200 μl Elution Buffer. IP Samples were incubated for 1 hour at 65°C at 300 rpm in a thermoshaker and finally supernatant was collected after centrifugation at 14,000 rpm for 3 minutes at room temperature using the magnetic rack. Elution Buffer was also added to the Input samples to reach a final volume of 200 μl and both IP and Input samples were incubated overnight at 65°C at 300 rpm. To remove proteins, 50 μg of Proteinase K (Qiagen 19131) was added and incubated at 56°C for 2 hours for 1 hour, and then 50 μg of RNAse A (Quiagen) was added and incubated at 37°C for 30 minutes. QIAquick PCR Purification Kit was used for purification, using 30 μl of pre-warmed DNAse-free molecular grade water and repeating the elution twice. Purified DNA was quantified using Qubit and the HS dsDNA Buffer. Libraries were prepared and run on the MiSeq by the DNA sequencing core at the NIEHS using 10 ng of each sample. Bioinformatic analysis including quality control, mapping and peak detection, was performed by Sara Grimm (Integrative Bioinformatics Support Group, NIEHS).

4.14 Wound healing Assay

MDA-MB-231 cells over-expressing ETV7 and their control were seeded in a 24-well plate and when reaching confluence a wound was created using a p200 tip. Pictures were taken immediately after the wound generation and after 16 hours. Wound diameter was measured using the Leica LASX software and percentage of reclosure was calculated as % (time 0 diameter-time 16 diameter/time 0 diameter).

4.15 Soft Agar colony formation Assay

In a 24-well plate, 500 μl of pre-heated base agar (0,5% agarose in DMEM1X) was distributed evenly in each well and left 10 minutes under the hood to solidify, on the top of it, 2500 cells (MDA-MB-231-ETV7 and MDA-MB-231-Empty) were mixed in the specific medium (DMEM 1X supplemented with 1% Non Essential amminoacids, 10% FBS, 2mM L-Glutamine and 2mM of Penicillin/Streptomycin, 400 μg/ml Geneticin) containing 0,35% agarose. After solidification of the top layer (15 minutes), 250 μl of specific medium was added on the top and replaced every 3 days. After 20 days colonies were stained for 2 hours using 0,005% methylene blue and extensively washed with deionized water. Pictures were taken at the stereomicroscope (EVOS XL Cell Imaging System) and manually counted.

4.16 Transient silencing

150.000 MDA-MB-231 cells were seeded in each well of a 6-well plate and 25 nM of siRNA for p53 and relative control siRNA were transfected using Interferin (Polyplus) transfectant agent. Cells were harvested 72 hours after transfection.

4.17 Statistical Analysis

Statistical analyses were performed by first applying a Fisher-test for comparing variance among two different groups. Relative results were used to set the T-test analysis as following: homoskedastic test (type 2) if p-value (Fisher-test) was higher than 0.05 and an heteroskedastic test (type 3) if p-value (Fisher-test) was lower than 0.05. T-test results were represented graphically using "*" for a p-value < 0.05 and "**" for a p-value < 0.01. The ANOVA test for variance was not chosen, given the interest in the comparison between two different groups (mainly treated and not treated) rather than a total analysis of the variance. Prism GraphPad software was chosen for graphical representation of data.

5. RESULTS

5.1 ETV7 can represent a promising transcription factor in chemotherapy-derived chemoresistance

Unexpectedly, chemotherapy itself can, in some cases, promote chemoresistance. Molecular mechanisms mediating this deleterious effect can often rely on the activity of transcription factors, that once stimulated by chemotherapy, can consequently control the expression of key target genes, leading eventually to drug resistance. My PhD project was specifically focused on the role of ETV7 as transcription factor in response to chemotherapy and its possible implication in mediating chemoresistance in breast cancer cells. I interrogated microarray data from breast cancer cells MCF7 treated with Doxorubicin already available in the lab (Gene Expression Omnibus, GEO, accession number: GSE24065). In particular, I considered only top differentially expressed genes (DEGs) showing a log[fold change(Doxorubicin to Untreated)] higher than 1 (considered as up-regulated) or lower than -1(considered as repressed) and searched for over-represented clusters of transcription factor binding sites using the oPOSSUM tool (http://opossum.cisreg.ca). Transcription factor binding sites (TFBS) best enrichment results are reported in Figure 1A and Figure 1B, indicating DEGs consistently up-regulated and repressed by Doxorubicin, respectively. According to gene ontologies, I then searched for transcription factor enrichment among the up-regulated DEGs by using the Panther Protein Class classification system (http://pantherdb.org) and the top up-regulated ones were reported in Figure 1C. Interestingly, ETV7 ranked as the transcription factor with the highest score among the ones activated by Doxorubicin in terms of gene expression (Fig. 1C). Moreover, a remarkably relevant enrichment for its binding site (ETS) was observable predominantly in in downregulated DEGs group (Figure 1B), in line with its known transcriptional repressive action, but it was also visible among the up-regulated DEGs (Fig.1A). Notably, ETV7 appeared as the only ETS factor consistently up-regulated by Doxorubicin in MCF7 cells from the microarray analysis data (GSE24065) (Fig. 1D). Conversely, two other ETS factors with reported tumor suppressive roles in cancer, SPDEF and ELF2, showed decreased expression upon Doxorubicin treatment in the microarray data from MCF7 cells, which was also confirmed by qPCR analysis (Fig. 1E). Given the encouraging data in support of a promising role for ETV7 as a transcriptional regulator in response to chemotherapy, I decided to

characterize the activation of ETV7 upon treatment with different DNA damaging agents in breast cancer cells. Specifically, I treated MCF7 cells with various drugs for 16 hours and analyzed ETV7 induction by qPCR analysis (Fig. 1F). DNA damaging drugs and, particularly, p53-activating agents proved to efficiently induce the ETV7 expression in MCF7 cells, suggesting that p53 could positively control the expression of this interesting transcription factor (Fig. 1F). To check whether ETV7 activation in response to DNA damaging drugs was a common feature also relevant for other breast cancer cells, I extended the analysis to a breast cancer cell line of a different histologic sub-type and bearing the R280K mutant p53 protein (MDA-MB-231). Notably, in these cells, ETV7 transcriptional activation was still observable, even if at a lower level in comparison to MCF7, and specifically only in response to the treatment with the topoisomerase inhibitors Doxorubicin, Etoposide, and Camptothecin (Fig. 1G). As expected, the MDM2 inhibitor Nutlin-3a wasn't able to affect ETV7 expression in MDA-MB-231. Also, 5-Fluorouracil, was unable to activate the expression of ETV7 in this cell line, possibly due to the fact that it is relying on a different DNA damaging mechanism with respect to Doxorubicin, Etoposide, and Camptothecin (Fig. 1G).

Curiously, in both MCF7 and MDA-MB-231 cells, Doxorubicin was the most efficient ETV7 inducer drug; therefore, the ETV7 activation upon Doxorubicin was also tested and positively confirmed in other cancer cell lines derived from melanoma (A375M), lung cancer (A549) and osteosarcoma (U2OS) (Fig. 1I).

To test whether the same transcriptional activation was also shared by normal cells, I tested ETV7 transcriptional activation in healthy donor-derived lymphocytes upon Doxorubicin, 5-Fluorouracil, Nutlin-3a and ionizing radiation. Despite the expected variability, the majority of samples showed a clear ETV7 induction upon all the treatment conditions (Fig. 1H). To better verify the conservation of ETV7 activation in normal cells, immortalized normal mammary cells (MCF10a), immortalized normal foreskin fibroblasts BJ1 cells and Human Umbilical Vein Endothelial Cells (HUVEC) were treated with Doxorubicin, and ETV7 was observed to be strongly induced also in these non-cancerous cell lines (Fig. 1I). ETV7 activation upon Doxorubicin was also responsible for an increased protein expression in nuclear extracts of MCF7 cells (Fig. 1J). Endogenous ETV7 expression was observable only when more than 50 μg of nuclear extracts were loaded, given that ETV7 protein levels in breast cancer cells are considerably low. To better explore if Doxorubicin-mediated ETV7 activation could be involved in drug resistance, I first checked if also a prolonged treatment with Doxorubicin could lead to an increase in ETV7 expression in breast cancer cells. I treated both MCF7 and MDA-MB-231 cells with Doxorubicin for 14 days and analyzed the ETV7 expression by qPCR

(Fig.1K). In MCF7 cells ETV7 activation revealed to be modest, whereas in MDA-MB-231 cells ETV7 activation was massive (Fig. 1K), in contrast with the results obtained upon transient Doxorubicin treatment, where a higher ETV7 activation was seen in MCF7 cells (Fig. 1F-G). These results are suggesting that ETV7 induction upon DNA damaging drugs, and especially Doxorubicin, could be a relevant mechanism involved in breast cancer drug resistance, and particularly in MDA-MB-231 cells, given the results upon prolonged Doxorubicin treatment.

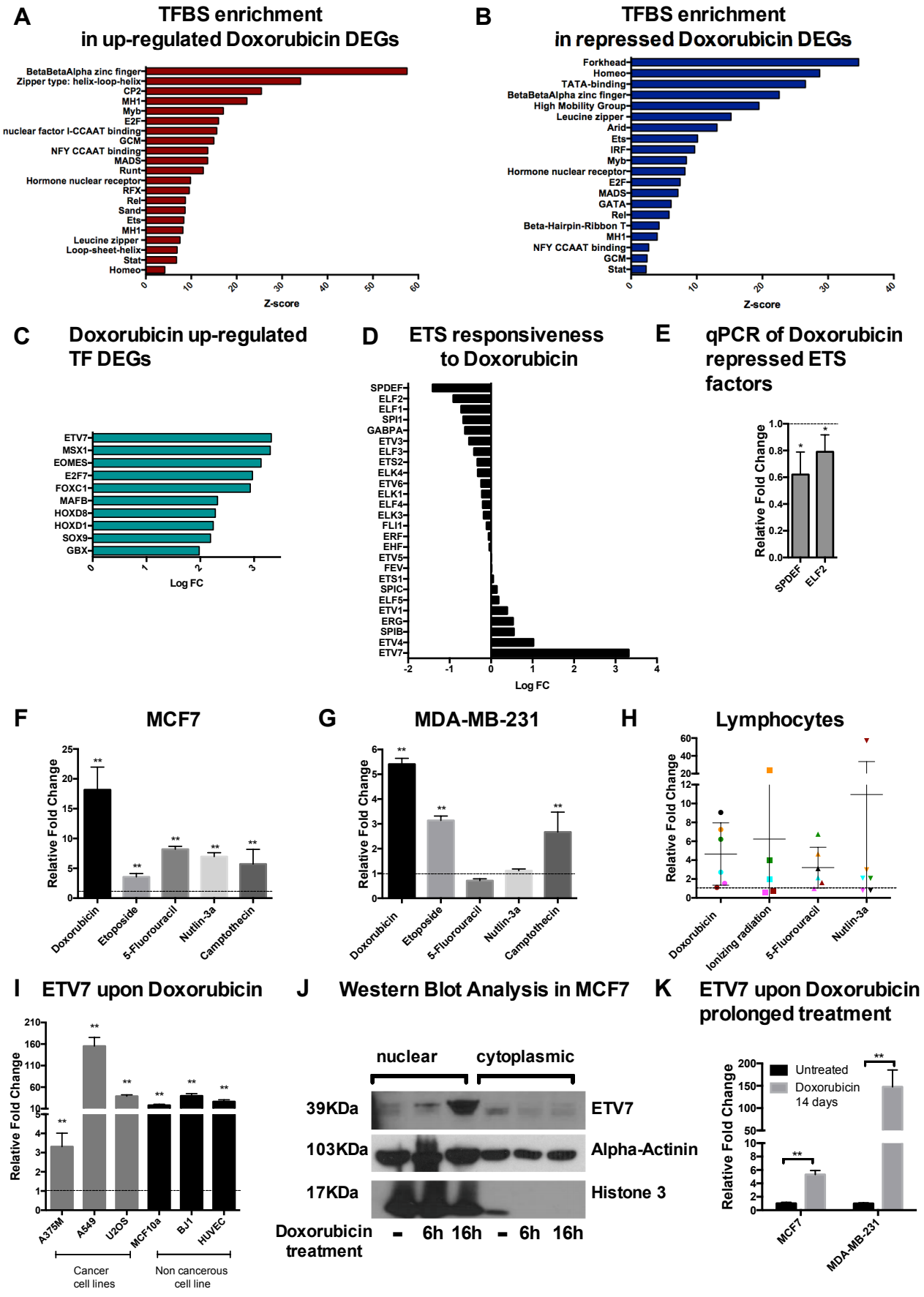

RESULTS-Figure 1: A-B) Transcription factor binding sites (TFBS) enrichment analysis in Doxorubicin up-regulated (A) and repressed (B) DEGs relative to microarray analysis in MCF7 cells. C) List of transcription factors with highest score among the ones up-regulated by Doxorubicin in microarray analysis from MCF7 cells.

D) Expression values for ETS genes from microarray data of MCF7 cells treated with Doxorubicin. E) qPCR validation of Doxorubicin-repressed ETS factors SPDEF and ELF2 in MCF7 cells F-G-H) qPCR analysis of ETV7 transcriptional activation upon DNA damaging and p53 activating drugs in MCF7 cells (F), MDA-MB-231 cells (G), and in healthy donor-derived lymphocytes (H, each color corresponds to a different donor). I) qPCR analysis of ETV7 expression upon Doxorubicin treatment in different cancer cell lines (A375 melanoma, A549 lung, U2OS osteosarcoma) and non cancerous cell lines (MCF10a, BJ1 and HUVEC). J) Western Blot Analysis of ETV7 expression from nuclear and cytoplasmic extracts of MCF7 cells treated with Doxorubicin (1,5 μM) for either 6 or 16 hours. Histone 3 is used as a control for nuclear extraction efficiency. K) qPCR analysis for ETV7 expression upon prolonged Doxorubicin treatment (14 days) using 0,5 μM and 0,8 μM Doxorubicin respectively for MCF7 and MDA-MB-231 cells. * indicates P-value (T test-treatment vs untreated control-) <0.05**,** ** if P-value <0.01.

5.2 ETV7 is synergistically activated by p53 and p65 upon combined treatment with Doxorubicin and TNF-α

Microarray data in MCF7 cells (GSE24065) showed that ETV7 was one of the top synergistically activated genes upon Doxorubicin and TNF-α treatment. I wanted to experimentally validate by qPCR the ETV7 activation upon Doxorubicin and TNF-α in MCF7 cells and also to check if this synergy was conserved in another breast cancer-derived cellular system, MDA-MB-231. Synergy was confirmed in both MCF7 and MDA-MB-231 cells but the reported ETV7 activation and synergy levels were lower in MDA-MB-231 cells in comparison to MCF7 cells, probably due to the fact that mutant p53 is not as effective as wild type p53 in recruiting transcriptional co-activators (Fig. 2A and Fig. 2B, parental cells). Given that both p53 and p65 transcription factors are strongly activated respectively by Doxorubicin and TNF-α treatment, I tested by ChIP-qPCR assays if they are able to bind the ETV7 promoter in MCF7 cells (Fig. 2G and Fig. 2H). MCP-1/CCL2 and p21 promoter regions were used as positive controls for testing the activation and the immunoprecipitation efficacy of respectively p53 and p65 proteins. Localization of p53 and p65 binding sites in the ETV7, p21 and MCP-1 genes and regions amplified by ChIP-qPCR experiments are depicted in Figure 2J. Both p53 and p65 showed occupancy within the ETV7 promoter and in their positive controls p21 and MCP-1 upon all treatments. Moreover, to better determine the involvement of these two transcription factors in ETV7 activation, I generated MCF7 and MDA-MB-231 cellular clones negative for the expression of either p53 and p65 using the CRISPR/Cas9 technology (Fig. 2C-D-E-F). In MCF7 cells, the transcriptional activation of ETV7 was decreased upon Doxorubicin and combined treatment in the absence of either p53 or p65 (Fig. 2A). Nevertheless, the synergistic activation of ETV7 was still observable, suggesting that these factors alone are not essential for the transcriptional activation (Fig. 2A). In MDA-MB-231 cells, the impact of p53 or p65 ablation was more substantial in comparison with MCF7 cells

(Fig. 2B). Synergy was lost upon deletion of either p53 or p65, suggesting that possibly also mutant p53 retained the potential to positively regulate ETV7 expression. Furthermore, to check if mutant p53 was able to bind to the ETV7 promoter, I performed ChIP-qPCR assays in MDA-MB-231 cells treated with Doxorubicin and I was able to detect occupancy of mutant p53 already in the mock condition, which was further increased upon Doxorubicin treatment (Fig. 2I). Mutant p53 and p65 cooperation was confirmed as a critical activatory stimuli for ETV7 expression in MDA-MB-231 cells, where even in basal conditions both are expressed at high level, thus justifying also the reduced increased in expression of ETV7 upon single and combined treatment with Doxorubicin and TNF-α treatment in comparison to what was seen with MCF7 cells.

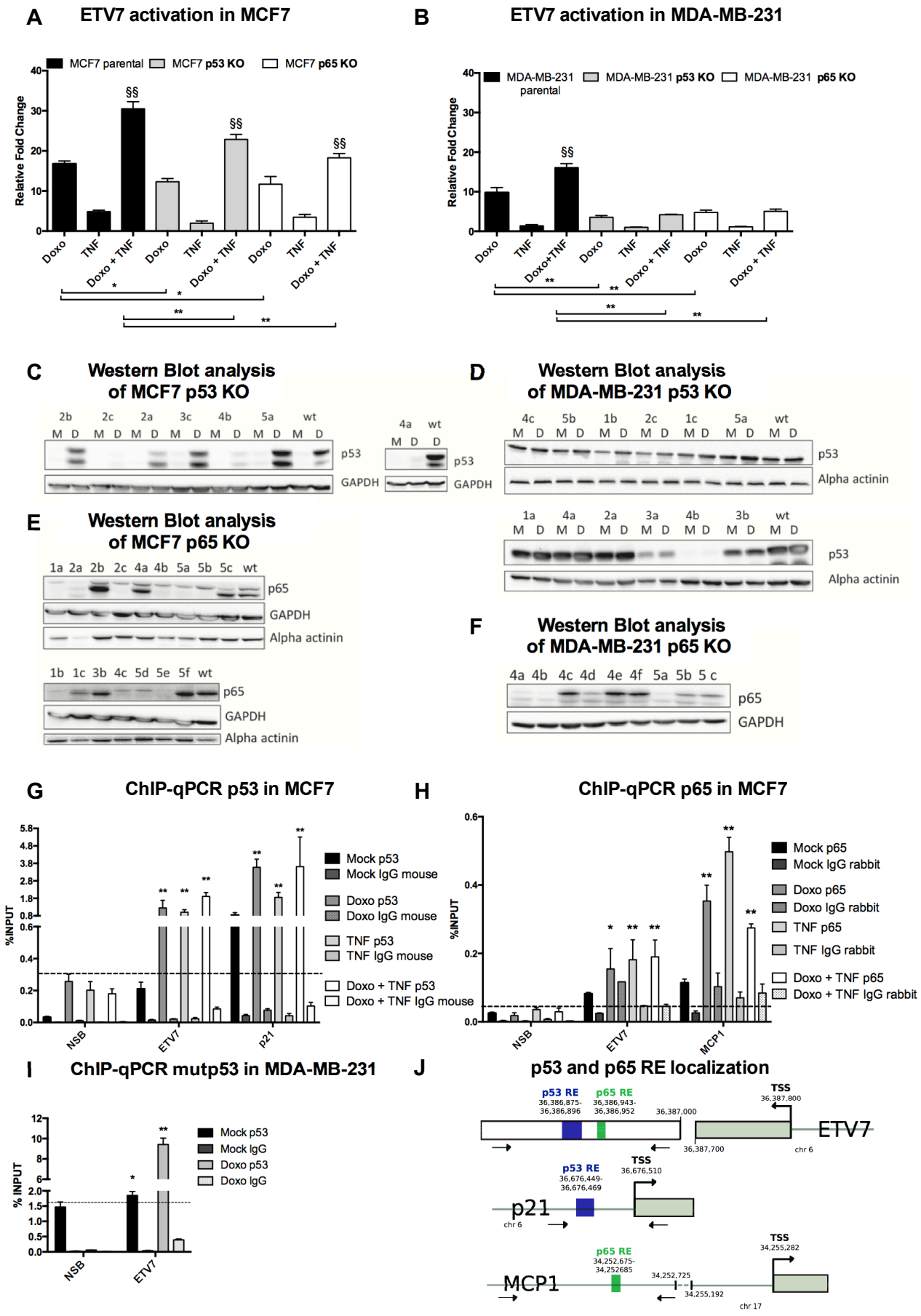

RESULTS-Figure 2: A-B) qPCR analysis of ETV7 activation upon Doxorubicin, TNF-α and combined treatment in parental or p53 knock-out (KO) or p65 KO MCF7 (A) or MDA-MB-231 cells (B). C-D) Western Blot analysis of

CRISPR/Cas9 for p53 generated in MCF7 cells (C) and in MDA-MB-231 cells (D); respectively, clone 4a for MCF7 cells and clone 4b for MDA-MB-231 cells have been selected for following experiments. E-F) Western Blot analysis of CRISPR/Cas9 for p65 generated in MCF7 (E) and in MDA-MB-231 cells (F); respectively, clone 5e for MCF7 cells and clone 4b for MDA-MB-231 cells have been selected for following experiments. G) ChIP-qPCR for p53 occupancy on ETV7 promoter in MCF7 cells upon Doxorubicin, TNF-α and combined treatment. P21 promoter region was used as positive control for p53 immunoprecipitation, whereas NSB represented the non specific binding control, setting the threshold for specific antibody binding. IgG was an additional control for the binding specificity of the p53 antibody. H) ChIP-qPCR for p65 occupancy on ETV7 promoter in MCF7 cells upon Doxorubicin, TNF-α and combined treatment. MCP1 promoter region was used as positive control for p65 activation and immunoprecipitation efficiency I) ChIP-qPCR analysis for mutant p53 occupancy on the ETV7 promoter upon Doxorubicin treatment in MDA-MB-231 cells. J) Graphical representation of the localization of predicted p53 and p65 Response Elements (RE) and the relative to the TSS (Transcriptional Start Site) in the ETV7, p21 and MCP1 genes. Arrows indicate regions amplified by the primers used for the ChIP-qPCR assays. Localization is reported using the human GRCh38/hg38 as reference genome. NSB was the control for non-specific binding. * indicates a P-value(T-test) < 0.05, ** if < 0.01. § indicates synergistic activation (sum of each treatment activation is statistically lower then the combined treatment activation, §§ p value(T-test) < 0.01; § p value(T-test) < 0.05).

5.3 STAT3 is involved in transcriptional activation of ETV7 in MDA-MB-231 cells

So far, the involvement of p53 and p65 in the induction of ETV7 has been considered, but additional transcription factors can cooperate in the activation of ETV7. Among the possible transcriptional controllers, I decided to focus on STAT3, being an important mediator linking inflammation and cancer. I decided to more precisely analyze the role of STAT3 in the induction of ETV7 transcription by generating cells negative for its expression using the CRISPR/Cas9 technology (Fig. 3E and 3F). In MCF7 cells, abrogation of STAT3 expression led to increased expression of ETV7, meaning that STAT3 exerts a negative regulation of ETV7 transcription (Fig. 3C). In fact, in MCF7 cells no STAT3 activation was seen upon all treatment conditions (Fig. 3A). Conversely, in MDA-MB-231 cells, where an increase of phosphorylated form of STAT3 (pSTAT3, the activate form of the protein) was seen upon Doxorubicin and the combined treatment (Fig. 3B), the depletion of STAT3 diminished the ETV7 activation, although it is still synergistically induced (Fig. 3D). This result suggests that STAT3 has probably a supporting role in ETV7 transcription in MDA-MB-231 cells, but it is not essential like p53 and p65.

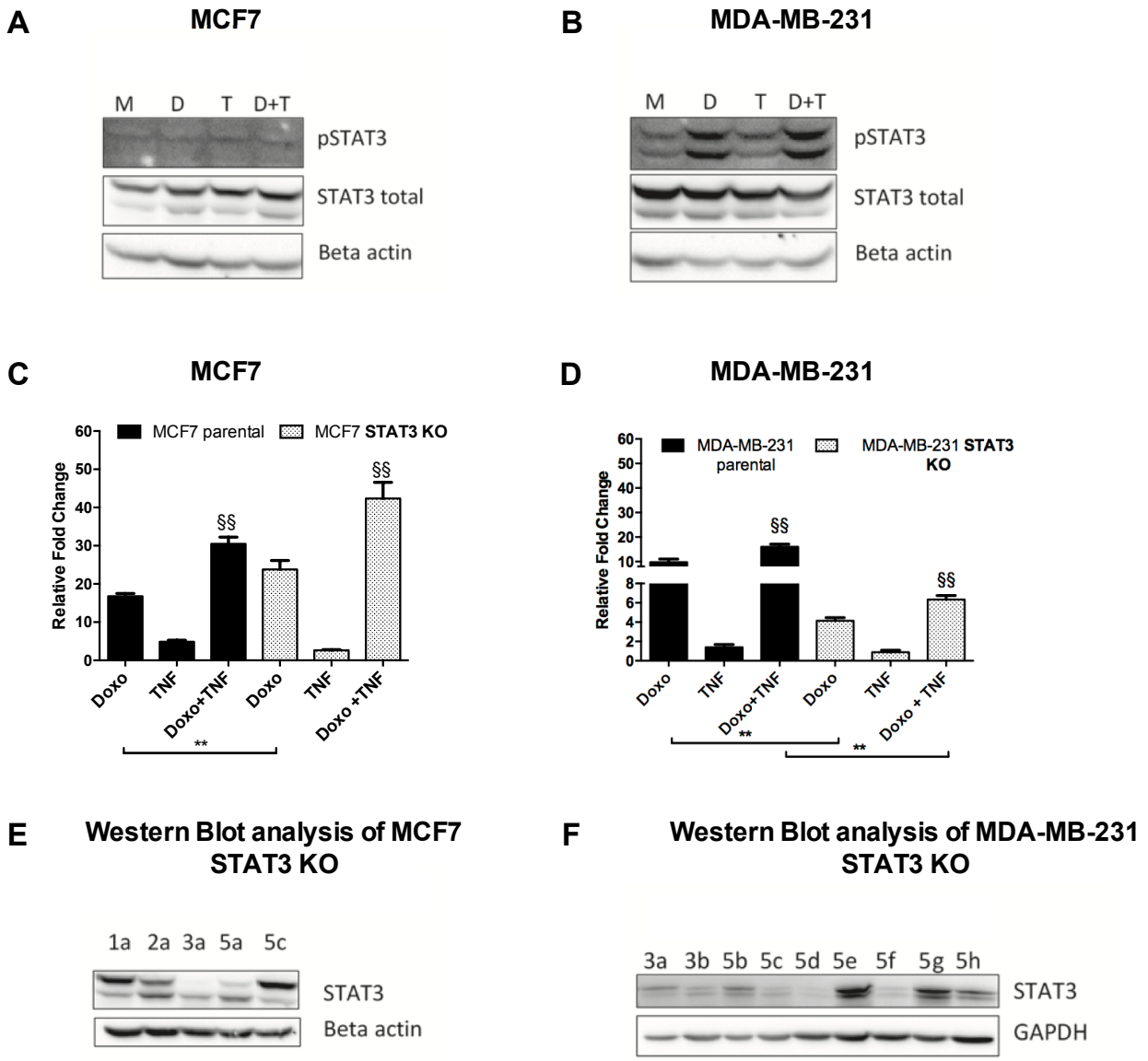

RESULTS-Figure 3: A) Western Blot analysis of STAT3 phosphorylation in MCF7 (A) and MDA-MB-231 cells (B) upon Doxorubicin, TNF-α and combined treatment. C-D) qPCR analysis of ETV7 activation upon Doxorubicin, TNF-α and combined treatment in parental or STAT3 KO MCF7 (C) or MDA-MB-231 cells (D). E-F) Western Blot analysis of CRISPR/Cas9 for STAT3 generated in MCF7 (E) and in MDA-MB-231 cells (F); respectively clone 3a for MCF7 cells and clone 5d for MDA-MB-231 cells have been selected for following experiments. ** indicates P-value (T-test) < 0.01; § indicates synergistic activation (sum of each treatment activation was statistically lower then the combined treatment activation, §§ p value (T-test) < 0.01).

5.4 ETV7 transcriptional activation is determined by an increase in H3K4me3

To investigate the epigenetic regulation of ETV7 transcription upon Doxorubicin and TNF-α, I performed a ChIP-qPCR analysis for three different histone marks of active transcription, one involving methylation of Histone 3 and the other the acetylation of Histone 4 (H3K4me3, H4PanAce, H4K16Ace). MCP-1 and p21 served as positive controls of activation. An increase in H3K4me3 upon Doxorubicin and TNF-α combined treatment, with respect to Mock

condition, was observable both in the region where p53 and p65 are binding (RE) and also in the region comprising the TATA box (TATA). Upon single treatment, an increase in H3K4me3 was observed only in the RE region (Fig. 4A). Acetylation of H4K16 didn't change upon the treatments, whereas Doxorubicin treatment was responsible for an enrichment in Histone 4 pan-acetylation at the ETV7 promoter (Fig. 4B).

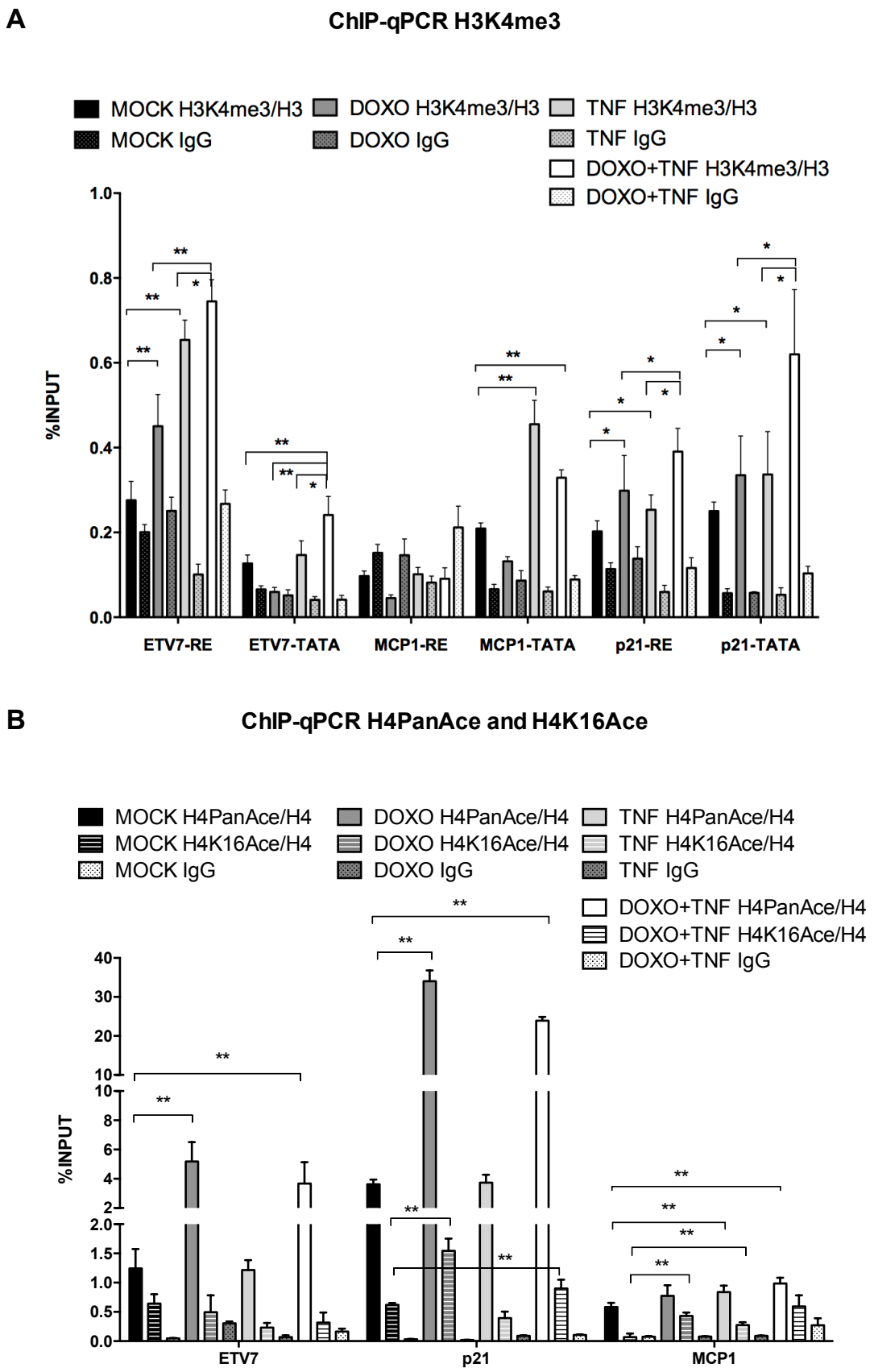

RESULTS-Figure 4: ChIP-PCR analysis for the occupancy of the transcriptional activation mark H3K4me3 (A) and H4 pan acetylation and H4K16ace (B) in MFC7 cells treated with Doxorubicin, TNF-α and combined treatment. IgG signal was a control for the specificity of the binding of H3K4me3 antibody, p21 and MCP1 served as a controls for activated genes upon the tested treatments. H3K4me3 is expressed as a ratio to total H3 signal and % of Input. * P-value(T-test) < 0.05; ** P-value(T-test) < 0.01.

5.5 ETV7 triggers breast cancer resistance to Doxorubicin

To test the possible role for ETV7 in improving cell survival upon Doxorubicin treatment and mediating a drug resistance phenotype, I generated a MDA-MB-231 cell line stably over-expressing ETV7. MDA-MB-231 cell line was chosen being representative for a triple negative and therefore more advanced breast cancer compared to MCF7, thus being a more suitable model for the clinical condition where chemotherapy with cytotoxic drugs is usually adopted. Furthermore, a higher ETV7 activation upon Doxorubicin prolonged treatment was observed in MDA-MB-231 cells with respect to MCF7 cells (Fig. 1K), thus suggesting a possible greater impact of ETV7 in drug resistance in this cell line. In addition, both p53 and p65 were reported to be responsible for ETV7 transcriptional activation upon Doxorubicin and TNF-α treatment, and in MDA-MB-231 cells both proteins are active even in basal conditions, being p53 kept stable in its mutant form and p65 fired by the presence of mutant p53. Therefore, I reasoned that MDA-MB-231 cell line itself could somehow recapitulate the Doxorubicin and TNF-α condition without the need of treatment. Lastly, given the observed massive mortality of cells upon ETV7 silencing (laboratory colleague's project) and the low protein levels of endogenous ETV7 , I was forced to use over-expression as a tool for studying ETV7-driven biological roles in breast cancer.

For the aforementioned reasons, I generated MDA- MB-231 cells stably over-expressing ETV7 and the respective empty control cells (Fig. 5B). I compared their survival upon 72 hours treatment with increasing concentration of Doxorubicin by MTT assay. ETV7 over-expressing cells were characterized by an increased survival at all tested doses (Fig. 5A). To determine if this better survival in ETV7 over-expressing cells could be linked to a different intra-cellular accumulation of drug, I decided to quantify the levels of Doxorubicin present inside the nuclei of the two cell lines. Notably, ETV7 over-expressing cells showed a decreased Doxorubicin accumulation inside nuclei with respect to cytoplasm, and the counted perinuclear area of Doxorubicin efflux was larger when compared with the empty counterpart (Fig. 5C and 5D). The observation of higher expression of the ABC transporter ABCB1 in MDA-MB-231-ETV7 cells may support the increased Doxorubicin efflux (Fig. 5E). To check whether ETV7-mediated resistance mechanism was also conserved in other types of cancer, I generated osteosarcoma U2OS cell line over-expressing ETV7 (Fig. 5G). One colleague demonstrated that also MCF7 cells over-expressing ETV7 better survived to Doxorubicin treatment (data submitted, see Annex 2.4). Similarly, U2OS over-expressing cells were more resistant to Doxorubicin treatment in comparison with their empty control (Fig. 5F), despite their

intrinsic higher sensitivity to Doxorubicin, thus suggesting that ETV7 could trigger Doxorubicin resistance in different types of cancer. Furthermore, U2OS cells over-expressing ETV7 showed a small increase in the expression of ABCB1, as seen in MDA-MB-231-ETV7 cells (Fig. 5H).

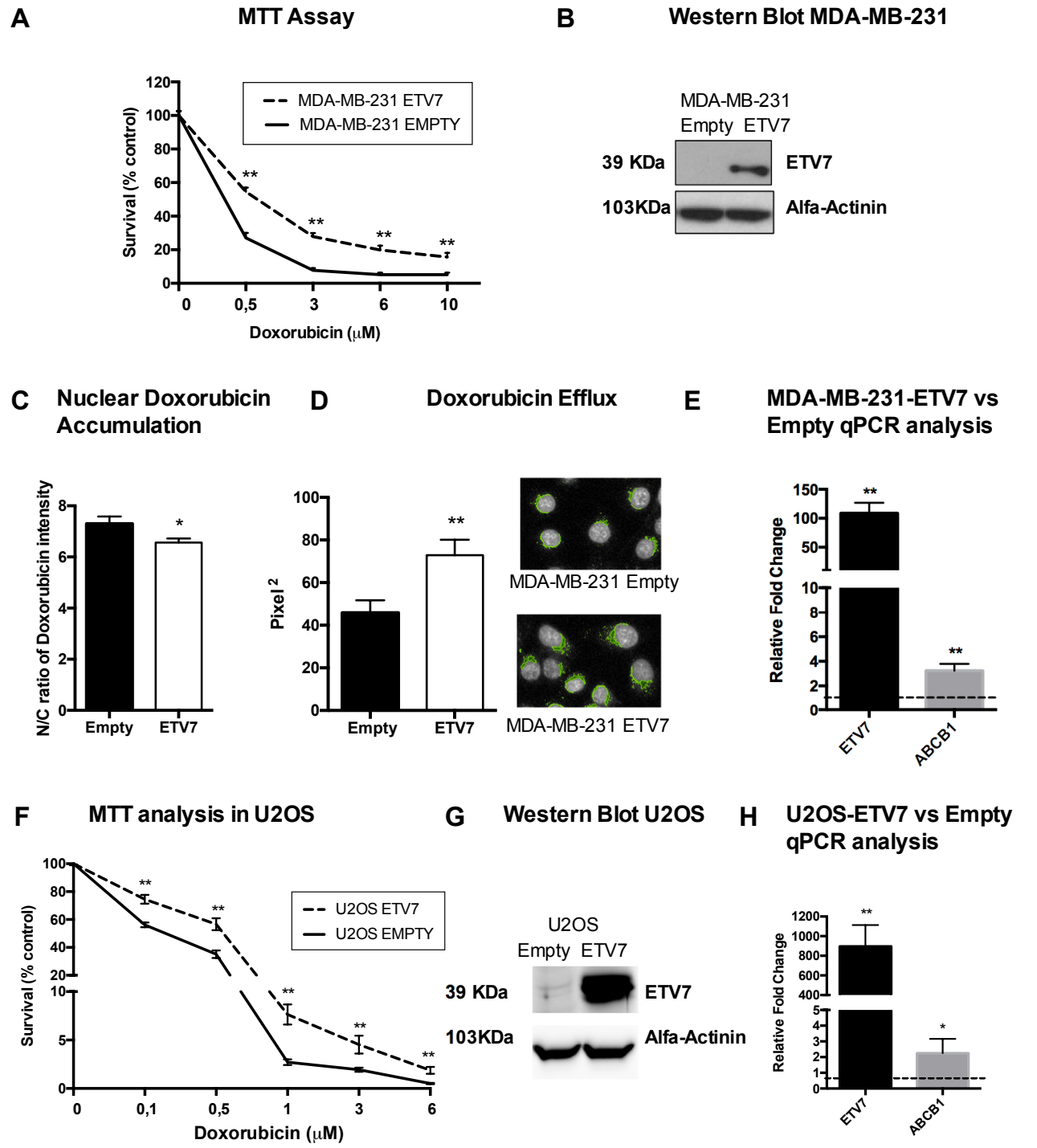

RESULTS-Figure 5: A) MTT assay for MDA-MB-231 cells over-expressing ETV7 and the empty control upon 72 hours of Doxorubicin treatment at increasing concentrations. B) Western Blot for checking the stable over-expression of ETV7 protein in MDA-MB-231 cells (20μg of total protein extract). C) Ratio of nuclear to cytoplasmic intensity of Doxorubicin (10μM, 3 hours treatment) in MDA-MB-231 cells over-expressing ETV7 compared with the empty control. D) Total cytoplasmic area of Doxorubicin efflux, represented as Pixel ^{2} (1 pixel in 20x WD is 0,5 μm). Pictures on the right show an example of Doxorubicin efflux observed at the Operetta Perkin

Elmer as green spots area. E) qPCR analysis of ETV7 over-expression and increase of ABCB1 expression in MDA-MB-231 cells over-expressing ETV7 compared with the empty control. F) MTT Assay for survival of ETV7 over-expressing U2OS cells upon Doxorubicin treatment (72 hours, increasing doses). G) Western Blot analysis of ETV7 over-expressing U2OS cells. H) qPCR analysis of ETV7 over-expression and increase of ABCB1 expression in U2OS cells over-expressing ETV7 compared with the empty control. * P-value(T-test) < 0.05; ** P-value(T-test) < 0.01.

5.6 DNAJC15 represents a good candidate for mediating ETV7-driven drug resistance

Given the relevant role observed for ETV7 in breast cancer drug resistance, I wanted to determine possible ETV7 targets playing key roles in mediating this ETV7-driven phenotype.
ETV7 is a transcriptional repressor, therefore when searching for putative ETV7 targets involved in the drug resistance phenotype, I considered a list of hypermethylated ,thus repressed genes, directly associated with drug resistance (Boettcher, Kischkel and Hoheise, 2010). I restricted the analysis to DNA methylation-type of regulation because it was recently highlighted as an important epigenetic hallmark for drug resistance, and found enriched for some ETS factors binding site (Hogart, Lichtenberg and Ajay, 2012; Strauss and Figg, 2016).
I then apply a filter for the search of putative ETV7 targets, by considering the expression of the reported genes in the microarray analysis performed in MCF7 cells upon Doxorubicin treatment available in the laboratory (Gene Expression Omnibus, GEO, accession number: GSE24065). Out of 6 genes , 3 were remarkably down-regulated (Fig. 6A). To further filter and confirm this data, I analyzed by qPCR the expression of these 3 genes upon Doxorubicin, TNF-α and the combined treatment (Fig. 6B). The only gene which was synergistically down-regulated by the combined treatment was DNAJC15 (Fig. 6B). Interestingly, DNAJC15 is a known negative modulator of ABCB1 expression by controlling c-Jun pathway (Hatle *et al.*, 2007), and thus could directly link the observed ABCB1 increased expression upon ETV7 over-expression. To further investigate ETV7 and DNAJC15 linkage, I analyzed by qPCR the DNAJC15 expression upon ETV7 activating stimuli in breast cancer cells and in lymphocytes (Fig. 6C-D-E). As expected, DNAJC15 repression was observed upon DNA damaging drugs in both MCF7 and MDA-MB-231 cells (Fig. 6C and 6D). Notably, similarly to ETV7 activation, Doxorubicin was the most effective drug in repressing DNAJC15 expression and this mechanism proved to be conserved also in normal cells, being down-regulated by DNA damaging and p53 activating drugs even in healthy donors-derived lymphocytes (Fig. 6E). By comparing ETV7 activation (Fig. 1C) and DNAJC15 repression in lymphocytes (Fig. 6E), a relevant inverse correlation was observable for some donors, such as the orange-depicted one in the case of Doxorubicin, 5-Fluorouracil and Nutlin-3a. Moreover, DNAJC15 repression was observed also upon prolonged exposure to Doxorubicin (14 days) in MCF7 and MDA-MB-231

cells, further supporting the promising involvement of DNAJC15 in breast cancer cells drug resistance (Fig. 6F).

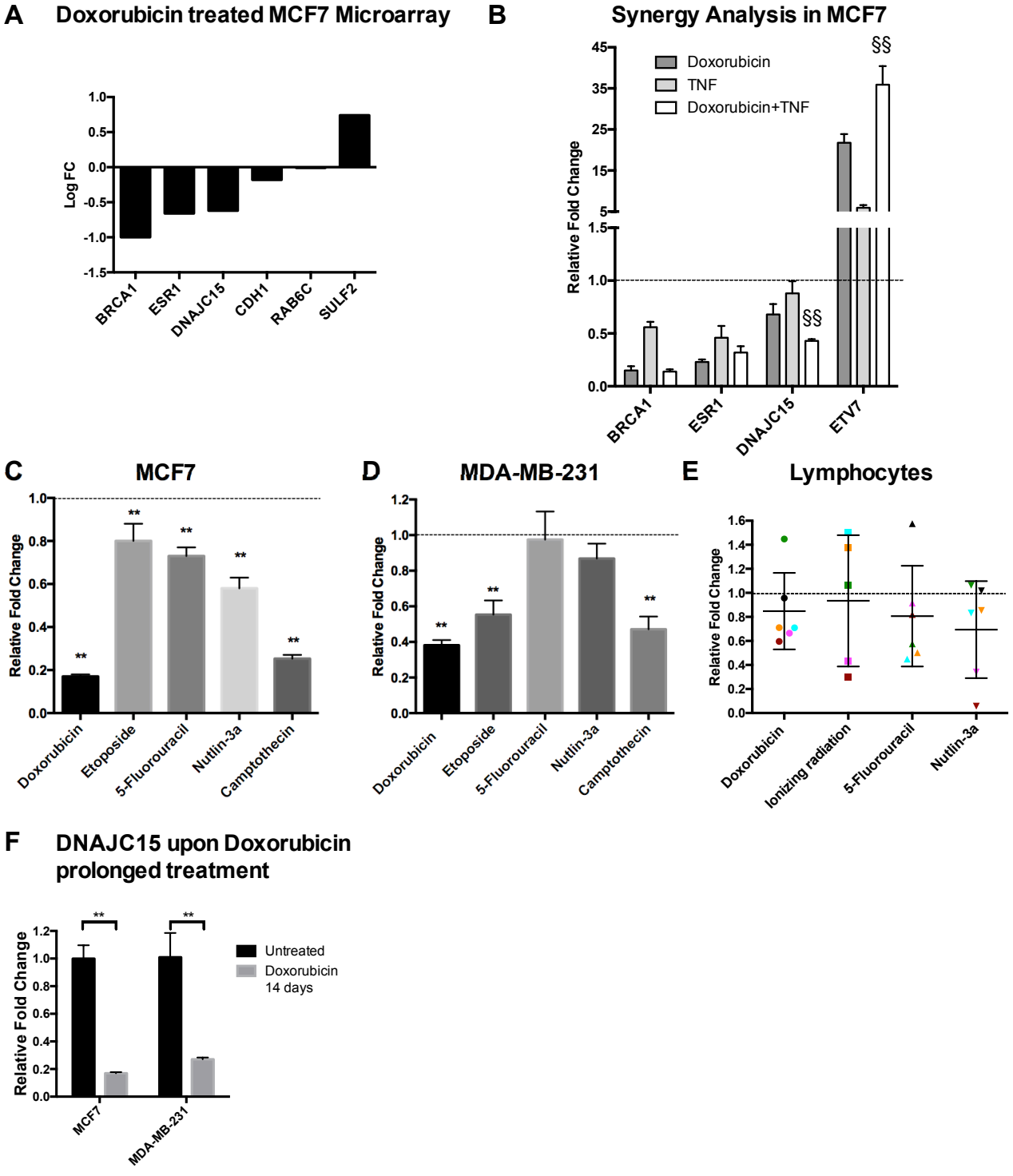

RESULTS-Figure 6 A) Expression microarray data of MCF7 cells treated with Doxorubicin for genes commonly found hypermethylated and repressed in drug resistant breast cancer. B) qPCR analysis for comparing repression of BRCA1, ESR1, DNAJC15 and activation of ETV7 upon Doxorubicin, TNF-α and combined treatment. § indicates synergistic activation (sum of each treatment activation is statistically lower then the combined treatment activation, §§ P-value T-test < 0.01). C-E) DNAJC15 repression upon different DNA damaging and p53 activating drugs in MCF7 (C), in MDA-MB-231 cells(D) and in healthy donor-derived lymphocytes (each color represents a different donor, the same used for ETV7 analysis) (E). F) DNAJC15 expression levels measured by

qPCR upon prolonged Doxorubicin treatment (14 days) in MCF7 cells (0,5μM Doxorubicin) and in MDA-MB-231 cells (0,8μM Doxorubicin). ** P-value T-test (treated versus untreated)< 0.01.

5.7 ETV7 can regulate DNAJC15 expression

To verify if DNAJC15 can be considered a direct ETV7 target, I checked DNAJC15 expression upon ETV7 transient transfection in MCF7 and in the generated ETV7 over-expressing MDA-MB-231 cells. DNAJC15 repression was observable upon both transient and stable overexpression of ETV7 (Fig. 7A and Fig. 7B). I then cloned an 800 bp portion of the DNAJC15 promoter region upstream the firefly luciferase reporter gene and monitored its expression upon ETV7 transient transfection. Using Gene Reporter Assays, the repression was observable as a decrease in Relative Light Units (RLU) in both MCF7 parental cells and also in the p53 deleted version (Fig. 7C); whereas in MDA-MB-231 cells the repression was observable only in the absence of mutant p53 (Fig. 7D). To specifically demonstrate the recruitment of ETV7 on the promoter of DNAJC15, I performed ChIP-qPCR Assays in MDA-MB-231 cells over-expressing ETV7. Experiments confirmed ETV7 occupancy on the DNAJC15 promoter, which consistently increased in the presence of Doxorubicin (Fig. 7E), an observation in line with the strongly increased amount of ETV7 protein in chromatin and nuclear fraction upon this treatment (Fig. 7F). Gene Reporter Assays also showed a significant decrease in basal RLU relative to MCF7 and MDA-MB-231 cells without p53 in comparison with the parental ones, thus suggesting that, probably, p53 may control DNAJC15 expression. To check if the decrease in DNAJC15 expression was not just linked to the procedures for the generation of this cell line, but directly dependent on the absence of p53, I transiently silenced p53 with oligonucleotides and checked DNAJC15 expression by qPCR in MDA-MB-231 cells (Fig. 7G). While effective in reducing the endogenous levels of p53, no statistically significant differences in the expression of DNAJC15 upon p53 silencing in the untreated condition were determined (Fig. 7G). Conversely, p53 silencing increased the DNAJC15 down-regulation potential upon Doxorubicin treatment. This could suggest that mutant p53-dependent control on DNAJC15 expression is more relevant upon Doxorubicin treatment rather than in basal conditions. To better investigate the role of p53 on the expression of DNAJC15, I also over-express transiently (48 hours) either the wild type p53 or two different type of mutant p53 (respectively, R282Q and G279E) in MDA-MB-231 p53 KO cells (Fig. 7H). There were no statistically relevant differences in DNAJC15 expression upon any type of the p53 over-expression, further supporting the conclusion that probably p53 alone without stimulation upon Doxorubicin is not able to influence DNAJC15 expression. Nevertheless, to better

understand the reasons why in MDA-MB-231 cells the promoter of DNAJC15 was not affected by ETV7 over-expression, I checked if p53 could bind nearby the ETV7 binding site within the DNAJC15 promoter, thus probably masking the binding site for ETV7 and impacting on its capability to bind to DNA. In fact, a half site consensus site for p53 was found nearby the ETV7 binding region (Fig. 7I). To verify this hypothesis, I performed a ChIP-qPCR by immunoprecipitating wild type p53 in MCF7 cells (Fig. 7J) and mutant p53 in MDA-MB-231 cells (Fig. 7L) and checking p53 occupancy in the same region where ETV7 is binding on the DNAJC15 promoter (Fig. 7I). In MCF7 cells wild type p53 was retrieved on the DNAJC15 promoter, which was decreased in presence of Doxorubicin (Fig. 7J), whereas mutant p53 was also able to bind to DNAJC15 promoter already in the untreated condition (even if at a lower extent), but its occupancy slightly increased upon Doxorubicin treatment (Fig. 7L). This binding ability of p53 suggests that probably in parental MDA-MB-231 cells ETV7 binding site within DNAJC15 promoter could be masked by mutant p53 or, alternatively, mutant p53 could possibly negatively interfere with the transcriptional function of ETV7. In fact, given the presence of high concentrations of reporter plasmid in the Gene Reporter Assays, the mutant p53-dependent negative effect on ETV7 repressive action can be more evident. The fact that wild type p53 binds, even with higher stronger potential compared with mutant p53, but in Gene Reporter Assays, doesn't inhibit ETV7 repressive action, could suggest that a possible direct or indirect link between ETV7 and p53 is more relevant in presence of mutant p53 rather than the wild type form. According to the hypothesis of a possible masking effect exerted by mutant p53, it can be that probably p53 could bind more tightly to the cloned promoter with respect to the endogenous DNAJC15 promoter, possibly due to different chromatin conformation or the presence of other transcription factors. Moreover, the putative binding of p65 to DNAJC15 promoter was also checked, to determine if wild type or mutant p53 and p65 eventually cooperate in controlling DNAJC15 expression (Fig.7K and 7M respectively). ChIP-qPCR assay showed that p65 can bind to the DNAJC15 promoter mainly in the mock condition and it is remarkably reduced (Fig. 7K, MCF7 cells) or abolished (Fig. 7M, MDA-MB-231) upon Doxorubicin treatment. This result can suggest that possibly p53 silencing alone was not sufficient to appreciate effects on DNAJC15 expression, because bound p65 could compensate the absence of p53, whereas upon Doxorubicin treatment being just p53 bound, p53 silencing resulted in a consistent down-regulation of DNAJC15 expression.

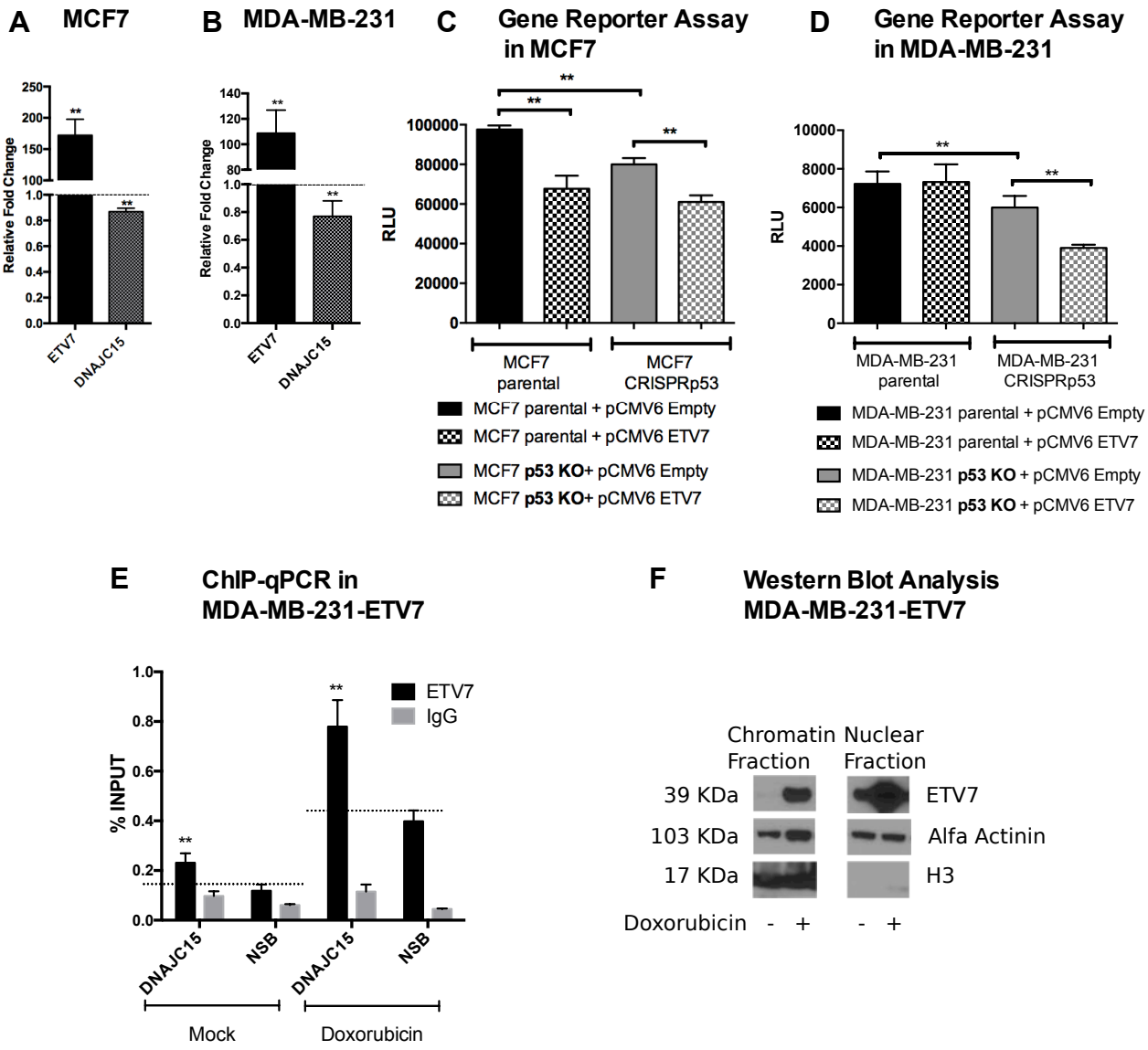
A MCF7
B MDA-MB-231
C Gene Reporter Assay in MCF7
D Gene Reporter Assay in MDA-MB-231
Relative Fold Change
RLU
ETV7
DNAJC15
MCF7 parental
MCF7 CRISPRp53
MDA-MB-231 parental
MDA-MB-231 CRISPRp53
MCF7 parental + pCMV6 Empty
MCF7 parental + pCMV6 ETV7
MCF7 p53 KO+ pCMV6 Empty
MCF7 p53 KO+ pCMV6 ETV7
MDA-MB-231 parental + pCMV6 Empty
MDA-MB-231 parental + pCMV6 ETV7
MDA-MB-231 p53 KO + pCMV6 Empty
MDA-MB-231 p53 KO + pCMV6 ETV7

E ChIP-qPCR in MDA-MB-231-ETV7
F Western Blot Analysis MDA-MB-231-ETV7
% INPUT
ETV7
IgG
DNAJC15
NSB
Mock
Doxorubicin
Chromatin Fraction
Nuclear Fraction
39 KDa
103 KDa
17 KDa
ETV7
Alfa Actinin
H3
Doxorubicin - + - +

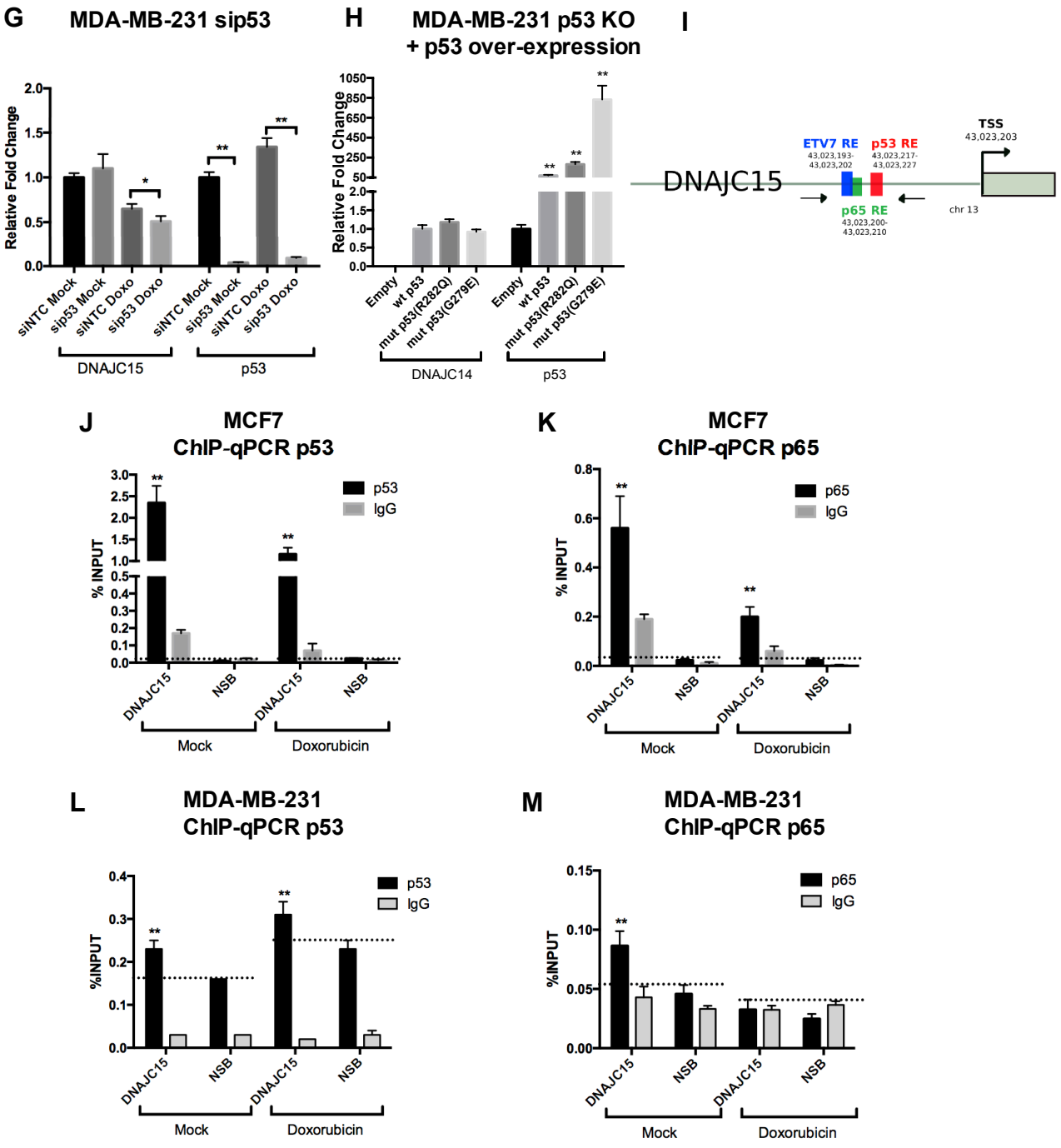

RESULTS-Figure 7: A-B) DNAJC15 repression upon transient ETV7 expression in MCF7 cells (A) and upon stable ETV7 expression in MDA-MB-231 cells (B). C-D) Gene Reporter Assay for ETV7 binding on DNAJC15 promoter reporter in parental or p53 KO MCF7 (C) or MDA-MB-231 cells (D). E) ChIP-qPCR for ETV7 occupancy on DNAJC15 promoter in MDA-MB-231 cells over-expressing ETV7 and treated with Doxorubicin. NSB is the non specific binding control (GTF2H5 was used). F) Western Blot analysis of chromatin and nuclear fraction of MDA-MB-231 cells over-expressing ETV7 upon Doxorubicin treatment. H3 was used as control for chromatin fractions. G) qPCR analysis for the measurement of DNAJC15 and p53 expression upon p53 silencing (25nM, 72 hours) and Doxorubicin treatment (1,5μM, 16 hours) in MDA-MB-231 cells. H) qPCR analysis for the measurement of DNAJC15 and p53 expression upon transient (48 hours) overexpression of p53 (wild type or mutant R282Q and G279E) in MDA-MB-231 p53 KO cells. I) Graphical representation of of the localization of predicted ETV7, p53 and p65 Response Elements (REs) and the TSS in the DNAJC15 promoter. Arrows indicate regions amplified by the primers used for the ChIP-qPCR assay. Localization is reported using the human UCSC GRCh38/hg38 as reference genome. J-M) ChIP-qPCR for mutant p53 occupancy (J,L) and p65 (K,M) on DNAJC15 promoter in MCF7 (J, K) and MDA-MB-231 cells(L,M) treated with Doxorubicin (1,5μM, 16 hours). NSB is the non

specific binding control (ACTB in MCF7 cells and GTF2H5 in MDA-MB-231 cells). * indicates a P-value(T-test) < 0.05 and ** a P-value(T-test) < 0.01.

5.8 ETV7 drug resistance phenotype can be rescued by DNAJC15 over-expression or flavonoids administration

To better check if DNAJC15 could really represent a key mediator in ETV7-driven resistance phenotype, I tried to rescue the resistant phenotype by performing an ectopic expression of DNAJC15 in the ETV7 over-expressing cell line and monitoring cell survival upon 72 hours Doxorubicin treatment. DNAJC15 over-expression revealed able to sensitize the ETV7 over-expressing cells to Doxorubicin (studied with two different concentrations) that was also associated with a down-regulation of ABCB1 expression (Fig. 8A and Fig. 8B). Furthermore, I wanted to analyze the clinical relevance of this novel ETV7-DNAJC15 circuitry in breast cancer patients using available expression data. In particular, the dataset GSE43502 gathered data similar to the *in vitro* condition studied, since Yu and co-workers collected expression data from recurrent or non-recurrent triple negative breast cancer patients after adjuvant chemotherapy (Yu *et al.*, 2013). ETV7 expression was increased in recurrent samples (P-value was not significant -0.08-, but a trend was clearly visible) while the expression of DNAJC15 was reduced in a statistically significant manner in the same patients (Fig. 8C). The online tool Kaplan Meier-plotter, allowing the analysis of the effects of different genes on breast cancer prognosis (Szász *et al.*, 2016), was interrogated for DNAJC15 expression in relation to relapse-free survival from breast cancer patients and showed a quite relevant Hazard Ratio of 0.73, supporting the association between its low expression and increased patients' susceptibility to cancer relapses (Fig. 8D). Given the relevance of the mechanism discovered, and the technical problems in the over-expression of a gene such as DNAJC15 for clinical applications, I decided to test if Quercetin was able to sensitize ETV7 over-expressing cells. The selection was motivated by the fact that it has been demonstrated that this flavonoid can increase Doxorubicin efficacy and reduce related cardiotoxicity in cancer patients. Interestingly, Quercetin can sensitize MDA-MB-231 over-expressing ETV7, and it is also able to repress ETV7 expression in MDA-MB-231 cells (Fig. 8E and Fig. 8F). This last observation was also evident from the treatment of MDA-MB-231 cells with another class of flavonoid, such as Genistein (Fig. 8F). Therefore, a combination of Doxorubicin with flavonoids could possibly improve treatment efficacy, by reducing associated ETV7 activation.

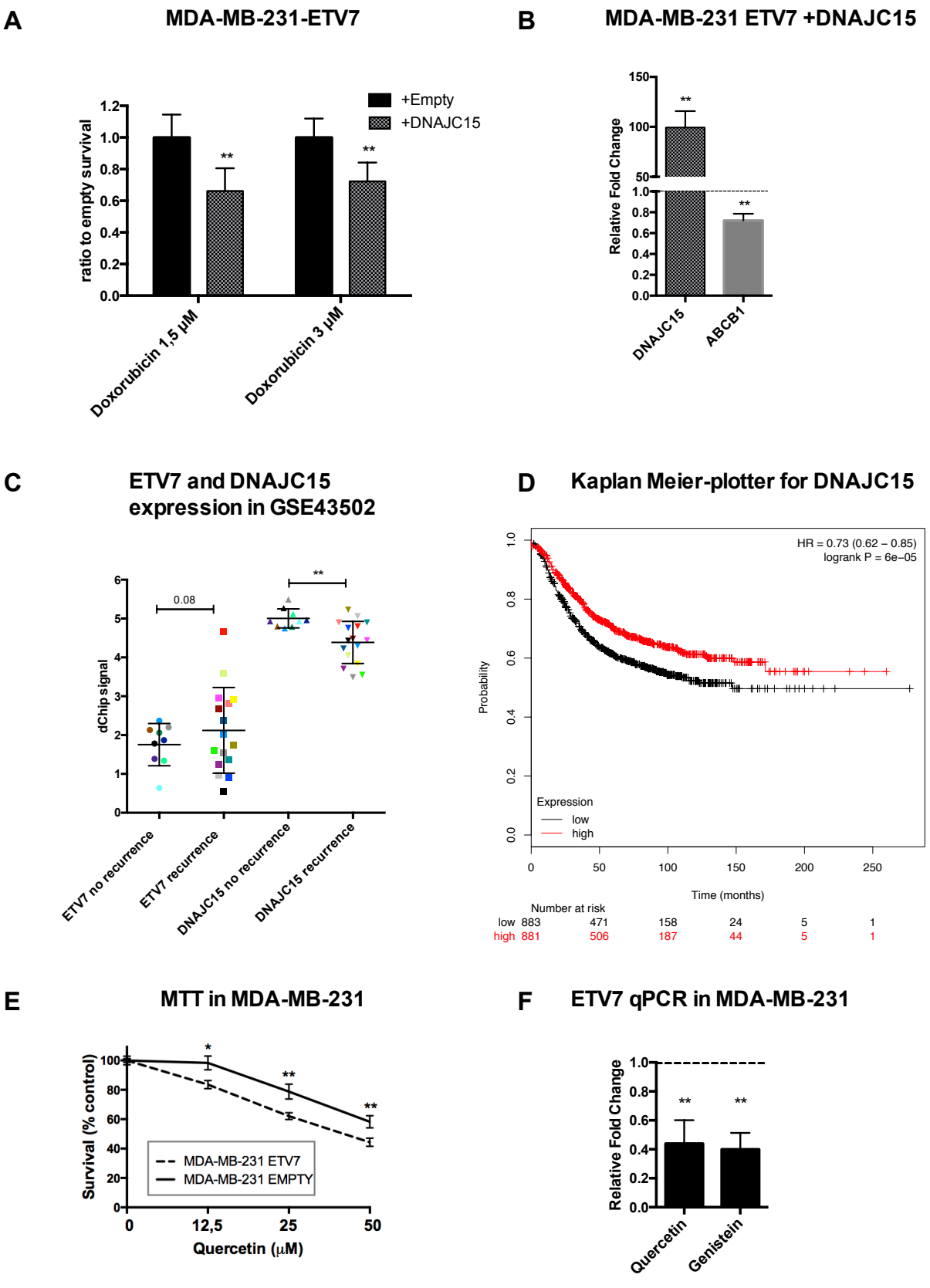

RESULTS-Figure 8: A) MTT Assay of MDA-MB-231 cells stably over-expressing ETV7 and transiently transfected with either DNAJC15 or Empty control. B) qPCR analysis for ABCB1 expression in MDA-MB-231 cells stably over-expressing ETV7 and transiently transfected with DNAJC15. C) ETV7 and DNAJC15 expression analysis in the dataset GSE43502, relative to recurrent or non-recurrent triple negative breast cancer patients after adjuvant chemotherapy (each color represents a different patient). D) Kaplan Meier-plotter analysis for DNAJC15 (probe 227808_at) expression in breast cancer patients and relapse free survival (RFS). E) MTT Assay for survival of

MDA-MB-231 cells stably over-expressing ETV7 and empty control, treated with Quercetin. F) qPCR analysis of ETV7 repression upon Quercetin and Genistein treatment in MDA-MB-231 cells. * P-value(T-test) < 0.05; ** P-value(T-test) < 0.01.

5.9 DNAJC family response to Doxorubicin and possible involvement of DNAJC14 in drug resistance

According to microarray data obtained by our group (GSE24065), Doxorubicin treatment in MCF7 cells can influence the expression of many DNAJC proteins, mainly in a repressive fashion (Fig. 9A). For this reason, I decided to investigate if other members of DNAJC family could be involved in drug resistance, given that many of them are poorly studied, especially in the cancer field. I analyzed the expression of the five highly repressed members by Doxorubicin treatment using the triple negative breast cancer dataset (GSE43502), and I found that only DNAJC14 was statistically down-regulated in recurrent triple negative breast cancers (Fig. 9B). Then, I checked DNAJC14 potential as predictive marker by Kaplan-Meier plotter, and observed a positive correlation between high expression and relapse-free survival, which motivated me in further exploring DNAJC14 role in breast cancer resistance and its possible link with ETV7 (Fig. 9C).

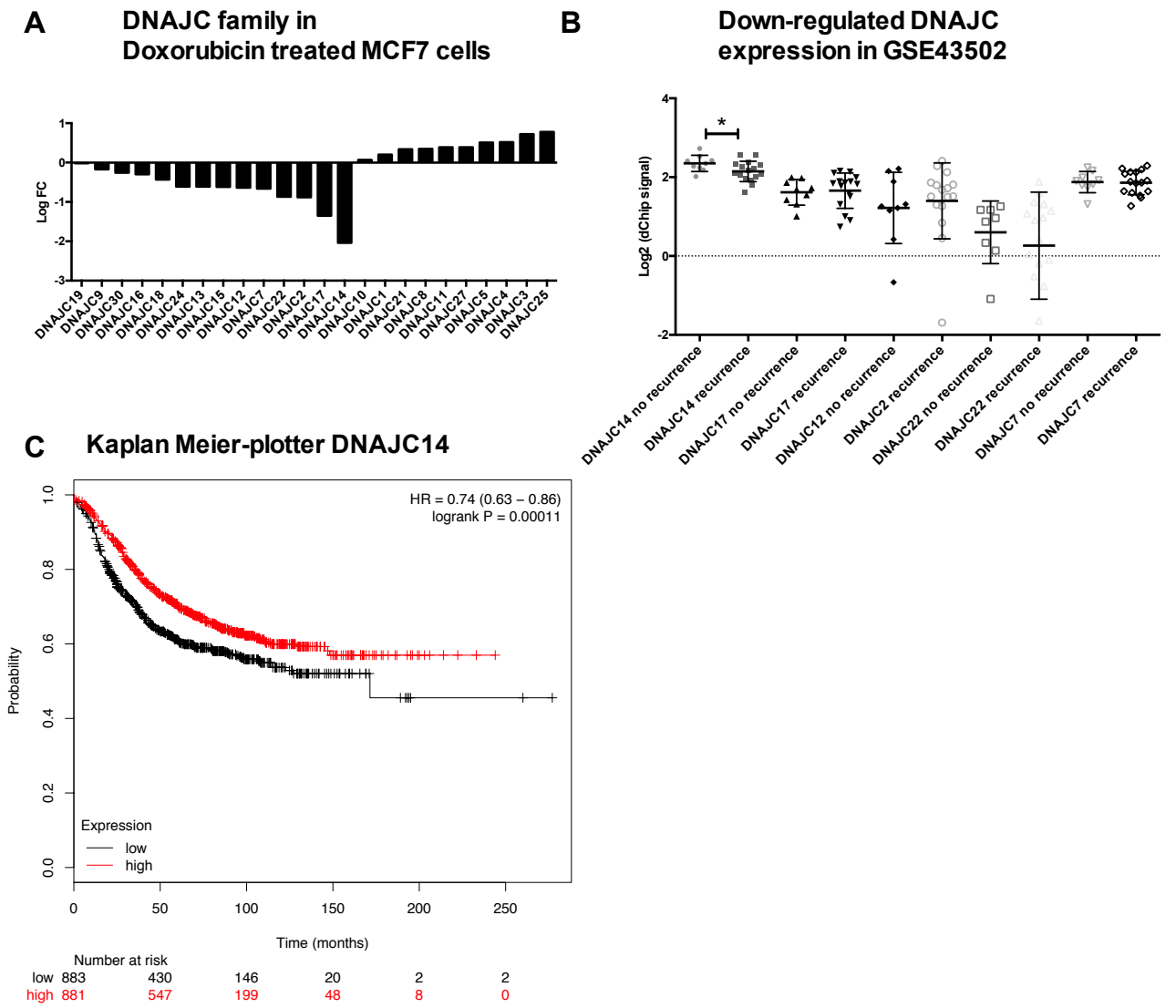

RESULTS-Figure 9: A) DNAJC family expression in microarrray data from MCF7 cells treated with Doxorubicin (GSE24065). B) Expression analysis of the highly down-regulated DNAJC genes upon Doxorubicin treatment in the dataset GSE43502 referred to breast cancer recurrence. C) Kaplan Meier-plotter analysis for relapse-free survival in breast cancer patients with high or low expression for DNAJC14. * indicates P-value (T -test)< 0.05.

5.10 DNAJC14 is a novel ETV7 target

Supported by the MCF7 microarray analysis reporting a strong repression of DNAJC14 upon Doxorubicin, I validated its transcriptional response to different DNA damaging drugs both in MCF7 and in MDA-MB-231 cells (Fig. 10A and Fig. 10B). DNAJC14 showed repression only upon Doxorubicin and 5-Fluorouracil in MCF7, and only upon Doxorubicin and Nutlin-3a in MDA-MB-231 cells. Doxorubicin was still representing the most effective drug in repressing DNAJC14, as was the case for DNAJC15, but prolonged Doxorubicin treatment was effectively repressing DNAJC14 only in MCF7 cells but not in MDA-MB-231 cells (Fig. 10D). DNAJC14 repression upon DNA damaging drugs was marginally recapitulated in lymphocytes (Fig.

10C). To determine if DNAJC14 expression could be controlled by ETV7, I performed ETV7 over-expression experiments in MCF7 cells (transient transfection) and quantified DNAJC14 expression by qPCR. Notably, ETV7 over-expression was associated with the repression of endogenous DNAJC14, supporting the hypothesis of DNAJC14 as an ETV7 target (Fig. 10G). Further determination of the role of ETV7 on DNAJC14 was performed by Gene Reporter Assay, which confirmed the ETV7-mediated repression of DNAJC14, both in MCF7 parental and MCF7 p53 KO cells, without any relevant difference between the two cell lines (Fig. 10E). Repression was observable also in MDA-MB-231 parental and p53 KO cells, with a statistically relevant reduction of the basal level of the reporter gene even upon the transfection of an empty vector in MDA-MB-231 p53 KO when compared to the parental MDA-MB-231 cells (Fig. 10F). To validate this observed effect of mutant p53 absence on DNAJC14 expression in MDA-MB-231 cells, I silenced p53 and checked how this could influence the expression levels of DNAJC14. Silencing of p53 alone resulted in a marked down-regulation of DNAJC14 expression, which was also increasing its Doxorubicin-mediated repression (Fig-10I). Conversely, neither wild type nor mutant p53 (R282Q and G279E) were able to shape DNAJC14 expression when simply over-expressed in MDA-MB-231 p53 KO cells, meaning that other transcription factors are needed for regulating its transcription (Fig. 10J). ChIP-qPCR experiments confirmed mutant p53 binding to DNAJC14 promoter in mock and more prominently in Doxorubicin-treated condition; in this particular case, the putative consensus p53 binding site is a full site (DNAJC15 promoter contains a p53 half site; Fig.10N). Also wild type p53 was able to be recruited on the DNAJC14 promoter in MCF7 cells both in mock and upon Doxorubicin treatment (Figure 10L). Given the possible cooperation between p53 and p65, I also checked p65 occupancy in DNAJC14 promoter in MCF7 and MDA-MB-231 cells (putative localization of p65,p53, and ETV7 response elements is reported in Figure 10K). In MCF7 cells, p65 was found in the DNAJC14 promoter in mock and upon Doxorubicin treatment (Fig. 10M), whereas in MDA-MB-231 cells p65 was not able to bind to DNAJC14 promoter (Fig. 10O). Therefore, the ETV7-mediated down-regulation of DNAJC14 seen in Gene Reporter Assays with MDA-MB-231 cells bearing mutant p53, can suggest that, probably, the presence of p65 on DNA can stabilize mutant p53 binding, especially when bound to an exogenous reporter plasmid. Moreover, to finally determine DNAJC14 as a direct target of ETV7, I performed ChIP-qPCR assays. ETV7 occupancy within the DNAJC14 promoter region was observed in mock condition and was further enhanced upon Doxorubicin treatment (Fig. 10H). Lastly, to understand if DNAJC14 repression was playing a role in ETV7-mediated chemoresistance, the sensitivity of MDA-MB-231 cells to increasing amount of

Doxorubicin and silencing of DNAJC14 with oligonucleotides (siRNA) was measured (Fig. 10P). Results provided conflicting data, since silencing was increasing breast cancer cells sensitivity to Doxorubicin at lower doses, and increasing resistance only at higher doses (Fig. 10P).

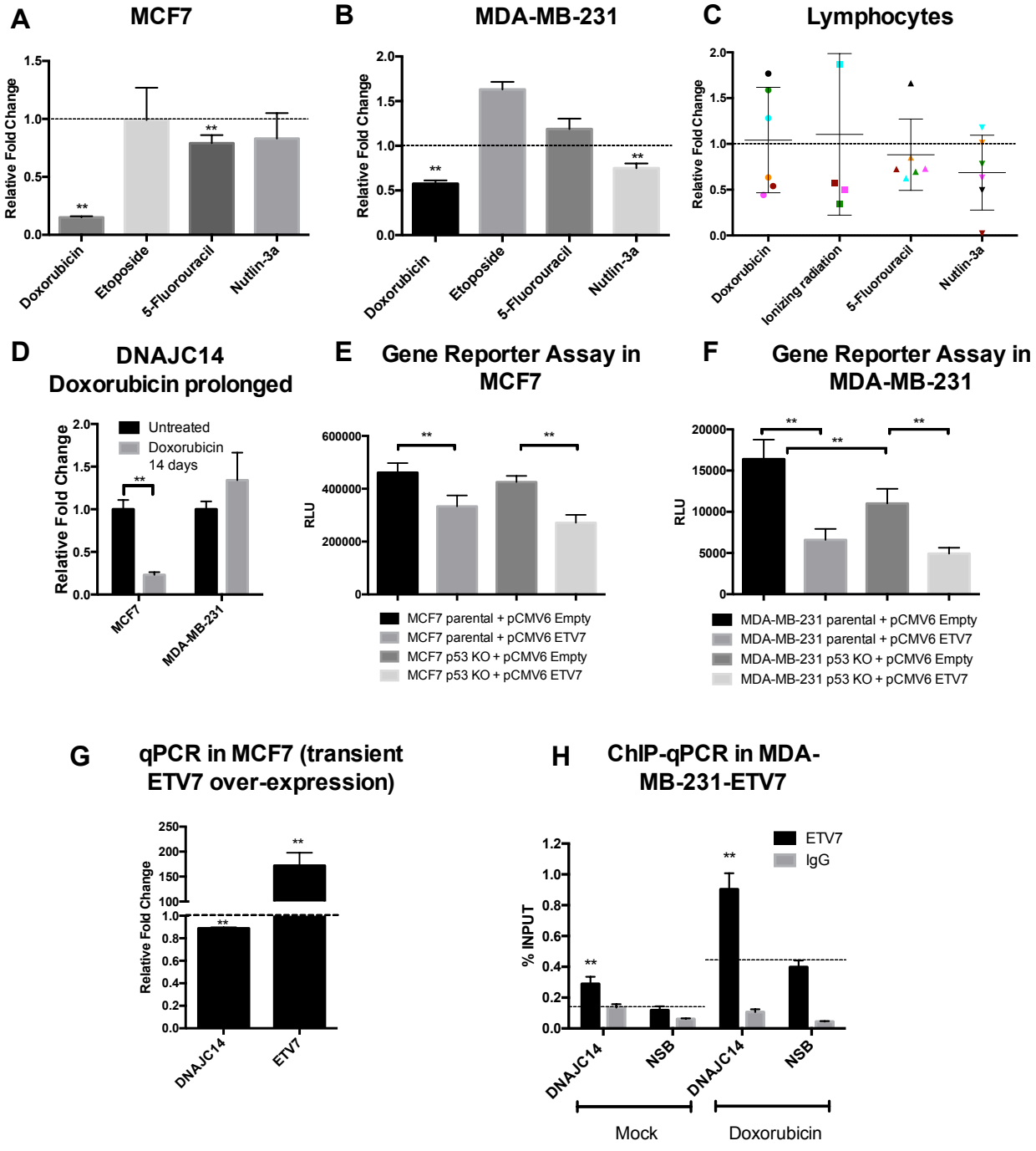

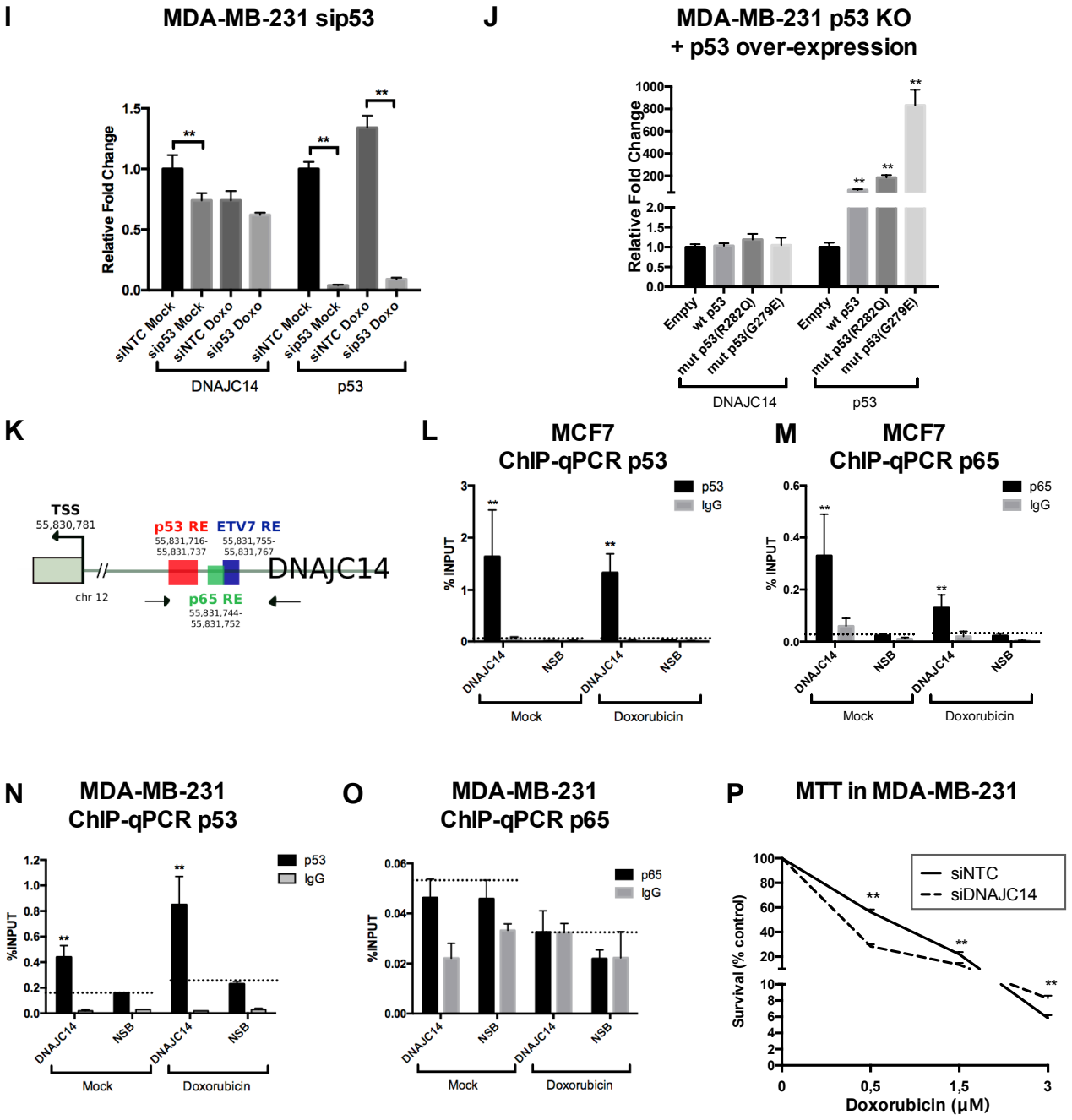

RESULTS-Figure 10: A-B-C) qPCR analysis of DNAJC14 expression upon different DNA damaging and p53 activating drug treatment in MCF7 (A), in MDA-MB-231 cells (B), and in healthy donors-derived lymphocytes (C, each color corresponds to a different patient). D) qPCR analysis of DNAJC14 expression upon prolonged (14 days) treatment in MCF7 and MDA-MB-231 cells. E-F) Gene Reporter Assay for DNAJC14 promoter upon ETV7 transient overexpression in parental or p53 KO MCF7 (E) and in MDA-MB-231 cells (F). G) qPCR analysis of DNAJC14 repression upon ETV7 transient expression in MCF7 cells. H) ChIP-qPCR for ETV7 occupancy on DNAJC14 promoter in MDA-MB-231 cells over-expressing ETV7, and treated with Doxorubicin. I) qPCR analysis for the measurement of DNAJC14 and p53 expression upon p53 silencing and Doxorubicin treatment (1,5µM, 16 hours) in MDA-MB-231 cells. J) qPCR analysis for the measurement of DNAJC14 and p53 expression upon wild type or mutant p53 over-expression (48 hours) in MDA-MB-231 KO cells. K) Graphical representation of of the localization of predicted ETV7, p53, and p65 Response Elements (REs) and the TSS in the DNAJC14 promoter. Arrows indicate regions amplified by the primers used for the ChIP-PCR assay. Localization is reported using the human UCSC GRCh38/hg38 as reference genome. L-N) ChIP-qPCR assay for wild type p53 (L) and mutant p53 (N) occupancy on the DNAJC14 promoter in MCF7 and MDA-MB-231 cells treated with Doxorubicin (1,5µM, 16 hours). M-O) ChIP-qPCR for p65 occupancy on the DNAJC14 promoter in MCF7 (M) and MDA-MB-231 cells (O) treated with Doxorubicin (1,5µM, 16 hours). P) MTT assay of MDA-MB-231 cells upon DNAJC14 silencing and Doxorubicin treatment of 72 hours. ** indicates P-value (T-test) < 0.01.

5.11 Doxorubicin and p53 might influence ETV7 protein stability

Given the findings obtained so far, I considered an ETV7 ChIP-seq experiment as next essential step to understand at a global scale which are the ETV7 targets and to try to identify a possible link between its activity as transcriptional repressor and its role in cancer cells drug resistance.

Therefore, in order to understand the optimal experimental conditions for ETV7 ChIP-seq analysis, I performed a chromatin and nuclear extraction in MDA-MB-231 parental and p53 KO cells both over-expressing ETV7, given the different responses observed in Gene Reporter Assays for DNAJC15 and DNAJC14. In particular, ETV7 expression in chromatin fraction was barely visible in MDA-MB-231 parental ETV7 over-expressing cells, whereas was already high in MDA-MB-231 p53 KO ETV7 over-expressing cells (Fig. 11A). In both cell lines, Doxorubicin treatment was increasing ETV7 expression in both the nuclear and chromatin fraction (Fig. 11A). To check if the different ETV7 expression in the absence of mutant p53 could be a consequence of the direct interaction of mutant p53 to ETV7, I performed a Co-IP experiment in MDA-MB-231 cells overexpressing ETV7, and I observed a weak interaction signal between mutant p53 and ETV7, which has to be better explored (Fig. 11B). Binding of mutant p53 to endogenous ETV7 was not possible to determine, since endogenous ETV7 protein levels are too low (Fig.11C). To further explore the possible role of mutant p53 on ETV7 protein stability, I transiently over-expressed two p53 mutants (respectively, R282Q and G279E) in MDA-MB-231 p53 KO cells and checked for ETV7 protein expression by Western Blot analyses (Fig. 11D). The over-expression of p53 was confirmed and interestingly, it appeared that both the p53 mutants tested were able to decrease protein levels of ETV7. This reduction in ETV7 signal was remarkably visible in the cytoplasmic extracts, but it was also evident in the nuclear ones. To better visualize this effect, I transiently over-expressed ETV7 in MDA-MB-231 cells, co-transfected along with the two p53 mutants and I checked the ETV7 expression by Western Blot (Fig. 11E). This analysis clearly showed how mutant p53 overexpression can decrease protein expression of ETV7 both at the cytoplasmic and at the nuclear level, thus confirming that the increased expression of ETV7 observed in nuclear and chromatin fractions in MDA-MB-231-ETV7 p53 KO cells are directly linked to the absence of p53, which possibly might influence ETV7 protein stability.

Bearing in mind that not always high protein levels are related to higher chromatin binding ability, I decided to include all these tested conditions in the ChIP-seq experiment. Given the redundant nature of ETS factors and the fact that their binding ability can change due to the presence of different cofactors, testing ETV7 binding in different contexts, could possibly lead to a more trustable *in vivo* consensus sequence.

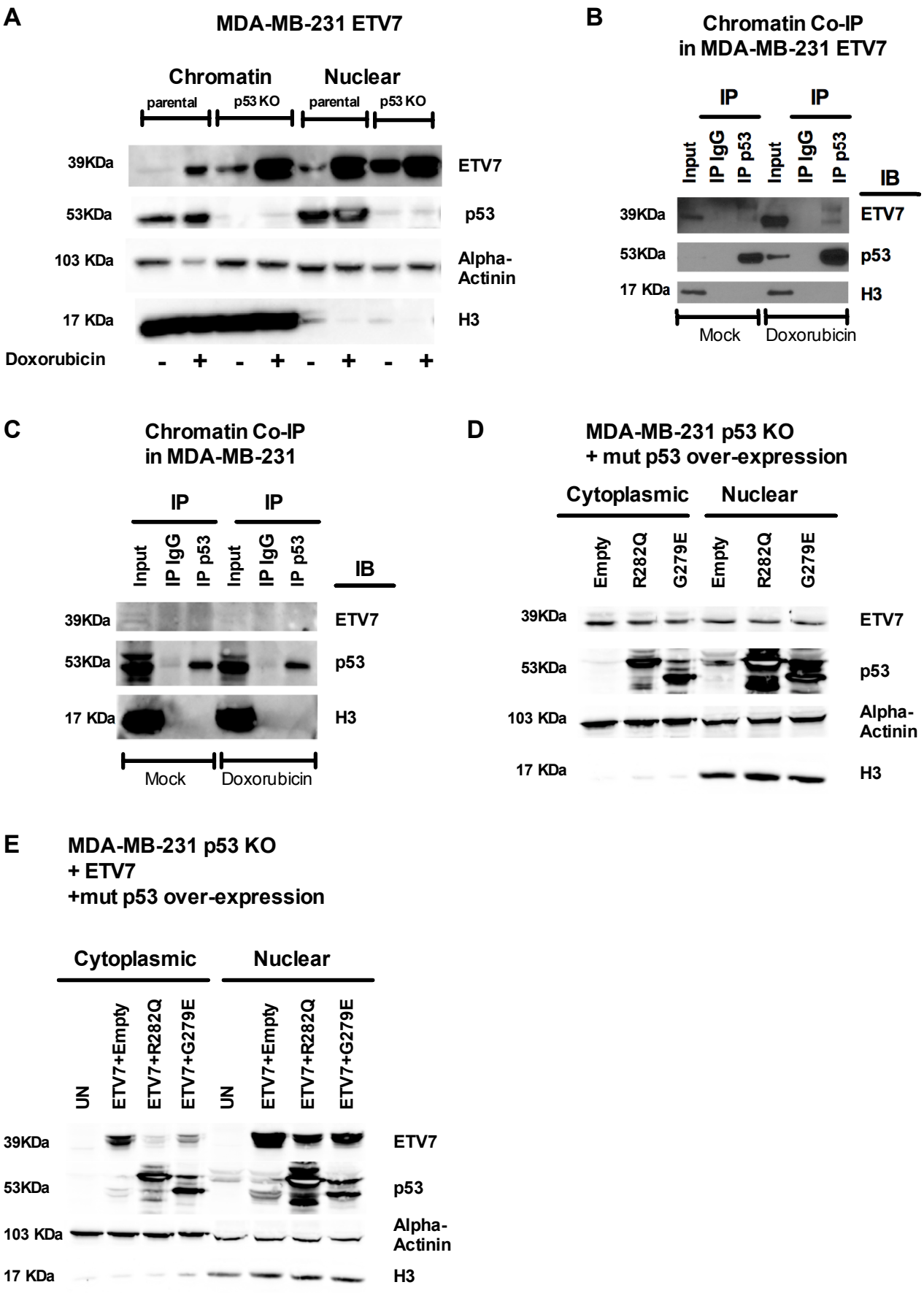

RESULTS-Figure 11: A) Western Blot analysis of chromatin and nuclear extracts of MDA-MB-231 cells over-expressing ETV7 and bearing mutant p53 or deleted for mutant p53 (p53 KO), and treated with Doxorubicin (1,5μM, 16 hours). B) Co-IP for studying the possible mutant p53 and ETV7 interactions by p53 immuno-

precipitation in MDA-MB-231 cells overexpressing ETV7 in mock and in Doxorubicin treated condition. C) Co-IP for studying the p53 and endogenous ETV7 putative interaction by p53 immuno-precipitation in MDA-MB-231 cells in mock and in Doxorubicin treated condition. D) Western Blot analysis of endogenous ETV7 protein expression upon mutant p53 transient overexpression (48 hours) in MDA-MB-231 p53 KO cells. E) Western Blot analysis of exogenous ETV7 protein expression upon transient transfection of ETV7 and mutant p53 in MDA-MB-231 p53 KO cells. Alpha actinin and H3 are used as respectively as controls for cytoplasmic and nuclear extracts. UN stands for the untransfected control.

5.12 ETV7 ChIP-seq analysis

The first ETV7 ChIP-seq experiment was performed using the best quality ChIP-grade antibody available in the market, which was validated in the laboratory like the one having the highest IP efficiency. MDA-MB-231 cells with or without p53 and over-expressing ETV7 were used since endogenous ETV7 protein level are not enough abundant to obtain a reasonable amount of material from immuno-precipitation with standard ChIP procedure to be used for the following NGS sequencing.

ETV7 ChIP-seq data that passed the quality control filters (Q20 filter, adapter trimming) and the de-duplication step were uniquely mapped and were in average 76.2% of the raw data (for each condition in average 4,937,893 reads). The average median length of fragments was 250 bases and SISSR peak calling method generated a very small number of peaks, especially for the MDA-MB-231 p53 KO cells treated with Doxorubicin (Fig. 12.1A). Overlap between peaks determined using IgG or Input as controls were highly similar, showing an average overlap higher than 80%, meaning that both can be used as good quality controls. Overlap between peaks found in different conditions was very low when compared to the p53 KO Doxorubicin condition, given the low number of peaks relative to this condition, but among all the other cases overlaps were of the order of 30% (Fig. 12.1B). Circos plots generated by Metascape (METASCAPE.ORG; Tripathi et al. 2015) graphically showed the overlap between targets found in different conditions and GO common to the targets highlighted in blue (Fig. 12.1C). Approximately more than half of the genes for each conditions are somehow connected and shared among conditions. In general, the presence of few overlapping genes among all different conditions underlines the importance of cofactors for ETV7 binding ability, and only two target genes were common in all four tested conditions: DPEP1 and MBOAT2.

A **Number of SISSR peaks and % overlap**

Query	vs IgG	vs Input	IgG to Input overlap	Input to IgG overlap
parental Mock	112	108	94,6%	98,1%
p53 KO Mock	107	72	58,9%	87,5%
parental Doxorubicin	104	101	93,5%	96,0%
p53 KO Doxorubicin	9	10	66,7%	60,0%

B **Overlap Peaksets Between Conditions**

vs IgG	Overlaps parental Mock	Overlaps p53 KO Mock	Overlaps parental Doxorubicin	Overlaps p53 KO Doxorubicin
parental Mock	self	33,0%	26,8%	1,8%
p53 KO Mock	33,6%	self	25,2%	2,8%
parental Doxorubicin	28,9%	26,0%	self	3,9%
p53 KO Doxorubicin	22,2%	33,3%	44,4%	self
vs Input	**Overlaps parental Mock**	**Overlaps p53 KO Mock**	**Overlaps parental Doxorubicin**	**Overlaps p53 KO Doxorubicin**
parental Mock	self	24,1%	26,9%	1,9%
p53 KO Mock	34,7%	self	31,9%	4,2%
parental Doxorubicin	28,7%	22,8%	self	3,0%
p53 KO Doxorubicin	20,0%	30,0%	30,0%	self

C **Metascape Gene overlap analysis**

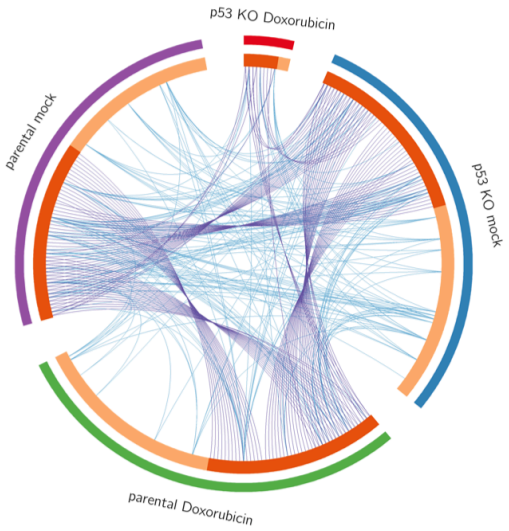

RESULTS-Figure 12.1: A-B) Tables reporting numbers of peaks and overlap across the different tested conditions by ETV7 ChIP-seq. C) Circos Plot obtained by Metascape analysis; purple lines are connecting shared genes across conditions and blue lines are connecting genes sharing similar gene ontologies. Red and Orange circle segments helps in visualizing shared genes across conditions.

To obtain information relative to the ETV7 *in vivo* consensus sequence, ChIP-seq data were subjected to HOMER analysis for unknown motifs, successfully obtaining a logo consistent with the *in vitro* data (with the exception of the base 5' to the GGAA core) (Fig. 12.2A).

Then, HOMER analysis was re-analyzed in relation to known motifs. The first 9 known motifs bound by ETV7 appeared to be the consensus sequences for other ETS factors, which confirmed the characteristic redundancy of ETS family binding to DNA (Fig. 12.2A). Motif of ETV6, the closest ETS member to ETV7, is unfortunately not present in the HOMER software and therefore, it is not listed.

In order to obtain information relative to the enrichment of ETV7 targets across the different tested conditions, I performed an enrichment analysis with the Metascape tool

METASCAPE.ORG (Tripathi *et al.*, 2015). Given the very small number of peaks relative to p53 KO Doxorubicin, this condition is not reported in the heatmap relative to the enrichment analysis by Metascape (Fig. 12.2B). The remaining 3 conditions showed all enrichment for Chagas disease, a tropical parasitic disease which in some cases can also lead to heart damage. They also all showed enrichment in processes relative to development, such as animal organ morphogenesis and cellular component biogenesis. An interesting enrichment especially in relation to cancer biology is represented by the regulation of the endopeptidase activity involved in apoptotic process, that could possibly mediate additional oncogenic properties of ETV7. In untreated/mock conditions either having or not mutant p53, ETV7 targets were enriched for other biological processes important for cancer progression and dissemination, such as migration (possible ETV7 control on migration is reported in Annex 1.1) , cell junction assembly, extracellular matrix organization, and TGF-β signaling. Other processes were enriched only in presence of mutant p53; specifically, the response to gamma radiation and the negative regulation of the immune system process, thus suggesting that the binding of ETV7 to these genes could be possibly directly or indirectly influenced by mutant p53. Conversely, other pathways were enriched only in absence of mutant p53, such as the TNF signaling. Doxorucibin treatment seems to influence ETV7 binding in terms of enrichment relative to ETV7 targets (as expected from the analysis in Western blot, where a stronger signal within chromatin enriched fraction was obtained; Fig. 11A), showing the biggest enrichment for embryonic pattern specification, in line with previous finding relative to inhibitory function of ETV7 in differentiation.

I then extended the enrichment analysis to the Enrichr tool considering ETV7 targets common in at least two conditions (http://amp.pharm.mssm.edu/Enrichr/)(Chen et al. 2013; Kuleshov et al. 2016 and Fig. 12.2C). The most enriched KEGG pathway and GO biological process was the TGF-β signaling, which was also present in the Metascape enrichment analysis together with Chagas disease. Other enriched pathways found were referring to pathogen response and respiratory burst, which are suggesting a role for ETV7 in shaping inflammatory response. In order to gain insights on possible ETV7 cofactors or transcription factors cooperating or counteracting the ETV7 transcriptional activity, I performed an enrichment analysis for transcription factors with reported ChIP-seq binding ability in the ETV7 targets (unfortunately p53 data are still not present in the ChIP-seq data considered by the tool). Among the enriched transcription factors, CTBP2 and SIN3A are both transcriptional repressors and have already been reported as interactors of ETV6, the closest ETS member to ETV7 (Wang and Hiebert, 2001; Roukens *et al.*, 2010). For this reason, they might represent

good putative ETV7 interactors, favoring the ETV7-mediated transcriptional repression. EGR1, PML, NR3C1, TEAD4 are all associated with tumor suppressive functions, thus probably they are mediating an increase in transcription of the ETV7 targets, acting in an opposite way, probably by recruiting EP300 (found as second most enriched transcription factor). Given that most of them are positive regulators of differentiation, this confirms again the reported role of ETV7 as negative regulators of cell differentiation (Carella *et al.*, 2006). CEBPB is more involved in inflammatory response, thus probably counteracting the negative action of ETV7 on inflammatory genes.

The diseases prevalently associated to ETV7 targets include anemia, in line with the ETV7 reported role in red blood cell development (Quintana *et al.*, 2014) and the Charcot-Marie-Tooth disease, an incurable genetic inheritable neuropathy.

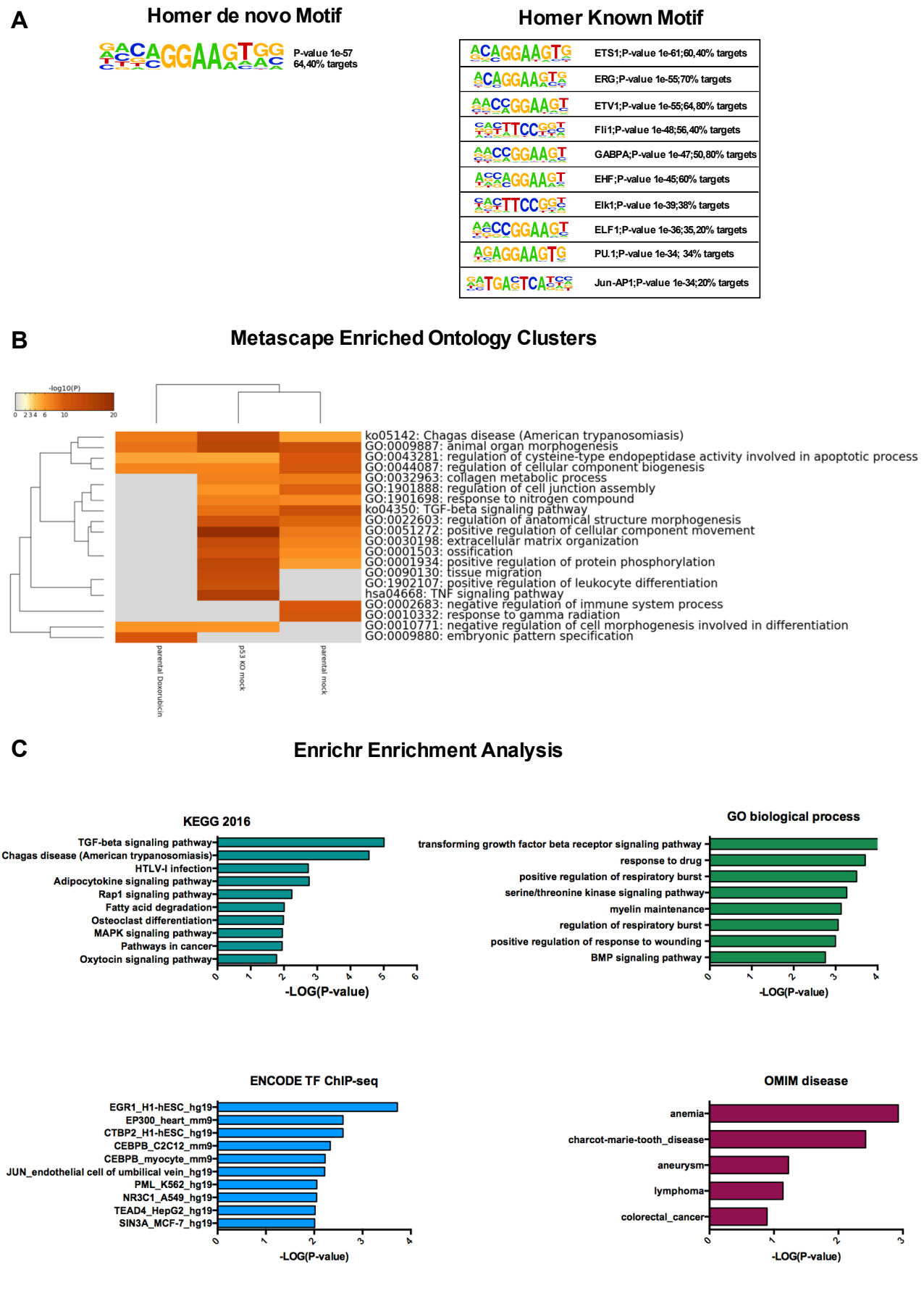

RESULTS-Figure 12.2: A) *in vivo* ETV7 consensus sequences calculated with Homer unknown Motif analysis performed on ETV7 ChIP-seq (left logo) and with Homer Analysis for known motifs (right logo) with indicated P-values and percentage of targets. B) Enrichment analysis performed with Metascape online tool and relative to

enriched ontology clusters specific to each ChIP-seq condition tested. C) Enrichment analysis performed with the Enrichr software on ETV7 ChIP-seq found targets, and relative to pathways, biological processes, transcription factors, and diseases. Reported P-values are referring to the enrichment statistical analysis performed by the two softwares, for which a detailed information is provided on the relative websites.

Furthermore, Metascape was interrogated to understand if localization of ETV7 binding sites was linked to different groups of genes belonging to similar ontologies. Figure 12.3 A reports the relative distribution of ETV7 peaks localization, showing a majority of binding peaks in the intragenic region and a relative small number of peaks within the promoter regions. Interestingly, Metascape analysis (Fig. 12.3B) showed that ETV7 binding regions relative to promoters were enriched in genes related to the interferon response, which is one of the most recognized processes in literature as activator of ETV7 (Park *et al.*, 2013; Rempel *et al.*, 2013; Contreras *et al.*, 2015; Ignatius Irudayam *et al.*, 2015). Conversely, ETV7 peaks present in intra- or inter-genic regions, were more enriched in cancer related processes, such as cell growth, apoptosis, and cell-substrate adhesion and, interestingly, TGF-β signaling enrichment was restricted to intergenic regions (Fig. 12.3B). ENCODE visualization of the ETV7 peak region relative to binding to DPEP1 in parental untreated cells is reported in Figure 12.3C. The calculated SISSR peak length is around 350 bp, but the actual peak length appears larger, thus possibly supporting the reported DNA binding of ETV7 in form of oligomer (Kar and Gutierrez-Hartmann, 2013; Selvaraj, Kedage and Hollenhorst, 2015).

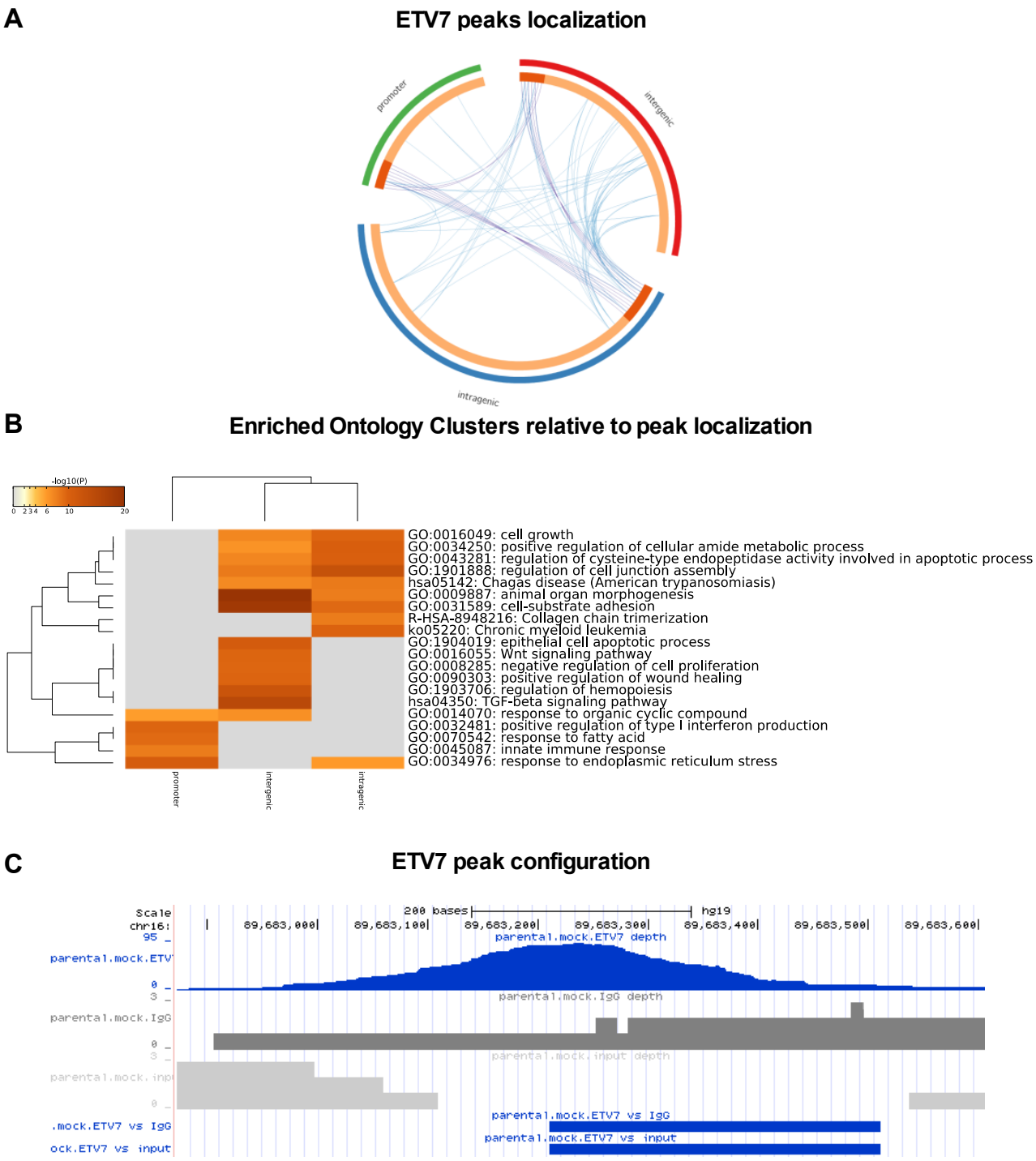

RESULTS-Figure12.3: A) Circos plot for genomic localization of ETV7 binding regions found by ChIP-seq analysis. B) Enriched ontology clusters relative to the genomic localization of ETV7 binding site (found by Metascape analysis). C) Configuration of the peak region (DPEP1) for ETV7 enrichment, visualized in the ENCODE genome browser (using UCSC hg19 as reference genome).

5.13 ETV7 can regulate the TGF-β pathway

Since TGF-β pathway was found among the enriched pathways relative to ETV7 targets both by Metascape and Enrichr analysis, some ETV7 targets involved in this signaling (SKI, SMAD6,

ID1 and FKBP1A) were validated by qPCR in ETV7 over-expressing cells (Fig. 13A). All these genes are negative regulators of TGF-β-mediated response, at different levels, meaning that a repression of these genes mediated by ETV7 could possibly lead to a constitutive TGF-β pathway activation. All tested genes were repressed in MDA-MB-231-ETV7 cells, except for SKI, whose expression was only slightly decreasing but did not reach statistical significance. ChIP-qPCR analysis in MDA-MB-231-ETV7 cells confirmed ETV7 occupancy in all these genes with an enrichment pattern reflecting the qPCR repression data (Fig. 13B). To assess the possible predictive prognostic value for these TGF-β pathway-related genes in breast cancer (SKI, SMAD6, ID1, FKBP1A: it will be called ETV7/TGF-β signature), Kaplan Meier-plotter relative to relapse-free survival (RFS) was exploited, and a modest correlation between low gene expression of the ETV7/TGF-β signature and worse prognosis in breast cancer patients was observable (Fig. 13C). GOBO online tool was also interrogated to check gene expression association with outcome for this group of genes, specifically relative to RFS (co.bmc.lu.se/gobo) (Ringnér *et al.*, 2011). Differently from Kaplan-Meier plotter, GOBO Hazard Ratio graph stratifies the expression data into three quantiles based on the expression levels of the interrogated genes, which are respectively depicted i) with a grey line for the low expression quantile, ii) with a red line for the intermediate and iii) with a light blue line for the high expression quantile. Furthermore, GOBO tool also allows a multivariate analysis using lymph node status, cancer size, ER status, histological grade and patients' age as covariates and RFS as endopoint. GOBO results, reported in Figure 13 D, confirmed the Kaplan Meier-plotter analysis, showing a correlation between low expression of the ETV7/TGF-β signature and worse prognosis relative to all breast cancer types. Moreover, multivariate analysis showed a relevant correlation between expression of these genes and both the tumor size and the lymph node status of patients (Fig. 13E). Specifically, low gene expression of the ETV7/TGF-β signature was mostly found in breast cancer with an average size larger than 20 mm and in lymph node-positive patients. The subgroup, where this signature can best predict patients' outcome, is represented by the ER positive and lymph node negative one, that i salso the largest group analyzed (Fig. 13F).

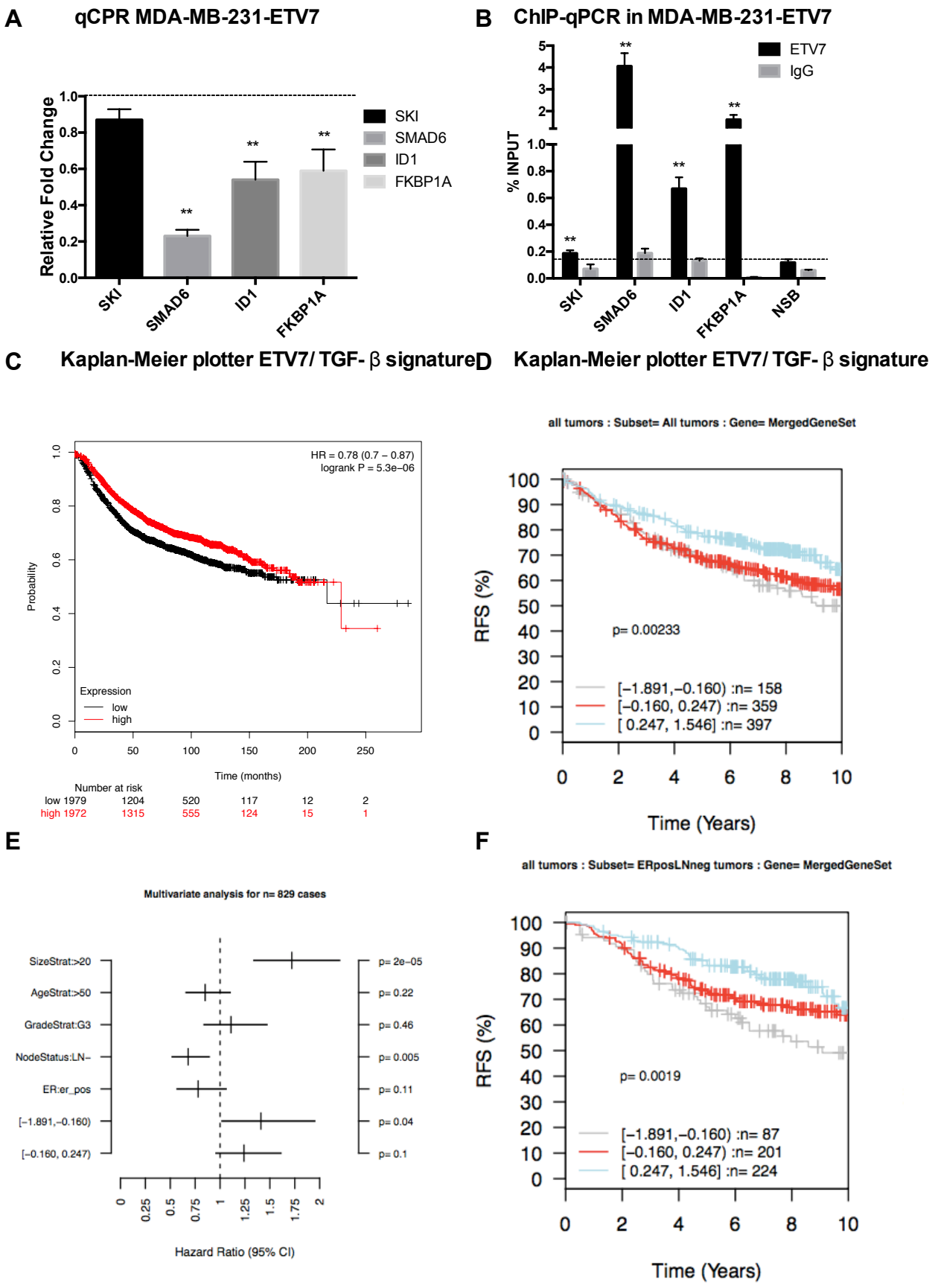

RESULTS-Figure 13: A) qPCR analysis of TGF-β signaling genes (found in ETV7 ChIP-seq) in MDA-MB-231 cells over-expressing ETV7. B) Validation of ETV7 binding to TGF-β signaling genes by ChIP-qPCR analysis in MDA-MB-231-ETV7 cells. NSB is the control for non specific binding of the ETV7 antibody (in this case GTF2H5 was used). C) Kaplan Meier-plotter analysis for the ETV7/ TGF-β signature (SKI, SMAD6, ID1, FKBP1A) and breast

cancer patients' outcome. Numbers below the x axis represent the number of patients analyzed at each time interval (50, 100, 150, 200, 250 months) during the follow-up study. HR stands for Hazard Ratio, a value above zero indicates a worse prognosis associated to high gene expression, whereas a value below zero indicates a worse prognosis associated to low gene expression. D) GOBO analysis for Relapse-Free survival in breast cancer patients and associated expression of the ETV7/ TGF-β signature. E) Multivariate analysis for the ETV7/ TGF-β signature and reported features, performed by GOBO analysis. F) Kaplan-Meier plot obtained by GOBO analysis of the ETV7/ TGF-β signature for the ER positive and lymph node negative patients subset. In Kaplan-Meier plots calculated by GOBO tool (D and F) above the x axis is reported the interval of each expression quantile and relative number of patients analysed. Grey line refers to the low expression quantile, red to the intermediate and light blue line to the high expression quantile. ** indicates P-value (T-test) <0.01

5.14 Novel ETV7 targets can predict breast cancer patients relapse-free survival

The ETV7 targets common to at least two conditions of ChIP-seq were interrogated in Kaplan Meier-plotter relative to breast cancer patients. Seventy-seven percent of the genes had a Hazard Ratio below zero, meaning that an increased expression of most of the ETV7 target genes was associated with a better prognosis in terms of relapse-free survival. Nine ETV7 target genes were showing a striking association with patients prognosis, with a Hazard Ratio less than 0.7 and an associated constistent statistically significant P-Value for the log rank test. Figure 14A reports these 9 ETV7 targets gene with predictive value in breast cancer patients. This ETV7-target signature of 9 genes (named as 9-gene signature) proved to be very effective in predicting patients' outcome when combined, reaching a Hazard Ratio of 0.48, meaning that the relapse-free time almost doubled in presence of high expression of these genes (Fig. 14B). Similarly to the ETV7/TGF-β signature, also this 9-gene signature showed a strong association between gene expression and both tumor size and lymph node status, and the subset where it best performed in terms of outcome prediction was the ER positive and lymphonode negative patients' one.

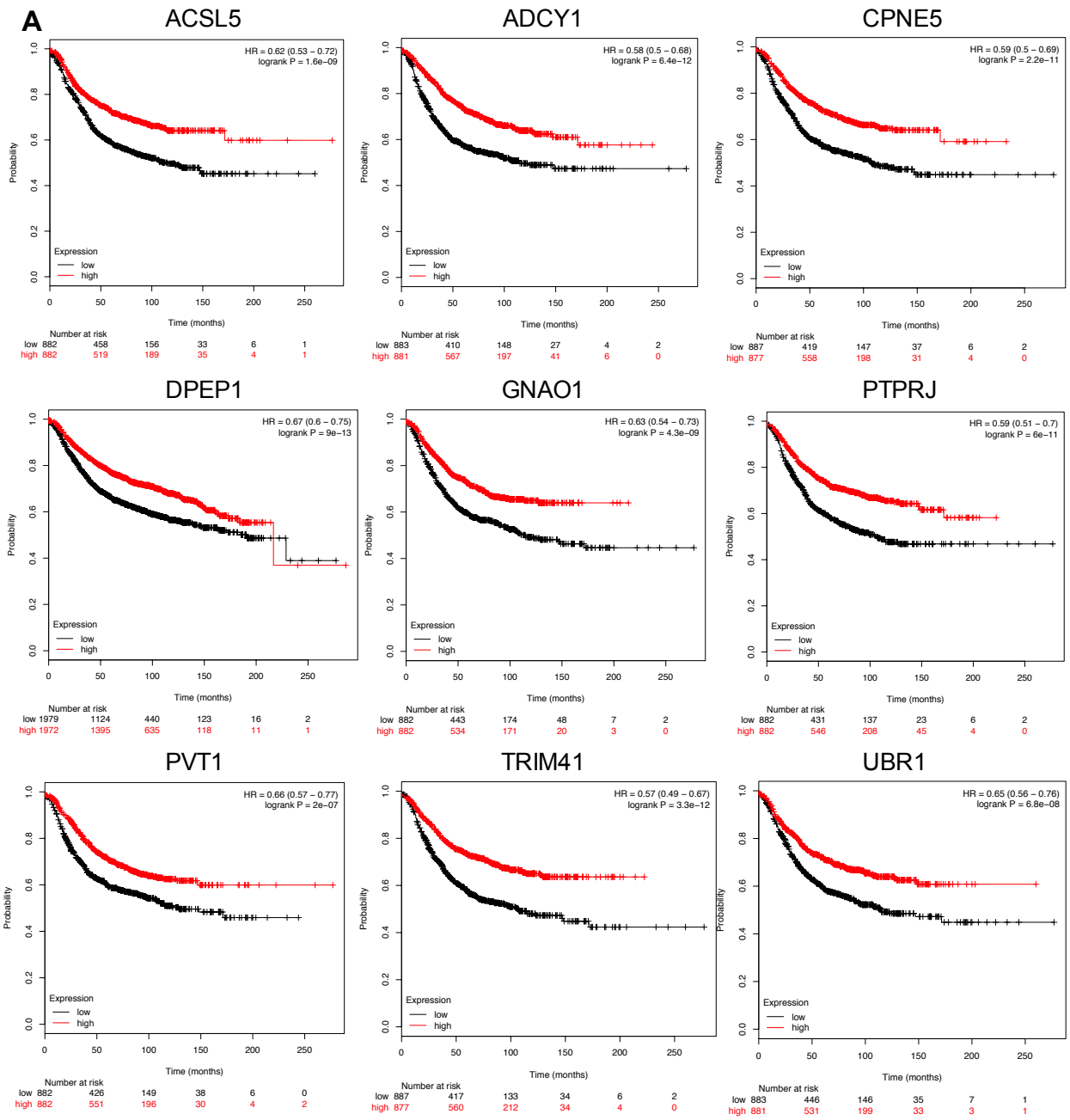
A
ACSL5
HR = 0.62 (0.53 – 0.72)
logrank P = 1.6e−09
Probability
Expression
low
high
Time (months)
Number at risk
low 882 458 156 33 6 1
high 882 519 189 35 4 1
ADCY1
HR = 0.58 (0.5 – 0.68)
logrank P = 6.4e−12
Probability
Expression
low
high
Time (months)
Number at risk
low 883 410 148 27 4 2
high 881 567 197 41 6 0
CPNE5
HR = 0.59 (0.5 – 0.69)
logrank P = 2.2e−11
Probability
Expression
low
high
Time (months)
Number at risk
low 887 419 147 37 6 2
high 877 558 198 31 4 0
DPEP1
HR = 0.67 (0.6 – 0.75)
logrank P = 9e−13
Probability
Expression
low
high
Time (months)
Number at risk
low 1979 1124 440 123 16 2
high 1972 1395 635 118 11 1
GNAO1
HR = 0.63 (0.54 – 0.73)
logrank P = 4.3e−09
Probability
Expression
low
high
Time (months)
Number at risk
low 882 443 174 48 7 2
high 882 534 171 20 3 0
PTPRJ
HR = 0.59 (0.51 – 0.7)
logrank P = 6e−11
Probability
Expression
low
high
Time (months)
Number at risk
low 882 431 137 23 6 2
high 882 546 208 45 4 0
PVT1
HR = 0.66 (0.57 – 0.77)
logrank P = 2e−07
Probability
Expression
low
high
Time (months)
Number at risk
low 882 426 149 38 6 0
high 882 551 196 30 4 2
TRIM41
HR = 0.57 (0.49 – 0.67)
logrank P = 3.3e−12
Probability
Expression
low
high
Time (months)
Number at risk
low 887 417 133 34 6 2
high 877 560 212 34 4 0
UBR1
HR = 0.65 (0.56 – 0.76)
logrank P = 6.8e−08
Probability
Expression
low
high
Time (months)
Number at risk
low 883 446 146 35 7 1
high 881 531 199 33 3 1

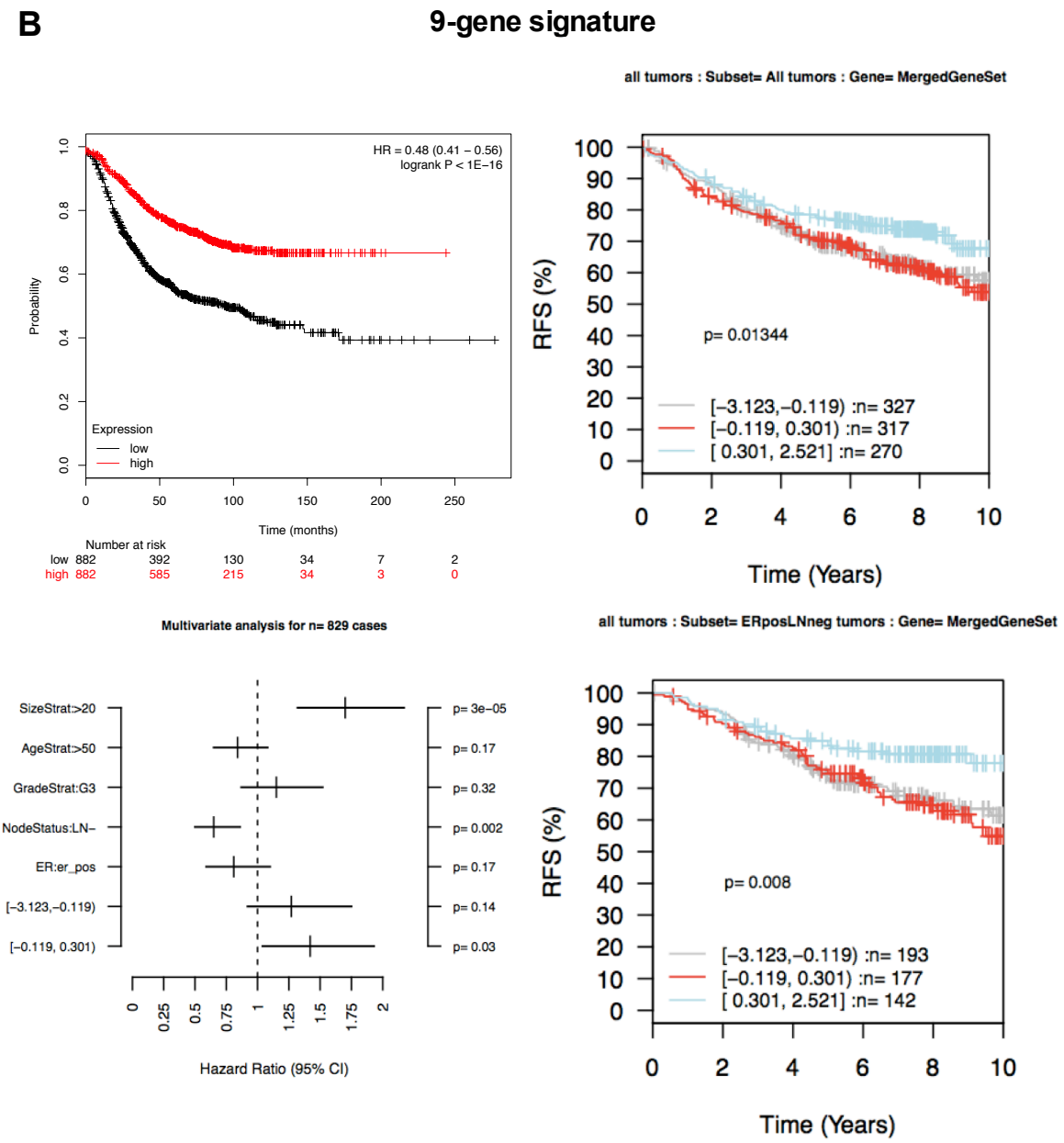

RESULTS-Figure 14: A) Kaplan Meier-plotter analysis for relapse-free surival in breast cancer patients expressing high or low levels of the novel ETV7 targets found by ChIP-seq. Numbers below the x axis represent the number of patients analyzed at each time interval (50, 100, 150, 200, 250 months) during the follow-up study. HR stands for Hazard Ratio; a value above zero indicates a worse prognosis associated to high gene expression, whereas a value below zero indicates a worse prognosis associated to low gene expression. B) Kaplan Meier-plotter and GOBO analyses for relapse-free survival in breast cancer patients expressing high or low levels of the 9 genes in average (9-gene signature). In Kaplan-Meier plots calculated by GOBO tool (on the right) the interval of each expression quantile and relative number of patients analysed is reported above the x axis. Grey line refers to the low expression quantile, red to the intermediate and light blue line to the high expression quantile.

5.15 DPEP1 and DPYD are novel ETV7 targets involved in drug resistance, also to 5-Fluorouracil

Upregulation of ABCB1 suggests that ETV7 is mediating a multi-drug resistant phenotype, but to better validate this hypothesis I decided to check ETV7 over-expressing cells survival to 5-Fluorouracil, a drug whose resistance has not been associated to ABCB1 but to different multi-drug tranporters (Pan *et al.*, 2016). Another reason, why I selected 5-Fluorouracil, is the fact that it is commonly used in combination with Doxorubicin and Cyclophosphamide for the treatment of advanced breast cancer, in the so-called FAC regimen (F = 5-Fluorouracil; A = Doxorubicin, also known as Adriamycin; C = Cyclophosphamide). Therefore, I performed MTT assay treating with increasing concentrations of 5-Fluorouracil (72 hours treatment) in both control and ETV7-overexpressing MDA-MB-231 cells (Fig. 15A). ETV7-mediated resistance was confirmed also for 5-Fluorouracil, underlying the importance of ETV7 in shaping the response to FAC therapy (Fig. 15A). Furthermore, ETV7-mediated resistance to 5-Fluorouracil was observable also in the osteosarcoma cell line U2OS over-expressing ETV7 (Fig. 15B). To widen the search for putative ETV7 targets involved in drug resistance to both Doxorubicin and 5-Fluorouracil, I took adavantage of the ChIP-seq results to search for known genes whose repression associates to drug resistance.

Among the 9 gene-signature, DPEP1 was the only one found in all tested ChIP-seq conditions, suggesting an important role of the regulation of this gene by ETV7. Furthermore, this gene is already known to exert relevant function in the drug response. For this reason, I decided to determine DPEP1 expression upon ETV7 over-expression in MDA-MB-231 cells, which showed a relevant repression of DPEP1 in comparison with the control cells (Fig. 15C). Then, to validate DPEP1 as a direct target of ETV7, I performed ChIP-qPCR assays in MDA-MB-231-ETV7 cells and validate ETV7 occupancy on the DPEP1 promoter (Fig. 15D). I then continue the research for putative targets by performing a comparative analysis between ETV7 ChIP-seq data and published microarray analysis in ETV7 over-expressing Lin- cells (Carella *et al.*, 2006). In both experiments I found DPYD, a gene involved in the 5-Fluorouracil catabolism. To validate the regulation of this gene mediated by ETV7, I measured by qPCR analysis the expression of DPYD in ETV7 over-expressing cells (Fig. 15C) and by ChIP-qPCR the binding of ETV7 to DPYD enhancer region (Fig. 15D). The DPYD repression upon ETV7 over-expression and ETV7 binding to DPYD enhancer, defined DPYD as a novel ETV7 direct target, critically important for 5-Fluorouracil-related cellular response and toxicity (Gross *et al.*, 2008; Deng *et al.*, 2014; Wu *et al.*, 2016). Once added to the 9-gene signature found by ChIP-seq, the newly validated DNAJC15 and DPYD genes were able to enhance the predictive power of the gene

signature, making it to reach the Hazard Ratio of 0.42 according to Kaplan Meier-plotter results (11-gene signature, Fig. 15E). Predictive power was confirmed also by GOBO analysis, and particularly relative to cancer size and lymph node status, and particularly in the subset of ER positive breast cancers.

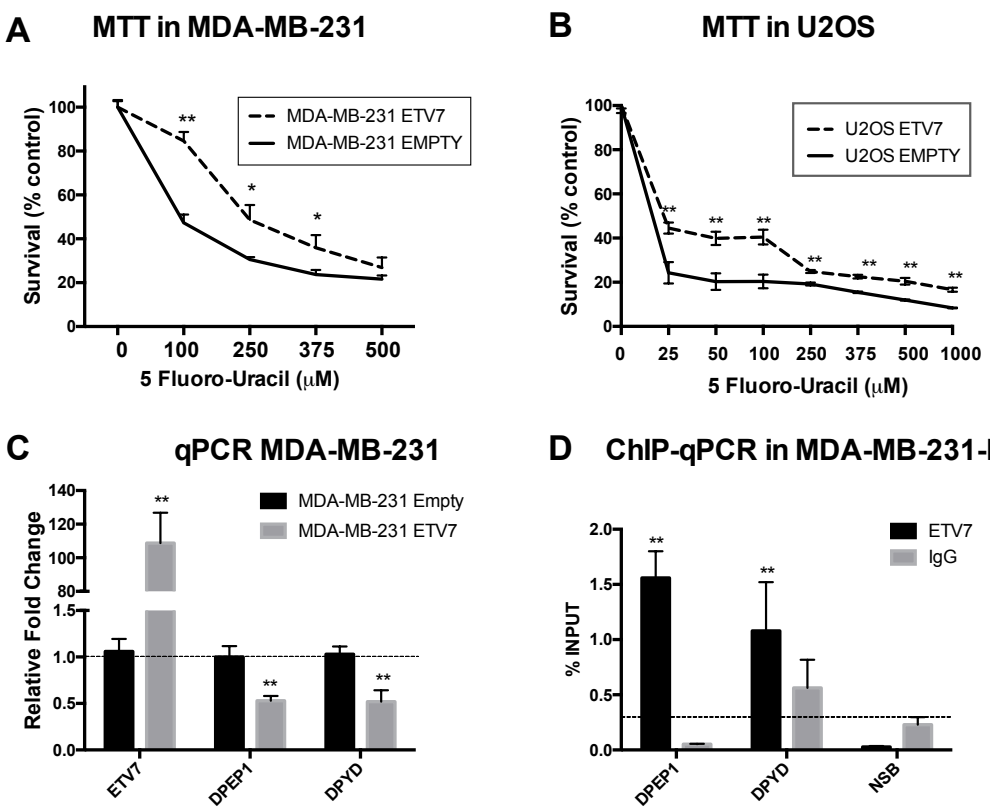
A
MTT in MDA-MB-231
Survival (% control)
MDA-MB-231 ETV7
MDA-MB-231 EMPTY
5 Fluoro-Uracil (μM)
B
MTT in U2OS
Survival (% control)
U2OS ETV7
U2OS EMPTY
5 Fluoro-Uracil (μM)
C
qPCR MDA-MB-231
Relative Fold Change
MDA-MB-231 Empty
MDA-MB-231 ETV7
ETV7
DPEP1
DPYD
D
ChIP-qPCR in MDA-MB-231-ETV7
% INPUT
ETV7
IgG
DPEP1
DPYD
NSB
E
11-gene signature
HR = 0.42 (0.36 – 0.5)
logrank P < 1E−16
Probability
Expression
low
high
Time (months)
Number at risk
low 882 384 116 29 6 2
high 882 593 229 39 4 0
all tumors : Subset= All tumors : Gene= MergedGeneSet
RFS (%)
p= 5e−05
[−2.520,−0.122) :n= 339
[−0.122, 0.236) :n= 302
[0.236, 1.792] :n= 273
Time (Years)
Multivariate analysis for n= 829 cases
SizeStrat:>20
AgeStrat:>50
GradeStrat:G3
NodeStatus:LN−
ER:er_pos
[−2.520,−0.122)
[−0.122, 0.236)
p= 6e−05
p= 0.23
p= 0.34
p= 9e−04
p= 0.16
p= 8e−04
p= 0.001
Hazard Ratio (95% CI)
all tumors : Subset= ER−positive tumors : Gene= MergedGeneSet
RFS (%)
p= 2e−05
[−2.520,−0.122) :n= 271
[−0.122, 0.236) :n= 246
[0.236, 1.792] :n= 221
Time (Years)

RESULTS-Figure 15: A) MTT analysis for survival of MDA-MB-231-ETV7 cells and empty control upon 5-Fluorouracil treatment (72 hours, increasing concentrations). B) MTT analysis for survival of U2OS-ETV7 cells and empty control upon 5-Fluorouracil treatment (72 hours, increasing concentrations). C) qPCR analysis for DPEP1 and DPYD expression in MDA-MB-231 cells overexpressing ETV7 compared to the empty control. D) ChIP-PCR analysis for ETV7 occupancy in DPEP1 and DPYD ETV7 binding sites in MDA-MB-231-ETV7 cells E) Expression analysis of the 11-gene signature (9-gene signature + DNAJC15 and DPYD) and associated breast cancer patients' relapse free survival, calculated starting from the left panel first by Kaplan Meier-plotter and then by GOBO analysis, relative to all breast cancer patients, and in the right panel the corresponding multivariate analysis and the Keplan Meier-plot for the ER positive breast cancer patients subset. In Kaplan-Meier plots calculated by GOBO tool (on the right) the interval of each expression quantile and relative number of patients analysed is reported above the x axis. Grey line refers to the low expression quantile, red to the intermediate and light blue line to the high expression quantile.

* indicates P-value(T-test) <0.05 and ** indicates P-value(T-test) <0.01.

6. DISCUSSION

Chemotherapy itself can lead to chemoresistance through a complex molecular network. Focusing on critical transcription factors, able to trigger and control this intricated network, could undercover key connections and promising targets involved in the outbreak of chemoresistance.

Specifically, DNA damaging drugs proved to effectively activate the expression of ETV7, a transcription factor belonging to the ETS family, with few reported oncogenic roles. ETV7 activation by DNA damaging drugs was observed in breast cancer cells, but proved to be a conserved mechanism, exploited by various cancer cells (lung, melanoma, osteosarcoma) and normal cells (lymphocytes, endothelial cells, fibroblasts). Conservation of the activation mechanism suggests its importance in cellular responses to certain drugs. This project focused on the role of ETV7 activation upon chemotherapy specifically in breast cancer cells. However, effectors and regulatory mechanisms involved in ETV7-mediated transcriptional repression in cancer cells can be shared with normal cells. Therefore, understanding the role of ETV7 in cancer cells could potentially help also to direct studies in normal cells.

ETV7 activation in breast cancer cells was studied respectively in two breast cancer cell lines, that differ in molecular and histopathological terms: luminal A breast cancer-derived MCF7 cells, expressing wild type p53, and triple negative breast cancer derived MDA-MB-231 cells, bearing the p53 mutant R280K. MCF7 cells showed a very strong response in terms of activation of ETV7 transcription, being Etoposide the least effective and Doxorubicin the most effective drug. Furthermore, transcriptional activation of ETV7 was also observed in response to prolonged Doxorubicin treatment in MCF7 cells, suggesting a potential key role for ETV7 activation in cell survival. Interestingly, an enrichment of ETS binding site was reported in genes differentially expressed upon Doxorubicin treatment, which supports the possible active role in transcription exerted by ETV7 or other ETS factors in response to Doxorubicin treatment. Nevertheless, Doxorubicin activation was not a typical response to this drug shared by other ETS factors. Microarray data from MCF7 cells clearly showed that ETV7 was the only ETS gene potently activated by Doxorubicin treatment, whereas SPDEF and ELF2 were repressed by this treatment, also confirmed by qPCR data. This might suggest that ETV7, SPDEF and ELF2 have different or even opposite biological functions, which is in line with the few data reporting tumor suppressor roles for the two latter proteins (Feldman *et al.*, 2003;

Turner, Moussa, *et al.*, 2007; Ando *et al.*, 2016; Guan *et al.*, 2017). Similarly to MCF7 cells, in MDA-MB-231 cells, Doxorubicin was the most potent inducer of ETV7 gene transcriptional activation, but the levels of induction were much lower with respect to MCF7 cells. Conversely, upon prolonged Doxorubicin treatment higher ETV7 activation was reported in MDA-MB-231 cells in comparison with MCF7 cells. Another relevant difference between these two cell lines is represented by the different occupancy of either wild type or mutant p53 on the ETV7 promoter. In fact, mutant p53 is already present on the ETV7 promoter in basal condition and increases its occupancy upon Doxorubicin treatment; whereas wild type p53 can be retrieved on the ETV7 promoter in MCF7 cells only in presence of Doxorubicin. Possibly, mutant p53 is already able to promote ETV7 transcription without Doxorubicin treatment and basal ETV7 expression is higher in MDA-MB-231 cells compared with MCF7 cells, as reported by He and colleagues in 2007 (He *et al.*, 2007). Thus, probably, a weaker induction of ETV7 is needed in these cells to activate its network. Alternatively, despite mutant p53 seems to retain the ability to bind ETV7 promoter, transactivation potential of wild type p53 in terms of recruiting cofactors (i.e. chromatin remodelers) could differ from mutant p53, and therefore ETV7 activation could be altered. Another difference between MCF7 and MDA-MB-231 cells stands in the expected different response to Nutlin-3a, that didn't show any ability to shape ETV7 expression in MDA-MB-231, confirming that mutant p53 R280K escapes the p53 protein stability control exerted by MDM2. 5-Fluorouracil was also not able to activate ETV7 expression in MDA-MB-231 cells, whereas Etoposide and Camptothecin activated ETV7, suggesting that the different mechanisms of DNA damage activation behind these different drugs are influencing ETV7 transcription. In this respect, the inhibition of topoisomerase is a more potent inducer with respect to the inhibition of the thymidylate synthase. This project reported a role for ETV7 in promoting drug resistance; therefore, the observation that ETV7 can be differently activated by cytotoxic drugs used in chemotherapy (based on their mechanism of action) with respect to the patient- and cancer-specific context, can be helpful in light of personalized medicine.

The critical role of inflammation in promoting chemoresistance and the role of ETV7 in triggering chemoresistance are directly linked, being ETV7 also activated by NFκB, belonging to a signature of genes associated with breast cancer aggressiveness and synergistically activated by the combined treatment of Doxorubicin and TNF-α in MCF7 cells (Bisio *et al.*, 2014).

An important finding came from the validation of p53's role in the activation of ETV7 transcription. p53 was shown to bind the ETV7 promoter upon Doxorubicin, TNF-α and the combined treatment in MCF7 cells. The transcriptional induction of ETV7, an oncogene, is unexpected and contradictory with the standard p53 tumor suppressor functions. Given the conservation of ETV7 activation in different cell types, it could be that p53-mediated transcription of ETV7 is meant to exert tumor suppressor roles in normal cells, but it acts differently in transformed cells. This is in line with the reported potential control of ETV7 on the TGF-β pathway, which controls cell death in normal cells but promotes metastasis in advanced cancers. p65 was also able to bind to the ETV7 promoter upon all treatments, confirming the positive control exerted by NFκB on ETV7 activation.

Synergistic transactivation potential of ETV7 upon Doxorubicin and TNF-α combined treatment was also observed in MDA-MB-231 cells, although at a lower magnitude compared to MCF7 cells. Probably other transcription factors, which are not present in MDA-MB-231 cells, can be involved in ETV7 activation in MCF7 cells. In fact, CRISPR/Cas9 experiments directed to knock-out the expression of either p53 and p65 showed a stronger impact in MDA-MB-231 cells with respect to MCF7 cells. It could also be that mutant p53, which proved to be able to bind to the ETV7 promoter, needs p65 to efficiently activate the transcription of target genes, and, similarly mutant p53 is essential to activate p65 in MDA-MB-231 cells, upon Doxorubicin treatment.

The complexity of the regulatory mechanisms controlling ETV7 transcription is amplified by the activatory roles played by STAT3 in MDA-MB-231, where an increase in phosphorylation of STAT3 was detected upon Doxorubicin treatment. In MCF7 cells there was no activation of STAT3 pathway and loss of STAT3 increased ETV7 activation. Furthermore, testing the response to a STAT3 activatory signal in MCF7 in terms of ETV7 transcription, could also help the understanding the role of STAT3 in this cell line.

Relatively recently, epigenetic modulators proved to be effective in enhancing chemotherapy potency in different types of cancer including breast cancer (Strauss and Figg, 2016). In the case of ETV7 activation, the histone mark H3K4 trimethylation was increased upon Doxorubicin, TNF-α and combined treatment, whereas only weak signal was seen for acetylation. This information could be useful to design a therapy, which minimizes ETV7 transcription upon chemotherapy.

Since no literature data are available relative to the specific role of ETV7 in breast cancer, and the reported significant activation upon DNA damaging drugs, I investigated the survival of MDA-MB-231 cells over-expressing ETV7 (MDA-MB-231-ETV7) upon Doxorubicin treatment. MDA-MB-231 cells were selected in order to have a model able to more closely resemble the clinical settings of most patients treated with chemotherapy (advanced stage and triple negative) and over-expression strategy was chosen instead of silencing, because previous results of the laboratory I am joining, showed a dramatic breast cancer cell death upon ETV7 silencing. ETV7 over-expressing cells were significantly more resistant to Doxorubicin treatment with respect to their empty control cells. This ETV7-mediated increased resistance to Doxorubicin was also observed in MCF7 cells (see Annex 2.3) and in osteosarcoma cell line U2OS, suggesting a conserved role for ETV7 in drug resistance. Furthermore, MDA-MB-231-ETV7 also showed an increased migratory potential and increased ability in anchorage-independent growth (see Annex 1.1), supporting a key oncogenic role for this protein in breast cancer cells. This study is mainly focused on the role of ETV7 in drug resistance especially in relation to its role as transcription factor, aiming at the investigation of novel key transcriptional circuitries that can be pharmacologically targeted, in order to ultimately improve breast cancer treatment efficacy. In support to ETV7 role in drug resistance, MDA-MB-231 cells over-expressing ETV7 showed an increased Doxorubicin efflux from nuclei and a consequent reduced nuclear accumulation of Doxorubicin. Another relevant characteristic of ETV7 over-expressing cells, was the increased expression of the ABC transporter ABCB1/MDR1/P-glycoprotein. Probably the increased efflux from nuclei could be directly linked to ABCB1 transporter, being able to localize also in the nuclear membrane (Molinari *et al.*, 2002). The calculated increased Doxorubicin efflux area from nuclei could eventually be indicative for an increased Doxorubicin accumulation inside cytoplasmic organelles, which could also be promoted by ABCB1 (Molinari *et al.*, 2002). A link between ETV7 and ABCB1 comes from the novel finding of DNAJC15 as an ETV7 target. DNAJC15 is a negative regulator of c-Jun pathway, blocking c-Jun-mediated ABCB1 transcription; DNAJC15 transcriptional repression mediated by ETV7 is, therefore, leading to an increased expression of ABCB1, as seen in ETV7 over-expressing cells (Hatle *et al.*, 2007).

To achieve the discovery of DNAJC15 as a mediator of ETV7-driven drug resistance phenotype, I first performed a comparative analysis of a list of genes often found hypermethylated and repressed in breast cancer, which were proven to be directly linked to drug response (Boettcher, Kischkel and Hoheise, 2010). ETV7 is a transcriptional repressor,

therefore I focused my attention on repressed genes and, particularly, I restricted the search for potential targets to hypermethylated genes, because ETS factor motifs are over-represented in methylated regions, particularly in hematopoietic stem and progenitor cells (Hogart, Lichtenberg and Ajay, 2012). I then applied two filters to get to the best predicted ETV7 targets: first, I analyzed the response to Doxorubicin of the six genes listed by Boettcher and co-workers (Boettcher, Kischkel and Hoheise, 2010), using the microarray analysis of Doxorubicin-treated MCF7 cells available in our group, and then I checked the most repressed genes by qPCR in MCF7 cells treated with Doxorubicin, TNF-α, and the combined treatment. DNAJC15 was the only gene synergistically repressed by the combined treatment. DNAJC15 repression was then tested upon treatment with p53 activating and DNA damaging drugs in MCF7, MDA-MB-231, and healthy donors-derived lymphocytes. The pattern of DNAJC15 repression very much mirrored the one of ETV7 activation, being Doxorubicin the most potent DNAJC15 repressor both in MCF7 and MDA-MB-231 cells, and being Etoposide the least effective drug in inducing ETV7 and repressing DNAJC15. DNAJC15 repression was found also upon prolonged Doxorubicin treatment, as for ETV7 activation, both in MCF7 and MDA-MB-231 cells. In MDA-MB-231 cells there was no response upon Nutlin-3a and 5-Fluorouracil treatment, as it was the case for ETV7 activation. DNAJC15 repression upon DNA damaging drugs was also conserved in lymphocytes derived from healthy donors. For some donors there was an appreciable inverse correlation between ETV7 and DNAJC15 expression, especially in Doxorubicin condition. These expression studies showed a clear inverse correlation between ETV7 and DNAJC15, which was recapitulated by ETV7 over-expression experiments, either transiently in MCF7 cells, or stably in MDA-MB-231 cells, both leading to DNAJC15 repression. ChIP-qPCR analysis confirmed ETV7 occupancy within the DNAJC15 promoter in MDA-MB-231 cells over-expressing ETV7. Increased occupancy was observed in the presence of Doxorubicin, which was associated with increased ETV7 abundance in chromatin and, more generally, in nuclear fractions. Doxorubicin could possibly activate specific pathways, responsible for ETV7 post-translational modifications which increase its protein stability. For example, ETV7 has a high affinity for p38 kinase, which is a kinase known to be induced by Doxorubicin, providing a link and a possible explanation for the increase in protein level, which, in the case of over-expression, cannot be simply related to increased transcription of endogenous ETV7 (Poizat *et al.*, 2005; Selvaraj, Kedage and Hollenhorst, 2015).

The ability of ETV7 to repress DNAJC15 transcription was confirmed by Gene Reporter Assay performed in MCF7 cells by co-transfecting ETV7 expression vector and a reporter plasmid harboring a fragment of the DNAJC15 promoter upstream the luciferase reporter gene. It was then asked if the presence or absence of either wild type or mutant p53 could influence ETV7-dependent repression of DNAJC15. According to ChIP-seq data of Nutlin-3a treated MCF7 cells, p53 itself can bind to the DNAJC15 promoter (chr13:42495669-42496026) (Nikulenkov *et al.*, 2012). It is also known that some ETS factors can interact with p53; among them, the interaction between ETS2 and mutant p53 is well studied and responsible for drug resistance to Etoposide (Do *et al.*, 2012). In MCF7 cells transiently over-expressing ETV7, ETV7-mediated repression of DNAJC15 didn't change in the absence of p53, meaning that, in these cells, the presence of p53 is not essential or not competing for ETV7-mediated repression of DNAJC15. In MDA-MB-231 cells the repression of DNAJC15 was not noticeable in parental cells upon ETV7 over-expression, but in the absence of mutant p53 there was a relevant decrease in the basal transactivation of DNAJC15 reporter plasmid, and a strong repression upon ETV7 over-expression, suggesting that possibly mutant p53 can somehow interfere or block ETV7 binding to the promoter. Therefore, I checked whether wild type and mutant p53 were able to bind nearby the ETV7 binding site in the DNAJC15 promoter, where a half site consensus region for p53 is present. ChIP-qPCR assays for p53, obtained by amplifying the same region used for ETV7 ChIP-qPCRs, showed p53 occupancy on the DNAJC15 promoter both in MCF7 and MDA-MB-231 cells. Notably, in MCF7 cells p53 occupancy substantially decreased upon Doxorubicin treatment, whereas ETV7 occupancy increased in presence of Doxorubicin, suggesting a possible competition between wild type p53 and ETV7, rather than a cooperation in binding. ChIP-qPCR assays in MDA-MB-231 cells showed that also mutant p53 could bind nearby the ETV7 binding region in the DNAJC15 promoter, despite the occupancy levels, in terms of % of Input, are much more reduced for mutant p53 and differently from wild type p53, are increasing upon Doxorubicin treatment. Given the increased repression of DNAJC15 observed in MDA-MB-231 cells both in Gene Reporter Assays in absence of p53, and the increased repression of DNAJC15 gene expression upon Doxorubicin and transient silencing of p53 in MDA-MB-231 cells, it seems that p53 and, especially mutant p53, could somehow compete with the repressive action of ETV7. Upon Doxorubicin treatment, ETV7 repressive action is winning against p53, leading to a relevant repression, which is mirrored by a decreased occupancy of wild type p53. Alternatively, even if an increased binding is observed for mutant p53 upon Doxorubicin treatment, it could be that probably alone it may not be able to actively promote DNAJC15 transcription. Among the

possible transcription factors reported to be able to assist mutant p53 transcriptional action, I focused on p65, which also has a good predicted binding site very near to both ETV7 and p53 response elements in the DNAJC15 promoter. Therefore, p65 ChIP-qPCR assays were performed in both MCF7 and MDA-MB-231 cells, which revealed that also p65 can bind to the DNAJC15 promoter and that its binding is decreasing upon Doxorubicin treatment, suggesting a possible competition in binding with ETV7 also for this transcription factor. Furthermore, the fact that Doxorubicin treatment totally abolished p65 occupancy in MDA-MB-231 cells, suggests that possibly p65 is essential to support mutant p53 negative action on ETV7 mediated repression, given the fact that ETV7-mediated repression is still winning against p53 despite an increased mutant p53 occupancy is visible in presence of Doxorubicin. Moreover, the fact that p53 over-expression alone in p53 KO cells wasn't able to shape DNAJC15 expression confirms the essential role of p65 or other cofactors in supporting p53 transcriptional control on DNAJC15 expression. This ChIP-qPCR data can also explain why the over-expression of ETV7 is already leading to DNAJC15 repression also in cells harboring mutant p53, whereas in Gene Reporter Assays this is not visible in presence of p53. It could be that the promoter region and organization cloned in the reporter plasmid is more prone for the binding of mutant p53 and p65 with respect to the "real" and more complex chromatin organization of the endogenous promoter, thus blocking the ETV7 binding and its related repressive actions.

In addition to these possible competitive interactions between p53 and ETV7, co-immunoprecipitation studies (using cell lysates enriched for the chromatin fraction from MDA-MB-231 cells over-expressing ETV7) suggested a possible physical interaction between mutant p53 and ETV7. This hypothesis has to be better explored in the future since over-expression experiments could eventually give a false-positive result of interaction, but unfortunately endogenous ETV7 protein levels are too low to appreciate a possible protein interaction by standard Co-IP technique. In line with this possible negative interaction between mutant p53 and ETV7 are the data showing a higher ETV7 protein expression in chromatin and nuclear extracts in MDA-MB-231 cells deleted for p53 but over-expressing ETV7, compared to the parental MDA-MB-231-ETV7 over-expressing cells. Doxorubicin treatment was responsible for an increased ETV7 protein expression in nuclear and chromatin fractions in both cell lines. It could be also that mutant p53 can indirectly shape ETV7 stability thanks to its reported control on proteasome, thereby leading to a decreased proteasomal degradation of ETV7 in absence of mutant p53 (Walerych *et al.*, 2016).

Doxorubicin treatment can also possibly influence cofactors needed by mutant p53 to exert its regulatory functions on ETV7 stability. Alternatively, Doxorubicin can possibly lead to an increased stability of ETV7 protein mediated by post-translational modifications such as phosphorylation, occurring independently from mutant p53, in line with the observed increased protein level of endogenous ETV7 seen in MCF7 cells treated with Doxorubicin. Nevertheless, it could be that this observed difference in protein levels could be related to the different position where the exogenous ETV7 integrated into the two different clones. Thus procedures to assess the chromatin and nuclear expression of ETV7 protein in different clones derived from MDA-MB-231 p53 KO cells over-expressing ETV7 are planned to be done in the near future. Furthermore, to better determine the possible effect of p53 on ETV7 protein stability, experiments with transient silencing of p53 in both parental MDA-MB-231 cells and MDA-MB-231 cells over-expressing ETV7 cells are needed. In support to the hypothesis of a mutant p53-dependent control of ETV7 protein stability are the data showing a decrease in ETV7 protein expression (both the endogenous and the ectopically transfected ETV7), as demonstrated by cytoplasmic and nuclear fractions, upon over-expression of different p53 mutants in MDA-MB-231 p53 KO cells. However, the two mutant forms of p53 used in these experiments (R282Q and G279E) are different from the one constitutively present in parental MDA-MB-231 cells (R280K), thus additional experiments using the p53 mutant R280K could be necessary to better confirm this hypothesis. Furthermore, it could be possible that wild type p53 might have a different effect on ETV7 protein stability, and, therefore, it might not be able to destabilize ETV7 protein as efficiently as mutant p53. Experiments in this direction could also possibly clarify the differences observed in DNAJC15 repression from Gene Reporter Assays performed in MCF7 and MDA-MB-231 cells, where, possibly, mutant p53 could better destabilize the chromatin-bound ETV7 protein with respect to wild type p53 (p53 and ETV7 REs are somewhat close within the DNAJC15 promoter, see Figure 7I).

To confirm that DNAJC15 represents a critical ETV7 target in mediating drug resistance, I transiently overexpressed DNAJC15 in MDA-MB-231-ETV7 cells and observed that, upon DNAJC15 increased expression, these cells became more sensitive to Doxorubicin, and concomitantly ABCB1 expression decreased, partially rescuing the ETV7-dependent resistant phenotype. To test the potential power of the discovered ETV7-DNAJC15 mechanism in predicting patients outcome, I interrogated the expression of ETV7 and DNAJC15 in the dataset GSE43502, which collected data on cancer recurrence of triple negative breast cancer

patients after neoadjuvant chemotherapy and, therefore, closely resembles the conditions used for the experiments done *in vitro*. ETV7 expression was increased in patients with recurrent disease, despite not in a statistically significant fashion. DNAJC15 was strongly and statistically significantly decreased in patients with recurrent disease. ETV7 activation levels upon chemotherapy can vary among patients, also according to the presence of other different transcription factors, the different level of ETV7 before the treatments, the different drugs used, as it was observed for breast cancer cells *in vitro*. Furthermore, being an unstable protein, ETV7 activation can be restricted in time, thus explaining the lack of statistical significance in ETV7 expression. Conversely, ETV7-mediated repression could potentially lead to stable epigenetic silencing of DNAJC15, because this gene is known to be controlled by DNA methylation (Shridhar *et al.*, 2001).

Given that DNAJC15 over-expression is difficult to pursue in clinical settings, a possible therapeutic strategy is to block ABCB1-mediated drug efflux and increase Doxorubicin therapeutical efficacy. This, associated with the concomitant decrease in the related cardiotoxicity, might be provided by the treatment with flavonoids, for instance Quercetin (Dong *et al.*, 2014; Cote *et al.*, 2015; Liu *et al.*, 2016; Lv *et al.*, 2016; Minaei *et al.*, 2016). ETV7 over-expressing cells were more sensitive to Quercetin cytotoxic action, that, given the pleiotropic action of this natural compounds, can only partially suggest an important role for ABCB1 expression in the survival of these cells. Interestingly, ETV7 expression was repressed upon Quercetin treatment in MDA-MB-231 cells, probably due to Quercetin negative action of NFκB pathway activation (Indra *et al.*, 2013). Genistein, an isoflavone, was also able to repress ETV7 expression in MDA-MB-231 cells, proposing that possibly ETV7 repression can generally occur upon flavonoids administration.

To broaden the analysis of ETV7 roles in breast cancer and possibly discover novel targets relevant for ETV7 drug resistant phenotype, I performed a ChIP-seq experiment for ETV7 in two different cell lines over-expressing ETV7, expressing or not mutant p53 (parental MDA-MB-231-ETV7 and MDA-MB-231-ETV7 p53 KO), either untreated or treated with Doxorubicin. In general the number of peaks found by ETV7 ChIP-seq was quite small (around 100 peaks for each condition, except MDA-MB-231-ETV7 p53 KO treated with Doxorubicin that only counted 10 peaks), in line with the previous microarray analysis of cells over-expressing ETV7, where only a limited number of genes was differentially expressed (Carella *et al.*, 2006). A possible explanation for this phenomenon can be related to the oligomeric

conformation of ETV7 in the process of binding DNA that made difficult the detection of binding peaks; in fact, the visualization of peaks showed that the peaks calculated by SISSR are actually representing just a part of the ETV7 binding region. Another important information that can be retrieved from peak visualization is the high fold change of ETV7 IP signal with respect to both the IgG and the Input signals. This might suggest that ETV7 can be a very specific transcription factor, able to reach very high occupancy in few specific regions, therefore potentially consistent with the low number of peaks obtained by ETV7 ChIP-seq analysis. Despite the low number of peaks detected in general, the overlap in terms of ETV7 targets present in different conditions or sharing a similar gene ontology was conspicuous, suggesting an important ETV7-mediated regulation of specific genes. In particular, as shown by Metascape analysis, ETV7 target genes mostly shared among different conditions were enriched for the response to Chagas disease (also observed in the enrichment analysis performed with Enrichr software), the animal organ morphogenesis, the regulation of cysteine-type endopepetidase activity involved in apoptotic process, and the regulation of cellular component biogenesis. This suggests that ETV7 might play an important role in the control of parasitic diseases, in addition to the reported control on viral infection (Rempel *et al.*, 2013; Ignatius Irudayam *et al.*, 2015). Nevertheless, being this project mostly inherent to cancer biology, emphasis should be given to the observed enrichment in the cysteine-type endopeptidase activity relative to apoptosis. This possible control exerted by ETV7 on caspase activity would confirm previously reported data regarding ETV7 over-expression and related decreased apoptotic rate observed in lymphoid and hematopoietic stem cells (Cardone *et al.*, 2005; Carella *et al.*, 2006). The enrichment observed in processes of animal organ morphogenesis and cellular component biogenesis can be linked to the reported ETV7 negative control on differentiation (Sakurai *et al.*, 2003; Kawagoe *et al.*, 2004; Quintana *et al.*, 2014). In general, processes found to be enriched in 3 different ChIP conditions, appeared to be related to previously reported biological roles of ETV7, and therefore could be helpful to better characterize how ETV7, in terms of transcriptional control, can regulate them. Among the enriched ontology clusters found in at least two conditions, and specifically in the untreated ones, both in presence and in absence of mutant p53, many cancer related pathways were found, such as regulation of extracellular matrix and collagen metabolism, migration, and cell junction assembly.

The TGF-β pathway was also found to be enriched in at least two ChIP-conditions both by Metascape and Enrichr analysis. Binding and repression of some ETV7 targets involved in

TGF-β pathway were validated, and notably, they were all negative regulators of the TGF-β signaling, thus suggesting a positive activation of this pathway upon ETV7 over-expression. Moreover, the expression of these TGF-β-related genes was able to predict breast cancer patients' outcome especially in terms of their lymphonode status and tumor size, and with the highest predictive power in ER positive cells. Possibly, crosstalk between ER and TGF-β could play a role in determining a worse outcome (Matsuda *et al.*, 2001). ETV7 control on this pathway could also suggest a growth arrest effect of ETV7 activation upon DNA damaging in normal cells, given that TGF-β in normal cells and in early stage cancer is responsible for growth inhibition. Furthermore, the positive control exerted by ETV7 on this pathway can be very meaningful in cells that have mutant p53 and activated Ras signaling, such as MDA-MB-231, given that their ternary complex with Smads promotes p63 inhibition and stimulates the metastatic spread (Adorno *et al.*, 2009).

A good enrichment among ETV7 targets in drug response process (seen by Enrichr analysis), confirmed the observed ETV7 role in drug resistance. Among the targets involved in drug response, DPEP1 (Dehydropeptidase I) showed a strong ETV7 peak, and it was one the two targets common in all four ChIP-seq conditions; therefore it represented an interesting target to validate. Binding and repression by ETV7 were confirmed by qPCR and ChIP-qPCR in MDA-MB-231-ETV7 cells, and DPEP1 was also interrogated for prognostic relevance using the Kaplan Meier-plotter web tool and interrogating breast cancer cases, where a low expression was indeed associated with reduced survival. DPEP1 is a metalloproteinase responsible for the that hydrolysis of dipeptides, and it is part of the glutathione metabolism, where high glutathione level resulting from DPEP1 loss can lead to drug resistance (Balendiran, Dabur and Fraser, 2004). A loss of DPEP1 expression was found in breast cancer and Wilm's tumor (Cohen-Salmon *et al.*, 1993; Green *et al.*, 2009), whereas an over-expression was found in colorectal carcinoma compared to adjacent tissue (Hao *et al.*, 2017). DPEP1 can positively regulate colon cancer metastasis (Park *et al.*, 2016) and, conversely, it can inhibit cancer invasion and promote chemosensitivity in pancreatic ductal carcinoma, where it can predict clinical outcome (G. Zhang *et al.*, 2012). This thesis reports a novel type of DPEP1 regulation mediated by ETV7, and proposes a role for DPEP1 in ETV7-mediated drug resistance and predictive role for DPEP1 in breast cancer aggressiveness, which could be further investigated also in other types on cancer.

ETV7-mediated drug resistance was also tested upon another unrelated cytotoxic drug, 5-Fluorouracil, which is frequently used in breast cancer chemotherapy in combination with Doxorubicin in the FAC regimen (5-Fluorouracil, Doxorubicin, Cyclophosphamide). MDA-MB-231 cells over-expressing ETV7, showed an increased survival also upon treatments with this drug, suggesting that the drug response-phenotype linked to ETV7 can be considered as a multi-drug resistance one. Resistance to both Doxorubicin and 5-Fluorouracil was monitored also in the U2OS osteosarcoma cells over-expressing ETV7. To explain the observed resistance to 5-Fluorouracil, I searched for potential putative targets, in addition to DPEP1, specifically involved in the metabolism of this drug, by merging the novel ETV7 ChIP-seq data with the reported ETV7 microarray analysis (Carella *et al.*, 2006). DPYD was present in both analyses and its repression by miR-21 was associated with increased resistance to 5-Fluorouracil in human colon cancer HT-29 (Deng *et al.*, 2014). qPCR and ChIP-qPCR analysis confirmed the ETV7-mediated repression of this gene, but additional rescue analysis is needed to prove the direct involvement of DPYD in ETV7-mediated 5-Fluorouracil resistance. Furthermore, given the conflicting evidences regarding its role in chemoresistance reported in colon and gastric cancer (Wu *et al.*, 2016) a deeper study of this gene involvement in breast cancer chemoresistance is of paramount importance.

ChIP-seq enrichment analysis also suggested a potential role for ETV7 in the control of inflammation, given the presence of many inflammation-related pathways, such as pathogen response (specifically Trypanosomiasis and HTLV-1), adipocytokine signaling, response to wounding, and respiratory burst, which represents an important response of immune cells to infection. ETV7 is a recognized interferon stimulated gene, but a better understanding the role of ETV7 in inflammation is needed and could uncover relevant information for cancer immunotherapy. This project reported an increased expression of ETV7 upon respiratory syncytial virus (RSV) infection, with an associated downregulation of DNAJC14 (Annex 1.2). DNAJC14 is a co-chaperone protein with a known role in viral replication of flavivirus and yellow fever virus (Yi *et al.*, 2012; Bozzacco *et al.*, 2016). It is here reported for the first time, as a novel ETV7 direct target confirmed by qPCR, Gene Reporter Assay and ChIP-qPCR analysis. DNAJC14 was the most repressed gene of the DNAJC family in MCF7 cells upon Doxorubicin treatment, and a DNAJC14 expression decrease was found in Doxorubicin and 5-Fluorouracil treated MCF7 cells and only upon Doxorubicin and Nutlin-3a in MDA-MB-231 cells. The mechanism of repression is also partially conserved in healthy donors-derived lymphocytes treated with DNA damaging agents. These differences in terms of repression

between DNAJC14 and DNAJC15 suggest that different co-repressors and epigenetic factors are involved in the repression of the two genes. ETV7 repression and binding within the DNAJC14 promoter were confirmed by ChIP-qPCR, with an increased occupancy upon Doxorubicin treatment, as demonstrated for DNAJC15. Its repression seen in Gene Reporter Assays was detected both in presence of wild type or mutant p53, but without p53, the basal levels of activation were much lower than in the presence of mutant 53. These observations are supported by the results from transient silencing of p53 in MDA-MB-231 cells, where the reduction in p53 levels was sufficient to lead to a relevant repression of DNAJC14 expression. Conversely, when either wild type or mutant p53 are transiently over-expressed in p53 KO MDA-MB-231 cells, there were no observable effect on DNAJC14 expression, suggesting that p53 needs other transcription factors or cofactors to support the basal expression levels of DNAJC14. To investigate whether p53 was able to bind nearby the ETV7 response element also in the DNAJC14 promoter, I first searched for p53 binding sites and found a consensus full site next to the ETV7 one. Then, I performed ChIP-qPCR analyses in both MCF7 and MDA-MB-231 cells, and I confirmed both wild type and mutant p53 occupancy on the DNAJC14 promoter, which was respectively decreasing in MCF7 and increasing in MDA-MB-231 cells upon Doxorubicin treatment, as it was observed for DNAJC15. In MCF7 cells, also p65 displayed positive occupancy in the DNAJC14 promoter, that decreased upon Doxorubicin, thus suggesting that p65 could be essential for supporting positive regulation of this gene together with p53. In MDA-MB-231 cells, p65 was not retrieved on the DNAJC14 promoter in any conditions and this could explain why, differently from DNAJC15, in Gene Reporter Assays repression of DNAJC14 transcription was also visible in presence of mutant p53, given that probably mutant p53 in absence of p65 is not able to bind enough tightly to mask ETV7 binding on the promoter region on the reporter plasmid.

DNAJC14 was also the only DNAJC member, besides DNAJC15, which was repressed by Doxorubicin, and at the same time was also down-regulated in a statistically significant way in recurrent breast cancer patients after neoadjuvant chemotherapy. Notably, its decreased expression was also associated with poorer prognosis in breast cancer patients, according to Kaplan Meier-plotter analysis. *In vitro* analysis, using MDA-MB-231 and silencing DNAJC14, showed conflicting results relative to its potential role in drug resistance, showing increased drug sensitivity at lower doses and increased resistance at higer doses. Probably ETV7-mediated DNAJC14 repression exerts a more prominent role in the control of immune responses rather than in cancer cell survival upon chemotherapy. Nevertheless, DNAJC14 overexpression studies are needed to better determine its involvement in drug resistance and

to effectively compare with results obtained with DNAJC15. In addition, survival analysis should be extended to other breast cancer cells, since in MDA-MB-231 there was no DNAJC14 repression upon prolonged Doxorubicin treatment, suggesting that probably in this cell line its repression is not relevant for drug resistance. Furthermore, extending the analysis of DNAJC14 repression and ETV7 activation upon other types of viral infection could potentially explain the link between viral infection types enriched in ETV7 ChIP-seq targets (Epstein-Barr, HIV1, and papilloma) and their increased predisposition to develop cancer.
ChIP-seq data enrichment referred to diseases and, in particular, anemia, confirming a previous reported role for ETV7 in the development of red blood cells (Quintana *et al.*, 2014) and also added novel ETV7 potential targets involved in this function (CUBN, RPS19, and TERC). An enrichment in lymphoma also agreed with the reported evidence as oncogene in this type of cancer (Cardone *et al.*, 2005). Furthermore, ChIP-seq analysis suggested a role for ETV7 in the rare genetic disorder Charcot-Marie-Tooth disease (through the targets SH3TC2 and NDRG1).

Another important achievement of the ChIP-seq was the discovery of the first reported *in vivo* binding site for ETV7, which as expected contained the GGAA core as in the previous *in vitro* consensus sequences reported so far. Interestingly, I was able to identify specific features of the boundary sequences, which are very critical for determining the specificity of ETS, as more similar to the first two reported consensus sequences (Potter *et al.*, 2000; Gu *et al.*, 2001) compared to the latest reported one obtained by microwell-based transcription factor-DNA-binding assays (Wei *et al.*, 2010). The ChIP-seq analysis showed that ETV7 could bind *in vivo* with very high affinity to motifs representing consensus sequence of other ETS factors, thus confirming the redundancy property of ETS factors. The best known consensus sequence bound by ETV7 was the one of ETS1. Given the high statistical relevance of the binding to the ETS1 motif and the low number of peaks detected by ChIP-seq, it is very unlikely that it resulted from indirect binding of ETV7 to DNA, mediated by ETS1; despite the interaction between ETS1 and ETV7 already reported in the literature (Vivekanand and Rebay, 2012). More probably, it can be that ETV7 and ETS1 can share some targets, but their activator signals can differ; for example low level of JNK1 phosphorylation could be enough to activate ETV7, whereas, based on the different affinities, ETS1 would require higher level of JNK1 phosphorylation for activation (Selvaraj, Kedage and Hollenhorst, 2015). In addition to the different phosphorylation regulation, it could be that these ETS are recruited to the same targets by different cofactors, varying among cancer type and context. The second best known

motif bound by ETV7, is the one of ERG, an oncogenic ETS factors, that contrarily from ETS1 and ETV7 mainly acts as transcriptional activator and is frequently over-expressed as a result of chromosomal translocations in prostate cancer. ERG was recently reported as downregulated in breast cancer compared to normal tissue, and expressed at low level especially in basal subtype, inversely correlating with the expression of ETV7, which was markedly increased in this subtype and in general in breast cancer (Piggin *et al.*, 2016). It can be that, in breast cancer, ERG regulates some common targets with ETV7, but the first exerts a transcriptional activation, whereas the second a repression, suggesting the reason why they negatively correlate. Furthermore, similarly to ETS1, different post-translational modifications control ERG, which has a really high affinity for ERK2 (Selvaraj, Kedage and Hollenhorst, 2015). As third best motif bound by ETV7 was classified the one for ETV1, an important ETS factor for prostate cancer metastasis, that can substitute ERG when it is not over-expressed; possibly ETV7 could represent another substitute when also ETV1 is missing (Watson *et al.*, 2010).

ChIP-seq data also provided some clues on possible ETV7 cofactors involved in transcriptional repression, for example CTBP2 and SIN3a represent very interesting candidates, being both co-repressors and able to associate to ETV6, which is the closest ETS factor related to ETV7 (Wang and Hiebert, 2001; Roukens *et al.*, 2010).
Other enriched transcription factors able to bind ETV7 response elements, were all tumor suppressor genes and linked to transcriptional activation, therefore they could probably represent ETV7 competitors rather than interactors. Nevertheless, it couldn't be excluded that upon specific condition, the interaction of ETV7 with some cofactors could also lead to transcriptional activation of certain targets.

Another feature of ETV7 binding highlighted by ChIP-seq analysis was the preferential binding to intragenic regions in the cell lines and conditions analyzed. It could be that in other cells, especially in normal cells, binding dynamics could differ. In fact, most of the intragenic ETV7 peaks, were present in genes enriched in cancer related processes, whereas promoter ETV7 peaks were mostly found on genes enriched for processes related to inflammation and interferon response. It could be that the presence of other factors in cancer cells can direct ETV7 binding to intragenic regions. Relatively recently, it was shown that Ets-1 can associate with Smad4 and this complex preferentially binds to intragenic region of FPGS gene (Raz, Stark and Assaraf, 2014). Ets-1 is the most similar gene to ETV7 in terms of consensus

sequence (according to Homer analysis), therefore it can be that Smad proteins can also interact with ETV7 and help its binding to intragenic region. This would also explain the observed control of ETV7 on the TGF-β signaling, that could sustain ETV7 transcription itself by activating specific Smads. Alternatively, the binding to intragenic region can suggest other type of transcriptional regulation mediated by ETV7, such as modulation of transcriptional elongation or prevention of spurious transcriptional initiation (Neri *et al.*, 2017).

ETV7 targets (common in at least two ChIP-seq conditions) were also interrogated using the Kaplan Meier-plotter and 9 targets genes (that I called 9-gene signature) showed a remarkable correlation between increased expression and better survival in breast cancer patients, each with a statistically significant Hazard Ratio lower than 0.7. When the mean expression of these genes was interrogated by both Kaplan Meier-plotter and GOBO analysis, it showed a strong predictive power, even increased if considering the additional ETV7 targets reported in this project, DNAJC15 and DPYD, generating the so-called 11-gene signature. Multivariate analysis showed that, both the 9- and the 11-gene signatures, were particularly powerful in predicting patients' cancer size and lymphonode status, especially in ER positive breast cancer. Usually, this type of breast cancer is treated with hormone therapy, however in case of i) hormone therapy failure or ii) in presence of a larger size cancer or iii) in the neoadjuvant setting also in this type of cancer, chemotherapy is commonly used as a treatment option in this type of cancer. Therefore, this signature could have a clinical relevance also in this group of patients, and these results can eventually suggest that ER could somehow influence or cooperate in the phenotype driven by the differential expression of these genes. Nevertheless, it has to be considered that these data could be influenced by the fact that the ER-positive group in the GOBO analysis has many more samples respect to the others analyzed (such as the ER-negative one); thus the statistical power could be improved simply because of the larger group analyzed. For some of the signature genes (ACSL5, PTPRJ, GNAO1, PVT1), there were already reported association with breast cancer (Keane *et al.*, 1996; Smart *et al.*, 2012; Spring *et al.*, 2015; Sarver *et al.*, 2016; Sharma *et al.*, 2016; W. C. Chen *et al.*, 2016; Yan *et al.*, 2017). Specifically, increased expression of ACSL5 predicted a good prognosis for breast cancer patients (W. C. Chen *et al.*, 2016), consistent with the results shown here by Kaplan Meier-plotter. PTPRJ was found to inhibit breast cancer growth and a decrease in its expression was observed in breast cancer tissue compared to normal mammary tissue and was associated to poor survival (Keane *et al.*, 1996; Smart *et al.*, 2012). Conflicting data reported an oncogenic role for PTPRJ in promoting breast cancer cell invasion

(Spring *et al.*, 2015). A breast tumor promoting role is reported also for GNAO1 and PVT1, respectively, mutated GNAO1 promotes growth of mammary epithelial cells and PVT1 accellerates mammary tumors also by cooperating with MYC (Sarver *et al.*, 2016; Sharma *et al.*, 2016; Yan *et al.*, 2017). Conversely, GNAO1 and PVT1 are reported here as ETV7 targets whose high expression is predictive for good prognosis in breast cancer; therefore a better understanding on their role in different breast cancer subtypes and stages could better clear out their role in cancer progression.

The remaining 5 genes have so far no reported evidence in breast cancer; therefore, they could represent promising novel targets and molecular markers for precise investigations. In particular, CPNE5 has a remarkable striking Hazard Ratio (0.59), and it is the most unexplored gene, with no publication referring to cancer, but having just 3 publications on rodent anxiety, alcohol dependence and obesity, and an hypothesized role in the development of murine central nervous system (Ding *et al.*, 2008, 2017; Wang *et al.*, 2015).

Some of the identified ETV7 target genes have already a reported role in drug resistance, supporting this novel ETV7 function that is the focus of this project. Specifically, TRIM41 is directly linked to the drug resistance process driven by ABCB1-mediated increased efflux. TRIM41 is an E3 ubiquitin ligase responsible for the degradation of PKC, and PKC promotes drug resistance through the increased efflux by ABCB1 (C. W. Kim *et al.*, 2015). Given that its mechanism of action closely resembles the ETV7-mediated drug resistance mechanism observed here, TRIM41 could represent another important ETV7 target involved in drug resistance. UBR1 is another E3 ubiquitin ligase, which was found to be associated with drug resistance to Imatinib (Eldeeb and Fahlman, 2014), to alkylating agents (Leng *et al.*, 2015), and to Hsp90 inhibitors (Sultana, Theodoraki and Caplan, 2012). PTPRJ loss was also found to be responsible for 5-Fluorouracil resistance in cervical carcinoma, representing an additional target besides DPEP1 and DPYD for the observed 5-Fluorouracil resistance mediated by ETV7 (Yan *et al.*, 2015). Tumor promoting roles and decreased expression of some of these ETV7 targets, have already been associated with increased metastasis and worse prognosis in some types of cancer. Therefore, they could play an important role also in breast cancer. TRIM41 decrease was associated with metastasis in colorectal cancer (P. Zhang *et al.*, 2012), UBR1 loss was observed to accelerate lymphomagenesis (Chen *et al.*, 2006), and ACSL5 was down-regulated in squamous cell lung cancer (Molina-Pinelo *et al.*, 2014). Furthermore, PTPRJ loss was seen to predict worse prognosis in esophageal squamous cell carcinoma and promoting migration of hepatocellular carcinoma (Luo *et al.*, 2015; Qiao *et al.*, 2016), and down-regulation of GNAO1 was linked to increased proliferation and senescence inhibition in

hepatocellular carcinoma (Pei *et al.*, 2013)**.** Finally, ADCY1 was found down-regulated in rectal adenocarcinoma metastasis (Hua *et al.*, 2017), found hypermethylated in glioblastoma (Ma *et al.*, 2015), and its loss represents a biomarker for osteosarcoma tumorigenesis and therapeutics (Li *et al.*, 2010).

Given all these cancer-associated reported roles for these novel ETV7 targets, it is worth to investigate whether also these genes can be regulated by ETV7 in other types of cancer.

7. CONCLUSIONS AND FUTURE PERSPECTIVES

In conclusion, this project reported a novel involvement for ETV7 in breast cancer, and specifically, in the regulation of drug resistance to Doxorubicin and 5-Fluorouracil, two drugs often used in combination for breast cancer treatment. The ETV7-mediated drug resistance was characterized by an increased Doxorubicin efflux from nuclei associated with an increased expression of the ABC transporter ABCB1. The co-chaperone DNAJC15 is a negative regulator of the ABCB1 transcriptional activation mediated by c-Jun, and ETV7 proved to be able to bind and repress DNAJC15, therefore leading to increased ABCB1 expression and the related resistance. However, ETV7-DNAJC15 circuitry represents only one mechanism of the complex drug resistance machinery triggered by ETV7. By performing the first reported ChIP-seq for ETV7, I provided evidence regarding the *in vivo* ETV7 consensus sequence and targets, which is planned to be further reinforced by performing RNA-seq analysis on ETV7 over-expressing cells combined with Doxorubicin treatment. Some targets were validated and showed biological implications in both drug resistance and the regulation of TGF-β pathway. Nevertheless, a better understanding of the ETV7-dependent control of TGF-β pathway has to be established in future, together with the contribution of ETV7 on the 5-FU resistance. DPEP1 and DPYD genes were validated as ETV7 repressed targets, but rescue experiments are further needed to confirm their direct involvement in ETV7-mediated 5-FU resistance. Furthermore, a group of ETV7 targets found by ChIP-seq showed a strong correlation between high expression and associated good prognosis in breast cancer patients. Among them, CPNE5, a completely unexplored gene in cancer, might probably open up new horizons for breast cancer research. By controlling this wide spectrum of targets, ETV7 targeting could represent a very promising therapeutic strategy to overcome or, better, to avoid the outbreak of drug resistance. A possible targeting strategy could either rely on triplex-forming oligonucleotide specifically targeting ETV7 promoter, as in the case of another ETS factor, ETS2 (Carbone *et al.*, 2004), or targeting the phosphorylation events responsible for ETV7 activation, as reported for the ETS factors ETV1 and ELK3 (Pop *et al.*, 2014; Semenchenko *et al.*, 2016). So far, there are no clear studies on post-translational modifications controlling ETV7 activation, except for the high affinity for JNK1 (Selvaraj, Kedage and Hollenhorst, 2015). In this project, I observed an increased ETV7 protein stability upon Doxorubicin

treatment, that could be probably mediated by post-translational modifications, and could be helpful to direct future studies in the field. Furthermore, a complex relationship between ETV7 and p53 is proposed by this study and it is aimed to be better clarified, both in terms of competition in binding of some ETV7 targets and in terms of possibly controlling ETV7 protein stability. The conserved ETV7 transcriptional activation upon DNA damaging drugs in normal cells and its influence on TGF-β pathway suggested that ETV7 could have a tumor suppressor role in normal cells, that needs to be better explored. Therefore, when planning ETV7 targeting, it will be of paramount importance to specifically target ETV7 in cancer cells. Notably, ETV7-mediated drug resistance to Doxorubicin and 5-Fluorouracil was also observed in the osteosarcoma cell line U2OS, and ETV7 novel targets were already associated with drug resistance in various cancer types. Therefore, extending to other cancer types the analysis of ETV7 role on drug resistance can hold important promises, especially in the light of simplifying the drug resistance complexity. Lastly, a possible role of ETV7 in controlling viral infection was also briefly evaluated and specifically in response to respiratory syncytial virus (Annex 1). A better understanding of the role for ETV7 activation and its novel target DNAJC14 in response to RSV infection, can also eventually clear out a possible link between infection and increased susceptibility to cancer.

8. ACKNOWLEDGMENTS

I first would like to acknowledge my advisor Prof. Yari Ciribilli, who selected me as first PhD student for his brand new laboratory and always provided to me scientific and moral support during this amazing PhD project. I am particularly grateful to him for being always present and showing interest in my ideas, and especially for having transmitted to me his passion for science. Special thanks also for his financial support and his time in critically reviewing this thesis report.

I would like to offer my special thanks to my tutor Prof. Alberto Inga, who financially supported a part of this project and, thanks to his great scientific experience and knowledge, helped me in reviewing this thesis and gave precious suggestions. Furthermore, he helped me in realizing my dream to experience research life in the US, thanks to its collaboration with NIEHS Chromosome Stability Group. I particularly appreciate the kind hospitality showed by Dr. Michael Resnick and Dr. Daniel Menendez during my stay at the NIEHS. I want to thank both of them for their time, financial support and scientific discussions, that made my research period abroad particularly productive.

I want to acknowledge all my present and past colleagues, who helped in creating an ideal working place. I gratefully acknowledge the University of Trento and CIBIO for all the funding sources and the institutional support that was essential for my PhD. I want to acknowledge all the CIBIO Facilities and in particular Valentina Adami and Michael Pancher from the HTS Facility for the work on Doxorubicin efflux dynamics measurements by Operetta.

I also want to thank my parents and my life mate, who always supported me. Thank you.

9. REFERENCES

Acharyya, S., Oskarsson, T., Vanharanta, S., Malladi, S., Seshan, V. E., Norton, L., Brogi, E. and Massagué, J. (2012) 'A CXCL1 paracrine network links cancer chemoresistance and metastasis.', *Cell*, 150(1), pp. 165–178. doi: 10.1016/j.cell.2012.04.042.A.

Adorno, M., Cordenonsi, M., Montagner, M., Dupont, S., Wong, C., Hann, B., Solari, A., Bobisse, S., Rondina, M. B., Guzzardo, V., Parenti, A. R., Rosato, A., Bicciato, S., Balmain, A. and Piccolo, S. (2009) 'A Mutant-p53/Smad Complex Opposes p63 to Empower TGF β-Induced Metastasis', *Cell*. Elsevier Ltd, 137(1), pp. 87–98. doi: 10.1016/j.cell.2009.01.039.

Al-Dhfyan, A., Alhoshani, A. and Korashy, H. M. (2017) 'Aryl hydrocarbon receptor/cytochrome P450 1A1 pathway mediates breast cancer stem cells expansion through PTEN inhibition and β-Catenin and Akt activation', *Molecular Cancer*, 16(1), p. 14. doi: 10.1186/s12943-016-0570-y.

Albino, D., Civenni, G., Dallavalle, C., Roos, M., Jahns, H., Curti, L., Rossi, S., Pinton, S., D'Ambrosio, G., Sessa, F., Hall, J., Catapano, C. V. and Carbone, G. M. (2016) 'Activation of the Lin28/let-7 axis by loss of ESE3/EHF promotes a tumorigenic and stem-like phenotype in prostate cancer', *Cancer Research*, 76(12), pp. 3629–3643. doi: 10.1158/0008-5472.CAN-15-2665.

Albino, D., Civenni, G., Rossi, S., Mitra, A., Catapano, V. and Carbone, G. M. (2016) 'The ETS factor ESE3 / EHF represses IL-6 preventing STAT3 activation and expansion of the prostate cancer stem – like compartment', 7(47). doi: 10.18632/oncotarget.12525.

Albino, D., Longoni, N., Curti, L., Mello-Grand, M., Pinton, S., Civenni, G., Thalmann, G., D'Ambrosio, G., Sarti, M., Sessa, F., Chiorino, G., Catapano, C. V. and Carbone, G. M. (2012) 'ESE3/EHF controls epithelial cell differentiation and its loss leads to prostate tumors with mesenchymal and stem-like features', *Cancer Research*, 72(11), pp. 2889–2900. doi: 10.1158/0008-5472.CAN-12-0212.

American Cancer Society (2016) 'Cancer Facts & Figures'. doi: 10.1101/gad.1593107.

Anders, C. K., Abramson, V., Tan, T. and Dent, R. (2016) 'The Evolution of Triple-Negative Breast Cancer: From Biology to Novel Therapeutics', *American Society of Clinical Oncology Educational Book*, 36, pp. 34–42. doi: 10.14694/EDBK_159135.

Ando, M., Kawazu, M., Ueno, T., Koinuma, D., Ando, K., Koya, J., Kataoka, K., Yasuda, T., Yamaguchi, H., Fukumura, K., Yamato, A., Soda, M., Sai, E., Yamashita, Y., Asakage, T., Miyazaki, Y., Kurokawa, M., Miyazono, K., Nimer, S. D., Yamasoba, T. and Mano, H. (2016) 'Mutational landscape and antiproliferative functions of ELF transcription factors in human cancer', *Cancer Research*, 76(7), pp. 1814–1824. doi: 10.1158/0008-5472.CAN-14-3816.

Balendiran, G. K., Dabur, R. and Fraser, D. (2004) 'The role of glutathione in cancer', *Cell Biochemistry and Function*, 22(6), pp. 343–352. doi: 10.1002/cbf.1149.

De Bessa, S. A., Salaorni, S., Patrão, D. F. C., Neto, M. M., Brentani, M. M. and Nagai, M. A. (2006) 'JDP1 (DNAJC12/Hsp40) expression in breast cancer and its association with estrogen receptor status', *International Journal of Molecular Medicine*, 17(2), pp. 363–367.

Bisio, A., Zámborszky, J., Zaccara, S., Lion, M., Tebaldi, T., Sharma, V., Raimondi, I., Alessandrini, F., Ciribilli, Y. and Inga, A. (2014) 'Cooperative interactions between p53 and NFκB enhance cell plasticity.', *Oncotarget*, 5(23), pp. 12111–25. doi: 10.18632/oncotarget.2545.

De Bock, C. E., Lin, Z., Mekkawy, A. H., Byrne, J. A. and Wang, Y. (2010) 'Interaction between urokinase receptor and heat shock protein MRJ enhances cell adhesion', *Int J Oncol*, 36(5), pp. 1155–1163.

Boettcher, M., Kischkel, F. and Hoheise, J. D. (2010) 'High-definition DNA methylation profiles from breast and ovarian carcinoma cell lines with differing doxorubicin resistance', *PLoS ONE*, 5(6). doi: 10.1371/journal.pone.0011002.

Bozzacco, L., Yi, Z., Andreo, U., Conklin, C. R., Li, M. M. H., Rice, C. M. and MacDonald, M. R. (2016) 'Chaperone-Assisted Protein Folding Is Critical for Yellow Fever Virus NS3/4A Cleavage and Replication.', *Journal of virology*, 90(January), pp. 3212–3228. doi: 10.1128/JVI.03077-15.

Buggy, Y., Maguire, T. M., McDermott, E., Hill, A. D. K., O'Higgins, N. and Duffy, M. J. (2006) 'Ets2 transcription factor in normal and neoplastic human breast tissue', *European Journal of Cancer*, 42(4), pp. 485–491. doi:

10.1016/j.ejca.2005.10.018.

Buggy, Y., Maguire, T. M., McGreal, G., McDermott, E., Hill, a D. K., O'Higgins, N. and Duffy, M. J. (2004) 'Overexpression of the Ets-1 transcription factor in human breast cancer.', *British journal of cancer*, 91(7), pp. 1308–15. doi: 10.1038/sj.bjc.6602128.

Cangemi, R., Mensah, a, Albertini, V., Jain, a, Mello-Grand, M., Chiorino, G., Catapano, C. V and Carbone, G. M. (2008) 'Reduced expression and tumor suppressor function of the ETS transcription factor ESE-3 in prostate cancer.', *Oncogene*, 27(20), pp. 2877–2885. doi: 10.1038/sj.onc.1210953.

Carbone, G. M., Napoli, S., Valentini, A., Cavalli, F., Watson, D. K. and Catapano, C. V. (2004) 'Triplex DNA-mediated downregulation of Ets2 expression results in growth inhibition and apoptosis in human prostate cancer cells', *Nucleic Acids Research*, 32(14), pp. 4358–4367. doi: 10.1093/nar/gkh744.

Cardone, M., Kandilci, A., Carella, C., Nilsson, J. A., Brennan, J. A., Sirma, S., Ozbek, U., Boyd, K., Cleveland, J. L. and Grosveld, G. C. (2005) 'The novel ETS factor TEL2 cooperates with Myc in B lymphomagenesis.', *Molecular and cellular biology*, 25(6), pp. 2395–405. doi: 10.1128/MCB.25.6.2395-2405.2005.

Carella, C., Potter, M., Bonten, J., Rehg, J. E., Neale, G. and Grosveld, G. C. (2006) 'The ETS factor TEL2 is a hematopoietic oncoprotein', *Blood*, 107(3), pp. 1124–1132. doi: 10.1182/blood-2005-03-1196.

Chakrabarti, R., Hwang, J., Blanco, M. A., Wei, Y., Romano, R., Smalley, K., Liu, S., Yang, Q., Mercatali, L., Amadori, D., Haffty, B. G. and Sinha, S. (2012) 'Elf5 inhibits epithelial mesenchymal transition in mammary gland development and breast cancer metastasis by transcriptionally repressing Snail2/Slug', *Nat Cell Biol.*, 14(11), pp. 1212–1222. doi: 10.1038/ncb2607.Elf5.

Chakrabarti, S. R. and Nucifora, G. (1999) 'The leukemia-associated gene TEL encodes a transcription repressor which associates with SMRT and mSin3A.', *Biochemical and biophysical research communications*, 264, pp. 871–877. doi: 10.1006/bbrc.1999.1605.

Champagne, D. P., Hatle, K. M., Fortner, K. A., D'Alessandro, A., Thornton, T. M., Yang, R., Torralba, D., Tomás-Cortázar, J., Jun, Y. W., Ahn, K. H., Hansen, K. C., Haynes, L., Anguita, J. and Rincon, M. (2016) 'Fine-Tuning of CD8+ T Cell Mitochondrial Metabolism by the Respiratory Chain Repressor MCJ Dictates Protection to Influenza Virus', *Immunity*, 44(6), pp. 1299–1311. doi: 10.1016/j.immuni.2016.02.018.

Chang, C. H., Scott, G. K., Kuo, W. L., Xiong, X., Suzdaltseva, Y., Park, J. W., Sayre, P., Erny, K., Collins, C., Gray, J. W. and Benz, C. C. (1997) 'ESX: a structurally unique Ets overexpressed early during human breast tumorigenesis.', *Oncogene*, 14(13), pp. 1617–1622. doi: 10.1038/sj.onc.1200978.

Chen, E., Kwon, Y. T., Lim, M. S., Dubé, I. D. and Hough, M. R. (2006) 'Loss of Ubr1 promotes aneuploidy and accelerates B-cell lymphomagenesis in TLX1/HOX11-transgenic mice.', *Oncogene*, 25(42), pp. 5752–63. doi: 10.1038/sj.onc.1209573.

Chen, E. Y., Tan, C. M., Kou, Y., Duan, Q., Wang, Z., Meirelles, G. V., Clark, N. R. and Ma'ayan, A. (2013) 'Enrichr: interactive and collaborative HTML5 gene list enrichment analysis tool.', *BMC bioinformatics*, 14(1), p. 128. doi: 10.1186/1471-2105-14-128.

Chen, Q., Wei, C., Wang, Z. and Sun, M. (2016) 'Long non-coding RNAs in anti-cancer drug resistance', 8(1), pp. 1–12.

Chen, W. C., Wang, C. Y., Hung, Y. H., Weng, T. Y., Yen, M. C. and Lai, M. D. (2016) 'Systematic analysis of gene expression alterations and clinical outcomes for long-chain acyl-coenzyme A synthetase family in cancer', *PLoS ONE*, 11(5). doi: 10.1371/journal.pone.0155660.

Cohen-Salmon, M., Van Cong, N., Brugèires, L., Béroud, C., Henry, I., Junien, C. and Jeanpierre, C. (1993) 'Isolation of Kidney Complementary DNAs Down-expressed in Wilms' Tumor by a Subtractive Hybridization Approach', *Cancer Research*, 53(12), pp. 2888–2894.

Contreras, D., Irudayam, J. I., French, S. and Funari, V. (2015) 'Identification of Novel Interferon Stimulated Genes in Differentiated Hepatocytes', *FASEB*, 29(1).

Conway, K., Edmiston, S. N., Tse, C.-K., Bryant, C., Kuan, P. F., Hair, B. Y., Parrish, E. A., May, R. and Swift-Scanlan, T. (2015) 'Racial variation in breast tumor promoter methylation in the Carolina Breast Cancer Study.', *Cancer epidemiology, biomarkers & prevention : a publication of the American Association for Cancer Research, cosponsored by the American Society of Preventive Oncology*, 24(6), pp. 921–30. doi: 10.1158/1055-9965.EPI-14-1228.

Conze, D., Weiss, L., Regen, P. S., Bhushan, A., Weaver, D., Johnson, P. and Rincón, M. (2001) 'Autocrine production of interleukin 6 causes multidrug resistance in breast cancer cells', *Cancer Research*, 61(24), pp. 8851–8858.

Cote, B., Carlson, L. J., Rao, D. A. and Alani, A. W. G. (2015) 'Combinatorial resveratrol and quercetin polymeric

micelles mitigate doxorubicin induced cardiotoxicity in vitro and in vivo.', *Journal of controlled release : official journal of the Controlled Release Society*, 213(December), pp. 128–133. doi: 10.1016/j.jconrel.2015.06.040.

Curtin, N. J., Harris, A. L. and Aherne, G. W. (1991) 'Mechanism of Cell Death following Thymidylate Synthase Inhibition : Accumulation , DNA Damage , and Growth Inhibition following Exposure to CB3717 and Dipyridamole', 51(9), pp. 2346–2353.

Dallavalle, C., Albino, D., Civenni, G., Merulla, J., Ostano, P., Mello-Grand, M., Rossi, S., Losa, M., D'Ambrosio, G., Sessa, F., Thalmann, G. N., Garcia-Escudero, R., Zitella, A., Chiorino, G., Catapano, C. V. and Carbone, G. M. (2016) 'MicroRNA-424 impairs ubiquitination to activate STAT3 and promote prostate tumor progression', *Journal of Clinical Investigation*, 126(12), pp. 4585–4602. doi: 10.1172/JCI86505.

Deng, J., Lei, W., Fu, J. C., Zhang, L., Li, J. H. and Xiong, J. P. (2014) 'Targeting miR-21 enhances the sensitivity of human colon cancer HT-29 cells to chemoradiotherapy in vitro', *Biochemical and Biophysical Research Communications*. Elsevier Inc., 443(3), pp. 789–795. doi: 10.1016/j.bbrc.2013.11.064.

Deng, Z., Rong, Y., Teng, Y., Zhuang, X., Samykutty, A., Mu, J., Zhang, L., Cao, P., Yan, J., Miller, D. and Zhang, H.-G. (2016) 'Exosomes miR-126a released from MDSC induced by DOX treatment promotes lung metastasis', *Oncogene*, 36(May), pp. 1–13. doi: 10.1038/onc.2016.229.

Ding, X.-F., Wang, H.-J., Qian, L., Hu, Z.-Y., Feng, S.-F., Wu, Y., Yang, H.-H., Wu, H.-T., Fan, W.-H. and Fan, M. (2017) 'Cpne5 is Involved in Regulating Rodent Anxiety Level', *CNS Neuroscience & Therapeutics*, 23(3), pp. 266–268. doi: 10.1111/cns.12674.

Ding, X., Jin, Y., Wu, Y., Wu, Y., Wu, H., Xiong, L., Song, X., Liu, S., Fan, W. and Fan, M. (2008) 'Localization and cellular distribution of CPNE5 in embryonic mouse brain', *Brain Research*, 1224, pp. 20–28. doi: 10.1016/j.brainres.2008.05.051.

Do, M., Vv, D., Oa, B., Os, M., Dk, K., Ov, T. and Oh, M. (2015) 'The expression of CCN2, IQSEC, RSPO1, DNAJC15, RIPK2, IL13RA2, IRS1, and IRS2 genes in blood of obese boys with insulin resistance.', *Fiziol Zh.*, 61(1).

Do, P. M., Varanasi, L., Fan, S., Li, C., Kubacka, I., Newman, V., Chauhan, K., Daniels, S. R., Boccetta, M., Garrett, M. R., Li, R. and Martinez, L. A. (2012) 'Mutant p53 cooperates with ETS2 to promote etoposide resistance', *Genes and Development*, 26(8), pp. 830–845. doi: 10.1101/gad.181685.111.

Dong, Q., Chen, L., Lu, Q., Sharma, S., Li, L., Morimoto, S. and Wang, G. (2014) 'Quercetin attenuates doxorubicin cardiotoxicity by modulating Bmi-1 expression', *British Journal of Pharmacology*, 171(19), pp. 4440–4454. doi: 10.1111/bph.12795.

Dote, H., Toyooka, S., Tsukuda, K., Yano, M., Ouchida, M., Doihara, H., Suzuki, M., Chen, H., Hsieh, J., Gazdar, A. F. and Shimizu, N. (2004) 'Aberrant Promoter Methylation in Human DAB2 Interactive Protein (hDAB2IP) Gene in Breast Cancer', 10, pp. 2082–2089.

Ehrlich, M., Jiang, G., Fiala, E., Dome, J. S., Yu, M. C., Long, T. I., Youn, B., Sohn, O.-S., Widschwendter, M., Tomlinson, G. E., Chintagumpala, M., Champagne, M., Parham, D., Liang, G., Malik, K. and Laird, P. W. (2002) 'Hypomethylation and hypermethylation of DNA in Wilms tumors.', *Oncogene*, 21(43), pp. 6694–6702. doi: 10.1038/sj.onc.1205890.

Eldeeb, M. A. and Fahlman, R. P. (2014) 'The anti-apoptotic form of tyrosine kinase Lyn that is generated by proteolysis is degraded by the N-end rule pathway.', *Oncotarget*, 5(9), pp. 2714–22. doi: 10.18632/oncotarget.1931.

Feldman, R. J., Sementchenko, V. I., Gayed, M., Fraig, M. M. and Watson, D. K. (2003) 'Pdef Expression in Human Breast Cancer Is Correlated with Invasive Potential and Altered Gene Expression 1', pp. 4626–4631.

Fernández-Cabezudo, M. J., Faour, I., Jones, K., Champagne, D. P., Jaloudi, M. A., Mohamed, Y. A., Bashir, G., Almarzooqi, S., Albawardi, A., Hashim, M. J., Roberts, T. S., El-Salhat, H., El-Taji, H., Kassis, A., O'Sullivan, D. E., Christensen, B. C., DeGregori, J., Al-Ramadi, B. K. and Rincon, M. (2016) 'Deficiency of mitochondrial modulator MCJ promotes chemoresistance in breast cancer.', *JCI insight*, 1(7). doi: 10.1172/jci.insight.86873.

Foekens, J. A., Atkins, D., Zhang, Y., Sweep, F. C. G. J., Harbeck, N., Paradiso, A., Cufer, T., Sieuwerts, A. M., Talantov, D., Span, P. N., Tjan-Heijnen, V. C. G., Zito, A. F., Specht, K., Hoefler, H., Golouh, R., Schittulli, F., Schmitt, M., Beex, L. V. A. M., Klijn, J. G. M. and Wang, Y. (2006) 'Multicenter validation of a gene expression-based prognostic signature in lymph node-negative primary breast cancer', *Journal of Clinical Oncology*, 24(11), pp. 1665–1671. doi: 10.1200/JCO.2005.03.9115.

Gajulapalli, V. N. R., Samanthapudi, V. S. K., Pulaganti, M., Khumukcham, S. S., Malisetty, V. L., Guruprasad, L., Chitta, S. K. and Manavathi, B. (2016) 'A transcriptional repressive role for epithelial-specific ETS factor ELF3 on oestrogen receptor alpha in breast cancer cells', *Biochemical Journal*, 473(8), pp. 1047–1061. doi: 10.1042/BCJ20160019.

Gallego-Ortega, D., Ledger, A., Roden, D. L., Law, A. M. K., Magenau, A., Kikhtyak, Z., Cho, C., Allerdice, S. L., Lee, H. J., Valdes-Mora, F., Herrmann, D., Salomon, R., Young, A. I. J., Lee, B. Y., Sergio, C. M., Kaplan, W., Piggin, C., Conway, J. R. W., Rabinovich, B., Millar, E. K. A., Oakes, S. R., Chtanova, T., Swarbrick, A., Naylor, M. J., O'Toole, S., Green, A. R., Timpson, P., Gee, J. M. W., Ellis, I. O., Clark, S. J. and Ormandy, C. J. (2015) 'ELF5 Drives Lung Metastasis in Luminal Breast Cancer through Recruitment of Gr1+ CD11b+ Myeloid-Derived Suppressor Cells', *PLoS Biology*, 13(12). doi: 10.1371/journal.pbio.1002330.

Ghadersohi, a and Sood, a K. (2001) 'Prostate epithelium-derived Ets transcription factor mRNA is overexpressed in human breast tumors and is a candidate breast tumor marker and a breast tumor antigen.', *Clinical cancer research : an official journal of the American Association for Cancer Research*, 7(9), pp. 2731–8.

Ginsburg, I. G. S., Lucas, J., Hill, C., Woods, C. W., Us, N. C., Carin, L., Us, N. C., Zaas, A. K., Hill, C., Us, N. C., Hero, A. and Arbor, A. (2014) '(12) United States Patent'.

van Gisbergen, M. W., Voets, A. M., Starmans, M. H. W., de Coo, I. F. M., Yadak, R., Hoffmann, R. F., Boutros, P. C., Smeets, H. J. M., Dubois, L. and Lambin, P. (2015) 'How do changes in the mtDNA and mitochondrial dysfunction influence cancer and cancer therapy? Challenges, opportunities and models', *Mutation Research - Reviews in Mutation Research*. Elsevier B.V., 764, pp. 16–30. doi: 10.1016/j.mrrev.2015.01.001.

Green, A. R., Krivinskas, S., Young, P., Rakha, E. A., Paish, E. C., Powe, D. G. and Ellis, I. O. (2009) 'Loss of expression of chromosome 16q genes DPEP1 and CTCF in lobular carcinoma in situ of the breast', *Breast Cancer Research and Treatment*, 113(1), pp. 59–66. doi: 10.1007/s10549-008-9905-8.

Gross, E., Busse, B., Riemenschneider, M., Neubauer, S., Seck, K., Klein, H. G., Kiechle, M., Lordick, F. and Meindl, A. (2008) 'Strong association of a common dihydopyramidine dehydrogenase gene polymorphism with flouropyrimidine-related toxicity in cancer patients', *PLoS ONE*, 3(12), pp. 1–7. doi: 10.1371/journal.pone.0004003.

Gu, X., Shin, B. H., Akbarali, Y., Weiss, A., Boltax, J., Oettgen, P. and Libermann, T. A. (2001) 'Tel-2 is a Novel Transcriptional Repressor Related to the Ets Factor Tel/ETV-6', *Journal of Biological Chemistry*, 276(12), pp. 9421–9436. doi: 10.1074/jbc.M010070200.

Guan, F. H. X., Bailey, C. G., Metierre, C., O'Young, P., Gao, D., Khoo, T. L., Holst, J. and Rasko, J. E. J. (2017) 'The antiproliferative ELF2 isoform, ELF2B, induces apoptosis in vitro and perturbs early lymphocytic development in vivo', *Journal of Hematology & Oncology*, 10(1), p. 75. doi: 10.1186/s13045-017-0446-7.

Gunawardane, R. N., Sgroi, D. C., Wrobel, C. N., Koh, E., Daley, G. Q. and Brugge, J. S. (2005) 'Novel role for PDEF in epithelial cell migration and invasion', *Cancer Research*, 65(24), pp. 11572–11580. doi: 10.1158/0008-5472.CAN-05-1196.

Gupta, J. and Tikoo, K. (2012) 'Involvement of insulin-induced reversible chromatin remodeling in altering the expression of oxidative stress-responsive genes under hyperglycemia in 3T3-L1 preadipocytes', *Gene*, 504(2), pp. 181–191. doi: 10.1016/j.gene.2012.05.027.

Hagemann, T., Balkwill, F. and Lawrence, T. (2008) 'Inflammation and Cancer : A Double-Edged Sword', *Cancer Cell*, 12(4), pp. 300–301. doi: 10.1016/j.ccr.2007.10.005.Inflammation.

Hagman, J. and Grosschedl, R. (1992) 'An inhibitory carboxyl-terminal domain in Ets-1 and Ets-2 mediates differential binding of ETS family factors to promoter sequences of the mb-1 gene.', *Proceedings of the National Academy of Sciences of the United States of America*, 89(19), pp. 8889–93. doi: 10.1073/pnas.89.19.8889.

Hao, J.-J., Zhi, X., Wang, Y., Zhang, Z., Hao, Z., Ye, R., Tang, Z., Qian, F., Wang, Q. and Zhu, J. (2017) 'Comprehensive Proteomic Characterization of the Human Colorectal Carcinoma Reveals Signature Proteins and Perturbed Pathways', *Scientific Reports*, 7(7), p. 42436. doi: 10.1038/srep42436.

Hatle, K. M., Gummadidala, P., Navasa, N., Bernardo, E., Dodge, J., Silverstrim, B., Fortner, K., Burg, E., Suratt, B. T., Hammer, J., Radermacher, M., Taatjes, D. J., Thornton, T., Anguita, J. and Rincon, M. (2013) 'MCJ/DnaJC15, an endogenous mitochondrial repressor of the respiratory chain that controls metabolic alterations.', *Molecular and cellular biology*, 33(11), pp. 2302–2314. doi: 10.1128/MCB.00189-13.

Hatle, K. M., Neveu, W., Dienz, O., Rymarchyk, S., Barrantes, R., Hale, S., Farley, N., Lounsbury, K. M., Bond, J. P., Taatjes, D. and Rincón, M. (2007) 'Methylation-controlled J protein promotes c-Jun degradation to prevent ABCB1 transporter expression.', *Molecular and cellular biology*, 27(8), pp. 2952–2966. doi: 10.1128/MCB.01804-06.

He, J., Pan, Y., Hu, J., Albarracin, C., Wu, Y. and Dai, J. Le (2007) 'Profile of Ets gene expression in human breast carcinoma.', *Cancer biology & therapy*, 6(1), pp. 76–82. doi: 10.4161/cbt.6.1.3551.

Heisig, P. (2009) 'Type II topoisomerases - Inhibitors, repair mechanisms and mutations', *Mutagenesis*, 24(6), pp. 465–469. doi: 10.1093/mutage/gep035.

Hoffmann, A., Natoli, G. and Ghosh, G. (2006) 'Transcriptional regulation via the NF-kappaB signaling module.', *Oncogene*, 25(51), pp. 6706–16. doi: 10.1038/sj.onc.1209933.

Hogart, A., Lichtenberg, J. and Ajay, S. (2012) 'Genome-wide DNA methylation profiles in hematopoietic stem and progenitor cells reveal overrepresentation of ETS transcription factor binding sites', *Genome Research*, pp. 1407–1418. doi: 10.1101/gr.132878.111.22.

Hollenhorst, P. C., McIntosh, L. P. and Graves, B. J. (2011) 'Genomic and biochemical insights into the specificity of ETS transcription factors.', *Annual review of biochemistry*, 80(1), pp. 437–471. doi: 10.1146/annurev.biochem.79.081507.103945.

Horn, H., Lawrence, M. S., Hu, J. X., Worstell, E., Ilic, N., Shrestha, Y., Kim, E., Kamburov, A., Kashani, A., Hahn, W. C., Boehm, J. S., Getz, G. and Lage, K. (2015) 'A comparative analysis of network mutation burdens across 21 tumor types augments discovery from cancer genomes', *bioRxiv*, p. 25445. doi: 10.1101/025445.

Hua, Y., Ma, X., Liu, X., Yuan, X., Qin, H. and Zhang, X. (2017) 'Identification of the potential biomarkers for the metastasis of rectal adenocarcinoma', *Apmis*, 125(2), pp. 93–100. doi: 10.1111/apm.12633.

Huang, J., Li, H. and Ren, G. (2015) 'Epithelial-mesenchymal transition and drug resistance in breast cancer (Review)', *International Journal of Oncology*, 47(3), pp. 840–848. doi: 10.3892/ijo.2015.3084.

Ignatius Irudayam, J., Contreras, D., Spurka, L., Subramanian, A., Allen, J., Ren, S., Kanagavel, V., Nguyen, Q., Ramaiah, A., Ramamoorthy, K., French, S. W., Klein, A. S., Funari, V. and Arumugaswami, V. (2015) 'Characterization of type I interferon pathway during hepatic differentiation of human pluripotent stem cells and hepatitis C virus infection', *Stem Cell Research*, 15(2), pp. 354–364. doi: 10.1016/j.scr.2015.08.003.

Indra, M. R., Karyono, S., Ratnawati, R. and Malik, S. G. (2013) 'Quercetin suppresses inflammation by reducing ERK1/2 phosphorylation and NF kappa B activation in Leptin-induced Human Umbilical Vein Endothelial Cells (HUVECs).', *BMC research notes*, 6(1), p. 275. doi: 10.1186/1756-0500-6-275.

Irvin, B. J., Wood, L. D., Wang, L., Fenrick, R., Sansam, C. G., Packham, G., Kinch, M., Yang, E. and Hiebert, S. W. (2003) 'TEL, a Putative Tumor Suppressor, Induces Apoptosis and Represses Transcription of Bcl-XL', *Journal of Biological Chemistry*, 278(47), pp. 46378–46386. doi: 10.1074/jbc.M305189200.

Jemal, A., Bray, F. and Ferlay, J. (2011) 'Global Cancer Statistics: 2011', *CA Cancer J Clin*, 49(2), p. 1,33-64. doi: 10.3322/caac.20107.Available.

Jubinsky, P. T., Short, M. K., Mutema, G., Morris, R. E., Ciraolo, G. M. and Li, M. (2005) 'Magmas expression in neoplastic human prostate', *Journal of Molecular Histology*, 36(1–2), pp. 69–75. doi: 10.1007/s10735-004-3840-8.

Kalyuga, M., Gallego-Ortega, D., Lee, H. J., Roden, D. L., Cowley, M. J., Caldon, C. E., Stone, A., Allerdice, S. L., Valdes-Mora, F., Launchbury, R., Statham, A. L., Armstrong, N., Alles, M. C., Young, A., Egger, A., Au, W., Piggin, C. L., Evans, C. J., Ledger, A., Brummer, T., Oakes, S. R., Kaplan, W., Gee, J. M. W., Nicholson, R. I., Sutherland, R. L., Swarbrick, A., Naylor, M. J., Clark, S. J., Carroll, J. S. and Ormandy, C. J. (2012) 'ELF5 Suppresses Estrogen Sensitivity and Underpins the Acquisition of Antiestrogen Resistance in Luminal Breast Cancer', *PLoS Biology*, 10(12). doi: 10.1371/journal.pbio.1001461.

Kar, A. and Gutierrez-Hartmann, A. (2013) 'Molecular mechanisms of ETS transcription factor-mediated tumorigenesis.', *Critical reviews in biochemistry and molecular biology*, 48(6), pp. 522–43. doi: 10.3109/10409238.2013.838202.

Kaul, S. C., Deocaris, C. C. and Wadhwa, R. (2007) 'Three faces of mortalin: A housekeeper, guardian and killer', *Experimental Gerontology*, 42(4), pp. 263–274. doi: 10.1016/j.exger.2006.10.020.

Kawagoe, H., Potter, M., Ellis, J. and Grosveld, G. C. (2004) 'TEL2, an ETS factor expressed in human leukemia, regulates monocytic differentiation of U937 cells and blocks the inhibitory effect of TEL1 on Ras-induced cellular transformation', *Cancer Research*, 64(17), pp. 6091–6100. doi: 10.1158/0008-5472.CAN-04-0839.

Keane, M. M., Lowrey, G. A., Ettenberg, S. A., Dayton, M. A. and Lipkowitz, S. (1996) 'The protein tyrosine phosphatase DEP-1 is induced during differentiation and inhibits growth of breast cancer cells.', *Cancer research*, 56(18), pp. 4236–43.

Kim, B., Stephen, S. L., Hanby, A. M., Horgan, K., Perry, S. L., Richardson, J., Roundhill, E. A., Valleley, E. M. A., Verghese, E. T., Williams, B. J., Thorne, J. L. and Hughes, T. A. (2015) 'Chemotherapy induces Notch1-dependent MRP1 up-regulation, inhibition of which sensitizes breast cancer cells to chemotherapy.', *BMC cancer*. BMC Cancer, 15(1), p. 634. doi: 10.1186/s12885-015-1625-y.

Kim, C. W., Asai, D., Kang, J.-H., Kishimura, A., Mori, T. and Katayama, Y. (2015) 'Reversal of efflux of an anticancer drug in human drug-resistant breast cancer cells by inhibition of protein kinase Cα (PKCα) activity', *Tumor*

Biology, 37(2). doi: 10.1007/s13277-015-3963-4.

Kim, S. W., Hayashi, M., Lo, J. F., Fearns, C., Xiang, R., Lazennec, G., Yang, Y. and Lee, J. D. (2005) 'Tid1 negatively regulates the migratory potential of cancer cells by inhibiting the production of interleukin-8', *Cancer Research*, 65(19), pp. 8784–8791. doi: 10.1158/0008-5472.CAN-04-4422.

Kok, M., Koornstra, R. H., Margarido, T. C., Fles, R., Armstrong, N. J., Linn, S. C., Van't Veer, L. J. and Weigelt, B. (2009) 'Mammosphere-derived gene set predicts outcome in patients with ER-positive breast cancer', *Journal of Pathology*, 218(3), pp. 316–326. doi: 10.1002/path.2544.

Kuleshov, M. V, Jones, M. R., Rouillard, A. D., Fernandez, N. F., Duan, Q., Wang, Z., Koplev, S., Jenkins, S. L., Jagodnik, K. M., Lachmann, A., McDermott, M. G., Monteiro, C. D., Gundersen, G. W. and Ma'ayan, A. (2016) 'Enrichr: a comprehensive gene set enrichment analysis web server 2016 update.', *Nucleic acids research*, 44(W1), pp. W90-7. doi: 10.1093/nar/gkw377.

Kunderfranco, P., Mello-Grand, M., Cangemi, R., Pellini, S., Mensah, A., Albertini, V., Malek, A., Chiorino, G., Catapano, C. V. and Carbone, G. M. (2010) 'ETS transcription factors control transcription of EZH2 and epigenetic silencing of the tumor suppressor gene Nkx3.1 in prostate cancer', *PLoS ONE*, 5(5). doi: 10.1371/journal.pone.0010547.

Lau, D. T., Hesson, L. B., Norris, M. D., Marshall, G. M., Haber, M. and Ashton, L. J. (2012) 'Prognostic significance of promoter DNA methylation in patients with childhood neuroblastoma', *Clinical Cancer Research*, 18(20), pp. 5690–5700. doi: 10.1158/1078-0432.CCR-12-0294.

Leng, S., Wu, G., Collins, L. B., Thomas, C. L., Tellez, C. S., Jauregui, A. R., Picchi, M. A., Zhang, X., Juri, D. E., Desai, D., Amin, S. G., Crowell, R. E., Stidley, C. A., Liu, Y., Swenberg, J. A., Lin, Y., Wathelet, M. G., Gilliland, F. D. and Belinsky, S. A. (2015) 'Implication of a chromosome 15q15.2 locus in regulating UBR1 and predisposing smokers to MGMT methylation in lung', *Cancer Research*, 75(15), pp. 3108–3117. doi: 10.1158/0008-5472.CAN-15-0243.

Levine, A. J. and Oren, M. (2009) 'The first 30 years of p53: growing ever more complex.', *Nature reviews. Cancer*, 9(10), pp. 749–58. doi: 10.1038/nrc2723.

Li, Y., Liang, Q., Wen, Y., Chen, L., Wang, L., Liu, Y., Luo, C., Liang, H., Li, M. and Li, Z. (2010) 'Comparative proteomics analysis of human osteosarcomas and benign tumor of bone', *Cancer Genetics and Cytogenetics*, 198(2), pp. 97–106. doi: 10.1016/j.cancergencyto.2010.01.003.

Lindsey, J. C., Lusher, M. E., Strathdee, G., Brown, R., Gilbertson, R. J., Bailey, S., Ellison, D. W. and Clifford, S. C. (2006) 'Epigenetic inactivation of MCJ (DNAJD1) in malignant paediatric brain tumours', *International Journal of Cancer*, 118(2), pp. 346–352. doi: 10.1002/ijc.21353.

Liu, R., Wang, X., Chen, G. Y., Dalerba, P., Gurney, A., Hoey, T., Sherlock, G., Lewicki, J., Shedden, K. and Clarke, M. F. (2007) 'The Prognostic Role of a Gene Signature from Tumorigenic Breast-Cancer Cells', *New England Journal of Medicine*, 356(3), pp. 217–226. doi: 10.1056/NEJMoa063994.

Liu, Z., Balasubramanian, V., Bhat, C., Vahermo, M., Mäkilä, E., Kemell, M., Fontana, F., Janoniene, A., Petrikaite, V., Salonen, J., Yli-Kauhaluoma, J., Hirvonen, J., Zhang, H. and Santos, H. A. (2016) 'Quercetin-Based Modified Porous Silicon Nanoparticles for Enhanced Inhibition of Doxorubicin-Resistant Cancer Cells', *Advanced Healthcare Materials*, 6(3), p. 1601009. doi: 10.1002/adhm.201601009.

Longoni, N., Sarti, M., Albino, D., Civenni, G., Malek, A., Ortelli, E., Pinton, S., Mello-Grand, M., Ostano, P., D'Ambrosio, G., Sessa, F., Garcia-Escudero, R., Thalmann, G. N., Chiorino, G., Catapano, C. V. and Carbone, G. M. (2013) 'ETS transcription factor ESE1/ELF3 orchestrates a positive feedback loop that constitutively activates NF-kB and drives prostate cancer progression', *Cancer Research*, 73(14), pp. 4533–4547. doi: 10.1158/0008-5472.CAN-12-4537.

Lopez, R. G., Carron, C., Oury, C., Gardellin, P., Bernard, O. and Ghysdael, J. (1999) 'TEL is a sequence-specific transcriptional repressor', *Journal of Biological Chemistry*, 274(42), pp. 30132–30138. doi: 10.1074/jbc.274.42.30132.

Luo, X., Yang, S., Zhou, C., Pan, F., Li, Q. and Ma, S. (2015) 'MicroRNA-328 enhances cellular motility through posttranscriptional regulation of PTPRJ in human hepatocellular carcinoma', *OncoTargets and Therapy*, 8, pp. 3159–3167. doi: 10.2147/OTT.S93056.

Lv, L., Liu, C., Chen, C., Yu, X., Chen, G., Shi, Y., Qin, F., Ou, J., Qiu, K. and Li, G. (2016) 'Quercetin and doxorubicin co-encapsulated biotin receptortargeting nanoparticles for minimizing drug resistance in breast cancer.', *Oncotarget*, 7(22). doi: 10.18632/oncotarget.8607.

Ma, J., Hou, X., Li, M., Ren, H., Fang, S., Wang, X. and He, C. (2015) 'Genome-wide methylation profiling reveals new biomarkers for prognosis prediction of glioblastoma', *Journal of Cancer Research and Therapeutics*, 11(6), p. 212. doi: 10.4103/0973-1482.168188.

Maeda, O., Ando, T., Ohmiya, N., Ishiguro, K., Watanabe, O., Miyahara, R., Hibi, Y., Nagai, T., Yamada, K. and Goto, H. (2014) 'Alteration of gene expression and DNA methylation in drug-resistant gastric cancer', *Oncology Reports*, 31(4), pp. 1883–1890. doi: 10.3892/or.2014.3014.

Majidinia, M. and Yousefi, B. (2017) 'Breast tumor stroma: A driving force in the development of resistance to therapies', *Chemical Biology & Drug Design*. doi: 10.1111/cbdd.12893.

Matos, J. M., Witzmann, F. A., Cummings, O. W. and Schmidt, C. M. (2009) 'A Pilot Study of Proteomic Profiles of Human Hepatocellular Carcinoma in the United States', *Journal of Surgical Research*, 155(2), pp. 237–243. doi: 10.1016/j.jss.2008.06.008.

Matsuda, T., Yamamoto, T., Muraguchi, A. and Saatcioglu, F. (2001) 'Cross-talk between transforming growth factor-beta and estrogen receptor signaling through Smad3', *J Biol Chem*, 276(46), pp. 42908–42914. doi: 10.1074/jbc.M105316200.

McFadyen, M. C. E., Melvin, W. T. and Murray, G. I. (2004) 'Cytochrome P450 enzymes: novel options for cancer therapeutics.', *Molecular cancer therapeutics*, 3(3), pp. 363–371.

Menendez, D., Inga, A. and Resnick, M. a (2009) 'The expanding universe of p53 targets.', *Nature reviews. Cancer*, 9(10), pp. 724–737. doi: 10.1038/nrc2730.

Menezes, M. E., Mitra, A., Shevde, L. A. and Samant, R. S. (2012) 'DNAJB6 governs a novel regulatory loop determining Wnt/β-catenin signalling activity', *Biochemical Journal*, 444(3), pp. 573–580. doi: 10.1042/BJ20120205.

Di Michele, M., Marcone, S., Cicchillitti, L., Della Corte, A., Ferlini, C., Scambia, G., Donati, M. B. and Rotilio, D. (2010) 'Glycoproteomics of paclitaxel resistance in human epithelial ovarian cancer cell lines: towards the identification of putative biomarkers', *Journal of Proteomics*, 73(5), pp. 879–898. doi: 10.1016/j.jprot.2009.11.012.

Minaei, A., Sabzichi, M., Ramezani, F., Hamishehkar, H. and Samadi, N. (2016) 'Co-delivery with nano-quercetin enhances doxorubicin-mediated cytotoxicity against MCF-7 cells', *Molecular Biology Reports*, 43(2), pp. 99–105. doi: 10.1007/s11033-016-3942-x.

Minin, G., Bellazzo, A., Ferro, M. D., Chiaruttini, G., Nuzzo, S., Bicciato, S., Piazza, S., Rami, D., Bulla, R., Sommaggio, R., Rosato, A. and Sal, G. Del (2014) 'Mutant p53 Reprograms TNF Signaling in Cancer Cells through Interaction with the Tumor Suppressor DAB2IP', *Molecular Cell*. Elsevier Inc., 56(5), pp. 617–629. doi: 10.1016/j.molcel.2014.10.013.

Mitra, A., Fillmore, R. a, Metge, B. J., Rajesh, M., Xi, Y., King, J., Ju, J., Pannell, L., Shevde, L. a and Samant, R. S. (2008) 'Large isoform of MRJ (DNAJB6) reduces malignant activity of breast cancer.', *Breast cancer research : BCR*, 10(2), p. R22. doi: 10.1186/bcr1874.

Mitra, A., Menezes, M. E., Shevde, L. A. and Samant, R. S. (2010) 'DNAJB6 induces degradation of β-catenin and causes partial reversal of mesenchymal phenotype', *Journal of Biological Chemistry*, 285(32), pp. 24686–24694. doi: 10.1074/jbc.M109.094847.

Mitra, A., Rostas, J. W., Dyess, D. L., Shevde, L. a and Samant, R. S. (2012) 'Micro-RNA-632 downregulates DNAJB6 in breast cancer', *Laboratory Investigation*, 92(9), pp. 1310–1317. doi: 10.1038/labinvest.2012.87.

Molina-Pinelo, S., Gutiérrez, G., Pastor, M. D., Hergueta, M., Moreno-Bueno, G., Garcia-Carbonero, R., Nogal, A., Suarez, R., Salinas, A., Pozo-Rodriguez, F., Lopez-Rios, F., Agullo-Ortuno, M. T., Ferrer, I., Perpin, A., Palacios, J., Carnero, A. and Paz-Ares, L. (2014) 'MicroRNA-dependent regulation of transcription in non-small cell lung cancer', *PLoS ONE*, 9(3). doi: 10.1371/journal.pone.0090524.

Molinari, a, Calcabrini, A., Meschini, S., Stringaro, A., Crateri, P., Toccacieli, L., Marra, M., Colone, M., Cianfriglia, M. and Arancia, G. (2002) 'Subcellular detection and localization of the drug transporter P-glycoprotein in cultured tumor cells.', *Current protein & peptide science*, 3(6), pp. 653–70. doi: 10.2174/1389203023380413.

Muthusamy, V., Duraisamy, S., Bradbury, C. M., Hobbs, C., Curley, D. P., Nelson, B. and Bosenberg, M. (2006) 'Epigenetic silencing of novel tumor suppressors in malignant melanoma', *Cancer Research*, 66(23), pp. 11187–11193. doi: 10.1158/0008-5472.CAN-06-1274.

Navasa, N., Martin-Ruiz, I., Atondo, E., Sutherland, J. D., Angel Pascual-Itoiz, M., Carreras-González, A., Izadi, H., Tomás-Cortázar, J., Ayaz, F., Martin-Martin, N., Torres, I. M., Barrio, R., Carracedo, A., Olivera, E. R., Rincón, M. and Anguita, J. (2015) 'Ikaros mediates the DNA methylation-independent silencing of MCJ/DNAJC15 gene expression in macrophages.', *Scientific reports*, 5(April), p. 14692. doi: 10.1038/srep14692.

Neri, F., Rapelli, S., Krepelova, A., Incarnato, D., Parlato, C., Basile, G., Maldotti, M., Anselmi, F. and Oliviero, S. (2017) 'Intragenic DNA methylation prevents spurious transcription initiation', *Nature*. Nature Publishing Group,

543(7643), pp. 72–77. doi: 10.1038/nature21373.

Nikulenkov, F., Spinnler, C., Li, H., Tonelli, C., Shi, Y., Turunen, M., Kivioja, T., Ignatiev, I., Kel, A., Taipale, J. and Selivanova, G. (2012) 'Insights into p53 transcriptional function via genome- wide chromatin occupancy and gene expression analysis', *Cell death and differentiation*, 19(12), pp. 1992–2002. doi: 10.1038/cdd.2012.89.

Paik, S., Shak, S., Tang, G., Kim, C., Baker, J., Cronin, M., Baehner, F. L., Walker, M. G., Watson, D., Park, T., Hiller, W., Fisher, E. R., Wickerham, D. L., Bryant, J. and Wolmark, N. (2004) 'A multigene assay to predict recurrence of tamoxifen-treated, node-negative breast cancer.', *The New England journal of medicine*, 351(27), pp. 2817–26. doi: 10.1056/NEJMoa041588.

Pan, S. T., Li, Z. L., He, Z. X., Qiu, J. X. and Zhou, S. F. (2016) 'Molecular mechanisms for tumour resistance to chemotherapy', *Clinical and Experimental Pharmacology and Physiology*, 43(8), pp. 723–737. doi: 10.1111/1440-1681.12581.

Park, J., Munagala, I., Xu, H., Blankenship, D., Maffucci, P., Chaussabel, D., Banchereau, J., Pascual, V. and Cunningham-Rundles, C. (2013) 'Interferon Signature in the Blood in Inflammatory Common Variable Immune Deficiency', *PLoS ONE*, 8(9). doi: 10.1371/journal.pone.0074893.

Park, S. Y., Lee, S., Cho, H. J., Kim, T. W., Kim, J., Kim, J. W., Lee, C., Kim, B., Yeom, Y. Il, Lim, J., Lee, Y. and Lee, H. G. (2016) 'Dehydropeptidase 1 promotes metastasis through regulation of E-cadherin expression in colon cancer', *Oncotarget*, 7(8). doi: 10.18632/oncotarget.7033.

Parker, J. S., Mullins, M., Cheung, M. C. U., Leung, S., Voduc, D., Vickery, T., Davies, S., Fauron, C., He, X., Hu, Z., Quackenhush, J. F., Stijleman, I. J., Palazzo, J., Matron, J. S., Nobel, A. B., Mardis, E., Nielsen, T. O., Ellis, M. J., Perou, C. M. and Bernard, P. S. (2009) 'Supervised risk predictor of breast cancer based on intrinsic subtypes', *Journal of Clinical Oncology*, 27(8), pp. 1160–1167. doi: 10.1200/JCO.2008.18.1370.

Pei, X., Zhang, J., Wu, L., Lü, B., Zhang, X., Yang, D. and Liu, J. (2013) 'The down-regulation of GNAO1 and its promoting role in hepatocellular carcinoma.', *Bioscience reports*, 33(5). doi: 10.1042/BSR20130001.

Perou, C. M., Sørlie, T., Eisen, M. B., van de Rijn, M., Jeffrey, S. S., Rees, C. a, Pollack, J. R., Ross, D. T., Johnsen, H., Akslen, L. a, Fluge, O., Pergamenschikov, a, Williams, C., Zhu, S. X., Lønning, P. E., Børresen-Dale, a L., Brown, P. O. and Botstein, D. (2000) 'Molecular portraits of human breast tumours.', *Nature*, 406(6797), pp. 747–752. doi: 10.1038/35021093.

Peters, G. J., Van Triest, B., Backus, H. H. J., Kuiper, C. M., Van Der Wilt, C. L. and Pinedo, H. M. (2000) 'Molecular downstream events and induction of thymidylate synthase in mutant and wild-type p53 colon cancer cell lines after treatment with 5-fluorouracil and the thymidylate synthase inhibitor raltitrexed', *European Journal of Cancer*, 36(7), pp. 916–924. doi: 10.1016/S0959-8049(00)00026-5.

Pferdehirt, L. M. (2015) 'The contribution of the ETS-domain transcription factor EHF to breast cancer dormancy and recurrence', *Penn Thesis Dissertation*.

Piggin, C. L., Roden, D. L., Gallego-Ortega, D., Lee, H. J., Oakes, S. R. and Ormandy, C. J. (2016) 'ELF5 isoform expression is tissue-specific and significantly altered in cancer', *Breast Cancer Research*. Breast Cancer Research, 18(1), p. 4. doi: 10.1186/s13058-015-0666-0.

Poirel, H., Lopez, R. G., Lacronique, V., Della Valle, V., Mauchauffé, M., Berger, R., Ghysdael, J. and Bernard, O. a (2000) 'Characterization of a novel ETS gene, TELB, encoding a protein structurally and functionally related to TEL.', *Oncogene*, 19(41), pp. 4802–6. doi: 10.1038/sj.onc.1203830.

Poizat, C., Puri, P. L., Bai, Y. and Kedes, L. (2005) 'Phosphorylation-dependent degradation of p300 by doxorubicin-activated p38 mitogen-activated protein kinase in cardiac cells.', *Molecular and cellular biology*, 25(7), pp. 2673–87. doi: 10.1128/MCB.25.7.2673-2687.2005.

Pop, M. S., Stransky, N., Garvie, C. W., Theurillat, J.-P., Hartman, E. C., Lewis, T. A., Zhong, C., Culyba, E. K., Lin, F., Daniels, D. S., Pagliarini, R., Ronco, L., Koehler, A. N. and Garraway, L. A. (2014) 'A small molecule that binds and inhibits the ETV1 transcription factor oncoprotein.', *Molecular cancer therapeutics*, 13(6), pp. 1492–502. doi: 10.1158/1535-7163.MCT-13-0689.

Porporato, P. E., Payen, V. L., Pérez-Escuredo, J., De Saedeleer, C. J., Danhier, P., Copetti, T., Dhup, S., Tardy, M., Vazeille, T., Bouzin, C., Feron, O., Michiels, C., Gallez, B. and Sonveaux, P. (2014) 'A mitochondrial switch promotes tumor metastasis', *Cell Reports*, 8(3), pp. 754–766. doi: 10.1016/j.celrep.2014.06.043.

Potter, M. D., Buijs, A., Kreider, B., van Rompaey, L. and Grosveld, G. C. (2000) 'Identification and characterization of a new human ETS-family transcription factor, TEL2, that is expressed in hematopoietic tissues and can associate with TEL1/ETV6.', *Blood*, 95(11), pp. 3341–8.

Prat, A. and Perou, C. M. (2011) 'Deconstructing the molecular portraits of breast cancer', *Molecular Oncology*,

5(1), pp. 5–23. doi: 10.1016/j.molonc.2010.11.003.

Prescott, J. D., Koto, K. S. N., Singh, M. and Gutierrez-Hartmann, A. (2004) 'The ETS transcription factor ESE-1 transforms MCF-12A human mammary epithelial cells via a novel cytoplasmic mechanism.', *Molecular and cellular biology*, 24(12), pp. 5548–64. doi: 10.1128/MCB.24.12.5548-5564.2004.

Qiao, D., Li, M., Pu, J., Wang, W., Zhu, W. and Liu, H. (2016) 'Loss of Protein Tyrosine Phosphatase Receptor J Expression Predicts an Aggressive Clinical Course in Patients with Esophageal Squamous Cell Carcinoma', *Pathology & Oncology Research*, 22(3), pp. 541–547. doi: 10.1007/s12253-015-0036-3.

Quintana, A. M., Picchione, F., Klein Geltink, R. I., Taylor, M. R. and Grosveld, G. C. (2014) 'Zebrafish ETV7 regulates red blood cell development through the cholesterol synthesis pathway.', *Disease models & mechanisms*, 7(2), pp. 265–70. doi: 10.1242/dmm.012526.

Raz, S., Stark, M. and Assaraf, Y. G. (2014) 'Binding of a Smad4 / Ets-1 complex to a novel intragenic regulatory element in exon12 of FPGS underlies decreased gene expression and antifolate resistance in leukemia', 5(19).

Rempel, H., Sun, B., Calosing, C., Abadjian, L., Monto, A. and Pulliam, L. (2013) 'Monocyte Activation in HIV/HCV Coinfection Correlates with Cognitive Impairment', *PLoS ONE*, 8(2). doi: 10.1371/journal.pone.0055776.

Ringnér, M., Fredlund, E., Häkkinen, J., Borg, Å. and Staaf, J. (2011) 'GOBO: Gene expression-based outcome for breast cancer online', *PLoS ONE*, 6(3), pp. 1–11. doi: 10.1371/journal.pone.0017911.

Risbridger, G. P., Davis, I. D., Birrell, S. N. and Tilley, W. D. (2010) 'Breast and prostate cancer: more similar than different', *Nature Reviews Cancer*, 10(3), pp. 205–12. doi: 10.1038/nrc2795.

Roberts, A. B. and Wakefield, L. M. (2003) 'The two faces of transforming growth factor in carcinogenesis', *Proceedings of the National Academy of Sciences*, 100(15), pp. 8621–8623. doi: 10.1073/pnas.1633291100.

Roesch, A., Vultur, A., Bogeski, I., Wang, H., Zimmermann, K., Speicher, D., Körbel, C., Laschke, M., Gimotty, P., Philipp, S., Krause, E., Pätzold, S., Villanueva, J., Krepler, C., Fukunaga-Kalabis, M., Hoth, M., Bastian, B., Vogt, T. and Herlyn, M. (2013) 'Overcoming intrinsic multidrug resistance in melanoma by blocking the mitochondrial respiratory chain of slow-cycling JARID1Bhigh cells', *Cancer Cell*, 23(6), pp. 811–825. doi: 10.1016/j.ccr.2013.05.003.

Van Rompaey, L., Dou, W., Buijs, A. and Grosveld, G. (1999) 'Tel, a frequent target of leukemic translocations, induces cellular aggregation and influences expression of extracellular matrix components.', *Neoplasia (New York, N.Y.)*, 1(6), pp. 526–36. doi: http://dx.doi.org/10.1038/sj.neo.7900064.

Roukens, M. G., Alloul-Ramdhani, M., Baan, B., Kobayashi, K., Peterson-Maduro, J., van Dam, H., Schulte-Merker, S. and Baker, D. a (2010) 'Control of endothelial sprouting by a Tel-CtBP complex.', *Nature cell biology*, 12(10), pp. 933–42. doi: 10.1038/ncb2096.

Saha, S., Mukherjee, S., Khan, P., Kajal, K., Mazumdar, M., Manna, A., Mukherjee, S., De, S., Jana, D., Sarkar, D. K. and Das, T. (2016) 'Aspirin suppresses the acquisition of chemoresistance in breast cancer by disrupting an NFkB-IL6 signaling axis responsible for the generation of cancer stem cells', *Cancer Research*, 76(7), pp. 2000–2012. doi: 10.1158/0008-5472.CAN-15-1360.

Sakasai, R. and Iwabuchi, K. (2015) 'The distinctive cellular responses to DNA strand breaks caused by a DNA topoisomerase I poison in conjunction with DNA replication and RNA transcription', *Genes Genet. Syst*, 90(4), pp. 187–194. doi: 10.1266/ggs.15-00023.

Sakurai, T., Yamada, T., Kihara-Negishi, F., Teramoto, S., Sato, Y., Izawa, T. and Oikawa, T. (2003) 'Effects of overexpression of the Ets family transcription factor TEL on cell growth and differentiation of K562 cells.', *International journal of oncology*, 22(6), pp. 1327–1333.

Sang, Y., Chen, M.-Y., Luo, D., Zhang, R.-H., Wang, L., Li, M., Luo, R., Qian, C.-N., Shao, J.-Y., Zeng, Y.-X. and Kang, T. (2015) 'TEL2 suppresses metastasis by down-regulating SERPINE1 in nasopharyngeal carcinoma.', *Oncotarget*, 6(30), pp. 29240–53. doi: 10.18632/oncotarget.5074.

Sarver, A. L., Murray, C. D., Temiz, N. A., Tseng, Y. Y. and Bagchi, A. (2016) 'MYC and PVT1 synergize to regulate RSPO1 levels in breast cancer', *Cell Cycle*, 15(7), pp. 881–885. doi: 10.1080/15384101.2016.1149660.

Schick, U. M., Jain, D., Hodonsky, C. J., Morrison, J. V., Davis, J. P., Brown, L., Sofer, T., Conomos, M. P., Schurmann, C., McHugh, C. P., Nelson, S. C., Vadlamudi, S., Stilp, A., Plantinga, A., Baier, L., Bien, S. A., Gogarten, S. M., Laurie, C. A., Taylor, K. D., Liu, Y., Auer, P. L., Franceschini, N., Szpiro, A., Rice, K., Kerr, K. F., Rotter, J. I., Hanson, R. L., Papanicolaou, G., Rich, S. S., Loos, R. J. F., Browning, B. L., Browning, S. R., Weir, B. S., Laurie, C. C., Mohlke, K. L., North, K. E., Thornton, T. A. and Reiner, A. P. (2016) 'Genome-wide Association Study of Platelet Count Identifies Ancestry-Specific Loci in Hispanic/Latino Americans', *American Journal of Human Genetics*. The American Society of Human Genetics, 98(2), pp. 229–242. doi: 10.1016/j.ajhg.2015.12.003.

Schusdziarra, C., Blamowska, M., Azem, A. and Hell, K. (2013) 'Methylation-controlled J-protein MCJ acts in the import of proteins into human mitochondria', *Human Molecular Genetics*, 22(7), pp. 1348–1357. doi: 10.1093/hmg/dds541.

Selvaraj, N., Kedage, V. and Hollenhorst, P. C. (2015) 'Comparison of MAPK specificity across the ETS transcription factor family identifies a high-affinity ERK interaction required for ERG function in prostate cells.', *Cell communication and signaling : CCS*, 13(1), p. 12. doi: 10.1186/s12964-015-0089-7.

Semenchenko, K., Wasylyk, C., Cheung, H., Tourrette, Y., Maas, P., Schalken, J. A., van der Pluijm, G. and Wasylyk, B. (2016) 'XRP44X, an Inhibitor of Ras/Erk Activation of the Transcription Factor Elk3, Inhibits Tumour Growth and Metastasis in Mice', *Plos One*, 11(7), p. e0159531. doi: 10.1371/journal.pone.0159531.

Shaikhibrahim, Z., Lindstrot, A., Ellinger, J., Rogenhofer, S., Buettner, R., Perner, S. and Wernert, N. (2012) 'The peripheral zone of the prostate is more prone to tumor development than the transitional zone: Is the ETS family the key?', *Molecular Medicine Reports*, 5(2), pp. 313–316. doi: 10.3892/mmr.2011.647.

Sharma, V., Young, L., Allison, A. B., Owen, K., Iorns, E., Gunn, W., Tan, F., Lomax, J., Perfito, N. and Errington, T. (2016) 'Registered report: Diverse somatic mutation patterns and pathway alterations in human cancers', *eLife*, 5(FEBRUARY2016). doi: 10.7554/eLife.11566.

Shridhar, V., Bible, K. C., Staub, J., Avula, R., Lee, Y. K., Kalli, K., Huang, H., Hartmann, L. C., Kaufmann, S. H. and Smith, D. I. (2001) 'Loss of expression of a new member of the DNAJ protein family confers resistance to chemotherapeutic agents used in the treatment of ovarian cancer', *Cancer Research*, 61(10), pp. 4258–4265.

Sinha, D. and D'Silva, P. (2014) 'Chaperoning mitochondrial permeability transition: regulation of transition pore complex by a J-protein, DnaJC15.', *Cell death & disease*, 5(3), p. e1101. doi: 10.1038/cddis.2014.72.

Sinha, D., Srivastava, S. and D'Silva, P. (2016) 'Functional diversity of human mitochondrial j-proteins is independent of their association with the inner membrane presequence translocase', *Journal of Biological Chemistry*, 291(33), pp. 17345–17359. doi: 10.1074/jbc.M116.738146.

Sinha, D., Srivastava, S., Krishna, L. and D'Silva, P. (2014) 'Unraveling the intricate organization of mammalian mitochondrial presequence translocases: existence of multiple translocases for maintenance of mitochondrial function.', *Molecular and cellular biology*, 34(10), pp. 1757–75. doi: 10.1128/MCB.01527-13.

Skibinski, A. and Kuperwasser, C. (2015) 'The origin of breast tumor heterogeneity', *Oncogene*, 34(November 2014), pp. 1–8. doi: 10.1038/onc.2014.475.

Smart, C. E., Askarian Amiri, M. E., Wronski, A., Dinger, M. E., Crawford, J., Ovchinnikov, D. A., Vargas, A. C., Reid, L., Simpson, P. T., Song, S., Wiesner, C., French, J. D., Dave, R. K., da Silva, L., Purdon, A., Andrew, M., Mattick, J. S., Lakhani, S. R., Brown, M. A. and Kellie, S. (2012) 'Expression and function of the protein tyrosine phosphatase receptor J (PTPRJ) in normal mammary epithelial cells and breast tumors', *PLoS ONE*, 7(7). doi: 10.1371/journal.pone.0040742.

Spring, K., Fournier, P., Lapointe, L., Chabot, C., Roussy, J., Pommey, S., Stagg, J. and Royal, I. (2015) 'The protein tyrosine phosphatase DEP-1/PTPRJ promotes breast cancer cell invasion and metastasis', *Oncogene*, 34(44), pp. 5536–5547. doi: 10.1038/onc.2015.9.

La Starza, R., Aventin, A., Matteucci, C., Crescenzi, B., Romoli, S., Testoni, N., Pierini, V., Ciolli, S., Sambani, C., Locasciulli, A., Di Bona, E., Lafage-Pochitaloff, M., Martelli, M. F., Marynen, P. and Mecucci, C. (2006) 'Genomic gain at 6p21: a new cryptic molecular rearrangement in secondary myelodysplastic syndrome and acute myeloid leukemia.', *Leukemia : official journal of the Leukemia Society of America, Leukemia Research Fund, U.K*, 20(6), pp. 958–64. doi: 10.1038/sj.leu.2404208.

Sterrenberg, J. N., Blatch, G. L. and Edkins, A. L. (2011) 'Human DNAJ in cancer and stem cells', *Cancer Letters*. Elsevier Ireland Ltd, 312(2), pp. 129–142. doi: 10.1016/j.canlet.2011.08.019.

Strathdee, G., Davies, B. R., Vass, J. K., Siddiqui, N. and Brown, R. (2004) 'Cell type-specific methylation of an intronic CpG island controls expression of the MCJ gene', *Carcinogenesis*, 25(5), pp. 693–701. doi: 10.1093/carcin/bgh066.

Strathdee, G., Vass, J. K., Oien, K. A., Siddiqui, N., Curto-Garcia, J. and Brown, R. (2005) 'Demethylation of the MCJ gene in stage III/IV epithelial ovarian cancer and response to chemotherapy', *Gynecologic Oncology*, 97(3), pp. 898–903. doi: 10.1016/j.ygyno.2005.03.023.

Strauss, J. and Figg, W. D. (2016) 'Using epigenetic therapy to overcome chemotherapy resistance', *Anticancer Research*, 36(1), pp. 1–4.

Sultana, R., Theodoraki, M. A. and Caplan, A. J. (2012) 'UBR1 promotes protein kinase quality control and sensitizes cells to Hsp90 inhibition', *Experimental Cell Research*, 318(1), pp. 53–60. doi:

10.1016/j.yexcr.2011.09.010.

Szász, A. M., Lánczky, A., Nagy, Á., Förster, S., Hark, K., Green, J. E., Boussioutas, A., Busuttil, R., Szabó, A., Győrffy, B., Szász, A. M., Lánczky, A., Nagy, Á., Förster, S., Hark, K., Green, J. E., Boussioutas, A., Busuttil, R., Szabó, A. and Győrffy, B. (2016) 'Cross-validation of survival associated biomarkers in gastric cancer using transcriptomic data of 1,065 patients', *Oncotarget*, 7(31), pp. 49322–49333. doi: 10.18632/oncotarget.10337.

Tripathi, S., Pohl, M. O., Zhou, Y., Rodriguez-Frandsen, A., Wang, G., Stein, D. A., Moulton, H. M., Dejesus, P., Che, J., Mulder, L. C. F., Yanguez, E., Andenmatten, D., Pache, L., Manicassamy, B., Albrecht, R. A., Gonzalez, M. G., Nguyen, Q., Brass, A., Elledge, S., White, M., Shapira, S., Hacohen, N., Karlas, A., Meyer, T. F., Shales, M., Gatorano, A., Johnson, J. R., Jang, G., Johnson, T., Verschueren, E., Sanders, D., Krogan, N., Shaw, M., Koenig, R., Stertz, S., Garcia-Sastre, A. and Chanda, S. K. (2015) 'Meta- and Orthogonal Integration of Influenza "oMICs" Data Defines a Role for UBR4 in Virus Budding', *Cell Host and Microbe*, 18(6), pp. 723–735. doi: 10.1016/j.chom.2015.11.002.

Turner, D. P., Findlay, V. J., Moussa, O. and Watson, D. K. (2007) 'Defining ETS transcription regulatory networks and their contribution to breast cancer progression', *Journal of Cellular Biochemistry*, 102(3), pp. 549–559. doi: 10.1002/jcb.21494.

Turner, D. P., Moussa, O., Sauane, M., Fisher, P. B. and Watson, D. K. (2007) 'Prostate-derived ETS factor is a mediator of metastatic potential through the inhibition of migration and invasion in breast cancer', *Cancer Research*, 67(4), pp. 1618–1625. doi: 10.1158/0008-5472.CAN-06-2913.

Veer, V. L., Dai, H., van de Vijver, M. J., He, Y. D., Hart, A. A., Mao, M., Peterse, H. L., van der Kooy, K., Marton, M. J., Witteveen, A. T., Schreiber, G. J., Kerkhoven, R. M., Roberts, C., Linsley, P. S., Bernards, R. and Friend, S. H. (2002) 'Gene expression profiling predicts clinical outcome of breast cancer.', *Nature*, 415(6871), pp. 530–536. doi: http://dx.doi.org/http://dx.doi.org/10.1038/415530a.

Vivekanand, P. and Rebay, I. (2012) 'The sam domain of human TEL2 can abrogate transcriptional output from TEL1 (ETV-6) and ETS1/ETS2', *PLoS ONE*, 7(5), pp. 5–10. doi: 10.1371/journal.pone.0037151.

Vyas, D., Laput, G. and Vyas, A. K. (2014) 'Chemotherapy-enhanced inflammation may lead to the failure of therapy and metastasis', *OncoTargets and Therapy*, 7, pp. 1015–1023. doi: 10.2147/OTT.S60114.

Walerych, D., Lisek, K., Sommaggio, R., Piazza, S., Ciani, Y., Dalla, E., Rajkowska, K., Gaweda-Walerych, K., Ingallina, E., Tonelli, C., Morelli, M. J., Amato, A., Eterno, V., Zambelli, A., Rosato, A., Amati, B., Wiśniewski, J. R. and Del Sal, G. (2016) 'Proteasome machinery is instrumental in a common gain-of-function program of the p53 missense mutants in cancer.', *Nature cell biology*, 18(8), pp. 897–909. doi: 10.1038/ncb3380.

Walerych, D., Napoli, M., Collavin, L. and Del Sal, G. (2012) 'The rebel angel: Mutant p53 as the driving oncogene in breast cancer', *Carcinogenesis*, 33(11), pp. 2007–2017. doi: 10.1093/carcin/bgs232.

Wang, C. C., Liao, Y. P., Mischel, P. S., Iwamoto, K. S., Cacalano, N. A. and McBride, W. H. (2006) 'HDJ-2 as a target for radiosensitization of glioblastoma multiforme cells by the farnesyltransferase inhibitor R115777 and the role of the p53/p21 pathway', *Cancer Research*, 66(13), pp. 6756–6762. doi: 10.1158/0008-5472.CAN-06-0185.

Wang, K. S., Zuo, L., Pan, Y., Xie, C. and Luo, X. (2015) 'Genetic variants in the CPNE5 gene are associated with alcohol dependence and obesity in Caucasian populations', *Journal of Psychiatric Research*, 71, pp. 1–7. doi: 10.1016/j.jpsychires.2015.09.008.

Wang, L. and Hiebert, S. W. (2001) 'TEL contacts multiple co-repressors and specifically associates with histone deacetylase-3.', *Oncogene*, 20(28), pp. 3716–3725. doi: 10.1038/sj.onc.1204479.

Wang, T., Srivastava, S., Hartman, M., Buhari, S. A., Chan, C.-W., Iau, P., Khin, L. W., Wong, A., Tan, S.-H., Goh, B.-C. and Lee, S.-C. (2016) 'High expression of intratumoral stromal proteins is associated with chemotherapy resistance in breast cancer', *Oncotarget*, 7(34), pp. 55155–55168.

Wasylyk, B., Hagman, J. and Gutierrez-hartmann, A. (1998) 'Ets transcription factors : nuclear effectors of the Ras – MAP-kinase signaling pathway', 4(June), pp. 213–216.

Wasylyk, C., Kerckaert, J. P. and Wasylyk, B. (1992) 'A novel modulator domain of Ets transcription factors', *Genes and Development*, 6(6), pp. 965–974. doi: 10.1101/gad.6.6.965.

Watson, D. K., Turner, D. P., Scheiber, M. N., Findlay, V. J. and Watson, P. M. (2010) 'ETS Transcription Factor Expression and Conversion During Prostate and Breast Cancer Progression', *The Open Cancer Journal*, 3(1), pp. 24–39. doi: 10.2174/1874079001003010024.

Wei, G.-H., Badis, G., Berger, M. F., Kivioja, T., Palin, K., Enge, M., Bonke, M., Jolma, A., Varjosalo, M., Gehrke, A. R., Yan, J., Talukder, S., Turunen, M., Taipale, M., Stunnenberg, H. G., Ukkonen, E., Hughes, T. R., Bulyk, M. L., Taipale, J., Agarkar, V., Babayeva, N., Wilder, P., Rizzino, A., Tahirov, T., Audic, S., Claverie, J., Bailey, T., Elkan, C., Bartel, F., Higuchi, T., Spyropoulos, D., Batchelor, A., Piper, D., Brousse, F. de la, McKnight, S., Wolberger, C., Beitel, G., Tuck,

S., Greenwald, I., Horvitz, H., Berger, M., Badis, G., Gehrke, A., Talukder, S., Philippakis, A., Pena-Castillo, L., Alleyne, T., Mnaimneh, S., Botvinnik, O., Chan, E., Khalid, F., Zhang, W., Newburger, D., Jaeger, S., Morris, Q., Bulyk, M., Hughes, T., Berger, M., Philippakis, A., Qureshi, A., He, F., Estep, P., Bulyk, M., Boros, J., Donaldson, I., O'Donnell, A., Odrowaz, Z., Zeef, L., Lupien, M., Meyer, C., Liu, X., Brown, M., Sharrocks, A., Brunner, D., Ducker, K., Oellers, N., Hafen, E., Scholz, H., Klambt, C., Bryne, J., Valen, E., Tang, M., Marstrand, T., Winther, O., Piedade, I. da, Krogh, A., Lenhard, B., Sandelin, A., Bult, C., Eppig, J., Kadin, J., Richardson, J., Blake, J., Choi, Y., Sinha, S., Cooper, S., Trinklein, N., Nguyen, L., Myers, R., Dahl, R., Ramirez-Bergeron, D., Rao, S., Simon, M., Dalton, S., Treisman, R., DeKoter, R., Lee, H., Singh, H., Delattre, O., Zucman, J., Plougastel, B., Desmaze, C., Melot, T., Peter, M., Kovar, H., Joubert, I., Jong, P. de, Rouleau, G., Echeverri, C., Beachy, P., Baum, B., Boutros, M., Buchholz, F., Chanda, S., Downward, J., Ellenberg, J., Fraser, A., Hacohen, N., Hahn, W., Jackson, A., Kiger, A., Linsley, P., Lum, L., Ma, Y., Mathey-Prevot, B., Root, D., Sabatini, D., Taipale, J., Falcon, S., Gentleman, R., Fitzsimmons, D., Hodsdon, W., Wheat, W., Maira, S., Wasylyk, B., Hagman, J., Fitzsimmons, D., Lutz, R., Wheat, W., Chamberlin, H., Hagman, J., Frey, B., Dueck, D., Galang, C., Muller, W., Foos, G., Oshima, R., Hauser, C., Gangwal, K., Sankar, S., Hollenhorst, P., Kinsey, M., Haroldsen, S., Shah, A., Boucher, K., Watkins, W., Jorde, L., Graves, B., Lessnick, S., Garvie, C., Hagman, J., Wolberger, C., Golub, T., Barker, G., Bohlander, S., Hiebert, S., Ward, D., Bray-Ward, P., Morgan, E., Raimondi, S., Rowley, J., Gilliland, D., Hallikas, O., Palin, K., Sinjushina, N., Rautiainen, R., Partanen, J., Ukkonen, E., Taipale, J., Hallikas, O., Taipale, J., Heintzman, N., Ren, B., Heintzman, N., Stuart, R., Hon, G., Fu, Y., Ching, C., Hawkins, R., Barrera, L., Calcar, S. Van, Qu, C., Ching, K., Wang, W., Weng, Z., Green, R., Crawford, G., Ren, B., Hollenhorst, P., Chandler, K., Poulsen, R., Johnson, W., Speck, N., Graves, B., Hollenhorst, P., Jones, D., Graves, B., Hollenhorst, P., Shah, A., Hopkins, C., Graves, B., Karim, F., Urness, L., Thummel, C., Klemsz, M., McKercher, S., Celada, A., Beveren, C. Van, Maki, R., Gunther, C., Nye, J., Kielbasa, S., Gonze, D., Herzel, H., Kodandapani, R., Pio, F., Ni, C., Piccialli, G., Klemsz, M., McKercher, S., Maki, R., Ely, K., Kumar-Sinha, C., Tomlins, S., Chinnaiyan, A., Laajala, T., Raghav, S., Tuomela, S., Lahesmaa, R., Aittokallio, T., Elo, L., Lamber, E., Vanhille, L., Textor, L., Kachalova, G., Sieweke, M., Wilmanns, M., Laudet, V., Hanni, C., Stehelin, D., Duterque-Coquillaud, M., Leprince, D., Gegonne, A., Coll, J., Taisne, C. de, Schneeberger, A., Lagrou, C., Stehelin, D., Li, H., Ruan, J., Durbin, R., Li, M., Elledge, S., Löytynoja, A., Goldman, N., Löytynoja, A., Goldman, N., Mahony, S., Benos, P., Matys, V., Kel-Margoulis, O., Fricke, E., Liebich, I., Land, S., Barre-Dirrie, A., Reuter, I., Chekmenev, D., Krull, M., Hornischer, K., Voss, N., Stegmaier, P., Lewicki-Potapov, B., Saxel, H., Kel, A., Wingender, E., Mavrothalassitis, G., Ghysdael, J., Messina, D., Glasscock, J., Gish, W., Lovett, M., Metivier, R., Penot, G., Hubner, M., Reid, G., Brand, H., Kos, M., Gannon, F., Mo, Y., Vaessen, B., Johnston, K., Marmorstein, R., Mo, Y., Vaessen, B., Johnston, K., Marmorstein, R., Nix, D., Courdy, S., Boucher, K., Noyes, M., Christensen, R., Wakabayashi, A., Stormo, G., Brodsky, M., Wolfe, S., Nunn, M., Seeburg, P., Moscovici, C., Duesberg, P., Nye, J., Petersen, J., Gunther, C., Jonsen, M., Graves, B., Oettgen, P., Finger, E., Sun, Z., Akbarali, Y., Thamrongsak, U., Boltax, J., Grall, F., Dube, A., Weiss, A., Brown, L., Quinn, G., Kas, K., Endress, G., Kunsch, C., Libermann, T., O'Neill, E., Rebay, I., Tjian, R., Rubin, G., Pepke, S., Wold, B., Mortazavi, A., Pufall, M., Lee, G., Nelson, M., Kang, H., Velyvis, A., Kay, L., McIntosh, L., Graves, B., Ravasi, T., Suzuki, H., Cannistraci, C., Katayama, S., Bajic, V., Tan, K., Akalin, A., Schmeier, S., Kanamori-Katayama, M., Bertin, N., Carninci, P., Daub, C., Forrest, A., Gough, J., Grimmond, S., Han, J., Hashimoto, T., Hide, W., Hofmann, O., Kawaji, H., Ray-Gallet, D., Mao, C., Tavitian, A., Moreau-Gachelin, F., Richardson, L., Venkataraman, S., Stevenson, P., Yang, Y., Burton, N., Rao, J., Fisher, M., Baldock, R., Davidson, D., Christiansen, J., Robertson, G., Hirst, M., Bainbridge, M., Bilenky, M., Zhao, Y., Zeng, T., Euskirchen, G., Bernier, B., Varhol, R., Delaney, A., Thiessen, N., Griffith, O., He, A., Marra, M., Snyder, M., Jones, S., Roepcke, S., Grossmann, S., Rahmann, S., Vingron, M., Schober, M., Rebay, I., Perrimon, N., Sharrocks, A., Shore, P., Sharrocks, A., Shore, P., Whitmarsh, A., Bhaskaran, R., Davis, R., Waltho, J., Sharrocks, A., Smyth, G., Sorensen, P., Lessnick, S., Lopez-Terrada, D., Liu, X., Triche, T., Denny, C., Taipale, J., Cooper, M., Maiti, T., Beachy, P., Tirode, F., Laud-Duval, K., Prieur, A., Delorme, B., Charbord, P., Delattre, O., Tomlins, S., Laxman, B., Dhanasekaran, S., Helgeson, B., Cao, X., Morris, D., Menon, A., Jing, X., Cao, Q., Han, B., Yu, J., Wang, L., Montie, J., Rubin, M., Pienta, K., Roulston, D., Shah, R., Varambally, S., Mehra, R., Chinnaiyan, A., Tomlins, S., Rhodes, D., Perner, S., Dhanasekaran, S., Mehra, R., Sun, X., Varambally, S., Cao, X., Tchinda, J., Kuefer, R., Lee, C., Montie, J., Shah, R., Pienta, K., Rubin, M., Chinnaiyan, A., Treisman, R., Marais, R., Wynne, J., Valouev, A., Johnson, D., Sundquist, A., Medina, C., Anton, E., Batzoglou, S., Myers, R., Sidow, A., Verger, A., Duterque-Coquillaud, M., Virbasius, J., Virbasius, C., Scarpulla, R., Vrieseling, E., Arber, S., Wang, Y., Feng, L., Said, M., Balderman, S., Fayazi, Z., Liu, Y., Ghosh, D., Gulick, A., Wasylyk, C., Bradford, A., Gutierrez-Hartmann, A., Wasylyk, B., Woods, D., Ghysdael, J., Owen, M., Workman, C., Yin, Y., Corcoran, D., Ideker, T., Stormo, G., Benos, P., Wu, Z., Irizarry, R., Gentleman, R., Martinez-Murillo, F. and Spencer, F. (2010) 'Genome-wide analysis of ETS-family DNA-binding in vitro and in vivo.', *The EMBO journal*. Nature Publishing Group, 29(13), pp. 2147–60. doi: 10.1038/emboj.2010.106.

Weichselbaum, R. R., Ishwaran, H., Yoon, T., Nuyten, D. S. A., Baker, S. W., Khodarev, N., Su, A. W., Shaikh, A. Y., Roach, P., Kreike, B., Roizman, B., Bergh, J., Pawitan, Y., van de Vijver, M. J. and Minn, A. J. (2008) 'An interferon-related gene signature for DNA damage resistance is a predictive marker for chemotherapy and radiation for breast cancer.', *Proceedings of the National Academy of Sciences of the United States of America*, 105(47), pp. 18490–5. doi: 10.1073/pnas.0809242105.

Witham, J., Vidot, S., Agarwal, R., Kaye, S. B. and Richardson, A. (2008) 'Transient ectopic expression as a method

to detect genes conferring drug resistance', *International Journal of Cancer*, 122(11), pp. 2641–2645. doi: 10.1002/ijc.23427.

Wu, R., Nie, Q., Tapper, E. E., Jerde, C. R., Dunlap, G. S., Shrestha, S., Elraiyah, T. A., Offer, S. M. and Diasio, R. B. (2016) 'Histone H3K27 trimethylation modulates 5-fluorouracil resistance by inhibiting PU.1 binding to the DPYD promoter', *Cancer Research*, 76(21), pp. 6362–6373. doi: 10.1158/0008-5472.CAN-16-1306.

Xie, D., Gore, C., Liu, J., Pong, R.-C., Mason, R., Hao, G., Long, M., Kabbani, W., Yu, L., Zhang, H., Chen, H., Sun, X., Boothman, D. a, Min, W. and Hsieh, J.-T. (2010) 'Role of DAB2IP in modulating epithelial-to-mesenchymal transition and prostate cancer metastasis.', *Proceedings of the National Academy of Sciences of the United States of America*, 107(6), pp. 2485–2490. doi: 10.1073/pnas.0908133107.

Yan, C., Chen, Y., Kong, W., Fu, L., Liu, Y., Yao, Q. and Yuan, Y. (2017) 'PVT1-derived miR-1207-5p promotes breast cancer cell growth by targeting STAT6', *Cancer Science*. doi: 10.1111/cas.13212.

Yan, C. M., Zhao, Y. L., Cai, H. Y., Miao, G. Y. and Ma, W. (2015) 'Blockage of PTPRJ promotes cell growth and resistance to 5-FU through activation of JAK1/STAT3 in the cervical carcinoma cell line C33A', *Oncology Reports*, 33(4), pp. 1737–1744. doi: 10.3892/or.2015.3769.

Yao, D., Ding, S., Burchell, B., Wolf, C. R. and Friedberg, T. (2000) 'Detoxication of vinca alkaloids by human P450 CYP3A4-mediated metabolism: implications for the development of drug resistance.', *The Journal of pharmacology and experimental therapeutics*, 294(1), pp. 387–395.

Yardley, D. A. (2013) 'Drug Resistance and the Role of Combination Chemotherapy in Improving Patient Outcomes', 2013.

Yi, Z., Sperzel, L., Nürnberger, C., Bredenbeek, P. J., Lubick, K. J., Best, S. M., Stoyanov, C. T., Law, L. M. J., Yuan, Z., Rice, C. M. and Macdonald, M. R. (2011) 'Identification and characterization of the host protein DNAJC14 as a broadly active Flavivirus replication modulator', *PLoS Pathogens*, 7(1). doi: 10.1371/journal.ppat.1001255.

Yi, Z., Yuan, Z., Rice, C. M. and MacDonald, M. R. (2012) 'Flavivirus Replication Complex Assembly Revealed by DNAJC14 Functional Mapping', *Journal of Virology*, 86(21), pp. 11815–11832. doi: 10.1128/JVI.01022-12.

Yu, K. Da, Zhu, R., Zhan, M., Rodriguez, A. A., Yang, W., Wong, S., Makris, A., Lehmann, B. D., Chen, X., Mayer, I., Pietenpol, J. A., Shao, Z. M., Symmans, W. F. and Chang, J. C. (2013) 'Identification of prognosis-relevant subgroups in patients with chemoresistant triple-negative breast cancer', *Clinical Cancer Research*, 19(10), pp. 2723–2733. doi: 10.1158/1078-0432.CCR-12-2986.

Zhang, G., Schetter, A., He, P., Funamizu, N., Gaedcke, J., Ghadimi, B. M., Ried, T., Hassan, R., Yfantis, H. G., Lee, D. H., Lacy, C., Maitra, A., Hanna, N., Alexander, H. R. and Hussain, S. P. (2012) 'DPEP1 inhibits tumor cell invasiveness, enhances chemosensitivity and predicts clinical outcome in pancreatic ductal adenocarcinoma', *PLoS ONE*, 7(2). doi: 10.1371/journal.pone.0031507.

Zhang, P., Ma, Y., Wang, F., Yang, J., Liu, Z., Peng, J. and Qin, H. (2012) 'Comprehensive gene and microRNA expression profiling reveals the crucial role of hsa-let-7i and its target genes in colorectal cancer metastasis', *Molecular Biology Reports*, 39(2), pp. 1471–1478. doi: 10.1007/s11033-011-0884-1.

10. ANNEXES

ANNEX 1.1: ETV7 can promote breast cancer cell migration and anchorage-independent growth

This study mainly focused on the transcriptional role of ETV7 in breast cancer cells chemoresistance. However, our group is also investigating whether ETV7 may promote breast cancer aggressiveness by influencing also other biological processes. ETV7 was identified as one of the top synergistically genes up-regulated by the combined treatment with Doxorubicin and TNF-α in MCF7 cells, a condition that has been associated by our group to increased migration as previously stated (Bisio *et al.*, 2014). Therefore, ETV7 may be directly implicated in promoting breast cancer cells migration. To verify this hypothesis, I performed wound healing assay in MDA-MB-231 cells stably over-expressing ETV7 compared to the clone stably transfected with an empty vector. MDA-MB-231 cells over-expressing ETV7 showed increased reclosure percentage (Annex Fig. 1.1A), therefore supporting the supposed theory of a possible role for ETV7 in breast cancer migration. Given the toxicity related to ETV7 silencing observed by our laboratory in breast cancer cells, it is not possible to further check the ETV7 role in migration by gene silencing. In addition, I explored the ability of ETV7 to promote anchorage-independent growth by the soft agar colony formation assay using as a a model the MDA-MB-231-ETV7 and the empty cells. Annex Figure 1.1B shows the higher number of colonies found in ETV7 over-expressing cells with respect to the empty control, thus supporting a relevant implication for ETV7 also in anchorage-independent cell growth.

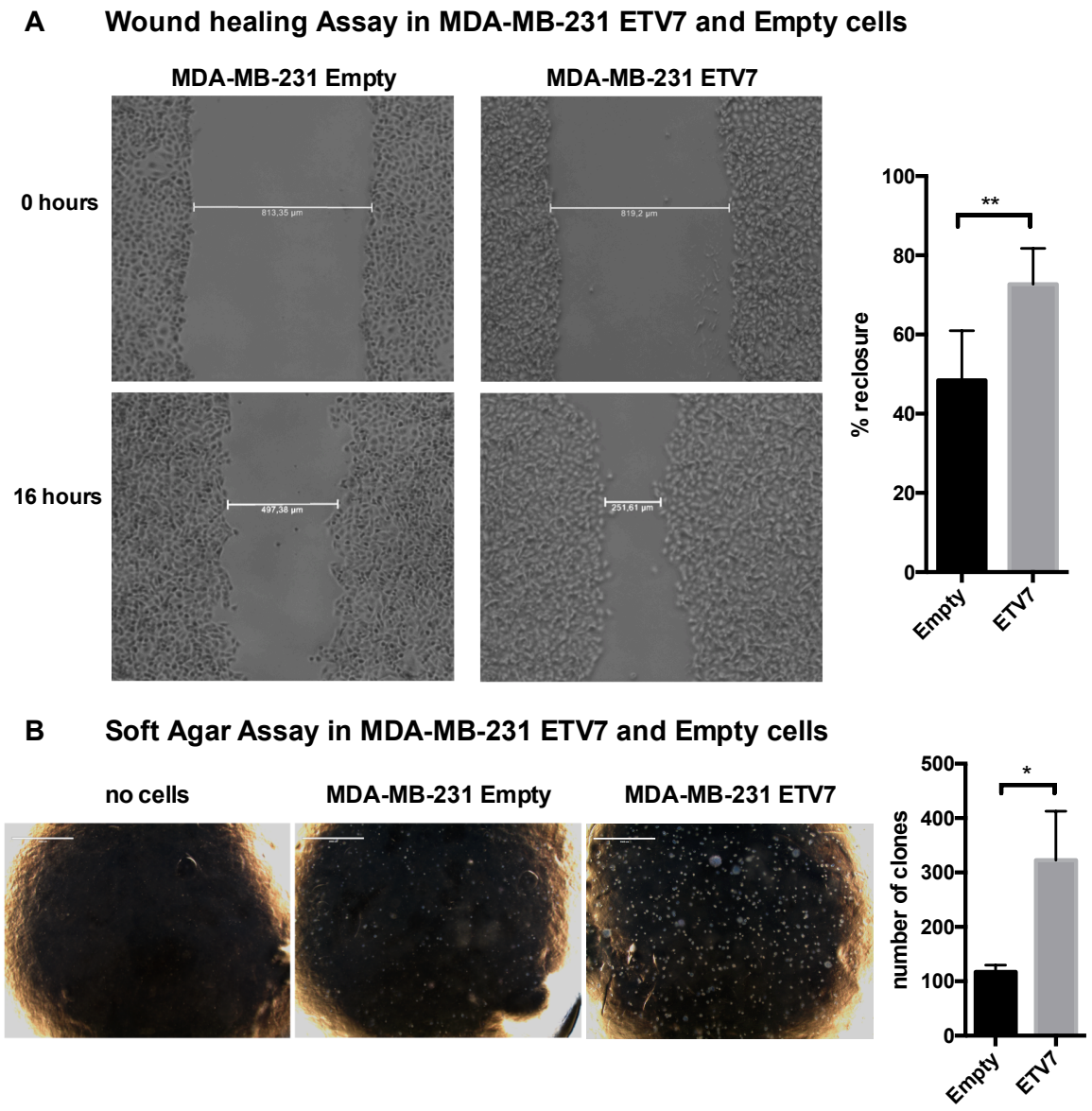

ANNEX-Figure1. 1: A) Representative pictures for wound healing assay in MDA-MB-231-ETV7 and Empty cells, showing the wound and the distance between the two edges at time 0 and after 16 hours from the generation of the wound. The graph on the right indicates calculated mean reclosing percentages of 8 indipendent samples. B) Representative results for soft agar assay in MDA-MB-231-ETV7 and Empty cells; on the left are presented images obtained at the stereomicroscope and, on the right, a graph of the counted number of colonies from three independent biological replicates. * indicates P-value (T-test)< 0.05 and ** indicates P-value (T-test)< 0.01.

ANNEX 1.2: A possible role for ETV7 in RSV infection

ChIP-seq enrichment analysis suggested a role for ETV7 in inflammation and response to pathogens, including viruses, for which the activation of ETV7 was already reported upon HCV infection (Rempel *et al.*, 2013). Therefore, I wanted to determine if ETV7 was also activated upon other types of viral infection. I observed ETV7 activation upon RSV infection

and a concomitant DNAJC14 repression in CRL4050 (an immortalized cell line from human normal lung airway tissue), MCF7 and MDA-MB-231 cells (Annex Fig. 1.2). This suggests that probably the decrease of DNAJC14 is more involved in the inflammation response rather than in the direct regulation of drug response. Nevertheless, from this data it is not possible to determine if ETV7 is the responsible for DNAJC14 repression or if this occours independently.

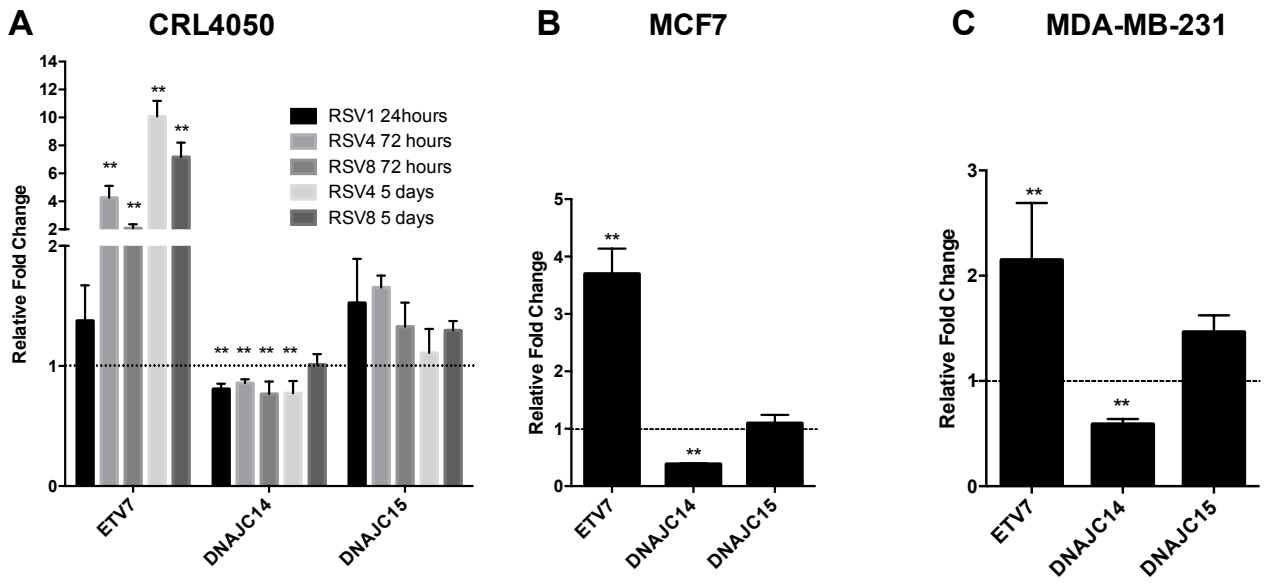

ANNEX-Figure1. 2: A) qPCR analysis of ETV7, DNAJC14 and DNAJC15 expression upon RSV infection in CRL4050 cells. B-C) qPCR analysis of ETV7, DNAJC14 and DNAJC15 expression upon RSV infection (RSV4, 5days) in MCF7 (B) and in MDA-MB-231 cells (C). ** indicates P-value (T-test)< 0.01.

ADDITIONAL ANNEXES: Personal contribution as author in published articles

During the first year of PhD project, I contributed to Bisio et al. 2014 manuscript, performing the nuclear and cytoplasmic protein fractionation followed by Western Blot analysis, and the ChIP-qPCR analysis of selected genes. This study was the starting point for my PhD project based on the analysis of ETV7 functions, one of the highly synergistically activated genes by Doxorubicin and TNF-α combined treatment in breast cancer cells (ANNEX2.1).

Among the list of genes synergistically activated, we identified also LAMP3, a member of the LAMP family, for which it was still missing in the literature a review summarizing the involvement of its family in cancer and that motivated my interest in writing a review, recently submitted to "Seminars in Oncology" journal in its revised version (ANNEX2.4).

Furthermore, my acquired experience in ChIP-qPCR assay was also exploited for contributing to the Tebaldi, Zaccara et al. 2015 manuscript (ANNEX2.2) for the validation of p53 targets discovered by bioinformatical analysis.

Lastly, most of the data presented in this thesis project are collected in the manuscript I wrote, which was recently submitted to "Breast Cancer Research" journal (ANNEX2.3).

ANNEX 2.1

www.impactjournals.com/oncotarget/ Oncotarget, Advance Publications 2014

Cooperative interactions between p53 and NFκB enhance cell plasticity

Alessandra Bisio[1], Judit Zámborszky[1,3], Sara Zaccara[1], Mattia Lion[1,4], Toma Tebaldi[2], Vasundhara Sharma[1], Ivan Raimondi[1], Federica Alessandrini[1], Yari Ciribilli[1], Alberto Inga[1]

[1]Laboratory of Transcriptional Networks, Centre for Integrative Biology, CIBIO, University of Trento, Trento, 38123, Italy

[2]Laboratory of Translational Genomics, Centre for Integrative Biology, CIBIO, University of Trento, Trento, 38123, Italy

[3]Institute of Enzymology, Research Centre for Natural Sciences, Budapest, Hungary

[4]Department of Genetics, Massachusetts General Hospital, Boston, MA, USA

correspondence to:
Yari Ciribilli, **e-mail:** ciribilli@science.unitn.it
Alberto Inga, **e-mail:** inga@science.unitn.it

Keywords: p53, NFkB, chemotherapy, doxorubicin, TNFα, EMT, synergy, breast cancer

Received: June 25, 2014 ***Accepted:*** October 01, 2014 ***Published:*** October 21, 2014

ABSTRACT

The p53 and NFκB sequence-specific transcription factors play crucial roles in cell proliferation and survival with critical, even if typically opposite, effects on cancer progression. To investigate a possible crosstalk between p53 and NFκB driven by chemotherapy-induced responses in the context of an inflammatory microenvironment, we performed a proof of concept study using MCF7 cells. Transcriptome analyses upon single or combined treatments with doxorubicin (Doxo, 1.5μM) and the NFκB inducer TNF-alpha (TNFα, 5ng/ml) revealed 432 up-regulated (log_2 FC> 2), and 390 repressed genes (log_2 FC< -2) for the Doxo+TNFα treatment. 239 up-regulated and 161 repressed genes were synergistically regulated by the double treatment. Annotation and pathway analyses of Doxo+TNFα selectively up-regulated genes indicated strong enrichment for cell migration terms. A panel of genes was examined by qPCR coupled to p53 activation by Doxo, 5-Fluoruracil and Nutlin-3a, or to p53 or NFκB inhibition. Transcriptome data were confirmed for 12 of 15 selected genes and seven (PLK3, LAMP3, ETV7, UNC5B, NTN1, DUSP5, SNAI1) were synergistically up-regulated after Doxo+TNFα and dependent both on p53 and NFκB. Migration assays consistently showed an increase in motility for MCF7 cells upon Doxo+TNFα. A signature of 29 Doxo+TNFα highly synergistic genes exhibited prognostic value for luminal breast cancer patients, with adverse outcome correlating with higher relative expression. We propose that the crosstalk between p53 and NFκB can lead to the activation of specific gene expression programs that may impact on cancer phenotypes and potentially modify the efficacy of cancer therapy.

INTRODUCTION

Cancer cells are continuously exposed to a number of signaling cues that reflect the distinct nature of the microenvironment at primary tumor site, metastastic lesions and potentially also during circulation in the blood stream [1–4]. Therapeutic intervention strategies can result in acute changes in microenvironment signaling, acting also through non-transformed cellular components resident at the primary tumor site [3, 5]. Cellular responses to changes in the microenvironment requires coordinated activation of sequence-specific transcription factors [6], among which NFκB and p53 have a prominent role and often opposing functions [7].

The p53 tumor suppressor gene is activated in response to a large number of cellular stress signals, including genotoxic stress, carbon and oxygen deficiencies, excessive proliferation signals [8, 9]. There are >150 established p53 target genes that link p53 to many different biological outcomes [10–14].

The NFκB family of sequence-specific transcription factors consists of essential regulators of immune, inflammatory, proliferative and apoptotic responses [15], and their activation generally results in the onset of pro-survival signals [16]. The most common form of the NFκB complexes is the p50/RELA (p65) heterodimer. p53 and NFκB activation occurs simultaneously in response to diverse stress conditions, including genotoxic stress and NFκB proteins are frequently de-regulated in cancer, resulting in constitutive activation [17]. Competition between p53 and NFκB for a common limiting cofactor such as p300 can result in mutual inhibition [17, 18]. However, examples of positive interactions have also been reported. For example, it was shown that p65 can induce the p53 target gene p21 by direct binding to its promoter [19] and participates in p53-dependent apoptosis [20]. Several human Toll-like receptors (TLRs), whose signaling leads to NFκB activation [21], were identified as direct p53 target genes both in cancer cells and primary cells [22] and it was demonstrated that p53 and NFκB can cooperate in the activation of pro-inflammatory genes in primary human monocytes and macrophages [23].

To investigate more globally the transcriptional crosstalk between p53 and NFκB we performed a proof of concept study using breast cancer-derived MCF7 cells treated with Doxorubicin, Tumor Necrosis Factor alpha (TNFα) and a combination of the two compounds (Doxo+TNFα). Our results demonstrated a synergistic interaction between p53 and NFκB transcription factors, which can lead to the reprogramming of cell fate and enhanced migratory potential. Seven genes (PLK3, LAMP3, ETV7, UNC5B, NTN1, DUSP5, SNAI1) were established as synergistically up-regulated after Doxo+TNFα and dependent both on p53 and NFκB. A 29-gene signature of highly synergistic genes up-regulated by Doxo+TNFα appeared to have prognostic value in a cohort of luminal breast cancer patients [24].

RESULTS

Striking transcriptome changes upon the combination of Doxorubicin and TNFα treatment of MCF7 cells

We first investigated the potential crosstalk between Doxorubicin (Doxo) and TNFα treatment using gene reporter assays in the human breast adenocarcinoma-derived MCF7 cells (Figure S1A). p53-dependent responsiveness of the P21 and MDM2 promoter plasmid constructs was observed following Doxo treatment and confirmed by p53 silencing. The transactivation of the P21 and MDM2 constructs was reduced upon addition of TNFα to Doxo, suggesting possible inhibition of p53 activity by NFκB. Mutual inhibition of the p53 and p65/RELA proteins has been previously shown on p21 [17], while both inhibition and cooperation were reported at the BAX gene [18, 20]. However, this effect was not observed at the level of the endogenous P21 and MDM2 genes (Figure S1B), which showed similar level of activation in response to either Doxo alone or Doxo+TNFα. An NFκB reporter construct was responsive to both Doxo and TNFα as single treatments and showed a strong increase following the double treatment that was unaffected by p53 silencing. On the contrary, the endogenous TNFα and MCP1 NFκB target genes were weakly responsive to Doxo alone, highly induced by TNFα treatment, and showed intermediate induction levels upon double treatment. Hence, canonical p53 or NFκB target genes did not exhibit synergistic transcriptional responses to the combined treatment with doxorubicin and TNFα.

Next we performed a genome-wide transcriptome analysis after Doxo, TNFα, or the combination of the two compounds using the Agilent 4 × 44k array and single color labeling. Differentially expressed genes (DEGs) were selected based on rank product test, setting a threshold of 0.05 on the percentage of false positives (pfp) and a threshold of 2 on the absolute log2 fold changes. The double treatment more than doubled the number of DEGs (Figure 1). The vast majority of DEGs resulting from the single treatments were also differentially expressed in the double treatment. Gene Ontology (GO) as well as pathway and upstream regulators analyses (DAVID, http://david.abcc.ncifcrf.gov/; IPA, http://www.ingenuity.com/) confirmed activation of p53 signaling upon Doxo treatment as most significant pathway, and apoptosis induction as the most significantly enriched GO terms among up-regulated DEGs (Figure 1A-C). TNFα treatment also resulted in gene annotation terms consistent with NFκB activation, such as regulation of T cell activation. The gene annotation of DEGs resulting from the double treatment was enriched for terms typical of the two single treatments (*e.g.* T cell activation and apoptosis regulation among the up-regulated DEGs). TP53 as an upstream regulator was less significant in the double treatment compared to the Doxo single treatment, while p65/RELA, NFKBIA, IRF7 and STAT1 appeared to be even more enriched in the double treatment compared to TNFα single treatment (Figure 1B). The double treatment not only led to a higher number of DEGs, but resulted in quantitative differences in gene expression levels compared to the single treatments. We applied a rigorous filter and identified 212 repressed, 361 induced DEGs that were synergistically regulated by the double treatment Doxo+TNFα (see Methods) (Figure 1D). Notably, this subgroup of up-regulated DEGs was enriched for cell migration GO biological process along with the expected canonical terms for p53 and NFκB. Collectively, our systematic analysis indicates a vast network of genes that can be mutually affected by combined activation of p53- and NFκB-dependent responses.

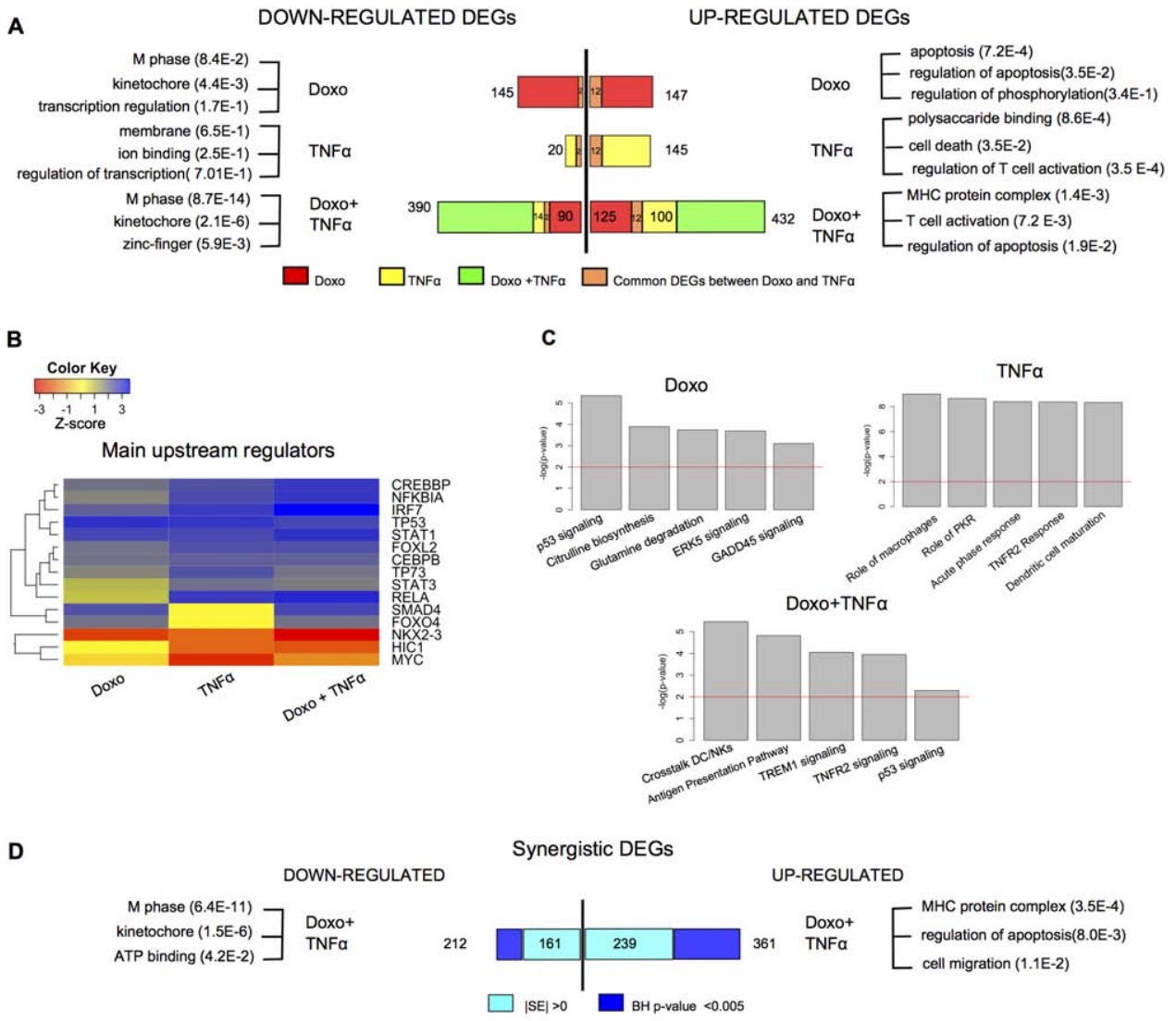

Figure 1: A vast array of genes responds selectively to Doxorubicin and TNFα in MCF7 cells. **(A)** Number of DEGs identified after single or combined treatment (see Methods for statistical filters). Most significant gene ontology terms of down- or up-regulated DEGs, according to DAVID (http://david.abcc.ncifcrf.gov). **(B)** Predicted upstream regulators of the DEGs for the indicated treatments, according to IPA (IPA, http://www.ingenuity.com). The color code reflects the enrichment or depletion of the listed transcription factors targeting the DEGs from the array analysis. **(C)** Statistically relevant pathways predicted to be modulated in response to the indicated treatments according to IPA. **(D)** Number of DEGs that are synergistically regulated by the double treatment according to two different statistical filters (see Materials and Methods). The most significant gene ontology terms are also indicated.

Doxorubicin + TNFα transcriptional synergy identifies new direct p53 and NFκB target genes

We selected fifteen genes for validation experiments based on (a) statistical analysis of synergistic up-regulated DEGs, (b) prior knowledge on direct regulation by either p53 or NFκB, (c) availability of ChIP-seq data for both transcription factors, and (d) gene functions in relation to cancer biology. The selected list contains genes encoding players of the control of various cellular processes, *e.g.* cell proliferation (PLK3, DUSP5, PLAU, GBX2, ETV7, EDN2), apoptosis (TNFRSF10B, UNC5B), inflammation (LAMP3, EGR2), development (GBX2, SOX9, NPPC, FOXC1) and cell migration (SNAI1, PLAU, UNC5B, NTN1, EDN2).

For twelve of the 15 genes we confirmed a synergistic response to the Doxo+TNFα treatment by qPCR (Figure 2A). Most of them were independently reported as putative targets of either p53, p65 or both according to published ChIP-seq data (for p65, http://genome.ucsc.edu/ENCODE) [14, 25]. A potential direct contribution of NFκB on the observed gene expression

changes was evaluates using the small molecule inhibitor BAY 11–7082 (BAY) used as single agent or in combination with Doxo or/and TNFα (Figure 2B). Eight of the twelve validated synergistic DEGs were tested and for five of them BAY markedly inhibited the effect of Doxo+TNFα, or of TNFα alone. TNFα treatment led to higher levels of nuclear p65, while Doxo alone or in the combined treatment did not significantly impact p65 nuclear protein levels. BAY treatment led to a slight reduction of p65 nuclear levels, which was paralleled by an increase in the cytoplasm (Figure 2C). p53 protein levels were induced to similar levels by the different treatment combinations (Figure S2).

The five genes that showed more convincing p65 dependence on the synergistic response to Doxo+TNFα (PLK3, NTN1, UNC5B, ETV7, LAMP3) were investigated more deeply to establish a direct role of wild type p53 in their transcription. MCF7 cells were treated with the chemotherapeutic agent 5-Fluorouracil (5FU) or with the MDM2 inhibitor Nutlin-3a, alone or in combination with TNFα. Both p53-inducing molecules were at least additive with TNFα in the responsiveness of the five genes (Figure 2D). Although the magnitude of the synergistic response was higher with Doxo, the fact that three different p53-activating treatments led to up-regulation of these five genes strongly suggested a direct role of p53. We next employed an MCF7 clone with stable knock-down of p53 and the HCT116 $p53^{-/-}$ cell line, to further establish p53-dependence of the five genes expression upon Doxo treatment. Matched MCF7 vector and HCT116 $p53^{+/+}$ were used as a comparison (Figure 2E, F). Invariably, Doxo responsiveness was strongly reduced in the p53-defective cells. Previous reports in the literature demonstrated or suggested p53-dependent regulation of PLK3, NTN1 and UNC5B. Our results confirm those findings and establish, for the first time, the possibility of synergistic regulation by NFκB. PLK3, a polo-like kinase, is an important regulator of the cell cycle and it is involved in the control of hypoxia signaling pathway [26]. NTN1 is ligand for both DCC1 and UNC5B receptors whose signaling can potentially modulate p53 activity, impacting on the decision between cell survival and cell death [27]. LAMP3 is a lysosomal membrane associated protein important in dendritic cells and potentially involved in tumor invasion [28], while ETV7 is a transcription factor associated to cell proliferation and tumorigenesis [29].

Given the lack of definitive evidence for LAMP3 and ETV7 being direct p53 targets and since our finding of synergistic responsiveness, we examined p53 and

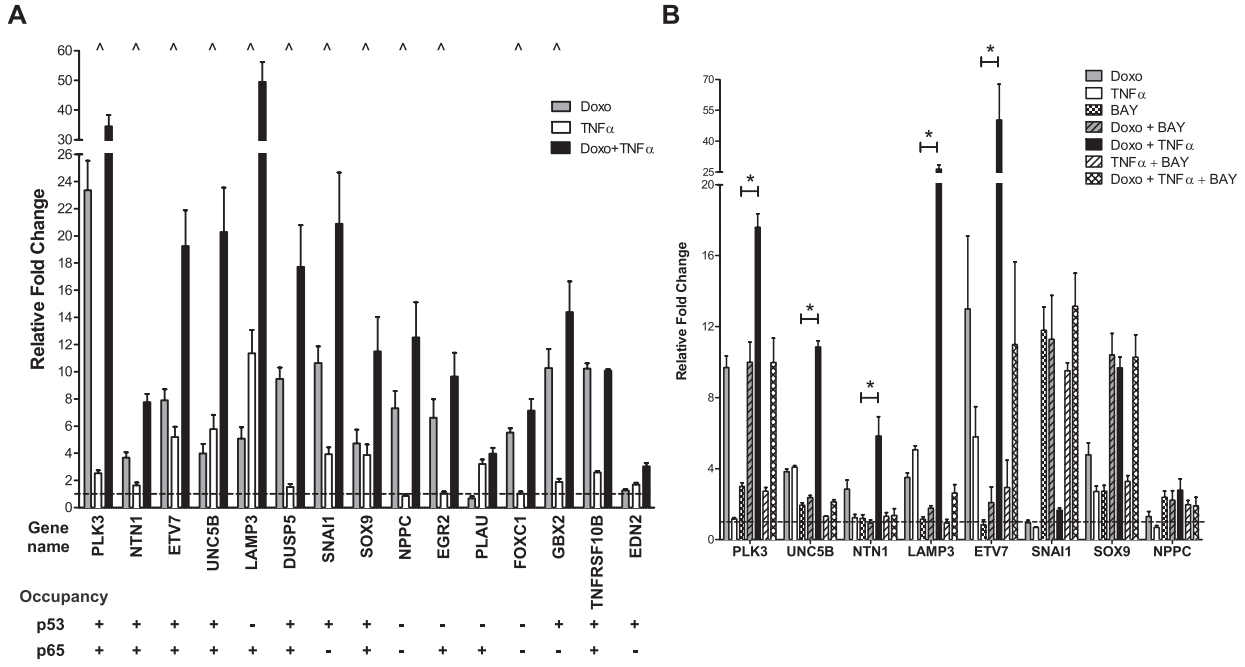

Figure 2: p53- and p65-dependent up-regulation of selected synergistic DEGs. (A) Twelve out of fifteen selected synergistic DEGs were validated by qPCR. Plotted are the average fold change relative to the mock condition and three reference genes (GAPDH, B2M, ACTB) and the standard deviations of three biological replicates. "^" marks genes responding in synergistic manner to the double treatment. p53 and p65 occupancy data from available ChIP-seq datasets are summarized below each gene name. **(B)** Impact of the NFκB inhibitor BAY 11-7082 on the synergistic gene expression response plotted as in panel A. "*" Significant inhibition of by BAY when combined to Doxo + TNFα (t-test, $p<0.01$). NPPC and SNAI1 were also tested but their expression levels were not affected by BAY treatment.

(*Continued*)

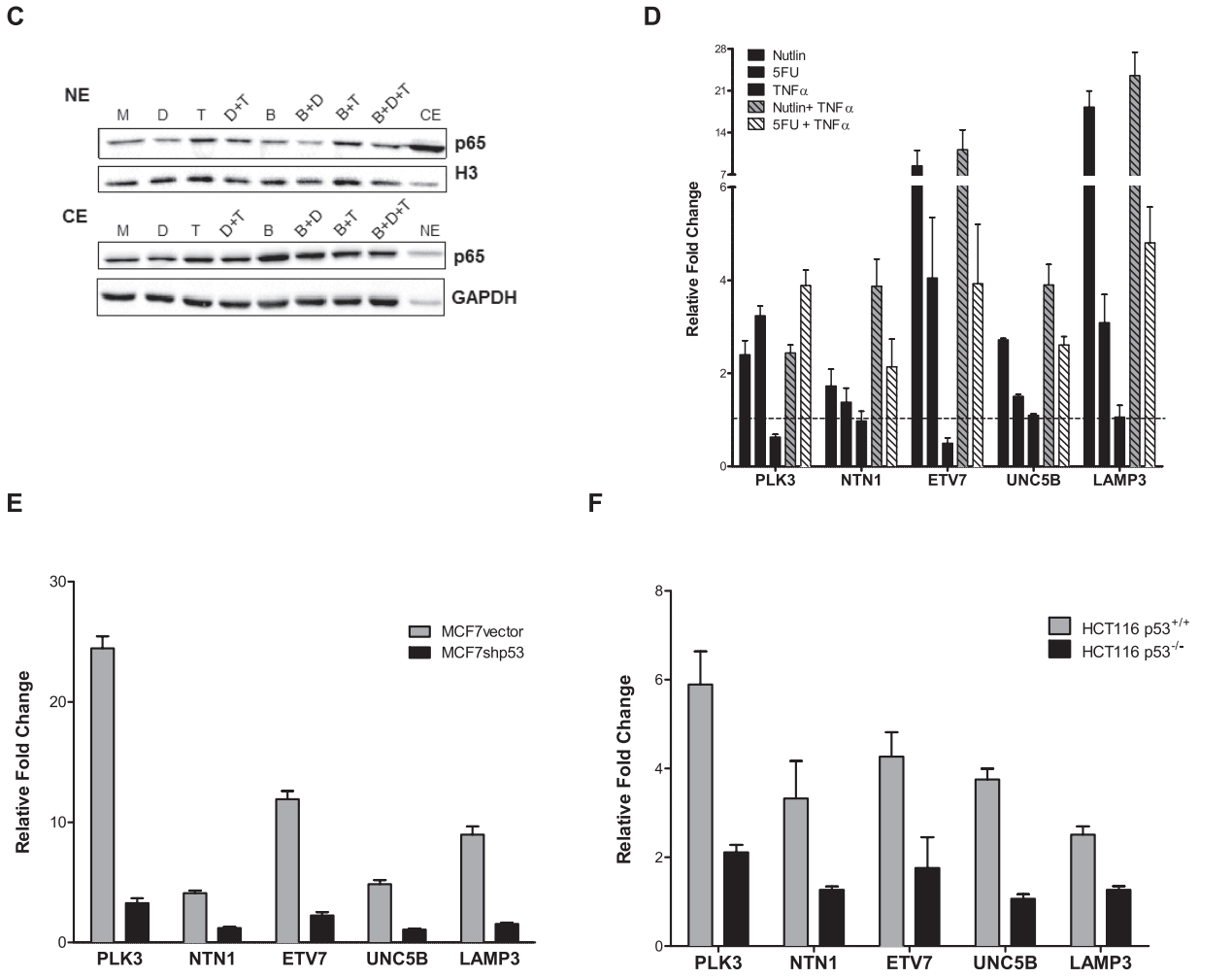

Figure 2: (C) p65 nuclear (NE) and cytoplasmic (CE) relative protein levels under the different treatments used in panel B. M = mock; D = Doxo; T = TNFα; B = BAY. Proteins were fractionated as described in Materials and Methods. GAPDH and histone 3 (H3) served as controls for cytoplasmic and nuclear fraction respectively. As controls, a cytoplasmic mock fraction sample (CE) is loaded together with the nuclear proteins and vice versa a nuclear mock sample (NE) in included in the cytoplasmic blot. **(D)** 5-fluorouracil and Nutlin-3a induced expression of 5 selected DEGs alone or in combination with TNFα. Results were obtained and are plotted as in A. **(E), (F)** The relative expression of the 5 selected genes shown in panel C was tested in doxorubicin treated matched cell lines differing for p53 status (MCF7 vector and shp53, D; HCT116 $p53^{+/+}$ and $p53^{-/-}$, E).

p65 occupancy in MCF7 cells treated with Doxo or TNFα (Figure 3). p53 occupancy was detected both for ETV7 and LAMP3 as well as for the positive control P21, in Doxo treated cells. For ETV7 p53 occupancy appeared to increase also after TNFα treatment. P21 was the only target for which p53 appeared to be bound also in the mock condition, a result consistent with previous data [30]. p53 occupancy levels were not distinguishable between Doxo and Doxo+TNFα treatment.

Both LAMP3 and ETV7 exhibited p65 occupancy in TNFα treated cells, although to a lower extent compared to the positive control MCP1. For the three promoter regions, occupancy was increased also by Doxo treatment alone, but no additive effect of the double treatment was apparent, except for a trend with LAMP3. On the contrary lower occupancy at MCP1 was detected in double treated cells. This latter result is consistent with the MCP1 mRNA expression changes (Figure S1B).

Hence, we identified genes whose expression is co-regulated by Doxo and TNFα. The gene expression studies conducted with different p53-activating molecules, the use of cells lines with different p53 status, and the chromatin immune-precipitation studies collectively established a direct role for p53 and p65 on the transcriptional regulation of PLK3, NTN1, ETV7, UNC5B and LAMP3. However, we did not find a direct correlation between occupancy levels at predicted promoter binding sites and gene expression changes.

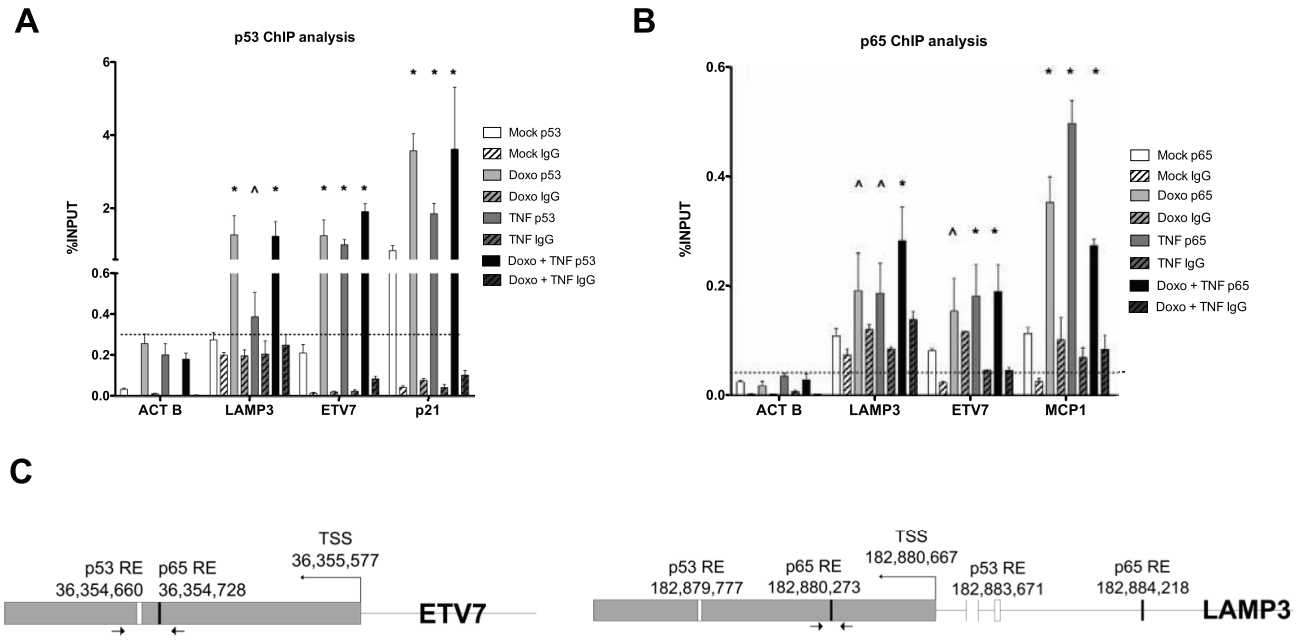

Figure 3: Occupancy analysis establishes ETV7 and LAMP3 as direct p65 and/or p53 target genes. (A) Relative quantification of immune-precipitated gene fractions by qPCR from MCF7 cells subjected to Doxo or TNFα single treatments and to the double treatment. The antibodies used for the immune-precipitations are listed. P21 was used as positive control, while ACTB was used as a negative control. Plotted are the average percentages relative to input signals. Error bars represent the standard errors of at least three biological replicates. **(B)** as in A, but probing p65 occupancy. MCP1 was used as positive control. The IgG antibody controls were anti-mouse (A) or anti-rabbit (B) to match the specific primary antibodies. **(C)** The position of the primers used for the qPCR and the location of predicted p53 and p65 binding sites in the ETV7 and LAMP3 genes are depicted.

Doxorubicin + TNFα treatment enhances the migration potential of MCF7 cells

Both the gene ontology enrichments of synergistic DEGs and the known function of the fifteen genes chosen for validation suggested the possible activation of gene expression programs influencing cell motility, epithelial mesenchymal transition (EMT) or even stem-like phenotypes. Projected to an *in vivo* context, the crosstalk of signals present in an inflammatory microenvironment could have a negative impact on the efficacy of chemotherapy, possibly by enhancing tumor cell plasticity. To begin exploring this hypothesis, we investigated migration and invasion potential of MCF7 cells treated with Doxo, TNFα or both. Three different experimental approaches consisting in real-time cell migration analysis (Figure 4A), transwell migration test (Figure 4B) and wound healing assay (Figure 4D) consistently showed higher migration potential of double-treated MCF7 cells, while the invasion phenotype was unaffected by all three types of treatment (Figure 4C).

Several studies suggest that EMT not only enhances the motility and invasiveness of cancer cells, but also provides additional aggressive features such as stemness and therapeutic resistance [31]. Indeed, several of the 15 synergistic DEGs we validated are directly or indirectly associated with acquisition of stem-like phenotypes in normal or cancer cells, particularly SNAI1 [32, 33], SOX9 [34] and GBX2 [35]. Different lines of evidence indicate that breast cancer stem cells (BCSCs) display increased cell motility, invasion, and overexpress genes that promote metastasis [36] and can be traced by $CD44^{+}/CD24^{-/low}$ surface marker expression [37]. We asked if the Doxo+TNFα treatment could enhance the stem-like subpopulation of the MCF7 cell line (Figure 4E). FACS analysis showed that the $CD44^{+}/CD24^{-}$ subpopulation virtually disappeared after all treatments. Therefore, the higher motility observed upon double treatment cannot be directly related to the expression of these surface markers, hence to putative stem-like features.

Prognostic value of Doxorubicin + TNFα synergistic DEGs

Since luminal type breast cancer, of which MCF7 is considered as a model, frequently retains wild type p53 and NFκB responsiveness, we asked if Doxo+TNFα synergistic DEGs could be endowed with prognostic significance. Up-regulated DEGs were further filtered by selecting genes that were strongly responsive to the double treatment but minimally responsive to the single ones (see Materials and Methods). A signature list of

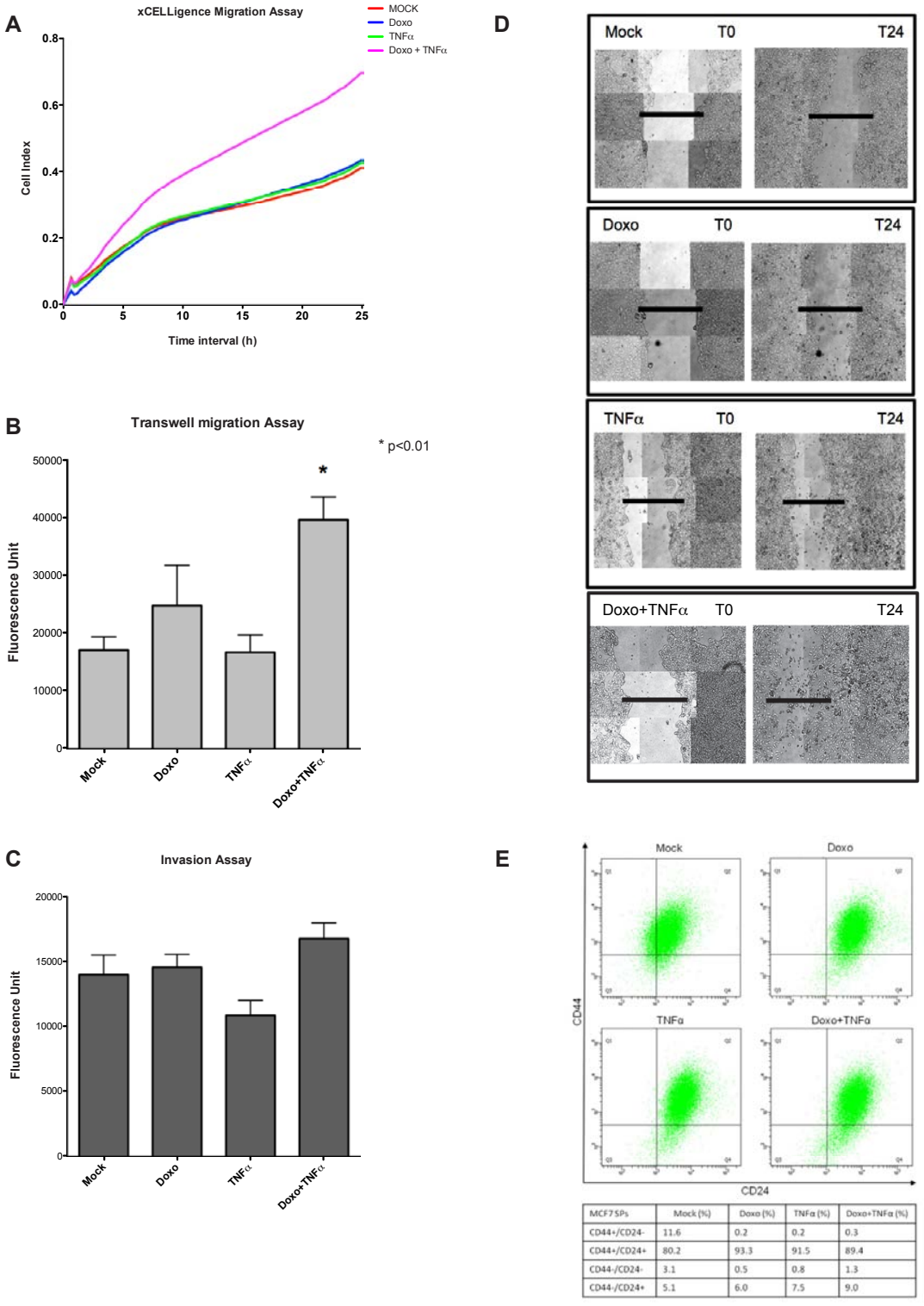

MCF7 SPs	Mock (%)	Doxo (%)	TNFα (%)	Doxo+TNFα (%)
CD44+/CD24-	11.6	0.2	0.2	0.3
CD44+/CD24+	80.2	93.3	91.5	89.4
CD44-/CD24-	3.1	0.5	0.8	1.3
CD44-/CD24+	5.1	6.0	7.5	9.0

Figure 4: Doxo+TNFα leads to enhanced MCF7 motility but ablates the stem-like side population. **(A)** Real-time migration assays examined by xCELLigence. Plotted are the average results of four biological repeats. Cell Index is proportional to the number of cells migrating through a hole in the culture plate. The treatments relative to the different curves are indicated. **(B)** Relative transwell migration values quantified by a fluorescence readout (see Materials and Methods). Average and standard deviation of triplicate biological replicates are presented. The applied treatments are listed on the x-axis. **(C)** As for B, but measuring the invasion potential of MCF7. **(D)** Images of a wound healing assay obtained at T0 or T24. Composite (3×3) images were acquired using an automated Zeiss microscope and the AxioVision3.1 software. **(E)** Cell sorting results based on intensity of CD44 and CD24 surface markers on 30000 cells. Q1 individuates the $CD44^{+}/CD24^{-(low)}$ cells, considered as stem-like. The percentages in the four quadrants after the various treatments are presented in the table.

29 genes (DT29) was generated (Figure 5A) and used to interrogate clinical data using the KM plotter tool [38]. Interestingly, breast cancer patients with luminal type A diagnosis who underwent chemotherapy and exhibited higher relative expression of DT29 genes showed poorer prognosis (Figure 5B). The same was true for luminal A patients with lymph node infiltration or luminal A grade 2 (Figure 5C, D).

Analysis of Doxorubicin and TNFα crosstalk in lung cancer-derived and HUVEC cells

We extended our analysis to another pair of cancer cell lines that differ for p53 status. A549 (p53 wild type) and H1299 (p53 null) lung cancer derived cells were treated with Doxo or/and TNFα or/and BAY. Expression of PLK3, NTN1, ETV7, UNC5B and LAMP3 was measured by qPCR (Figure 6A-E). The impact of the various treatments on p65 nuclear and cytoplasmic, p53 and p21 protein levels was also evaluated (Figure 6F, 6G). In the p53 null H1299 cells the relative expression changes of all the genes was invariably much lower compared to A549 cells. However, NTN1 was weakly TNFα inducible and ETV7 was weakly Doxo+TNFα responsive. Instead in A459 cells NTN1, ETV7 and LAMP3 were synergistically up-regulated by Doxo+TNFα, while PLK3 and UNC5B were additive. The magnitude of induction upon Doxo was often one order of magnitude higher compared to TNFα alone. Transient transfection assays with the κB luciferase reporter construct were performed using different concentrations of TNFα or BAY (Figure S3). Based on the results, 10ng/ml TNFα and/or 20μM BAY were chosen for the qPCR experiments, although the reduction of TNFα-induced reporter activity was modest, albeit significant. At the endogenous gene level in A549 cells we did not observe the inhibitory effect of BAY on either TNFα-induced changes or Doxo+TNFα, with the possible exception of UNC5B (Figure 6A-E). However, BAY treatment reduced the Doxo responsiveness of these genes, which might be dependent on its effect on the activation of NFκB by endogenous production of TNFα. In the p53 wild type A549 cells, p53 and p21 protein levels were induced by Doxo and not affected by the treatment with TNFα. Total p65 levels were unaffected by all treatments in both cell lines (Figure 6F). Nuclear p65 protein levels were increased in response to TNFα or

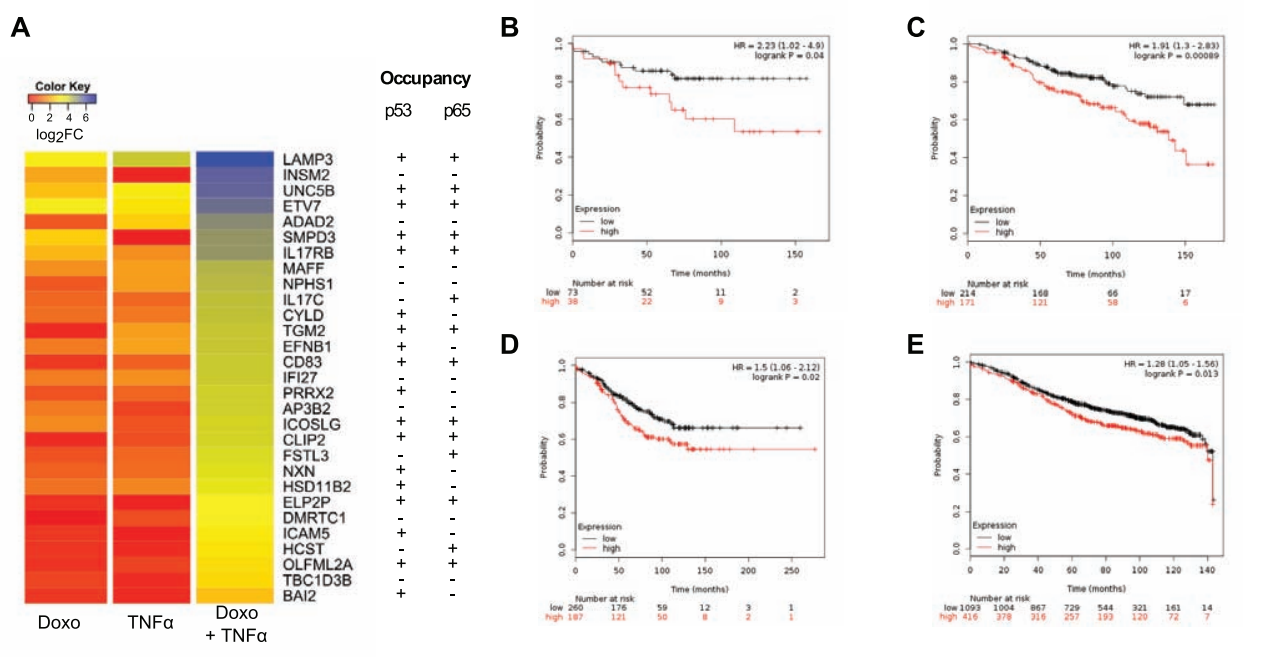

Figure 5: Prognostic significance of a 29-gene list of synergistic Doxo+TNFα DEGs. (A) Top list of 29 genes (DT-29) exhibiting minimal responsiveness to Doxo or TNFα as single agents, but strong synergy upon combined treatment. A heat map view of the gene expression results is presented (see Materials Methods for statistical filters). Occupancy of both for p65 and p53 in the vicinity of the transcription start sites of these genes has been summarized from ChIP-seq data available in the literature. **(B-E)** Kaplan-Meier plots stratifying a breast cancer patient cohort based on the relative expression of the DT-29 gene list and relapse free survival. Graphs were generated with the KM-plotter tool (ref). Patients' numbers are listed below the graph. Hazardous Ratio and the statistical analysis is reported for selected patients subgroups: **(B)** luminal A patients who underwent chemotherapy treatment (n = 111); **(C)** luminal A patients with a Grade 2 cancer at diagnosis (n = 385); **(D)** luminal A patients with lymph node infiltration at diagnosis (n = 447) and **(E)** the entire cohort of luminal A patients (n = 1509). Patients with a diagnosis of Luminal A breast cancer subtype were selected as the p53 status is not available in KM plotter, but this subgroup of breast cancer is expected to be strongly enriched for cases retaining wild type p53 protein.

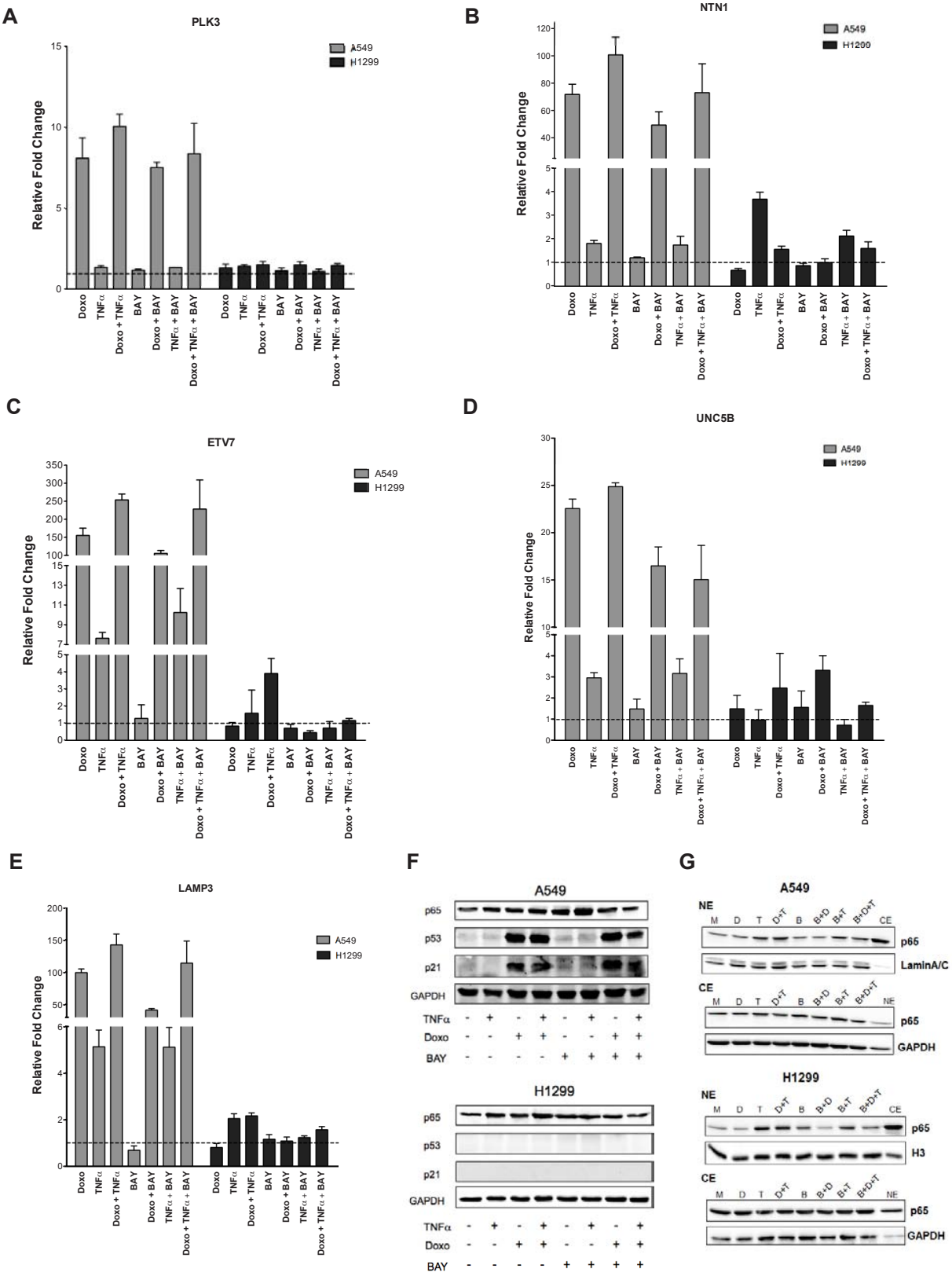

Figure 6: PLK3, NTN1, ETV7, UNC5B and LAMP3 responsiveness in lung cancer cell lines. (A-E) Relative fold change expression of the indicated genes and after the listed treatments in A549 (p53 wild type) and H1299 (p53 null) cells, measured by qPCR. Average and standard deviations of three biological replicates are presented. **(F)** Western blot of total p65, p53 and the p53 target p21. GAPDH was used as loading control. **(G)** Western blot of nuclear and cytoplasmic protein fractions were performed as for Figure 2C.

Doxo+TNFα in both A549 and H1299 cells (Figure 6G). Interestingly, BAY treatment alone or in combination led to a reduction in p65 nuclear accumulation (Figure 6G).

HUVEC primary cells were also subjected to Doxo and TNFα single or double treatment and the expression of the same panel of five genes was tested by qPCR (Figure S4). Results among biological repeats varied, but in the majority of tests, all genes with the exception of LAMP3 were Doxo responsive; NTN1 and ETV7 were also TNFα responsive. No synergistic up-regulation by the double treatment could be consistently established. p53 and p65 protein levels confirmed i) the activation of p53, with a similar level of p53 protein in the double treatment, and ii) the p65 proficiency of this cell line.

DISCUSSION

Wild type p53 functions are intricately related to multiple tumor suppressor pathways, primarily acting in cell autonomous manner to restrain cell proliferation and including cell death and senescence in response to genotoxic and many other types of cellular stresses [8, 9]. Furthermore, p53 also contributes to modulate the microenvironment in a non-cell autonomous manner [39]. p53 has also been linked to inhibition of EMT, for example through an indirect stimulation of E-cadherin expression [40]. At the same time, paracrine signaling in mice triggered by Doxorubicin were found to stimulate EMT and metastatic potential of cancer cells, in part through NFκB activation [3]. Many studies have highlighted the potential contribution of NFκB-induced signaling in the acquisition of cancer cell traits conducive to chemoresistance and higher metastasis risk [2] [41]. While, the canonical functions of p53 and NFκB are consistent with the co-occurrence of p53 inactivation and NFκB hyper-activation that is frequent in cancer [7], recent studies provided examples of positive cooperation between p53 and NFκB that would occur in specific cell types, such as antigen presenting cells or macrophages, and contribute to physiological responses, such as for example in the process of innate immunity and inflammation [12, 22, 23, 42].

Here we modeled the impact of a first line chemotherapeutic drug leading to genotoxic stress and p53 activation, using exposure to the immune cytokine and NFκB activator molecule TNFα as a variable, mimicking the effect of an inflammatory microenvironment. We used transcriptome analysis as primary endpoint and uncovered a vast network of differentially expressed genes that selectively responds to combined treatment with Doxorubicin and TNFα. Furthermore, genes that were synergistically up-regulated by both treatments appeared to endow cells with higher motility potential *in vitro*. Analyses of the annotated gene functions related to the aforementioned genes also revealed the possibility of an induced epithelial mesenchymal transition upon combination of the treatments. For example, SNAI1 appeared to be regulated in more than additive manner by the double treatment, as well as LAMP3, a lysosomal protein previously associated with metastasis risk [28, 43]. Multiple cytokines and secreted factors, including IL6, IL17, IL15 and its receptor, S100A8 and S100A9, CXCL12 and several Serpins were also identified as synergistic DEGs (Table S1). The presence of S100A8, S100A9 and CXCL12 among synergistic DEGs raises the possibility that, unlike the case of the triple negative cell line MDA-MB-231 for which S100A8-mediated signaling appeared to require heterotypic cell interactions [3] contributing to metastasis potential, in MCF7 cells this signaling could become homotypic or even autocrine. A marked difference in secreted factors and associated signaling among MDA and MCF7 cells was elegantly shown in recent studies [4].

A direct contribution of p65/RELA and p53 in the observed gene expression changes elicited by Doxorubicin and TNFα was inferred for some of the synergistic DEGs by modulating pharmacologically or genetically p65 or p53 activities. However, we cannot exclude at this stage a (Doxo+TNFα)-dependent, but p53- or NFκB- independent gene expression changes. For example, NFkB can functionally interact with AP-1 [44–46] or ER [47], which in turn can modulate p53-dependent responses [48] [49] [50].

Among the most synergistic genes, 29 appear to be prognostic in luminal A breast cancer patients who underwent chemotherapy, where their higher expression correlated with adverse outcome. The majority of luminal A breast cancers are wild type for p53 [51], although data is not available to stratify patients for p53 status in the KM plotter tool [24]. Based on available ChIP-seq data [14, 25, 52, 53], 20 of these 29 genes are putative targets of either p53 or p65 and 10 of them are putative targets of both factors (Figure 5). This result raises the possibility of an unexpected negative outcome of chemotherapy in the context of an inflammatory microenvironment. The prognostic significance of this gene signature needs in-depth evaluation in independent patients cohorts. If confirmed, the results would further support the value of combining treatments activating p53 and repressing NFκB [7].

Given that the crosstalk between Doxorubicin and TNFα and the interplay between p53 and NFκB would occur in cells residing or infiltrating the tumor microenvironment, the ultimate *in vivo* outcome of these functional interactions may vary and cannot be directly predicted from our study using a pure culture of MCF7 cells *in vitro*. Here we have explored Doxo+TNFα impact on HUVEC cells and also on a p53 wild type lung adenocarcinoma-derived cancer cell line. Although limited by the number of genes tested, the results suggest that a positive crosstalk between Doxorubicin and TNFα can be a general characteristic of different cell types and is

at least in part p53-dependent, based on the results with a p53 null lung cancer cell line. Furthermore, while we have addressed here the functional interactions between two small molecules, cells are constantly exposed to a complex milieu of signaling factors. However, both p53 and NFκB are master regulators, often contributing a dominant trait in gene expression changes to their target genes. Nuclear receptors, including Estrogen Receptors (ERs) can also modulate NFκB as well as p53 functions [54–56] and have critical roles in breast cancer etiology. We also explored the impact of ER function in the transcriptional programs responding to Doxorubicin and TNFα exposure, using estrogen-depleted culture conditions and adding 17β-estradiol (10^{-9}M, E2) as variable (Table S2 and GSE 24065). However, the combination of E2 to Doxo and TNFα resulted only in 15 and 11 selective up- and down-regulated DEGs, respectively (Table S3). A hierarchical cluster analysis of all the treatments confirmed graphically the large difference between TNFα- and Doxo-induced transcriptomes and also the significant impact of TNFα when combined to Doxo, while E2 had a minor effect both in the combination with Doxo and with Doxo + TNFα (Figure S5).

With this study we established an example of positive cooperation between p53 and NFκB, in the context of the responses of an epithelial cancer cell to standard chemotherapy but in the presence of active signaling by a pleiotropic inflammatory cytokine, such as TNFα. A signature gene of the consequent transcriptional reprogramming appears to be prognostic in breast cancer patients. Associated gene functions indicate the potential acquisition of enhanced cell plasticity and motility and provide a rationale to investigating mechanisms resulting in acquired chemoresistance, particularly for luminal A breast cancer, but potentially with general implication for p53 wild type tumors of different tissue types, and for overcoming such resistance by targeting NFκB. The unexpected positive crosstalk between p53 and NFκB emerging from our and other very recent studies [23] may represent an evolutionary consequence of anti-viral and infection responses towards which NFκB is an established master regulator [57], but the p53 and p73 family member are emerging as important/critical contributors [42, 58, 59].

MATERIALS AND METHODS

Cell lines and culture conditions

MCF7 (p53 wild type, expressing p65 and positive for ERs) and HUVEC (Human Umbilical Vein Endothelial Cells) cells were obtained from ICLC (Genoa, Italy), while A549 from ATCC (Manassas, VA, USA). H1299 cells were a gift of Dr. Resnick's laboratory (NIEHS, NIH, RTP, NC, USA); HCT116 $p53^{+/+}$ and $p53^{-/-}$ of Dr. Vogelstein's (John Hopkins Kimmel Cancer Center, Baltimore, MD, USA). MCF7-shp53 or control MCF7-vector cells were provided by Dr. Agami (Netherlands Cancer Institute, Amsterdam, The Netherlands). Cells were cultured in DMEM or RPMI media supplemented with 10% FBS, or Medium 199 (Lonza Milan, Italy) supplemented with 50 units/ml Low Serum Growth Supplements (Life Technologies, Milan, Italy) in the case of HUVEC cells that were also cultured on 0.1% gelatin pre-coated plastics. Media were supplemented by 2mM L-Glutamine and 1XPenicillin/Streptomycin mixture (Pen/Strep), and Puromycin (0.5 μg/mL) in the case of MCF7-shp53 and –vector cells. When appropriate, cells were maintained in DMEM without Phenol Red (Lonza) supplemented with Charcoal/Dextran treated FBS (Hyclone, GE Healthcare, South Logan, UT, USA).

Drug treatments

Doxorubicin (Doxo, 1.5 μM), 5-Fluorouracil (5FU, 375 μM), Nutlin-3a (10 μM) were used to stabilize p53 protein. When needed TNFα (5ng/ml in MCF7 and 10ng/ml in H1299, A549 and HUVEC cells –based on dose-response tests with gene reporter assays) or BAY11-7082 (10μM or 20μM in H1299 and A549) were added to the culture medium. All compounds were from Sigma-Aldrich (Milan, Italy).

Microarray experiment and data analysis

Total RNA was extracted from 4 biological replicates using the Agilent Total RNA Isolation Mini Kit (Agilent Technologies, Santa Clara, CA, USA). Samples with RNA Integrity Number (RIN) above 9 (Agilent 2100 BioAnalyzer) were processed. Details are provided with the Gene Expression Omnibus (GEO) (www.ncbi.nlm.nih.gov/geo) submission (GSE24065) and in [56]. The output of Feature Extraction (Agilent standard protocol GE1_107_Sep09) was analyzed with the R software for statistical computing and the Bioconductor library of biostatistical packages. Probes with low signals were removed in order to filter out the unexpressed genes and keep only probes with acceptable signals in most of the replicates. Signal intensities across arrays were normalized by quantile normalization. Signal intensities from probes associated with the same gene were averaged. This procedure resulted in quantitative signals for 14095 HGNC genes. To identify potential target genes of Doxorubicin and TNFα, we compared the signals after the double treatment (Doxo+TNFα) and the two single treatments relative to the untreated control (mock). DEGs were selected applying a statistical test based on rank products implemented in RankProd Bioconductor package, setting a threshold of 0.05 on the percentage of false positives (pfp) and a threshold of 2 on the absolute log2 fold changes [60]. Every treatment was compared to the mock condition (Table S1, S2 and Figure S5).

To select genes with synergistic effect, i.e. genes whose expression variations were more than additive in the double treatment with respect to single treatments, a further comparison between the double treatment samples and all the remaining samples (single treatments and control samples) was performed (double treatment vs all). Synergistic DEGs were selected applying an additional pfp filter (pfp<0.005) derived from this comparison, to the list of DEGs resulting from the "double treatment vs mock" comparison. A more stringent criterion was obtained by calculating the synergistic effect (SE) of the double treatment as the observed difference between the fold change of the double treatment and the sum of the fold changes of the single treatments (SE=log2 FC double treatment – (log2 FC Doxorubicin + log2 FC TNFα). We filtered genes with SE>0 for up-regulated DEGs, SE<0 for down-regulated genes (Figure 1). To select genes where the up-regulation contribution of each single treatment was low respect to the up-regulation of the double treatment, the ratio of the single/double treatments was calculated, applying a 0.25 filter on them (FC Doxorubicin/FC double treatment <0.25 and FC TNFα/ FC double treatment <0.25) (see Table S1, S2).

RNA isolation and quantitative qPCR

Total RNA was extracted using Qiagen RNeasy Kit (Qiagen). cDNA was converted from 1 μg of RNA using M-MuLV reverse transcritptase and RevertAid cDNA Synthesis kit (ThermoFisher, Milan, Italy). qPCR was performed on a Bio-Rad CFX384 (Bio-Rad, Milan, Italy). TaqMan gene expression assays (Applied Biosystems, Life Technologies) and Probe MasterMix (Kapa Biosystems, Resnova, Rome, Italy) were used starting with 25ng of cDNA as previously described [56, 61]. GAPDH, B2M or ACTB served as reference genes.

Western blot

Protein extraction and immunodetections were performed as previously described [62], using ECL Select detection reagent (GE Healthcare) and anti-p53 (DO-1) anti-RelA/p65 (C-20) anti- p21 (C19), anti-GAPDH (6C5) (Santa Cruz Biotechnology, Heidelberg, Germany). When appropriate, nuclear and cytoplasmic fractionation was performed. MCF7, A549 and H1299 cell lines were seeded on 100mm Petri dishes and treated at 80% confluence with Doxo, TNFα, BAY or the combination of the drugs for 16 hours. Cells were harvested and cytoplasmic and nuclear proteins were extracted using NE-PER Nuclear and Cytoplasmic Extraction Kit (Pierce, ThermoFisher Scientific), following the instructions provided by the manufacturer. 20 μg of nuclear and cytoplasmic extracts were loaded on a 12% poly-acrylamide gel and transferred to nitrocellulose membranes. Antibodies used for detection were: anti-Histone H3 (clone #: ab1791, AbCam, Milan, Italy) and anti-Lamin A/C (clone #: 2032, Cell Signaling, Milan, Italy) used as nuclear loading control, and anti-GAPDH used as cytoplasmic loading control.

Chromatin immunoprecipitation assay

We used previously described protocols [63, 64]. The following antibodies were used: anti-p53 (DO-1), anti-p65 (C-20) and IgG (sc-2025 or sc-2027) (Santa Cruz Biotechnology). ChIP-qPCR experiments were performed using Sybr MasterMix (Kapa Biosystems) and 2 μl of enriched DNA. Results were analyzed by the comparative Ct method (ΔCt) and normalized as % of input. Regions in the promoter of GAPDH or ACTB and p21 or MCP1 genes served as negative and positive controls, respectively. Primers were selected using Primer 3 (http://primer3.ut.ee/).

Migration and wound healing assays

The migration potential of MCF7 cells was monitored by a real-time technique using the xCELLigence Instrument (Acea Biosciences, Euroclone) and CIM-16 plates, following manufacturer's instructions. Prior to the analysis, cells were grown in estrogen-free medium for two days and left untreated (mock) or treated with Doxo, TNFα or the combination. 16 hours after the treatments, cells were detached and added to the top chamber in serum-free medium. Migration was detected every 10 minutes for 24 hours. We used 0.5% and 5% FBS as chemo-attractant. Migration and Invasion were also measured by QCM™ Fluor 24-Well Cell Migration and Cell Invasion kits (Merck-Millipore, Milan, Italy), according to manufacturer's instructions. For wound healing, cells were seeded in 12-well plates and treated with Doxo, TNFα or the combination. After 16 hours a scratch was introduced using a 10 μl pipette tip. Images of the same field were acquired immediately (T0) and after 24 hours (T24) using an automated Zeiss microscope and the AxioVision3.1 software in multidimensional mode with mosaic (3x3) acquisition.

Flow cytometry

MCF7 cells, seeded and treated as described above, were washed with PBS and harvested by 0.05% trypsin/0.025% EDTA. The cells were washed again with PBS containing 2% FBS before being subjected to antibody binding, a combination of fluorochrome-conjugated monoclonal antibodies against human CD44 (APC) and CD24 (FITC) or their respective isotype controls (BD Biosciences, Milan, Italy) and incubated on ice in the dark for 30 minutes. Cells were then washed twice with PBS/2% FBS and resuspended in PBS. Flow cytometry analysis was conducted using a FACSCanto II instrument (BD Biosciences).

ACKNOWLEDGEMENTS

We thank Dr. Valentina Adami (CIBIO High-throughput screening facility), Dr. Isabella Pesce (CIBIO Cell Separation facility), Ms. Sonia Leonardelli, Mr. Dennis Pedri for technical support. This work was supported by the Italian Association for Cancer Research, AIRC (IG grant # 12869 to AI). IR is supported by a Fellowship from the Pezcoller Foundation.

Competing interests

The authors declare no conflict of interest.

REFERENCES

1. Hanahan D, Weinberg RA. Hallmarks of cancer: the next generation. Cell. 2011; 144:646–674.
2. Labelle M, Begum S, Hynes RO. Direct signaling between platelets and cancer cells induces an epithelial-mesenchymal-like transition and promotes metastasis. Cancer Cell. 2011; 20:576–590.
3. Acharyya S, Oskarsson T, Vanharanta S, Malladi S, Kim J, Morris PG, Manova-Todorova K, Leversha M, Hogg N, Seshan VE, Norton L, Brogi E, Massague J. A CXCL1 paracrine network links cancer chemoresistance and metastasis. Cell. 2012; 150:165–178.
4. Kuznetsov HS, Marsh T, Markens BA, Castano Z, Greene-Colozzi A, Hay SA, Brown VE, Richardson AL, Signoretti S, Battinelli EM, Mc Allister SS. Identification of luminal breast cancers that establish a tumor-supportive macroenvironment defined by proangiogenic platelets and bone marrow-derived cells. Cancer Discov. 2012; 2: 1150–1165.
5. Cooke VG, Le Bleu VS, Keskin D, Khan Z, O'Connell JT, Teng Y, Duncan MB, Xie L, Maeda G, Vong S, Sugimoto H, Rocha RM, Damascena A, Brentani RR, Kalluri R. Pericyte depletion results in hypoxia-associated epithelial-to-mesenchymal transition and metastasis mediated by met signaling pathway. Cancer Cell. 2012; 21:66–81.
6. Darnell JE Jr. Transcription factors as targets for cancer therapy. Nat Rev Cancer. 2002; 2:740–749.
7. Dey A, Tergaonkar V, Lane DP. Double-edged swords as cancer therapeutics: simultaneously targeting p53 and NF-kappaB pathways. Nat Rev Drug Discov. 2008; 7: 1031–1040.
8. Vogelstein B, Lane D, Levine AJ. Surfing the p53 network. Nature. 2000; 408:307–310.
9. Vousden KH, Prives C. Blinded by the Light: The Growing Complexity of p53. Cell. 2009; 137:413–431.
10. Espinosa JM. Mechanisms of regulatory diversity within the p53 transcriptional network. Oncogene. 2008; 27: 4013–4023.
11. Riley T, Sontag E, Chen P, Levine A. Transcriptional control of human p53-regulated genes. Nat Rev Mol Cell Biol. 2008; 9:402–412.
12. Vousden KH. Outcomes of p53 activation--spoilt for choice. J Cell Sci. 2006; 119(Pt 24):5015–5020.
13. Menendez D, Inga A, Resnick MA. The expanding universe of p53 targets. Nat Rev Cancer. 2009; 9:724–737.
14. Nikulenkov F, Spinnler C, Li H, Tonelli C, Shi Y, Turunen M, Kivioja T, Ignatiev I, Kel A, Taipale J, Selivanova G. Insights into p53 transcriptional function via genome-wide chromatin occupancy and gene expression analysis. Cell Death Differ. 2012.
15. Karin M. Nuclear factor-kappaB in cancer development and progression. Nature. 2006; 441:431–436.
16. Chen LF, Greene WC. Shaping the nuclear action of NF-kappaB. Nat Rev Mol Cell Biol. 2004; 5:392–401.
17. Webster GA, Perkins ND. Transcriptional cross talk between NF-kappaB and p53. Mol Cell Biol. 1999; 19:3485–3495.
18. Kawauchi K, Araki K, Tobiume K, Tanaka N. Activated p53 induces NF-kappaB DNA binding but suppresses its transcriptional activation. Biochem Biophys Res Commun. 2008; 372:137–141.
19. Ma S, Tang J, Feng J, Xu Y, Yu X, Deng Q, Lu Y. Induction of p21 by p65 in p53 null cells treated with Doxorubicin. Biochim Biophys Acta. 2008; 1783:935–940.
20. Ryan KM, Ernst MK, Rice NR, Vousden KH. Role of NF-kappaB in p53-mediated programmed cell death. Nature. 2000; 404:892–897.
21. Kawai T, Akira S. Signaling to NF-kappaB by Toll-like receptors. Trends in molecular medicine. 2007; 13:460–469.
22. Menendez D, Shatz M, Azzam K, Garantziotis S, Fessler MB, Resnick MA. The Toll-like receptor gene family is integrated into human DNA damage and p53 networks. PLoS Genet. 2011; 7:e1001360.
23. Lowe JM, Menendez D, Bushel PR, Shatz M, Kirk EL, Troester MA, Garantziotis S, Fessler MB, Resnick MA. p53 and NF-kappaB Coregulate Proinflammatory Gene Responses in Human Macrophages. Cancer Res. 2014; 74:2182–2192.
24. Gyorffy B, Lanczky A, Eklund AC, Denkert C, Budczies J, Li Q, Szallasi Z. An online survival analysis tool to rapidly assess the effect of 22,277 genes on breast cancer prognosis using microarray data of 1,809 patients. Breast Cancer Res Treat. 2010; 123:725–731.
25. Menendez D, Nguyen TA, Freudenberg JM, Mathew VJ, Anderson CW, Jothi R, Resnick MA. Diverse stresses dramatically alter genome-wide p53 binding and transactivation landscape in human cancer cells. Nucleic Acids Res. 2013; 41:7286–7301.
26. Xu D, Yao Y, Lu L, Costa M, Dai W. Plk3 functions as an essential component of the hypoxia regulatory pathway by direct phosphorylation of HIF-1alpha. J Biol Chem. 2010; 285:38944–38950.

27. Arakawa H. Netrin-1 and its receptors in tumorigenesis. Nat Rev Cancer. 2004; 4:978–987.
28. Nagelkerke A, Bussink J, Mujcic H, Wouters BG, Lehmann S, Sweep FC, Span PN. Hypoxia stimulates migration of breast cancer cells via the PERK/ATF4/LAMP3-arm of the unfolded protein response. Breast Cancer Res. 2013; 15:R2.
29. Cardone M, Kandilci A, Carella C, Nilsson JA, Brennan JA, Sirma S, Ozbek U, Boyd K, Cleveland JL, Grosveld GC. The novel ETS factor TEL2 cooperates with Myc in B lymphomagenesis. Mol Cell Biol. 2005; 25:2395–2405.
30. Espinosa JM, Verdun RE, Emerson BM. 2003; p53 functions through stress- and promoter-specific recruitment of transcription initiation components before and after DNA damage. Mol Cell. :1015–1027.
31. Gupta PB, Chaffer CL, Weinberg RA. Cancer stem cells: mirage or reality? Nat Med. 2009; 15:1010–1012.
32. Lim S, Becker A, Zimmer A, Lu J, Buettner R, Kirfel J. SNAI1-mediated epithelial-mesenchymal transition confers chemoresistance and cellular plasticity by regulating genes involved in cell death and stem cell maintenance. PLoS One. 2013; 8:e66558.
33. Deep G, Jain AK, Ramteke A, Ting H, Vijendra KC, Gangar SC, Agarwal C, Agarwal R. SNAI1 is critical for the aggressiveness of prostate cancer cells with low E-cadherin. Molecular cancer. 2014; 13:37.
34. Sun L, Mathews LA, Cabarcas SM, Zhang X, Yang A, Zhang Y, Young MR, Klarmann KD, Keller JR, Farrar WL. Epigenetic regulation of SOX9 by the NF-kappaB signaling pathway in pancreatic cancer stem cells. Stem cells. 2013; 31:1454–1466.
35. Tai CI, Ying QL. Gbx2, a LIF/Stat3 target, promotes reprogramming to and retention of the pluripotent ground state. J Cell Sci. 2013; 126(Pt 5):1093–1098.
36. Shipitsin M, Campbell LL, Argani P, Weremowicz S, Bloushtain-Qimron N, Yao J, Nikolskaya T, Serebryiskaya T, Beroukhim R, Hu M, Halushka MK, Sukumar S, Parker LM, Anderson KS, Harris LN, Garber JE, et al. Molecular definition of breast tumor heterogeneity. Cancer Cell. 2007; 11:259–273.
37. Al-Hajj M, Wicha MS, Benito-Hernandez A, Morrison SJ, Clarke MF. Prospective identification of tumorigenic breast cancer cells. Proc Natl Acad Sci U S A. 2003; 100: 3983–3988.
38. Gyorffy B, Lanczky A, Szallasi Z. Implementing an online tool for genome-wide validation of survival-associated biomarkers in ovarian-cancer using microarray data from 1287 patients. Endocrine-related cancer. 2012; 19: 197–208.
39. Lujambio A, Akkari L, Simon J, Grace D, Tschaharganeh DF, Bolden JE, Zhao Z, Thapar V, Joyce JA, Krizhanovsky V, Lowe SW. Non-cell-autonomous tumor suppression by p53. Cell. 2013; 153:449–460.
40. Muller PA, Vousden KH, Norman JC. p53 and its mutants in tumor cell migration and invasion. J Cell Biol. 2011; 192:209–218.
41. Dalmases A, Gonzalez I, Menendez S, Arpi O, Corominas JM, Servitja S, Tusquets I, Chamizo C, Rincon R, Espinosa L, Bigas A, Eroles P, Furriol J, Lluch A, Rovira A, Albanell J, et al. Deficiency in p53 is required for doxorubicin induced transcriptional activation of NF-small ka, CyrillicB target genes in human breast cancer. Oncotarget. 2014; 5:196–210.
42. Wang B, Niu D, Lai L, Ren EC. p53 increases MHC class I expression by upregulating the endoplasmic reticulum aminopeptidase ERAP1. Nat Commun. 2013; 4:2359.
43. Kanao H, Enomoto T, Kimura T, Fujita M, Nakashima R, Ueda Y, Ueno Y, Miyatake T, Yoshizaki T, Buzard GS, Tanigami A, Yoshino K, Murata Y. Overexpression of LAMP3/TSC403/DC-LAMP promotes metastasis in uterine cervical cancer. Cancer Res. 2005; 65:8640–8645.
44. Fujioka S, Niu J, Schmidt C, Sclabas GM, Peng B, Uwagawa T, Li Z, Evans DB, Abbruzzese JL, Chiao PJ. NF-kappaB and AP-1 connection: mechanism of NF-kappaB-dependent regulation of AP-1 activity. Mol Cell Biol. 2004; 24:7806–7819.
45. Redhu NS, Saleh A, Halayko AJ, Ali AS, Gounni AS. Essential role of NF-kappaB and AP-1 transcription factors in TNF-alpha-induced TSLP expression in human airway smooth muscle cells. American journal of physiology Lung cellular and molecular physiology. 2011; 300:L479–485.
46. Westwick JK, Weitzel C, Minden A, Karin M, Brenner DA. Tumor necrosis factor alpha stimulates AP-1 activity through prolonged activation of the c-Jun kinase. J Biol Chem. 1994; 269:26396–26401.
47. Sas L, Lardon F, Vermeulen PB, Hauspy J, Van Dam P, Pauwels P, Dirix LY, Van Laere SJ. The interaction between ER and NFkappaB in resistance to endocrine therapy. Breast Cancer Res. 2012; 14:212.
48. Shaulian E, Karin M. AP-1 in cell proliferation and survival. Oncogene. 2001; 20:2390–2400.
49. Sayeed A, Konduri SD, Liu W, Bansal S, Li F, Das GM. Estrogen receptor alpha inhibits p53-mediated transcriptional repression: implications for the regulation of apoptosis. Cancer Res. 2007; 67:7746–7755.
50. Lion M, Bisio A, Tebaldi T, De Sanctis V, Menendez D, Resnick MA, Ciribilli Y, Inga A. Interaction between p53 and estradiol pathways in transcriptional responses to chemotherapeutics. Cell Cycle. 2013; 12:1211–1224.
51. Cancer Genome Atlas N: Comprehensive molecular portraits of human breast tumours. Nature. 2012; 490:61–70.
52. Consortium EP. A user's guide to the encyclopedia of DNA elements (ENCODE). PLoS biology. 2011; 9:e1001046.

53. Wang B, Niu D, Lam TH, Xiao Z, Ren EC. Mapping the p53 transcriptome universe using p53 natural polymorphs. Cell Death Differ. 2014; 21:521–532.

54. Quaedackers ME, van den Brink CE, van der Saag PT, Tertoolen LG. Direct interaction between estrogen receptor alpha and NF-kappaB in the nucleus of living cells. Molecular and cellular endocrinology. 2007; 273:42–50.

55. Thomas C, Gustafsson JA. The different roles of ER subtypes in cancer biology and therapy. Nat Rev Cancer. 2011; 11:597–608.

56. Lion M, Bisio A, Tebaldi T, De Sanctis V V, Menendez D, Resnick MA, Ciribilli Y, Inga A. Interaction between p53 and estradiol pathways in transcriptional responses to chemotherapeutics. Cell Cycle. 2013; 12.

57. Vallabhapurapu S, Karin M. Regulation and function of NF-kappaB transcription factors in the immune system. Annual review of immunology. 2009; 27:693–733.

58. Yang A, Walker N, Bronson R, Kaghad M, Oosterwegel M, Bonnin J, Vagner C, Bonnet H, Dikkes P, Sharpe A, Mc Keon F, Caput D. p73-deficient mice have neurological, pheromonal and inflammatory defects but lack spontaneous tumours. Nature. 2000; 404:99–103.

59. Menendez D, Shatz M, Resnick MA. Interactions between the tumor suppressor p53 and immune responses. Curr Opin Oncol. 2013; 25:85–92.

60. Breitling R, Armengaud P, Amtmann A, Herzyk P. Rank products: a simple, yet powerful, new method to detect differentially regulated genes in replicated microarray experiments. FEBS Lett. 2004; 5733:83–92.

61. Raimondi I, Ciribilli Y, Monti P, Bisio A, Pollegioni L, Fronza G, Inga A, Campomenosi P. P53 family members modulate the expression of PRODH, but not PRODH2, via intronic p53 response elements. PLoS One. 2013; 8:e69152.

62. Ciribilli Y, Monti P, Bisio A, Nguyen HT, Ethayathulla AS, Ramos A, Foggetti G, Menichini P, Menendez D, Resnick MA, Viadiu H, Fronza G, Inga A. Transactivation specificity is conserved among p53 family proteins and depends on a response element sequence code. Nucleic Acids Res. 2013; 41:8637–8653.

63. Ciribilli Y, Andreotti V, Menendez D, Langen JS, Schoenfelder G, Resnick MA, Inga A. The coordinated p53 and estrogen receptor cis-regulation at an FLT1 promoter SNP is specific to genotoxic stress and estrogenic compound. PLoS One. 2010; 5:e10236.

64. Bisio A, De Sanctis V V, Del Vescovo V, Denti MA, Jegga AG, Inga A, Ciribilli Y. Identification of new p53 target microRNAs by bioinformatics and functional analysis. BMC Cancer. 2013; 13:552.

ANNEX 2.2

Tebaldi et al. BMC Genomics (2015) 16:464
DOI 10.1186/s12864-015-1643-9

BMC Genomics

RESEARCH ARTICLE Open Access

Whole-genome cartography of p53 response elements ranked on transactivation potential

Toma Tebaldi*†, Sara Zaccara†, Federica Alessandrini, Alessandra Bisio, Yari Ciribilli and Alberto Inga*

Abstract

Background: Many recent studies using ChIP-seq approaches cross-referenced to trascriptome data and also to potentially unbiased *in vitro* DNA binding selection experiments are detailing with increasing precision the p53-directed gene regulatory network that, nevertheless, is still expanding. However, most experiments have been conducted in established cell lines subjected to specific p53-inducing stimuli, both factors potentially biasing the results.

Results: We developed *p53retriever*, a pattern search algorithm that maps p53 response elements (REs) and ranks them according to predicted transactivation potentials in five classes. Besides canonical, full site REs, we developed specific pattern searches for non-canonical half sites and 3/4 sites and show that they can mediate p53-dependent responsiveness of associated coding sequences. Using ENCODE data, we also mapped p53 REs in about 44,000 distant enhancers and identified a 16-fold enrichment for high activity REs within those sites in the comparison with genomic regions near transcriptional start sites (TSS). Predictions from our pattern search were cross-referenced to ChIP-seq, ChIP-exo, expression, and various literature data sources. Based on the mapping of predicted functional REs near TSS, we examined expression changes of thirteen genes as a function of different p53-inducing conditions, providing further evidence for PDE2A, GAS6, E2F7, APOBEC3H, KCTD1, TRIM32, DICER, HRAS, KITLG and TGFA p53-dependent regulation, while MAP2K3, DNAJA1 and potentially YAP1 were identified as new direct p53 target genes.

Conclusions: We provide a comprehensive annotation of canonical and non-canonical p53 REs in the human genome, ranked on predicted transactivation potential. We also establish or corroborate direct p53 transcriptional control of thirteen genes. The entire list of identified and functionally classified p53 REs near all UCSC-annotated genes and within ENCODE mapped enhancer elements is provided. Our approach is distinct from, and complementary to, existing methods designed to identify p53 response elements. *p53retriever* is available as an R package at: http://tomateba.github.io/p53retriever.

Keywords: p53, Response element, Transactivation potential, Distal enhancer

Background

The p53 tumor suppressor is certainly one of the most studied sequence-specific transcription factor to date. Yet, much has still to be learned to fully describe its transcriptional regulatory network, both in terms of the crosstalk with other transcription factors and in terms of the entire spectrum of regulated transcriptional target genes, that can be both up-regulated or down-regulated [1–6].

Recently, several genome-scale techniques such as ChIP-on-chip, ChIP-seq, and, more recently, ChIP-exo, have provided us with different and largely non-overlapping maps of p53 bound sites in the human genome in response to specific stimuli [7–17]. Correlation between occupancy data and modulation of transcription levels of nearby genes helped identifying additional direct p53 target genes, of which >200 have been established [2, 15]. Furthermore, new methodologies are refining the potential to map the p53 network taking also into account the kinetics of transcriptional initiation [18, 19]. It is worth noting that, to date, most experiments have been developed in cancer-derived cell lines that may represent an adapted environment potentially biasing a comprehensive annotation of physiological p53 target sites [7, 20]. To this respect, the impact of specific p53-inducing stimuli and the differentiation/

* Correspondence: t.tebaldi@unitn.it; alberto.inga@unitn.it
†Equal contributors
Centre for Integrative Biology (CIBIO), University of Trento, via delle Regole 101, 38123 Mattarello, TN, Italy

tissue context of the cell have not been systematically investigated [4, 7, 8, 21, 22].

Considerable attention has been given to the sequence and structural features of p53 binding sites that provide for p53 recruitment to target sites [2, 5, 6]. It is now more clear that the loose definition of p53 response element (RE) [23] that has been used for many years comprises a wide range of DNA binding affinity, occupancy rates and transactivation potentials measured by various types of assays, and that specific differences in the definition of p53 REs are evident between purely *in vitro* biochemical assays and *in vivo* occupancy measurements [24–28].

The canonical p53 consensus found in many identified binding sites of mostly up-regulated p53 target genes consists of two copies of the palindromic half-site RRRCWWGYYY separated by a spacer of 0–13 bp, in which R = purine, W = A or T and Y = pyrimidine. Theoretically, each p53 monomer binds five nucleotides – i.e., one monomer binds the I° quarter site $R_1R_2R_3C_1W_1$ and the second monomer the II° quarter site $W_2G_1Y_1Y_2Y_3$-. As reviewed previously, the rather degenerate p53 consensus sequence, reflects the established observation that in virtually all cases of validated p53 REs, an optimal consensus site is not found, because of mismatches, in some cases resulting in partial binding sites, referred to as non-canonical REs [5, 24, 29]. This has raised the hypothesis of a selection pressure to limit the intrinsic potential of p53 proteins to target binding sites, thereby allowing for modulation of p53-induced transcriptional changes by signal transduction pathways affecting p53 protein amount, DNA binding potential, quaternary structures and/or availability of multiple trans-factors [30–36]. For example, p53 REs with lower DNA binding affinity appear to be more frequent in target genes involved in apoptosis [28]. Consistent with this hypothesis, optimized p53 REs have been recently studied in experimental models and *in vitro* for their kinetic and thermodynamic interactions with p53 as well as transactivation potential and shown to provide for high level of p53-mediated transactivation even at low p53 protein levels [25].

Functional assays in a defined experimental setting provided by the yeast *S. cerevisiae* have been extensively used to characterize the transactivation potential of p53 RE in isogenic conditions and exploit variable expression of p53 under an inducible promoter to yield a matrix of transactivation results, to some extent comparable in precision to that of a biochemical assay in a test tube [5, 24, 26, 28, 37–41]. Further, high correlation was reported between results in yeast and transactivation or occupancy data in cancer cell lines [24, 27]. For example, experiments in this model system led to identify functionally active half-site and 3/4 site (3Q) p53 REs, a group of REs collectively considered as non-canonical that were then mapped and validated also in human cells [7].

Here we have combined all the data obtained so far with the yeast-based p53 transactivation assay and developed an algorithm, p53retriever, to scan DNA sequences, identify p53 REs and classify them based on predicted transactivation potential into five broad categories. As unique features, this algorithm takes into account cooperative interactions between groups of mismatches in two p53 dimers and scores also non-canonical REs.

Specifically we used this approach to map functional p53 REs in the proximity of all annotated coding genes, searched for high affinity p53 REs in the entire genome, and mapped functional p53 REs within ENCODE-defined distant enhancer regions. The predictive power of mapping p53 REs with high functional score near transcription start sites (TSS) was validated for a panel of 13 genes, using cell lines differing for p53 status, two p53-inducing stimuli and measuring relative expression by qPCR at three time points. APOBEC3H, E2F7, GAS6, TRIM32, PDE2A, KCTD1, DICER, MAP2K3, DNAJA1, HRAS, KITLG, TGFA and potentially YAP1 were confirmed or identified as p53 target genes.

Results and discussion

Development and implementation of p53retriever, a pattern search code that identifies canonical and non-canonical p53 REs based on predictions from transactivation assays

In general, the degree of p53 binding depends on various factors including the state of the p53 protein, its cofactors, and the sequence composition of the p53-RE [5, 32]. Because easier to predict than the p53 state, computational algorithms were developed to explore p53 binding through sequence motif analysis. The majority of these algorithms, such as p53MH [42], do not directly consider the response element (RE) potential to drive p53-dependent transactivation. On the contrary, p53retriever is based on a set of manually curated rules, derived from a compendium of p53 transactivation data obtained using a yeast-based assay [24, 26, 37, 43, 44].

REs are scored from five (= highly functional REs activity) to one (= unlikely functional REs) (Fig. 1a). The grade represents the inferred transactivation potential rather than being an indication of the percent similarity to the canonical p53 consensus sequence. For full site p53 REs the grade considers a severe negative impact of a spacer between the two half sites larger than two nucleotides (Fig. 1c). Variable p53-RE spacer lengths are known to affect transactivation capacity. Only two previous studies tried to incorporate the spacer length as one of the relevant features [11, 45], calculating a penalty score directly proportional to spacer length. Also in our algorithm, based on previous results, we attribute high

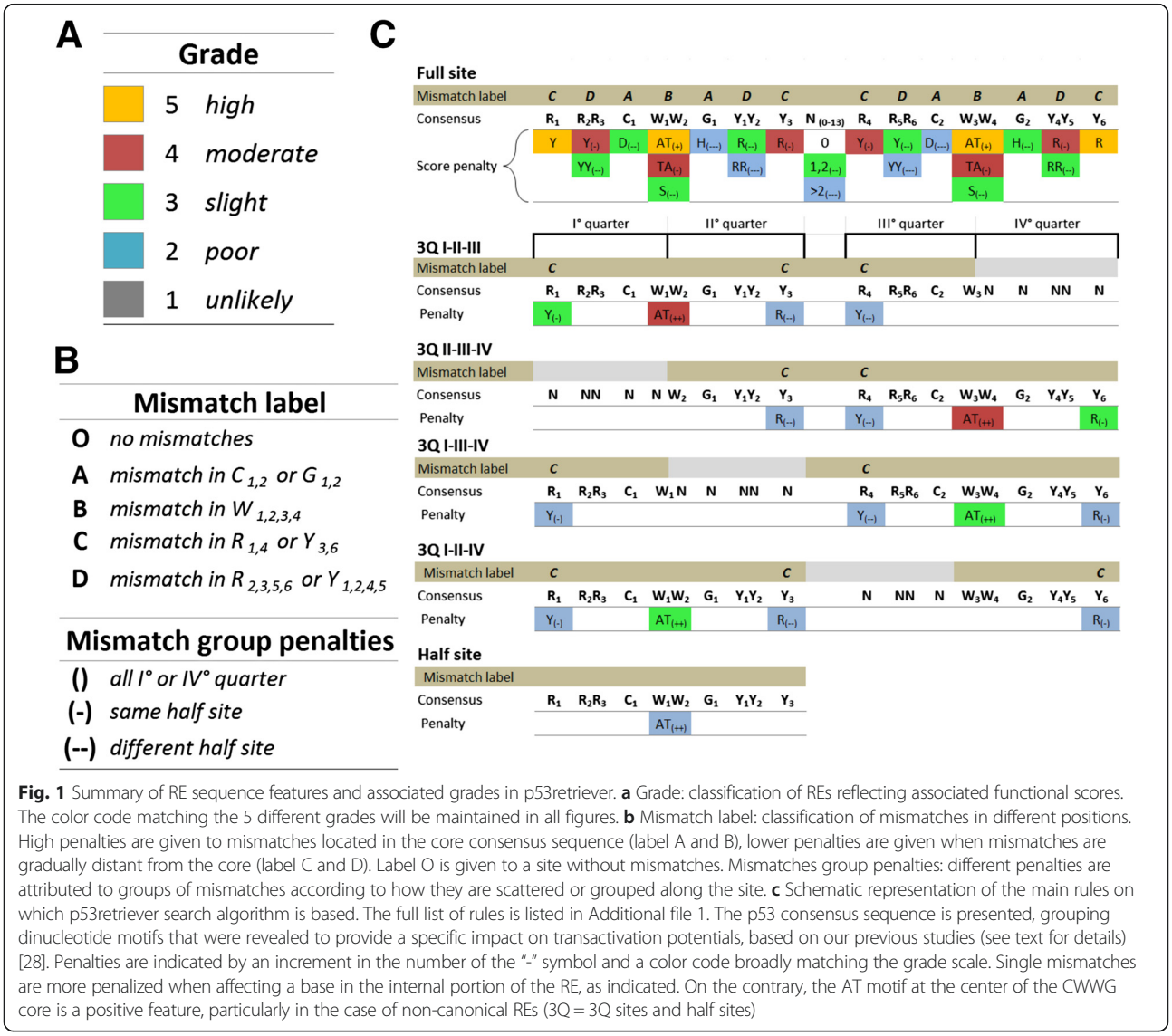

Fig. 1 Summary of RE sequence features and associated grades in p53retriever. **a** Grade: classification of REs reflecting associated functional scores. The color code matching the 5 different grades will be maintained in all figures. **b** Mismatch label: classification of mismatches in different positions. High penalties are given to mismatches located in the core consensus sequence (label A and B), lower penalties are given when mismatches are gradually distant from the core (label C and D). Label O is given to a site without mismatches. Mismatches group penalties: different penalties are attributed to groups of mismatches according to how they are scattered or grouped along the site. **c** Schematic representation of the main rules on which p53retriever search algorithm is based. The full list of rules is listed in Additional file 1. The p53 consensus sequence is presented, grouping dinucleotide motifs that were revealed to provide a specific impact on transactivation potentials, based on our previous studies (see text for details) [28]. Penalties are indicated by an increment in the number of the "-" symbol and a color code broadly matching the grade scale. Single mismatches are more penalized when affecting a base in the internal portion of the RE, as indicated. On the contrary, the AT motif at the center of the CWWG core is a positive feature, particularly in the case of non-canonical REs (3Q = 3Q sites and half sites)

negative impact to spacers longer than two nucleotides (Fig. 1c). Indeed, REs with a long spacer length are also confirmed to be rarely bound by p53 *in vivo* [7, 14, 46, 47]. Many of the computational approaches for identifying putative p53-REs define how similar that putative binding site is to the consensus, but do not consider the local context of single mismatches within the RE. In our approach mismatches from consensus are also weighted depending on their position within the RE 20-mer sequence, given the finding that mismatches in the quarter sites at the interface between the two half sites have a more severe impact likely due to cooperative interactions among two p53 dimers [28] (Fig. 1b). In addition, interaction effects between groups of mismatches are also considered. In general, any combination of mismatches is penalized in a different way according to their location, considering that p53 is functionally active as a tetramer, that each p53 monomer interacts with a 5 nt motif (quarter site) and that the p53 tetramer is thought to be assembled as a dimer of dimers [48]. If groups of mismatches are localized in the same "quarter" of the RE, the score is less penalized than if the same mismatches were scattered in different quarters (Fig. 1b). Importantly, non-canonical REs consisting of 3Q sites and ½ sites [5, 7] are considered functional p53 REs with specific pattern searches. A graphical view of these features presented as "penalty matrix" summarizes the main features of our pattern search (Fig. 1c). The complete list of the rules used to attribute the functional score is presented (Additional file 1). The p53retriever pattern search algorithm, together with functions to better visualize search results, has been implemented as an R package and is available for download at: http://tomateba.github.io/p53retriever.

Distribution of identified p53 response elements around human promoters

We applied p53retriever to the set of sequences in the human genome placed around annotated transcriptional start sites (TSS), selecting a window from -10 kb to 10 kb. The entire list of identified REs, chromosomal coordinates, official gene name, distance from TSS and RE sequence features resulting in the given grade, is available in Additional file 2.

The distribution of identified p53 REs grouped based on the functional score, shows a very large preponderance of "grade 1" REs, that are considered as unlikely functional (Fig. 2a). Also, the distribution of RE scores is highly skewed, with only 0.05 % of REs obtaining the highest grade, supporting the hypothesis of a selecting pressure to reduce p53 binding affinity and provide plasticity in the modulation of p53-mediated stress responses *in vivo* [4, 28]. Very recent analyses confirmed that p53 REs that are more highly conserved in evolution are relatively weak p53 RE sites displaying lower levels of occupancy compared to higher affinity REs that exhibit low evolutionary conservation [47]. Grade five sequences either lack entirely mismatches, or contain two or fewer mismatches in the external positions (R1,Y6/R4,Y3, see Fig. 1c), and contain the positive AT motif in the CWWG core. The vast majority of REs that can be considered functional are in the grade two category. Predicted to be poorly responsive on their own, these REs could participate in the regulation of gene expression conditional to other features, such as the local sequence context of promoter architecture. Included in the grade two category are ~30 % of all half sites mapped (Fig. 2a). A unique feature of our search tool is the specific pattern search for non-canonical 3Q sites. Interestingly, even though mismatches in the two internal quarter sites have an higher impact on p53 transactivation for 3Q sites compared to full sites, and thus result in a final lower grade, many 3Q sites obtained a grade higher than 2. Hence, a great number (13,744) of p53 REs are predicted to be functional even though the entire motif is not present. This observation strongly supports recent reports suggesting that p53 REs match the consensus in one half site, with the two central quarter sites being somehow less variable [14]. It is also consistent with the recent report of the frequent identification of p53 half-sites among p53 ChIP-seq peaks lacking full sites [47].

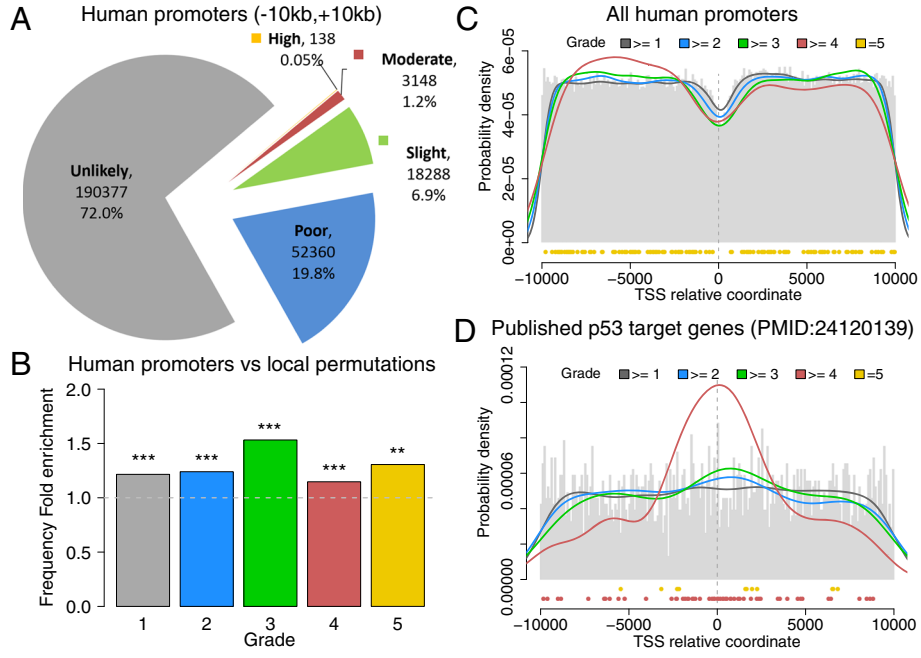

Fig. 2 Analysis of p53 REs found in human promoters. **a** Pie chart displaying the distribution of grades associated to REs found in all human promoters. **b** Comparison between the frequencies of REs found in human promoters, and the frequencies of REs found in scrambled promoter sequences after applying local permutations (to preserve the local GC content). The comparison is shown for each grade. The ratio is 1 if the frequency is the same, > 1 if the frequency is higher in real promoters, <1 if the frequency is higher in scrambled promoters. All enrichments are significant, the binomial test p-value is 4.84E-04 for grade 5 (**), <1E-15 for all the other grades (***). **c** p53 occupancy metaprofile, based on the position of REs in all human promoters, centered on the TSS position. The grey histogram displays the probability distribution of all REs independently from the grade. Colored lines represent the density distribution of REs with higher grades (the grade threshold corresponding to each color is displayed in the legend). The specific positions of grade 5 REs are dotted in yellow under the histogram. **d** p53 occupancy metaprofile, based on the position of REs in the human promoters of 228 p53 target genes, published in [15]. The color scheme is the same as in panel C. The specific positions of grade 4 and 5 REs are dotted under the histogram (in yellow for grade 5, red for grade 4)

We compared the results obtained searching within human promoters with what we would expect by chance, by applying p53retriever to sets of scrambled sequences obtained by local permutations of real promoter sequences (see Methods and Additional file 3: Table S1). Local permutations allowed us to preserve the local GC content of promoter regions, showing in fact an increase in GC content around the TSS (see Additional file 3: Figure S1). From this analysis we could determine that the frequency of REs in the global set of human promoters is slightly but significantly higher than the frequency of REs in scrambled sequences (Fig. 2b). This soft enrichment is plausible, given that we are considering all known human TSS and not specific populations of genes. Grade five and three are the most enriched class of REs when comparing the frequency of each grade (Fig. 2b).

Mapping all the REs considering their position with respect to the TSS, we obtained an occupancy metaprofile of p53 REs, displayed in Fig. 2c. This occupancy profile reveals a general decrease of REs in the region proximal to TSS (from -2 kb to +2 kb). This decrease affects all REs, independently from the grade, and appears to be a consequence of the local increase in GC content, since we observed the same effect in scrambled sequences when applying local permutations (Additional file 3: Figure S2). Overall the REs reduction (approximately of ¼.) could be interpreted as a selection against a high density of active p53 REs from promoter regions of non-target genes that is limited to about 2 kbs from TSS. This reduction is driven by the general increase in GC content around the TSS, which more globally is instrumental in the interplay between chromatin conformation and transcription processes. On the other hand, when restricting our analysis to the promoter region of known p53 targets, we found an entirely different landscape. Fig. 2d displays the promoter occupancy metaprofile of REs identified by p53retriever in a group of 189 HGNC genes listed as targets of p53 in literature and collected in [15, 45]. Interestingly, this profile shows the highest probability density in the region closer to the TSS, especially for functional REs with grade four and five (red line in Fig. 2d). Indeed, recent data reported a prevalence of p53 REs nearby the TSS of known target genes [16, 47].

Comparison with other p53 binding site datasets and search tools

To further verify if p53retriever recognized already established p53 binding sites, we compared our approach with lists of p53 target genes and REs previously reported. The detailed results of all comparisons are contained in Additional file 4.

First, we used our method to score 81 REs sequences that are consistently bound by p53 according to seven different ChIP-seq datasets, reported in [15]. All these sequences were picked by p53retriever as potentially functional. Interestingly, excluding one sequence, all p53 REs from this list obtained a grade greater than one with the majority being of grade 5, confirming that our tool can discriminate functional and well-known REs (Fig. 3a).

Next, we applied p53retriever on p53 REs obtained by Chip-exo analysis [14], providing near-nucleotide resolution of p53 bound sites in response to a variety of genotoxic stresses. (Fig. 3b). While 28 % of sites were not classified, the majority of bound sequences from ChIP-exo obtained a grade greater than 1, with a predominance of grade four and five, (Fig. 3b, left panel). Interestingly, we saw a clear correlation between higher relative occupancy and higher RE grade (Fig. 3b, right panel). Looking in more detail to the "no grade" group, we noticed that all non-scored sequences differed from the canonical RE site for features which are highly penalized by our algorithm, like a number of mismatches higher than three scattered on three different quarter sites. Nevertheless, we could show that these not-scored sequences are mostly characterized by low occupancy values (white boxplot in Fig. 3b right panel, Wilcoxon rank sum test p-value=1.29E-09). Consistently, when considering the subset of regions increasingly bound by p53 after all the stimuli used in [14], the percentage of "no grade" drops to 17.6 % (Additional file 3: Figure S3).

We also extended the comparison to a Chip-seq dataset, reported in [17] (Fig. 3c) and obtained an overall similar distribution of RE grades. The percentage of regions with "no grade" is 22.8 %.

Next, we extended the comparisons to other lists of REs, starting from two small collections of reported p53 REs, based on heterogeneous experimental approaches [2, 15, 45]. Only a minority of those REs obtained the highest grade, and the proportion of sequences not scored as potentially functional was approximately 40 % (Additional file 3: Figure S4). It has to be said that the REs reported in those lists are not guaranteed to be the ones actually or solely responsible for the responsiveness of the associated genes to p53.

Even though total mRNA levels are an indirect measurement of p53 transcriptional activity, they reflect the transcriptome status upon p53 activation. Thus, we did an additional comparison using microarray data obtained after p53 activation upon Doxorubicin treatment of MCF7 cells [49]. The majority of differentially expressed, up-regulated genes turned out to have a p53 binding sites with grade three (Fig. 3d), and exhibited a specific enrichment of REs with grade >3 near the TSS (Additional file 3: Figure S5). Similar comparisons were done with lists of p53 target genes in curated databases such as TRANSFAC and IPA. Again, the majority of these genes have a RE of grade three predicted by p53retriever in their promoter region (Fig. 3d). Using Ingenuity Pathway analysis (IPA), grade five and grade four human promoters revealed a strong p53 pathway signature (Additional file 5).

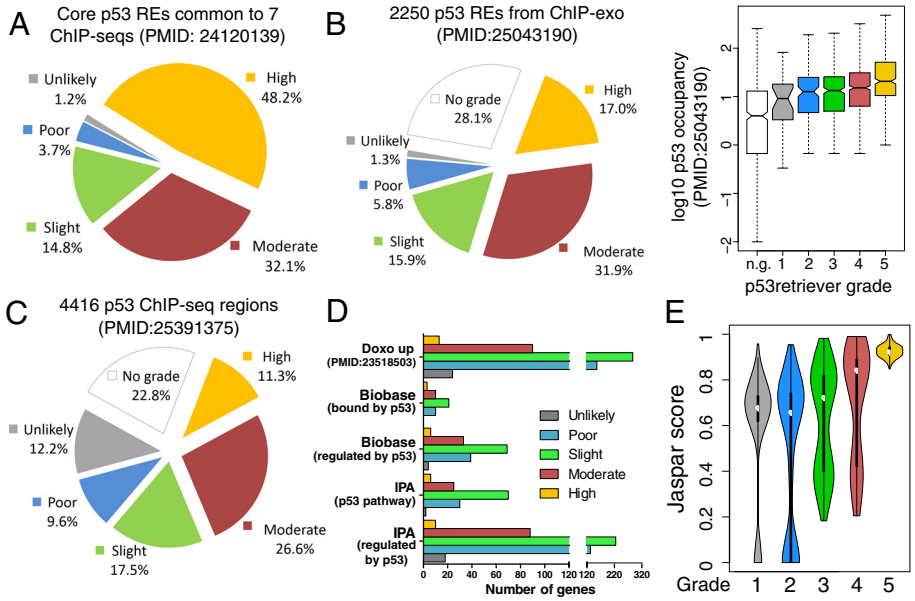

Fig. 3 Comparison of p53retriever with other p53 binding site datasets and tools. **a** Pie chart displaying p53retriever classification on a list of 81 regions commonly identified by 7 different ChIP-seq experiments [15]. **b** Left panel: pie chart displaying p53retriever classification on a list of 2250 regions identified by ChIP-exo [14]. Right panel: boxplot displaying for each grade assigned by p53retriever to ChIP-exo sequences, the distribution of the corresponding ChIP-exo occupancies, measured in [14]. n.g. = no grade given by p53retriever. **c** Pie chart displaying p53retriever classification on a list of 4416 regions identified by ChIP-seq in [17]. **d** p53 target gene lists from curated databases (Biobase and IPA) or from expression datasets (Doxo up: genes up-regulated upon doxorubicin treatment) were compared to the list of p53 promoter REs obtained with p53retriever. Presented in the bar graph are the predicted p53 REs grouped by the maximum functional grade identified by p53retriever in their promoter. **e** Comparison between p53 REs identified in human promoters by p53retriever, and the corresponding score given by Jaspar p53 PWM (MA0106.2), based on ChIPseq data. REs are divided in 5 groups along the horizontal axis, corresponding to the grade assigned by p53retriever. For each group, the distribution of the scores given by Jaspar PWM is represented as a violin plot, i.e., a box plot with a rotated kernel density plot on each side. Jaspar scores range from 0 (the RE is not identified) to 1 (the RE is optimal)

Finally, we compared p53retriever results with the standard PWM approach, using two PWMs provided by the JASPAR database (see Methods). All REs identified by p53retriever in the set of human promoters were scored in parallel with both JASPAR PWMs: the comparison with the JASPAR PWM derived from ChIPseq data is shown in Fig. 3e. Although there is a high agreement on REs with the maximum grade, very close to the optimal p53 consensus, the comparison shows divergences between the two methods for the lower grades. For example, a considerable population of REs assigned to grade four by p53retriever receives very low scores from JASPAR. This is likely due to the presence of ¾ sites that are over-penalized by the PWM approach. On the other hand, many REs with low grades are highly scored by JASPAR, that doesn't penalize groups of scattered mismatches. Apart from grade 1, we can observe a linear trend between the two scoring systems if we look at the median values of the boxplots displayed in Fig. 3e, so we can conclude that the two approaches are distinct and complementary. On the other hand, the second JASPAR matrix, based on SELEX data, gives misleading results, since even optimal REs (grade 5) receive low scores (Additional file 3: Figure S6).

High grade p53 REs are enriched in distant enhancers

Recent functional genomics approaches, particularly resulting from the ENCODE initiative, have revealed that transcription is rather pervasive, that enhancer sequence can be very distant, at least in terms of primary sequence, from genes, and that active enhancers can be mapped based on specific histone code marks [50, 51]. Hence, we exploited this rich body of available information to map p53 REs in distal enhancer sites, using DNAse hypersensitive sites tracks. We filtered out sites overlapping with promoter regions defined in the previous sections, and considered a population of 43,787 distal regions, whose length distribution is displayed in Fig. 4a. p53retriever was run on this set of regions, and the complete results are provided in Additional file 6. The grade distribution of REs found in distal DNAse regions is displayed in Fig. 4b. The frequency of REs in these regions is significantly higher than the frequency found in human promoters and also in random sequences (Fig. 4c and Additional file 3: Figure S7). The overall fold enrichment is 3.54, but this trend grows proportionally to the grade of the REs, reaching a peak with grade 5. In fact, 144 high grade REs are found within DNAse hypersensitive sites (Fig. 4b), more than in the

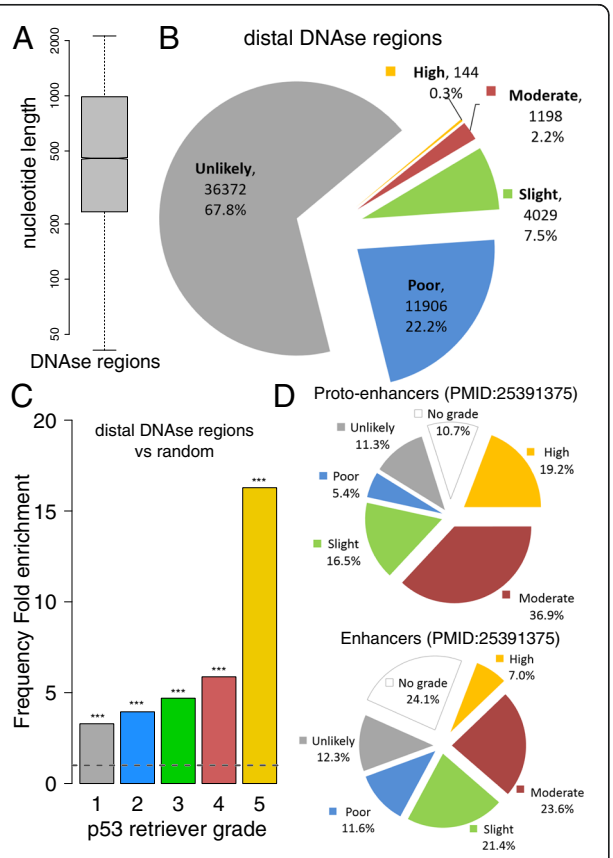

Fig. 4 Analysis of p53 REs found in distal DNAse hypersensitive regions. **a** Boxplot of the nucleotide length of human distal DNAse hypersensitive regions, determined as described in Methods. **b** Pie chart displaying the distribution of grades associated to REs found in human distal DNAse hypersensitive regions. **c** Comparison between the frequencies of REs found in human distal DNAse hypersensitive regions, and the frequencies of REs found in random sequences with the same GC content. The comparison is shown for each grade. The ratio is 1 if the frequency is the same (horizontal dotted line), > 1 if the frequency is higher in DNAse regions, <1 if the frequency is higher in random sequences. All enrichments of REs mapped to distal DNAse hypersensitive regions are highly significant (Binomial test p-value < 1E-20). **d** Pie charts displaying p53retriever classification on two lists of regions identified by ChIP-seq in [17] as proto-enhancers (upper panel) and enhancers (lower panel)

entire human promoter dataset. The fold enrichment of grade five REs is 16.3 (Fig. 4c). Presently, it is undetermined if this enrichment for high quality binding sites reflects a common trend for sequence-specific transcription factors or a distinct feature of p53 family proteins. Consistent with our results, higher levels of p53 occupancy in distal enhancers compared to promoters was very recently reported based on ChIP-seq analysis of lymphoblastoid cell lines treated with doxorubicin [47]. Additionally, Chip-seq analysis reported in [17] allowed us to expand the study of p53 REs in enhancers regions. In fact that paper provided p53 bound regions classified as enhancers based on ENCODE annotation or as proto-enhancers, where p53 could act as pioneer transcription factor. Interestingly, this latter group showed an enrichment for high scoring (grade four and grade five) p53 REs according to p53retriever and a lower proportion of sequences with no grade (Fig. 4d, top panel).

New direct p53 target genes identified based on the p53 RE functional search tool

High-activity, or non-canonical p53 REs predicted to be moderately active were mapped by our tools near the TSS of genes that are not completely established or novel putative direct p53 target genes. To infer the predictive power of the pattern search on p53-dependent transcriptional changes, 13 genes were selected and their expression was tested followed by qPCR in cell lines differing for p53 status (MCF7, two derivative clone so called MCF7 vector and MCF7shp53, HCT $p53^{+/+}$ and HCT $p53^{-/-}$) and at different time points (8, 16, 24 h) after p53 activation by two different treatments, i.e., Doxorubicin -a genotoxic chemotherapeutic drug- and Nutlin-3A -an MDM2 inhibitor- (Fig. 5a) (Additional file 7). Results support p53-dependent up-regulation for most genes. The p53-dependency is confirmed by the absence of induction in HCT $p53^{-/-}$ and MCF7shp53 cell lines, despite the different p53 status between the two cells lines (a p53-null and a partial knockdown cell line, respectively). In some cases, the increase in gene expression compared to the mock condition was time-dependent. Differences in these kinetic features were apparent between the two treatments applied. E2F7 was inducible by Doxorubicin at different time points, while after Nutlin-3A treatment an early up-regulation was followed by repression, which appeared to be p53-dependent. GAS6 and KCTD1 had a similar trend especially in MCF7 cells. Differences were noted between MCF7 and the MCF7-vector derivative clone in the magnitude or the kinetics of relative expression changes (*e.g.*, PDE2A, APOBEC3H, KCTD1, DNAJA1, DICER). Nine of the thirteen candidates (PDE2A, GAS6, E2F7, APOBEC3H, KCTD1, TRIM32, TGFA, KITLG, HRAS) were selected among the list of genes having both a predicted binding sites in our algorithm output with a grade higher or equal to 2, and a reported p53 binding sites on ChIPseq datasets [7, 8]. For all of them except TRIM32, total mRNA levels are also reported as upregulated after Doxorubicin treatment by microarray data [49]. Although the induction is not directly proportional to the grade, we confirmed p53 dependent induction by qPCR for all of them in time/cell line dependent manner. Even though TRIM32 is not upregulated after Doxorubicin treatment in all the tested cell lines, it is upregulated upon Nutlin-3A treatment, confirming ChIP-seq data. Besides their p53 binding sites, these candidates were selected because of their reported involvement in cell-cycle control

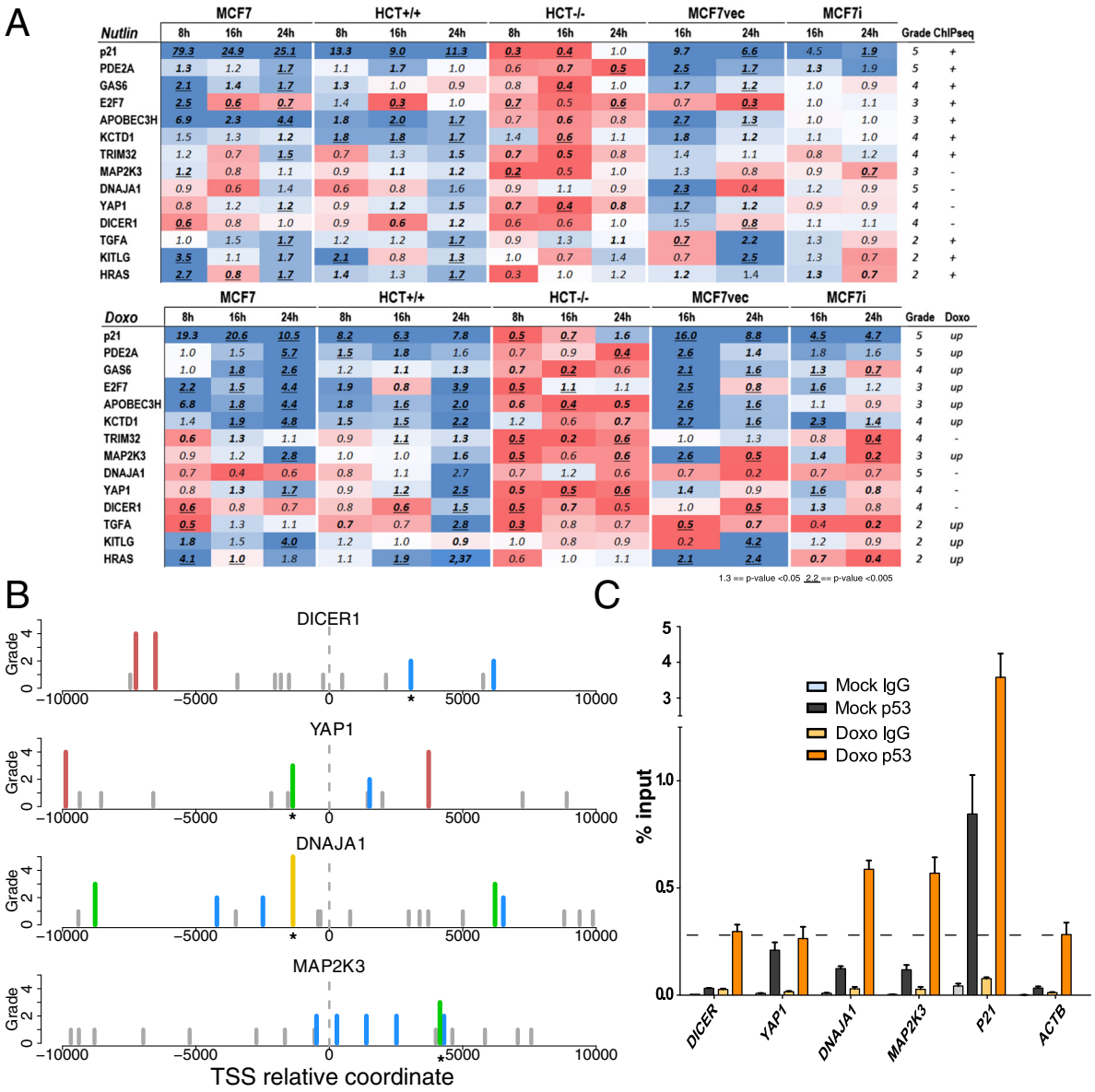

Nutlin	MCF7 8h	MCF7 16h	MCF7 24h	HCT+/+ 8h	HCT+/+ 16h	HCT+/+ 24h	HCT-/- 8h	HCT-/- 16h	HCT-/- 24h	MCF7vec 16h	MCF7vec 24h	MCF7i 16h	MCF7i 24h	Grade	ChIPseq
p21	79.3	24.9	25.1	13.3	9.0	11.3	0.3	0.4	1.0	9.7	6.6	4.5	1.9	5	+
PDE2A	1.3	1.2	1.7	1.1	1.7	1.0	0.6	0.7	0.5	2.5	1.7	1.3	1.9	5	+
GAS6	2.1	1.4	1.7	1.3	1.0	0.9	0.8	0.4	1.0	1.7	1.2	1.0	0.9	4	+
E2F7	2.5	0.6	0.7	1.4	0.3	1.0	0.7	0.5	0.6	0.7	0.3	1.0	1.1	3	+
APOBEC3H	6.9	2.3	4.4	1.8	2.0	1.7	0.7	0.6	0.8	2.7	1.3	1.0	1.0	3	+
KCTD1	1.5	1.3	1.2	1.8	1.8	1.7	1.4	0.6	1.1	1.8	1.2	1.1	1.0	4	+
TRIM32	1.2	0.7	1.5	0.7	1.3	1.5	0.7	0.5	0.8	1.4	1.1	0.8	1.2	4	+
MAP2K3	1.2	0.8	1.1	0.9	1.1	1.2	0.2	0.5	1.0	1.3	0.8	0.9	0.7	3	-
DNAJA1	0.9	0.6	1.4	0.6	0.8	1.6	0.9	1.1	0.9	2.3	0.4	1.2	0.9	5	-
YAP1	0.8	1.2	1.2	0.9	1.2	1.5	0.7	0.4	0.8	1.7	1.2	0.9	0.9	4	-
DICER1	0.6	0.8	1.0	0.9	0.6	1.2	0.6	0.6	1.0	1.5	0.8	1.1	1.1	4	-
TGFA	1.0	1.5	1.7	1.2	1.2	1.7	0.9	1.3	1.1	0.7	2.2	1.3	0.9	2	+
KITLG	3.5	1.1	1.7	2.1	0.8	1.3	1.0	0.7	1.4	0.7	2.5	1.3	0.7	2	+
HRAS	2.7	0.8	1.7	1.4	1.3	1.7	0.3	1.0	1.2	1.2	1.4	1.3	0.7	2	+

Doxo	MCF7 8h	MCF7 16h	MCF7 24h	HCT+/+ 8h	HCT+/+ 16h	HCT+/+ 24h	HCT-/- 8h	HCT-/- 16h	HCT-/- 24h	MCF7vec 16h	MCF7vec 24h	MCF7i 16h	MCF7i 24h	Grade	Doxo
p21	19.3	20.6	10.5	8.2	6.3	7.8	0.5	0.7	1.6	16.0	8.8	4.5	4.7	5	up
PDE2A	1.0	1.5	5.7	1.5	1.8	1.6	0.7	0.9	0.4	2.6	1.4	1.8	1.6	5	up
GAS6	1.0	1.8	2.6	1.2	1.1	1.3	0.7	0.2	0.6	2.1	1.6	1.3	0.7	4	up
E2F7	2.2	1.5	4.4	1.9	0.8	3.9	0.5	1.1	1.1	2.5	0.8	1.6	1.2	3	up
APOBEC3H	6.8	1.8	4.4	1.8	1.6	2.0	0.6	0.4	0.5	2.6	1.6	1.1	0.9	3	up
KCTD1	1.4	1.9	4.8	1.5	1.5	2.2	1.2	0.6	0.7	2.7	1.6	2.3	1.4	4	up
TRIM32	0.6	1.3	1.1	0.9	1.1	1.3	0.5	0.2	0.6	1.0	1.3	0.8	0.4	4	-
MAP2K3	0.9	1.2	2.8	1.0	1.0	1.6	0.5	0.6	0.6	2.6	0.5	1.4	0.2	3	up
DNAJA1	0.7	0.4	0.6	0.8	1.1	2.7	0.7	1.2	0.6	0.7	0.2	0.7	0.7	5	-
YAP1	0.8	1.3	1.7	0.9	1.2	2.5	0.5	0.5	0.6	1.4	0.9	1.6	0.8	4	-
DICER1	0.6	0.8	0.7	0.8	0.6	1.5	0.5	0.7	0.5	1.0	0.5	1.3	0.8	4	-
TGFA	0.5	1.3	1.1	0.7	0.7	2.8	0.3	0.8	0.7	0.5	0.7	0.4	0.2	2	up
KITLG	1.8	1.5	4.0	1.2	1.0	0.9	1.0	0.8	0.9	0.2	4.2	1.2	0.9	2	up
HRAS	4.1	1.0	1.8	1.1	1.9	2.37	0.6	1.0	1.1	2.1	2.4	0.7	0.4	2	up

1.3 == p-value <0.05 2.2 == p-value <0.005

Fig 5 p53-responsiveness of target genes associated with predicted functional REs. **a** qPCR results of 13 selected genes. Fold of changes values (ΔΔCq) upon each treatment are presented as a heatmap. Upper part shows mRNAs level after Nutlin-3A treatment while the lower shows the same after Doxorubicin (Doxo) treatment. Expression levels were tested in different cell lines (MCF7, HCT +/+, HCT –/–, MCF7 vector and MCF7 shp53) and at different time points (8, 16 and 24 h) (Details are presented in Additional file 7). For each gene, the "Grade" column presents the binding site grade reported by our algorithm. "ChIPseq" column shows the presence (+) or absence (–) of reported p53 binding sites [8]. "Doxo" column presents mRNA levels obtained by microarray data [49]. **b** Positional representation of p53 binding sites in TSS proximity for DICER, YAP1, DNAJA1, MAP2K3. Bar height is proportional to the binding site grade. Grade 5 is yellow, grade 4 is red, grade 3 is green, grade 2 is blue and grade 1 is grey. **c** p53 occupancy on the promoter of DICER, YAP1, DNAJA1 and MAP2K3 comparing Mock and Doxo condition in MCF7 cells. P21, well-known p53 direct target, is a positive control. ACTB is used as a reference. Sites validated by ChIP are indicated by a * symbol in Figure 5b

and tumor progression (PDE2A, E2F7, GAS6, TRIM32, HRAS, KITLG and TGFA), in transcription (KCTD1), and DNA editing (APOBEC3H) (see Supplementary Text in Additional file 3).

For the remaining four genes, whose REs are displayed in Fig. 5b, we performed a chromatin-immunoprecipitation experiment in MCF7 cells treated with Doxorubicin for 16 h. Weak p53 occupancy was observed by qPCR at DNAJA1 and MAP2K3 loci after doxorubicin treatment, while a region containing a predicted grade 3 category p53 RE in the YAP1 gene showed evidence for p53 occupancy in the mock condition. Our results did not support direct p53 binding to the DICER promoter, consistent with a previous study [52] (Fig. 5c).

Overall, we propose DNAJA1, MAP2K3 and potentially YAP1 as new direct p53 target genes, although the level of transactivation was relatively low.

DNAJA1 can act as a co-chaperone of Hsc70 that was previously associated to radioresistance phenotype in wild type p53 glioblastoma cells treated with farnesyltransferase inhibitors [53]. Recently, overexpression of DNAJA1 was associated with a reduction of pancreatic cancer cell survival and with c-Jun repression [54].

MAP2K3 participates in the MAP kinase cascade and can phosphorylate p38. This protein was identified as a senescence-promoting factor in human breast epithelial cells [55]. However, it has also been associated to tumor invasion potential and to be regulated at transcriptional level by NFY, NF-κB and gain-of-function mutant p53 [56].

The Yes-associated protein 1 (YAP1) is a transcriptional regulator involved in the Hippo signaling pathway. Evidences support both an oncogenic and a tumor suppressor role for YAP1, linked to ABL1-induced apoptosis [57]. YAP1 protein was found capable to bind the p53 promoter and a positive feedback loop was proposed based on the finding that p53 can bind the YAP promoter [58]. In part consistent with this view we found p53-dependent YAP1 gene up-regulation both after doxorubicin and Nutlin-3A treatment.

Conclusions

Several previous tools were developed to identify bona fide p53 response elements, starting with pioneering *in vitro* selection experiments that led to the initial and still accepted definition of the consensus p53 RE [11, 42, 45, 59, 60]. The majority of these tools were based on position weight matrices derived from results of *in vitro* approaches, namely competitive gel shift assays and SELEX, more recently integrated with results obtained from Chromatin immunoprecipitation experiments. A systematic effort to quantify changes in DNA binding affinity (dissociation constants) using fluorescence anisotropy titration led to the development of a p53 binding site predictor algorithm [60]. This tool was also used to search genome wide for high affinity p53 REs and to map naturally occurring single nucleotide polymorphisms (SNPs) that can impact on the DNA binding affinity of p53. The functional relevance of SNPs within p53 REs has been established in several reports [15, 24, 27, 44, 61].

All position weight matrix approaches assume additive contributions of the individual positions within the RE sequence, and except for [45] and [11], all tools do not specifically weigh the impact of spacers between half site decameric RE motifs in the 0-13 nt range. This spacer length was in fact considered neutral in the initial *in vitro* experiments [23]. However, DNA binding assays where RE sequence are embedded in longer DNA molecules, competitive binding experiments in microfluidics, Chromatin Immunoprecipitation assays, yeast- and mammalian-cell based transactivation assays all indicate that even a single nucleotide spacer between p53 RE half sites can reduce transactivation potential [5, 24, 27, 44]. In fact, when the spacer is longer than 2–3 nt the two decameric half sites no longer show cooperative interactions [24, 28, 62], although when the distance in primary sequence approach one helical pass, transactivation potential appears to increase beyond additivity [24], yet remaining much lower compared to the absence of a spacer. The negative impact of spacer is even more dramatic for TAp73 [62] and TAp63 proteins, but not for ΔNp63 [63], suggesting that the structure as well as the sequence of DNA binding sites can lead to conformational changes in the quaternary tetrameric structure of p53 family proteins, and that intrinsic differences exist in the oligomerization state of these proteins [64].

We have coded in p53retriever sequence and structural features of p53 REs impacting on transactivation potential that were revealed in the past several years using our yeast-based transactivation assay [5, 26, 28, 63, 65, 66]. The resulting algorithm has several distinctive features compared to previous tools, particularly for scoring interactions among groups of mismatches, non-canonical 3Q sites and half sites p53 REs, weighing the impact of consensus mismatches considering their position within the full site RE sequence, i.e., giving higher penalty to mismatches in the two internal quarter sites, and weighs consensus sequence variations within dinucleotide motifs in the core and flanking regions [28] (Fig. 1, Additional file 1). Possible interactions between nearby half site p53 REs or clusters of full site and 3Q sites are currently not considered by our algorithm.

We mapped and ranked functional REs near TSS for all annotated transcripts in UCSC (Additional file 2). Further, we exploited ENCODE data and provide a cartography of ranked p53 REs within distant DNAse hypersensitive sites, considered as distant enhancers (Additional file 6). In these regions we found a significant 16-fold enrichment of high grade REs with respect to the basal frequency expected by chance or observed in promoter regions. An enrichment for high grade REs was also found among proto-enhancer sequences bound by p53 identified by ChIP-seq [17]. It is worth noting that our results represent a projection from all DNAse hypersensitive sites, irrespective of the specific tissues in which they are active. Tissue variability may influence which REs are selectively bound. An additional layer of complexity is represented by the known interplay between different transcription factors. This important aspect is not included in our analysis that is focused on p53 alone.

Although the data on which the algorithm is construed are the outcome of transactivation assays measured from chromatinized promoter-reporter construct, the isogenic nature of the yeast-based functional assays, minimizes

most variables potentially impacting on transactivation by p53; at the same time distinct chromatin features of the natural context of the REs' location *in vivo* may certainly influence the associated gene transcriptional responsiveness to p53. Hence the yeast-based results might be more similar to ChIP-seq and ChIP-exo results, albeit with a more quantitative power.

Undoubtedly different ChIP-seq experiments do not agree with each other and there is limited overlap among the results obtained with different cell lines or using different treatments to activate p53. While global differences in occupancy could be related to differences in accessibility between different tissue-derived cells or to distinct p53 post-translational modifications or cofactors activated by different treatments, it was interesting to find that the list of p53 bound sites that are common to multiple ChIP-experiments were highly enriched for high scoring (grade four and grade five) REs and none of them failed to be classified by our tool (Fig. 3a). Instead, when examining individual ChIP-seq or even, although to a lower extent, ChIP-exo data, 20 % to 30 % of p53 bound fragments did not contain a motif scored by p53retriever. While those sites may represent examples of p53 proteins tethered to DNA by protein interactions, the manual inspection of "no grade" sites from the ChIP-exo datasets showed that the majority of these sites resemble p53 response elements but contain several (three or more) "core" mismatches scattered on three different quarter sites. These multiple mismatched REs are not presently scored by p53retriever, but would probably result in weak responsiveness. Consistently, the majority of no grade ChIP-exo REs showed lower occupancies (Fig. 3b right panel).

Finally, we decided to validate a few of the predictions from the pattern search, particularly for non-canonical 3Q sites using cell lines as a model. 13 genes with mapped functional REs were chosen. Overall, despite our algorithm doesn't consider the system complexity of transcriptional regulation in living cells and the response variability upon each different p53 stimulus, results support p53-dependent transactivation for the majority of them. Based on the combined qPCR and ChIP results we conclude that DNAJA1, MAP2K3, and potentially YAP1 can be considered new direct p53 target genes, linking p53 to yet additional potential biological outcomes. Furthermore, our data further establish the very recent findings of PDE2A, GAS6, E2F7, APOBEC3H, KCTD1, TRIM32, HRAS, KITLG and TGFA as p53 target genes.

Methods

Implementation of pattern search rules in p53retriever

We implemented the set of manually curated rules (Additional file 1) in an R package called p53retriever. p53retriever source and binary files are available on Github, at (http://tomateba.github.io/p53retriever/). p53retriever contains a main function that identifies potential REs. This function needs as input an arbitrary DNA sequence, and returns a table containing information about the identified REs, such as position, sequence, spacer length, mismatch label and grade. The format of the output is similar to Additional file 6. Many functions are also provided in order to graphically display the results. The package is documented with usage examples, and fully integrated with other CRAN and Bioconductor packages. In particular, p53retriever depends only on the previous installation of the Bioconductor Biostrings package.

Human promoters dataset

Human promoter sequences were extracted from the UCSC database (http://genome.ucsc.edu/) considering, for each transcript with a distinct TSS, the 20 kB region surrounding the transcription binding site (genome build GRCh37/hg19). The final dataset consists of 23,541 promoter sequences, associated to distinct UCSC identifiers and corresponding to 18,355 HGNC genes.

Human distal DNase regions dataset

Encode DNase-seq regulatory regions (genome build GRCh37/hg19) were obtained from the following cell lines: Gm12878, H1hesc, Helas3, Hepg2, Hmec, Hsmm, Hsmmt, Huvec, K562, Monocd14, Nha, Nhdfad, Nhek, Nhlf, Osteobl, Hsmmfshd, Lncap, Nb4, Nt2d1,Panc1. The consensus was defined as the merge of all the regions that were present in at least two cell lines. Only distal regions, with more than 10 kb from the nearest annotated TSS, were kept in the dataset, in order to avoid overlap with promoter regions. The final dataset consists of 43,787 regions, with a mean length of 673.3 bases.

Simulations with random sequences

Sets of scrambled promoter sequences were generated by local permutations (bin size = 500 nt) of human promoter sequences (−10 kb, +10 kb from TSS). This allowed to preserve the local GC content in the random model; p53 REs were then identified and classified with p53retriever. The random simulation was run ten times, and the results were compared to REs identified in real human promoters.

Set of random sequences were generated, with the same number and the same GC content (44 %) of human DNA sequences; p53 REs were then identified and classified with p53retriever. The random simulation was run ten times, and the results were compared to REs identified in human distal DNase regions promoters.

Pathway analysis of DEGs

All pathways analyses were performed using IPA (www.ingenuity.com). Only direct interactions were considered in the setting parameters.

Comparison with other datasets

Several lists of p53 targets, identified by their HGNC symbol, were extracted from online databases such as Biobase TRANSFAC (http://www.biobase-international.com/product/transcription-factor-binding-sites) and IPA, or from previous publications, referenced in the main text. These lists were used to select populations of genes among our dataset of human promoters, and analyze the grade of the REs identified by p53retriever (as shown in Fig. 2d).

Several sets of p53 RE sequences or p53 bound regions were taken from previous publications, referenced in the main text. p53retriever was run directly on these sequences (as shown in Fig. 3a, b, c).

Comparison with JASPAR PWMs

Two PWMs for p53 were downloaded from the JASPAR database (http://jaspar.genereg.net/). One PWM, MA0106.1, is built on SELEX data, while the second, MA0106.2, is built on ChIPseq data. The original values of the downloaded PWMs were based on nucleotide frequencies and therefore more similar to Positional Frequency Matrices. These frequency values were transformed in log2 probability ratio values with the PWM function implemented in the Bioconductor Biostring package, using a multinomial model with a Dirichlet conjugate prior to calculate the estimated probability of base b at position i. The final score of a match ranges from 0 to 1. All REs identified by p53retriever in the set of human promoters were scored with JASPAR PWMs: the comparison with MA0106.2 is shown in Fig. 3d, while the comparison with MA0106.1 is shown in Additional file 3: Figure S2.

Cell lines and culture conditions

The human breast adenocarcinoma-derived MCF7 cell line (p53 wild type) was obtained from the InterLab Cell Line Collection bank, ICLC (Genoa, Italy) while the colon adenocarcinoma HCT116 ($p53^{+/+}$) cell line and its $p53^{-/-}$ derivative were a gift from B. Vogelstein (The Johns Hopkins Kimmel Cancer Center, Baltimore, Maryland, USA). MCF7 cells stably expressing an shRNA targeting p53 (MCF7shp53) or control cells (MCF7vector) were kindly provided by Dr. Agami (Netherlands Cancer Institute, Amsterdam). Cells were normally maintained in DMEM or RPMI (BioWhittaker, Lonza, Milan, Italy) supplemented with 10 % FCS, antibiotics (100 units/ml penicillin plus 100 mg/ml streptomycin) and 2 mM glutamine. Puromycin (Sigma-Aldrich, Milan, Italy) was used to maintain the selection, at 0.5 μg/mL as final concentration.

RNA extraction

Cells were seeded into 6-well plates and allowed to reach 70-80 % of confluence before treating with 1.5 μM Doxorubicin or 10 Mm Nutlin-3A. Doxorubicin was purchased from Sigma-Aldrich (Milan, Italy) while Nutlin-3A was obtained from Alexis Biochemicals (Enzo Life Science, Exeter, UK). After 8 h, 16 h or 24 h of treatment cells were harvested and total RNA was extracted using RNeasy Mini Kit (Qiagen, Milan, Italy) according to the manufacturer's instructions. In-column DNAse treatment (RNase-Free DNase Set, Qiagen, Hilden, Germany) was performed to remove DNA contamination during the extraction. Purity of RNAs (A260/A280 value of 1.8–2.1) and concentration were measured using the Nanodrop spectrophotometer.

qPCR

cDNA was generated starting from 1 μg of RNA by using the RevertAidTM First Strand cDNA Synthesis Kit (Fermentas, Milan, Italy) in 20 μL as final volume following manufacturer's instructions. Primers were designed by Primer-BLAST performing in silico analysis as well as standard curves to define assay specificity and efficiency (Additional file 7). All qPCR assays were performed on CFX Touch Real-Time PCR Detection System (Bio-rad, Milan, Italy) in a 384-well plate format. Optimal primer concentrations (200nM-400nM) were determined by identifying conditions resulting in the lowest C_q combined with absence of primer dimer formation. Reaction volumes were set at 10 μl. SYBR Green assays contained 5X KAPA SYBR FAST qPCR Mastermix (Kapa Biosystems, Resnova, Rome, Italy), 400 nM each primer (MWG, Operon, Ebersberg, Germany) and 25 ng of cDNA. Initial thermal cycling conditions were 1 cycle of 95 °C for 3 mins, followed by 40 cycles of 95 °C for 30 s, 60 °C for 20 s, 72 °C for 60 s. At the end a melt curve analysis was performed. Post-run relative mRNA quantification was obtained using the comparative C_q method ($\Delta\Delta C_q$), where glyceraldehyde 3-phosphate dehydrogenase (GAPDH) and β-2microglobulin (B2M) served as reference genes.

ChIP assays

MCF7 cells were cultured in complete medium in a 150-mm Petri dishs and when reaching 70/80 % confluence were treated for 16 h with Doxo. The procedure for cross-linking, sonication, IP and analysis followed a previously described protocol [49]. Antibodies used for ChIP assays were: p53 (DO-1) and IgG (sc-2025 or sc-2027) (Santa Cruz Biotechnology®) (Millipore). ChIP analysis was performed with the comparative Cq method (ΔΔCq) and normalized as % of input, using β-actin gene as negative control and p21 as positive control for p53 enrichment.

Availability of supporting data

The data sets supporting the results of this article are included within the article and its additional files. p53-retriever source and binary files are available on Github, at (http://tomateba.github.io/p53retriever/).

Additional files

Additional file 1: Complete list of the rules used to attribute the functional score in the pattern search algorithm.

Additional file 2: Complete list of identified REs within human propoter regions (−10 kb, 10 kb from TSS). The list contains chromosomal coordinates, official gene name, distance from TSS and RE sequence features resulting in the given functional grade.

Additional file 3: Figures S1–S7, Table S1 and Supplementary Information.

Additional file 4: Comparison between p53retriever classification and lists of published p53 bound regions.

Additional file 5: Gene lists from data curated Ingenuity Pathway (TP53 Canonical Pathway) were compared to prediction and functional ranking of p53 REs. The RE grade is stated in the name of the various worksheets. A) Grade four and grade five. B) All grade 3, 4, and 5.

Additional file 6: Complete list of identified REs within ENCODE distal DNAse regions. The list contains chromosomal coordinates and RE sequence features resulting in the assigned functional grade.

Additional file 7: qPCR data summarized in Figure 5. For each gene, time point and treatment time, the average fold change of three biological repeats is presented along with the Standard Deviation. The results obtained with different cell lines are presented in different worksheets

Abbreviations
RE: Response element; TSS: Transcription start site; 3Q: 3/4 binding site.

Competing interests
The authors declare that they have no competing interests.
The authors declare that none of the work required ethical approval.

Authors' contributions
TT: implemented the tool and performed computational experiments. SZ, AB, YC, AI: curated the pattern search rules. SZ, FA: performed biological experiments. AI, TT, SZ: designed the study. TT, SZ, FA, AB, YC, AI: analyzed the data. TT, SZ, AI: wrote the manuscript. All authors read and approved the final manuscript.

Acknowledgements
We thank Dr. Francesca Demichelis and Alessandro Romanel for providing human DNAse hypersensitive regions from ENCODE data. We thank Dr. Paola Monti, Mattia Lion and Ivan Raimondi, for critical discussion.
This work was partially supported by the Italian Association for Cancer Research, AIRC (IG grant 12869 to AI).

Received: 10 October 2014 Accepted: 20 May 2015
Published online: 17 June 2015

References
1. Lane D, Levine A. p53 Research: The Past Thirty Years and the Next Thirty Years. Cold Spring Harb Perspect Biol. 2010;2(12):a000893.
2. Riley T, Sontag E, Chen P, Levine A. Transcriptional control of human p53-regulated genes. Nat Rev Mol Cell Biol. 2008;9:402–12.
3. Beckerman R, Prives C. Transcriptional regulation by p53. Cold Spring Harb Perspect Biol. 2010;2(8):a000935.
4. Sullivan KD, Gallant-Behm CL, Henry RE, Fraikin JL, Espinosa JM. The p53 circuit board. Biochim Biophys Acta. 2012;1825(2):229–44.
5. Menendez D, Inga A, Resnick MA. The expanding universe of p53 targets. Nature Rev Cancer. 2009;9:724–37.
6. Wang B, Xiao Z, Ren EC. Redefining the p53 response element. Proc Natl Acad Sci U S A. 2009;106(34):14373–8.
7. Menendez D, Nguyen TA, Freudenberg JM, Mathew VJ, Anderson CW, Jothi R, et al. Diverse stresses dramatically alter genome-wide p53 binding and transactivation landscape in human cancer cells. Nucleic Acids Res. 2013;41(15):7286–301.
8. Nikulenkov F, Spinnler C, Li H, Tonelli C, Shi Y, Turunen M, et al. Insights into p53 transcriptional function via genome-wide chromatin occupancy and gene expression analysis. Cell Death Differ. 2012;19(12):1992–2002.
9. Wang B, Niu D, Lam TH, Xiao Z, Ren EC. Mapping the p53 transcriptome universe using p53 natural polymorphs. Cell Death Differ. 2014;21(4):521–32.
10. Wang B, Niu D, Lai L, Ren EC. p53 increases MHC class I expression by upregulating the endoplasmic reticulum aminopeptidase ERAP1. Nat Commun. 2013;4:2359.
11. Smeenk L, van Heeringen SJ, Koeppel M, van Driel MA, Bartels SJ, Akkers RC, et al. Characterization of genome-wide p53-binding sites upon stress response. Nucleic Acids Res. 2008;36:3639–54.
12. Hearnes JM, Mays DJ, Schavolt KL, Tang L, Jiang X, Pietenpol JA. Chromatin immunoprecipitation-based screen to identify functional genomic binding sites for sequence-specific transactivators. Mol Cell Biol. 2005;25(22):10148–58.
13. Wei CL, Wu Q, Vega VB, Chiu KP, Ng P, Zhang T, et al. A global map of p53 transcription-factor binding sites in the human genome. Cell. 2006;124(1):207–19.
14. Chang GS, Chen XA, Park B, Rhee HS, Li P, Han KH, et al. A Comprehensive and High-Resolution Genome-wide Response of p53 to Stress. Cell Reports. 2014;8(2):514–27.
15. Zeron-Medina J, Wang X, Repapi E, Campbell MR, Su D, Castro-Giner F, et al. A polymorphic p53 response element in KIT ligand influences cancer risk and has undergone natural selection. Cell. 2013;155(2):410–22.
16. Allen MA, Andrysik Z, Dengler VL, Mellert HS, Guarnieri A, Freeman JA, et al. Global analysis of p53-regulated transcription identifies its direct targets and unexpected regulatory mechanisms. eLife. 2014;3, e02200.
17. Sammons MA, Zhu J, Drake AM, Berger SL. TP53 engagement with the genome occurs in distinct local chromatin environments via pioneer factor activity. Genome Res. 2015;25(2):179–88.
18. Gomes NP, Espinosa JM. Gene-specific repression of the p53 target gene PUMA via intragenic CTCF-Cohesin binding. Genes Dev. 2010;24(10):1022–34.
19. Melo CA, Leveille N, Agami R. eRNAs reach the heart of transcription. Cell Res. 2013;23(10):1151–2.
20. Shaked H, Shiff I, Kott-Gutkowski M, Siegfried Z, Haupt Y, Simon I. Chromatin immunoprecipitation-on-chip reveals stress-dependent p53 occupancy in primary normal cells but not in established cell lines. Cancer Res. 2008;68(23):9671–7.
21. Kaeser MD, Iggo RD. Promoter-specific p53-dependent histone acetylation following DNA damage. Oncogene. 2004;23(22):4007–13.
22. Vousden KH. Outcomes of p53 activation–spoilt for choice. J Cell Sci. 2006;119:5015–20.
23. El-Deiry WS, Kern SE, Pietenpol JA, Kinzler KW, Vogelstein B. Definition of a consensus binding site for p53. Nat Genet. 1992;1(1):45–9.
24. Jordan JJ, Menendez D, Inga A, Nourredine M, Bell D, Resnick MA. Noncanonical DNA motifs as transactivation targets by wild type and mutant p53. PLoS Genet. 2008;4(6), e1000104.
25. Jordan JJ, Menendez D, Sharav J, Beno I, Rosenthal K, Resnick MA, et al. Low-level p53 expression changes transactivation rules and reveals superactivating sequences. Proc Natl Acad Sci U S A. 2012;109(36):14387–92.
26. Inga A, Storici F, Darden TA, Resnick MA. Differential transactivation by the p53 transcription factor is highly dependent on p53 level and promoter target sequence. Mol Cell Biol. 2002;22(24):8612–25.
27. Noureddine MA, Menendez D, Campbell MR, Bandele OJ, Horvath MM, Wang X, et al. Probing the functional impact of sequence variation on p53-DNA interactions using a novel microsphere assay for protein-DNA binding with human cell extracts. PLoS Genet. 2009;5(5), e1000462.
28. Ciribilli Y, Monti P, Bisio A, Nguyen HT, Ethayathulla AS, Ramos A, et al. Transactivation specificity is conserved among p53 family proteins and depends on a response element sequence code. Nucleic Acids Res 2013;41(18):8637–53.
29. Menendez D, Inga A, Snipe J, Krysiak O, Schonfelder G, Resnick MA. A single-nucleotide polymorphism in a half-binding site creates p53 and estrogen receptor control of vascular endothelial growth factor receptor 1. Mol Cell Biol. 2007;27(7):2590–600.
30. Wieczorek AM, Waterman JL, Waterman MJ, Halazonetis TD. Structure-based rescue of common tumor-derived p53 mutants. Nat Med. 1996;2(10):1143–6.
31. Donner AJ, Szostek S, Hoover JM, Espinosa JM. CDK8 is a stimulus-specific positive coregulator of p53 target genes. Mol Cell. 2007;27(1):121–33.
32. Espinosa JM. Mechanisms of regulatory diversity within the p53 transcriptional network. Oncogene. 2008;27:4013–23.

33. Samuels-Lev Y, O'Connor DJ, Bergamaschi D, Trigiante G, Hsieh JK, Zhong S, et al. ASPP proteins specifically stimulate the apoptotic function of p53. Mol Cell. 2001;8:781–94.
34. Schlereth K, Beinoraviciute-Kellner R, Zeitlinger MK, Bretz AC, Sauer M, Charles JP, et al. DNA binding cooperativity of p53 modulates the decision between cell-cycle arrest and apoptosis. Mol Cell. 2010;38(3):356–68.
35. Timofeev O, Schlereth K, Wanzel M, Braun A, Nieswandt B, Pagenstecher A, et al. p53 DNA binding cooperativity is essential for apoptosis and tumor suppression in vivo. Cell Reports. 2013;3(5):1512–25.
36. Anderson CW, Appella E. Signaling to the p53 Tumor Suppressor through Pathways Activated by Genotoxic and Non-Genotoxic Stresses. In: Handbook of cell signaling. Edited by Dennis RABaEA, vol. Second edition. Amsterdam: Elsevier; 2009: part III, section C.
37. Jegga AG, Inga A, Menendez D, Aronow BJ, Resnick MA. Functional evolution of the p53 regulatory network through its target response elements. Proc Natl Acad Sci U S A. 2008;105(3):944–9.
38. Raimondi I, Ciribilli Y, Monti P, Bisio A, Pollegioni L, Fronza G, et al. P53 family members modulate the expression of PRODH, but not PRODH2, via intronic p53 response elements. PLoS One. 2013;8(7), e69152.
39. Flaman JM, Frebourg T, Moreau V, Charbonnier F, Martin C, Chappuis P, et al. A simple p53 functional assay for screening cell lines, blood, and tumors. Proc Natl Acad Sci U S A. 1995;92(9):3963–7.
40. Kato S, Han SY, Liu W, Otsuka K, Shibata H, Kanamaru R, et al. Understanding the function-structure and function-mutation relationships of p53 tumor suppressor protein by high-resolution missense mutation analysis. Proc Natl Acad Sci U S A. 2003;100(14):8424–9.
41. Shiraishi K, Kato S, Han SY, Liu W, Otsuka K, Sakayori M, et al. Isolation of temperature-sensitive p53 mutations from a comprehensive missense mutation library. J Biol Chem. 2004;279(1):348–55.
42. Hoh J, Jin S, Parrado T, Edington J, Levine AJ, Ott J. The p53MH algorithm and its application in detecting p53-responsive genes. Proc Natl Acad Sci U S A. 2002;99(13):8467–72.
43. Menendez D, Inga A, Resnick MA. Estrogen receptor acting in cis enhances WT and mutant p53 transactivation at canonical and noncanonical p53 target sequences. Proc Natl Acad Sci U S A. 2010;107(4):1500–5.
44. Tomso DJ, Inga A, Menendez D, Pittman GS, Campbell MR, Storici F, et al. Functionally distinct polymorphic sequences in the human genome that are targets for p53 transactivation. Proc Natl Acad Sci U S A. 2005;102(18):6431–6.
45. Gowrisankar S, Jegga AG. Regression based predictor for p53 transactivation. BMC Bioinformatics. 2009;10:215.
46. Jolma A, Yan J, Whitington T, Toivonen J, Nitta KR, Rastas P, et al. DNA-binding specificities of human transcription factors. Cell. 2013;152(1–2):327–39.
47. Su D, Wang X, Campbell MR, Song L, Safi A, Crawford GE, et al. Interactions of Chromatin Context, Binding Site Sequence Content, and Sequence Evolution in Stress-Induced p53 Occupancy and Transactivation. PLoS Genet. 2015;11(1), e1004885.
48. Nicholls CD, McLure KG, Shields MA, Lee PW. Biogenesis of p53 involves cotranslational dimerization of monomers and posttranslational dimerization of dimers. Implications on the dominant negative effect. J Biol Chem. 2002;277(15):12937–45.
49. Lion M, Bisio A, Tebaldi T, De Sanctis V, Menendez D, Resnick MA, et al. Interaction between p53 and estradiol pathways in transcriptional responses to chemotherapeutics. Cell Cycle. 2013;12(8):1211–24.
50. Kaneshiro K, Tsutsumi S, Tsuji S, Shirahige K, Aburatani H. An integrated map of p53-binding sites and histone modification in the human ENCODE regions. Genomics. 2007;89(2):178–88.
51. Consortium EP. An integrated encyclopedia of DNA elements in the human genome. Nature. 2012;489(7414):57–74.
52. Su X, Chakravarti D, Cho MS, Liu L, Gi YJ, Lin YL, et al. TAp63 suppresses metastasis through coordinate regulation of Dicer and miRNAs. Nature. 2010;467(7318):986–90.
53. Wang CC, Liao YP, Mischel PS, Iwamoto KS, Cacalano NA, McBride WH. HDJ-2 as a target for radiosensitization of glioblastoma multiforme cells by the farnesyltransferase inhibitor R115777 and the role of the p53/p21 pathway. Cancer Res. 2006;66(13):6756–62.
54. Stark JL, Mehla K, Chaika N, Acton TB, Xiao R, Singh PK, et al. Structure and function of human DnaJ homologue subfamily a member 1 (DNAJA1) and its relationship to pancreatic cancer. Biochemistry. 2014;53(8):1360–72.
55. Jia M, Souchelnytskyi N, Hellman U, O'Hare M, Jat PS, Souchelnytskyi S. Proteome profiling of immortalization-to-senescence transition of human breast epithelial cells identified MAP2K3 as a senescence-promoting protein which is downregulated in human breast cancer. Proteomics Clin Appl. 2010;4(10–11):816–28.
56. Gurtner A, Starace G, Norelli G, Piaggio G, Sacchi A, Bossi G. Mutant p53-induced up-regulation of mitogen-activated protein kinase kinase 3 contributes to gain of function. J Biol Chem. 2010;285(19):14160–9.
57. Cottini F, Hideshima T, Xu C, Sattler M, Dori M, Agnelli L, et al. Rescue of Hippo coactivator YAP1 triggers DNA damage-induced apoptosis in hematological cancers. Nat Med. 2014;20(6):599–606.
58. Bai N, Zhang C, Liang N, Zhang Z, Chang A, Yin J, et al. Yes-associated protein (YAP) increases chemosensitivity of hepatocellular carcinoma cells by modulation of p53. Cancer Biol Ther. 2013;14(6):511–20.
59. Ma B, Pan Y, Zheng J, Levine AJ, Nussinov R. Sequence analysis of p53 response-elements suggests multiple binding modes of the p53 tetramer to DNA targets. Nucleic Acids Res. 2007;35(9):2986–3001.
60. Veprintsev DB, Fersht AR. Algorithm for prediction of tumour suppressor p53 affinity for binding sites in DNA. Nucleic Acids Res. 2008;36:1589–98.
61. Resnick MA, Tomso D, Inga A, Menendez D, Bell D. Functional diversity in the gene network controlled by the master regulator p53 in humans. Cell Cycle. 2005;4(8):1026–9.
62. Ethayathulla AS, Tse PW, Monti P, Nguyen S, Inga A, Fronza G, et al. Structure of p73 DNA-binding domain tetramer modulates p73 transactivation, Proceedings of the National Academy of Sciences of the United States of America. 2012.
63. Monti P, Ciribilli Y, Bisio A, Foggetti G, Raimondi I, Campomenosi P, et al. DN-P63alpha and TA-P63alpha exhibit intrinsic differences in transactivation specificities that depend on distinct features of DNA target sites. Oncotarget. 2014;5(8):2116–30.
64. Luh LM, Kehrloesser S, Deutsch GB, Gebel J, Coutandin D, Schafer B, et al. Analysis of the oligomeric state and transactivation potential of TAp73alpha. Cell Death Differ. 2013;20(8):1008–16.
65. Campomenosi P, Monti P, Aprile A, Abbondandolo A, Frebourg T, Gold B, et al. p53 mutants can often transactivate promoters containing a p21 but not Bax or PIG3 responsive elements. Oncogene. 2001;20(27):3573–9.
66. Resnick MA, Inga A. Functional mutants of the sequence-specific transcription factor p53 and implications for master genes of diversity. Proc Natl Acad Sci U S A. 2003;100(17):9934–9. Epub 2003 Aug 9938.

ANNEX 2.3

Breast Cancer Research

ETV7-mediated DNAJC15 repression leads to Doxorubicin resistance in breast cancer cells

--Manuscript Draft--

Manuscript Number:		
Full Title:	ETV7-mediated DNAJC15 repression leads to Doxorubicin resistance in breast cancer cells	
Article Type:	Research article	
Funding Information:	CIBIO Start-up funds	Dr. Yari Ciribilli
	Intramural NIH Research Program NIEHS (Z01-ES065079)	Dr. Michael A. Resnick
Abstract:	Background: Breast cancer treatment often includes Doxorubicin as adjuvant as well as neoadjuvant chemotherapy. Despite its cytotoxicity, cells can develop drug resistance to Doxorubicin. Transcription factors have important roles in shaping cell responses to chemotherapy. Among them is ETV7, a poorly characterized ETS transcription repressor that is involved in different cancer types. Here, we investigated the effects of ETV7 expression on Doxorubicin-resistance in breast cancer, and the regulation of its novel identified target DNAJC15. Methods: Using MCF7 and MDA-MB-231 as breast cancer cell models, cells were treated with several chemotherapeutic drugs and mRNA expression was analyzed by RT-qPCR. We assessed doxorubicin-resistance by cell viability assay (MTT) and drug efflux dynamics by imaging. Direct binding of ETV7 was tested by site-directed mutagenesis, gene reporter assays, and ChIP. Methylation analysis was performed by bisulfite PCR followed by sequencing and by 5-Aza-2'-deoxycytidine treatment. Publicly available microarrays from breast cancer patients were interrogated to evaluate the prognostic value of ETV7 and DNAJC15 expression. Results: We found that Doxorubicin and other chemotherapeutic drugs induced the expression of ETV7, which led to down-regulation of DNAJC15, a co-chaperone protein whose low expression was previously associated with drug resistance in breast and ovarian cancer. There was a corresponding reduction in Doxorubicin sensitivity of MCF7 and MDA-MB-231 cells. We identified the binding site for ETV7 within the promoter of DNAJC15 and also found that DNA methylation may be a factor in ETV-mediated transcriptional repression at the DNAJC15 promoter. This inverse correlation between ETV7 and DNAJC15 expression in breast cancer cells in terms of Doxorubicin resistance correlated well with treatment responses of breast cancer patients with recurrent disease. In addition, we demonstrated that ETV7-mediated Doxorubicin resistance involves increased Doxorubicin efflux via nuclear pumps, which could be rescued in part by DNAJC15 up-regulation. Conclusions: We propose a novel role for ETV7 in breast cancer, and we identify DNAJC15 as a new target gene responsible for ETV7-mediated Doxorubicin-resistance. A better understanding of the opposing impacts of Doxorubicin could improve the design of combinatorial adjuvant regimens with the aim of avoiding resistance and relapse.	
Corresponding Author:	Yari Ciribilli, PhD Universita degli Studi di Trento Povo (TN), TN ITALY	
Corresponding Author Secondary Information:		
Corresponding Author's Institution:	Universita degli Studi di Trento	
Corresponding Author's Secondary Institution:		
First Author:	Federica Alessandrini	
First Author Secondary Information:		
Order of Authors:	Federica Alessandrini	

	Laura Pezzè
	Daniel Menendez, PhD
	Michael A. Resnick, PhD
	Yari Ciribilli, PhD
Order of Authors Secondary Information:	

ETV7-mediated DNAJC15 repression leads to Doxorubicin resistance in breast cancer cells

Federica Alessandrini[1,*,§], Laura Pezzè[1,*], Daniel Menendez[2], Michael A. Resnick[2], Yari Ciribilli[1,§]

[1]Laboratory of Molecular Cancer Genetics, Centre for Integrative Biology (CIBIO), University of Trento, Via Sommarive 9, 38123, Povo (TN), Italy; [2]Genome Integrity and Structural Biology Laboratory, National Institute of Environmental Health Sciences (NIHES), NIH, Research Triangle Park, NC 27709, USA

[*] = These authors contributed equally to this work

[§] = Correspondence: yari.ciribilli@unitn.it; f.alessandrini@unitn.it

Keywords: ETV7, DNAJC15, Doxorubicin, DNA-methylation, chemotherapy, resistance, ABCB1, Breast cancer

ABSTRACT

Background: Breast cancer treatment often includes Doxorubicin as adjuvant as well as neoadjuvant chemotherapy. Despite its cytotoxicity, cells can develop drug resistance to Doxorubicin. Transcription factors have important roles in shaping cell responses to chemotherapy. Among them is ETV7, a poorly characterized ETS transcription repressor that is involved in different cancer types. Here, we investigated the effects of ETV7 expression on Doxorubicin-resistance in breast cancer, and the regulation of its novel identified target DNAJC15.

Methods: Using MCF7 and MDA-MB-231 as breast cancer cell models, cells were treated with several chemotherapeutic drugs and mRNA expression was analyzed by RT-qPCR. We assessed doxorubicin-resistance by cell viability assay (MTT) and drug efflux dynamics by imaging. Direct binding of ETV7 was tested by site-directed mutagenesis, gene reporter assays, and ChIP. Methylation analysis was performed by bisulfite PCR followed by sequencing and by 5-Aza-2'-deoxycytidine treatment. Publicly available microarrays from breast cancer patients were interrogated to evaluate the prognostic value of ETV7 and DNAJC15 expression.

Results: We found that Doxorubicin and other chemotherapeutic drugs induced the expression of ETV7, which led to down-regulation of DNAJC15, a co-chaperone protein whose low expression was previously associated with drug resistance in breast and ovarian cancer. There was a corresponding reduction in Doxorubicin sensitivity of MCF7 and MDA-MB-231 cells. We identified the binding site for ETV7 within the promoter of *DNAJC15* and also found that DNA methylation may be a factor in ETV-mediated transcriptional repression at the *DNAJC15* promoter. This inverse correlation between ETV7 and DNAJC15 expression in breast cancer cells in terms of Doxorubicin resistance correlated well with treatment responses of breast cancer patients with recurrent disease. In addition, we demonstrated that ETV7-mediated Doxorubicin resistance involves increased Doxorubicin efflux via nuclear pumps, which could be rescued in part by DNAJC15 up-regulation.

Conclusions: We propose a novel role for ETV7 in breast cancer, and we identify DNAJC15 as a new target gene responsible for ETV7-mediated Doxorubicin-resistance. A better understanding of the opposing impacts of Doxorubicin could improve the design of combinatorial adjuvant regimens with the aim of avoiding resistance and relapse.

BACKGROUND

Chemotherapy is commonly adopted for the pre- and post-surgical treatment of many solid tumors, including breast cancer, and it is still the only therapeutic option for most cases of metastatic spread. Among the drugs used in different regimens, Doxorubicin is often employed and is one of the most effective [1]. This drug is an anthracyclin intercalator that poisons topoisomerase II, thereby causing DNA damage and subsequent cytotoxicity [2]. As for most chemotherapeutic agents, several unwanted side-effects have been reported and, unfortunately, Doxorubicin is also known for late-onset cardiotoxicity determined by a complex cascade of events [3]. Despite the efficacy of Doxorubicin and other chemotherapeutic drugs, cancer cells may develop chemoresistance, resulting in treatment failure and recurrence. Indeed, there are many survival strategies available to cancer cells and some of them can even be activated by chemotherapy itself. Some activation mechanisms can lay the groundwork for unwanted future resistance to treatment, which can be driven or stimulated by the activation of pro-survival or pro-tumorigenic transcription factors, such as NF-κB [4, 5] and FOXM1 [6, 7]. Moreover, Doxorubicin can lead to an increased expression of drug efflux pumps such as MRP1 in breast cancer [8] and to activation of the anti-apoptotic cascade HER3-PI3K-AKT in ovarian cancer [9].

ETV7 (Ets Variant Gene 7) is a transcription factor belonging to the ETS (E26 transformation-specific) family of transcriptional regulators. Various ETS factors, such as ETS1, ETS2, PU1, FLI1 and ERG, are distinguished for their pro-tumorigenic functions and are involved in chromosomal translocations often associated with Ewing's sarcoma and prostate cancer [10]. ETV7 is a poorly characterized protein that can act as a transcriptional repressor, which presents an 85-amino acid ETS domain responsible for binding a purine rich GGAA core motif in the regulatory regions of target genes. The protein also has a conserved pointed (PNT) protein-protein interaction domain, required for the formation of homo-/hetero-dimers and oligomers and involved in transcriptional repression [11, 12]. Given the presence of the PNT domain, ETV7 can either self-associate or form hetero-dimers/oligomers with ETV6/TEL, a highly related ETS family member with tumor suppressor functions that also acts as transcriptional repressor [13]. In contrast, ETV7 is generally acknowledged to be an oncoprotein, and some of its pro-tumorigenic functions result from its ability to directly bind and inhibit ETV6-mediated gene repression [14].

Deregulated high ETV7 expression levels has been linked to hepatocellular carcinoma [15] and to leukemia [10, 16]. Over-expressed ETV7 can also cooperate with Eμ-MYC in promoting lymphomagenesis and blocking Myc-induced apoptosis [17]. Furthermore, ETV7 is able to enhance the Ras-driven transformation in fibroblasts and shows pro-proliferative and anti-differentiation roles observed in myeloid and lymphoid cells [10, 17]. In contrast, ETV7 can act as a tumor suppressor in nasopharingeal carcinoma through binding *SERPINE1* promoter and decreasing its expression [18]. Further, ETV7 down-regulation has been reported in drug resistant gastric cancer cells [19].

We recently observed in human breast cancer cells that *ETV7* can be transcriptionally activated upon Doxorubicin treatment and synergistically induced by the combined treatment with Doxorubicin and TNFα. Among the possible activators of its transcription, we identified tumor suppressor p53 and NFκB (p65) as transcription factors able to directly bind to *ETV7* promoter [20].

Interestingly, ETV7 and DNAJC15 expression appear to inversely correlate upon Doxorubicin treatment and also upon interferon gamma expression. ETV7 is recognized as an interferon stimulated gene, whereas down-regulation of DNAJC15 has been reported in interferon gamma treated macrophages [21]. DNAJC15 plays an intriguing role among the tumor suppressor genes whose repression is associated with tumor aggressiveness and chemoresistance. It belongs to the HSP40/DNAJ family of co-chaperones, mostly involved in helping ATP hydrolysis and thus the activation of the HSP70 chaperone with its roles in protein folding, trafficking, interaction, import and export [22, 23].

DNAJC15 is often hyper-methylated and repressed in malignant pediatric tumors [24], neuroblastoma [25], Wilm's tumor and melanoma [26]. Furthermore, its down-regulation associates with increased drug resistance in ovarian and breast cancer [27, 28]. Using MCF7 breast cancer cells, Hatle and colleagues observed that in Doxorubicin-resistant clones, the low expression of DNAJC15 in the Golgi network was responsible for the degradation of some proteins including the transcription factor c-JUN [29]. Therefore, inhibition of DNAJC15 resulted in increased levels of c-JUN protein, which was ultimately responsible for increased transcription of

the multidrug transporter ABCB1/MDR1 [29]. Other studies have reported the localization of DNAJC15 inside the mitochondrial inner membrane where it can control the respiratory chain and thus the production of ROS [30]. Inside the mitochondria it can also help mitochondrial import of proteins by favoring the ATP hydrolysis of a chaperone member of the TIMP23 translocase [26]. DNAJC15 exerts its tumor suppressor role also by promoting the release of pro-apoptotic molecules through the mitochondrial permeability transition pore complex [31].

In this study we identify a novel circuitry for Doxorubicin resistance in breast cancer cells where ETV7 acts as major player. Given the pro-tumorigenic roles of ETV7, its activation upon Doxorubicin treatment represents one of the unwanted side-effects that could possibly unleash a drug resistance mechanism. In particular, ETV7 appears to trigger the activation of a resistance circuitry by directly binding and, therefore, repressing the transcription of some tumor suppressor genes. Specifically, we demonstrate that ETV7 can repress DNAJC15 in a methylation-dependent manner. We propose a novel drug resistance mechanism directly driven by Doxorubicin whereby Doxorubicin itself induces the up-regulation of ETV7 that, in turn, down-regulates DNAJC15 expression giving rise to Doxorubicin resistance in breast cancer cells.

METHODS

Cell culture conditions and treatments

MCF7 and U2OS were obtained from Interlab Cell Line Collection bank (Genoa, Italy). A549 were from ATCC (Manassas, VA, USA), while A375M and MDA-MB-231 were a gift from, respectively, Dr. D. Bergamaschi (Centre for Cell Biology and Cutaneous Research, Blizard Institute, Barts and The London School of Medicine & Dentistry, UK) and Prof. A. Provenzani (CIBIO, University of Trento, Italy). MCF7 and U2OS cells were grown in DMEM medium supplemented with 10% FBS, 2mM L-Glutamine and 2mM of Penicillin/Streptomycin; MDA-MB-231 cells in the same medium with the addition of 1% Non-Essential Amino acids. A549 and A375M were cultured in RPMI medium + 10% FBS, 2mM L-Glutamine and 2mM of Penicillin/Streptomycin.

BJ1-hTERT cells were obtained from Dr. K Lobachev (Georgia Institute of Technology, GA, USA) and were grown in MEM medium supplemented with 10% FBS, 2mM L-Glutamine, 2mM of Penicillin/Streptomycin and Puromycin.

Lymphocytes were obtained from healthy donors through the facilities of the Clinical Research Unit and NIEHS. For lymphocytes culture and treatment conditions please refer to Methods section in Menendez *et al.*, 2011 [47].

Doxorubicin (Sigma-Aldrich, Milan, Italy) was used at the concentration of 1.5μM (for all cells except for U2OS and BJ1-hTERT cells, which were treated with 0.5μM Doxorubicin) for 16 hours treatment in the case of qPCR analysis and western blotting and at different concentrations for 72 hours for MTT viability assays.

24 hours treatments were performed with the following drugs and concentrations: Etoposide 50μM (Enzo Life Science, Rome, Italy), Nutlin-3a 10μM, 5-FluoroUracil (5FU) 375μM, Camptothecin 0.5μM, Everolimus 50 nM, Tamoxifen 1μM, Imatinib 3μM (Selleckchem, Aurogene, Rome, Italy). Compounds were purchased from Sigma-Aldrich when not specifically indicated.

5-Aza-2'-deoxycytidine (Sigma-Aldrich) treatment was performed for 48 hours at the concentration of 5μM.

Quercetin and Genistein were purchased from Extrasynthese (Genay, Lyon, France), and treatments were performed for 16 hours at the concentration of 50μM for Quercetin and 30μM for Genistein.

Plasmids

The expression vectors pCMV6-Entry-Empty, pCMV6-Entry-ETV7 and pCMV6-Entry-DNAJC15 C-terminally tagged with DDK-Myc tags were purchased from Origene (Tema Ricerca, Bologna, Italy). pGL4.26-DNAJC15 reporter was obtained by cloning the promoter region of DNAJC15 (-299 to +512 bp from TSS according to the Eukaryotic Promoter Database, http://epd.vital-it.ch/) amplified with Q5 High Fidelity DNA Polymerase (New England Biolabs, Euroclone, Milan, Italy) and the following primers (Eurofins Genomics, Ebersberg, Germany): Fw: GCCTCGAGCAGCACAAACTCATTTGAGGG and Rv: GCAAGCTTAGGCGGCCCGGAGACTCAAG. Purified PCR product was inserted into pGL4.26 backbone using Xho I and Hind III restriction endonucleases. Cloning was checked by restriction analysis and direct sequencing (Eurofins Genomics). For site-directed mutagenesis of this vector please refer to the section below. The pRL-SV40 (Promega) vector constitutively expressing the *Renilla reniformis* luciferase cDNA was used as transfection efficiency control for gene reporter assays.

Generation of stable pCVM6-Entry-ETV7 and Empty MCF7 and MDA-MB-231 cells

In order to get MCF7 and MDA-MB-231 cells stably over-expressing ETV7 and the empty control, cells were seeded in 6-well plates and subsequently transfected for 48 hours with 1 μg of pCMV6-Entry-Empty or pCMV6-Entry-ETV7 (Origene) using Lipofectamine LTX and Plus Reagent (Life Technologies, Thermo Fisher Scientific, Milan, Italy) or FuGene HD (Promega, Milan, Italy) respectively for MCF7 and MDA-MB-231 cells. Afterwards, cells were splitted and Geneticin (Life Technologies) was added at a concentration of 600 and 800μg/ml respectively for MCF7 and MDA-MB-231 cells; each 3 days medium was replaced and after 4 cycles of selection, single cell cloning was performed according to the Corning protocol for cell cloning by Serial dilution in 96 well plate. During the single cell cloning procedure Geneticin concentration was gradually reduced till 300 (MCF7) and 400μg/ml (MDA-MB-231).

RNA isolation and RT-qPCR

Total RNA was extracted using the Illustra RNA spin Mini Kit (GE Healthcare, Milan, Italy), converted to cDNA with the RevertAid First Strand cDNA Synthesis Kit (Thermo Fisher Scientific) and RT-qPCR was performed with 25 ng of template cDNA in 384 wells-plate (BioRad, Milan, Italy) using the Kapa Sybr Fast qPCR Master Mix (Kapa Biosystems, Resnova, Ancona, Italy) and the CFX384 Detection System (BioRad). YWHAZ and B2M genes were used as housekeeping genes to obtain the relative fold change by the ΔΔCt method as previously described [48]. Primer

sequences were designed using Primer-BLAST designing tool (https://www.ncbi.nlm.nih.gov/tools/primer-blast/), checked for specificity and efficiency, and are listed in Supplementary Table 1 (Eurofins Genomics).

Western Blot

Total protein extracts were obtained by lysing the cells in RIPA buffer and proteins were quantified by the BCA method (Pierce, Thermo Fisher Scientific); 20-50 μg of protein extracts were loaded on 7.5% and 12% polyacrylamide gels and western blotting was performed as previously described [49, 50]. Transferred proteins were probed over-night at 4°C with specific antibodies diluted in 1% non-fat skim milk-PBS-T solution: GAPDH (6C5, sc-32233), ETV7/TEL2 (F-8, sc-376137X), ETV7/TEL2 (H-88, sc-292509), Histone H3 (FL-136, sc-10809), α-Actinin (H-2, sc-17829), DNMT3A (GTX129125, GeneTex, Prodotti Gianni, Milan, Italy). Antibodies were obtained from Santa Cruz Biotechnologies (Milan, Italy) when not specifically indicated. Detection was performed with ECL Select reagent (GE Healthcare) using a ChemiDoc XRS+ (BioRad) or UVITec Alliance LD2 (UVITec Cambridge, UK) imaging systems.

In order to separate cytoplasmic and nuclear fractions of proteins, MCF7 cells were seeded in p150 dishes and treated with Doxorubicin for either 6 or 16 hours. Cytoplasmic proteins were extracted following the instructions of NE-PER kit (Thermo Fisher Scientific). Alternatively, in order to enrich the nuclear extracts for chromatin-associated proteins, pellets remaining from cytoplasmic extraction were directly resuspended in 1x Loading Buffer and boiled. Approximately, 150 μg of nuclear protein extracts and 50 μg of cytoplasmic protein extracts were loaded on a polyacrylamide gel, blotted and detected as described above. Histone H3 and GAPDH were used respectively as controls for nuclear and for cytoplasmic extracts.

Gene reporter Assay

24 hours prior transfection, 7 x 10^4 MCF7 cells were seeded in 24 well-plate. Cells were transfected with Lipofectamine LTX and Plus Reagent (Thermo Fisher Scientific) along with 250ng pGL4.26-DNAJC15 reporter, 250ng pCMV6-Entry-Empty or pCMV6-Entry-ETV7 vectors, and 50ng pRL-SV40 for each well. After 48 hours, cells were washed once in PBS and lysed in 1X PLB buffer and luciferase activity measurements were performed using the Dual-Luciferase Reporter Assay System (Promega) as previously described [45, 51] and detected using the Infinite M200 plate

reader (Tecan, Milan, Italy). Renilla luciferase activity was used as indicator of transfection efficiency and used to obtain the Relative Light Unit (RLU) measure.

Site-directed mutagenesis

Site-directed mutagenesis was performed using GENEART Site-Directed Mutagenesis kit (Life Technologies) according to manufacturer's instructions. In order to mutate ETV7 binding sites within pGL4.26-DNAJC15 (substituting the GGA conserved bases with ATC random sequence), the reporter plasmid was first methylated and then amplified with AccuPrime *Pfx* DNA Polymerase (InVitrogen, Life Technologies) in a mutagenesis reaction with the following primers (Eurofins Genomics):

BS1_Fw: GGGAAGAAAGGCTGCCCatcAGGGGGTCAGGAAAGC;

BS1_Rv: GCTTTCCTGACCCCCTgatGGGCAGCCTTTCTTCCC;

BS2_Fw: GGTGAGAAGGGTATCTgatGGGAACCTCGCCTTTAA;

BS2_Rv: TTAAAGGCGAGGTTCCCatcAGATACCCTTCTCACC.

Mutagenesis was then followed by an *in vitro* recombination reaction to enhance efficiency and colony yield. Mutated plasmids (pGL4.26-DNAJC15-BS1 and -BS2) were subsequently transformed into DH5α-T1^{R} *E. coli* competent cells, which circularize the linear mutated DNA and exploits McrBC endonuclease activity to digest methylated DNA. Complete and correct mutagenesis was verified by direct sequencing (Eurofins Genomics).

Bisulfite-conversion

Genomic DNA was extracted from MCF7 cells left untreated, treated with Doxorubicin or over-expressing pCMV6-Entry-Empty or -ETV7 vectors. DNA and RNA extractions were obtained from the same samples using the AllPrep DNA/RNA/Protein Mini Kit (Qiagen, Milan Italy).

Purified DNA was then denaturated and subjected to bisulfite conversion with the EZ DNA Methylation-Lightning™ Kit (Zymo Research, Euroclone) according to manufacturer's recommendations. The resulting product was subsequently PCR amplified and sequenced using the following bisulfite-specific primers (Eurofins Genomics): Fw: TTGGTAGGATTTATTAGTTTTTGTTGG; Rv: CACCCAACTAATCTTTATATTTTTAATAAA.

Doxorubicin Efflux Analysis

1.5 x 10^4 MDA-MB-231 cells were seeded in a 96 well-plate; the subsequent day, 10 or 20μM Doxorubicin was added for 3 hours and cells were analyzed with the Operetta High Content Imaging System (Perkin Elmer, Milan, Italy) at CIBIO High Throughput Screening Facility exploiting the intrinsic fluorescence of Doxorubicin. By using the Harmony 4.1 PhenoLOGIC software nuclear and cytoplasmic regions were detected; successively, the relative ratio of nuclear respect to cytoplasmic fraction from Doxorubicin signal was calculated. To measure the Doxorubicin efflux area, the Doxorubicin spot area into the cytoplasm was measured (see Suppl. Fig2a for details).

Viability Assay

Cells were seeded in a 96 well-plate and treated with different concentrations of Doxorubicin for 72 hours. Medium was removed and wells were washed with 1X PBS to avoid possible reduction effects of the added compound with MTT reagent (Sigma-Aldrich). Ten μl of MTT was added to 100 μl of fresh medium and left in incubation for 3 hours. Afterwards, medium was accurately removed and cells were lysed in 100 μl of DMSO (Sigma-Aldrich), and a colorimetric measure was performed at the Infinite M200 plate reader (Tecan). Viability was calculated as a % ratio of viable cells treated with the indicated drug respect to an untreated control.

Chromatin Immunoprecipitation Assay

MDA-MB-231-ETV7 and MDA-MB-231-Empty cells were seeded in p150 dishes (four dishes each condition) and ChIP-PCR was performed following a revised version of Myers Lab protocol. Mouse monoclonal anti-ETV7/TEL2 antibody (F-8, sc-376137X, Santa Cruz Biotechnologies) and normal mouse IgG (sc-2025, Santa Cruz Biotechnologies) were used for immunoprecipitation. Two μl of purified immmunoprecipitated DNA was then used for qPCR analysis and calculation was performed using the ΔCt method in respect to non-immunoprecipitated DNA (% of input) as previously detailed described [52]. A genomic region within GTF2H5 gene was used a negative control. A list of the primers sequences that were used for ChIP-PCR analysis is presented in Supplementary Table 1 (Integrated DNA Technologies, Coralville, IA, USA and Eurofins Genomics).
MCF7 cells were seeded in p150 dishes and transiently transfected with 10μg of pCMV6-Entry-Empty or -ETV7 vectors using Lipofectamine LTX and Plus Reagent (Thermo Fisher Scientific) for 48 hours. ChIP was performed using the same protocol used for MDA-MB-231 using anti-ETV7/TEL2 (H-88, sc-292509) and normal rabbit IgG (sc-2027, Santa Cruz Biotechnologies) for

immunoprecipitation. qPCR on purified immunoprecipitated DNAs was performed as indicated above.

Co-Immunoprecipitation

MCF7 were seeded in p150 dishes and transiently transfected with pCMV6-Entry-ETV7 as above (Origene). 48 hours post-transfection cells were lysed in CHAPS buffer and then incubated over-night with an anti-ETV7 antibody (H-88, sc-292509) or normal rabbit IgG (sc-2027) previously bound to Dynabeads protein A magnetic beads (Life Technologies). Beads were then washed and the immunoprecipitated lysate was eluted and loaded on a polyacrylamide gel for SDS-PAGE.

Analysis of genome-wide data

Available expression arrays from our group (GSE24065, Agilent-014850 Whole Human Genome Microarray 4x44K G4112F) were analyzed for the specific genes of interest as previously described [20, 34].

Expression data of MCF7 cells resistant to Adriamycin -MCF7/ADR- (e.g. Doxorubicin) were obtained from Affymetrix Human Genome U133 Plus 2.0 Array platform and downloaded from GEO (GSE76540). Two transcripts for each gene of interest (ETV7, DNAJC15 and ABCB1) were available and expression averages were calculated.

Expression levels of ETV7 and DNAJC15 were obtained from microarray data of Triple Negative Breast Cancer patients who underwent neoadjuvant chemotherapy protocols (GSE43502, Affymetrix Human Genome U133 Plus 2.0 Array). The study included 25 patients (out of 47) showing recurrence.

Statistical analysis

When appropriate, Student's t-test was applied for statistical significance. We selected throughout the manuscript the two-sample Student's t-test for unequal variance.

RESULTS

ETV7 is activated by Doxorubicin and other DNA damaging drugs in cancer and normal cells

To investigate the differential expression of ETV7 in response to various stimuli in breast cancer cells we tested a panel of cytotoxic drugs in MCF7 cells. We observed a substantial induction of ETV7 expression with many of the treatments, especially DNA damaging drugs, among which Doxorubicin was the most effective inducer of ETV7 expression in comparison with 5FU, Camptothecin and Etoposide (Figure 1A). The treatment with Nutlin-3a, a p53 specific activator [32] also triggered an increment in ETV7 mRNA levels while Everolimus (mTOR inhibitor), Imatinib (tyrosine kinase inhibitor) and Tamoxifen (estrogen modulator) had no effect (Figure 1A). Moreover, ETV7 transcriptional activation by Doxorubicin in MCF7 cells was reflected by an increase in protein levels in the nuclear compartment (Suppl. Figure 1A), highlighting its role as a transcriptional regulator.

We extended the analysis to the breast cancer cell line MDA-MB-231 and confirmed the induction of ETV7 upon treatments with DNA damaging agents, especially Doxorubicin (Figure 1B). Nevertheless, the levels of ETV7 induction in this cell line were not as high as in MCF7. The reduced level might be explained by the presence of a mutant nonfunctional form of p53 in MDA-MB-231, since p53 is an activator of ETV7 transcription [20]. Doxorubicin treatment also induced ETV7 in other cancer-derived cell lines: lung adenocarcinoma (A549), osteosarcoma (U2OS) and melanoma (A375M) (Suppl. Figure 1B). Given the activation in the various cancer cell lines, we investigated ETV7 expression in normal cells. We treated lymphocytes obtained from healthy donors and two non-cancerous cell lines (immortalized normal fibroblasts BJ1-hTERT and immortalized normal mammary cells MCF10A). These results along with those from cancer cell lines establish that ETV7 induction is a conserved response to DNA damaging treatments (Figure 1C and Suppl. Figure 1B).

ETV7 can promote resistance to Doxorubicin in breast cancer cells

Given the observation that ETV7 is potently activated in response to Doxorubicin treatment, we hypothesized that it may be involved in drug resistance. To test this, we generated stable MCF7 and MDA-MB-231 cell lines over-expressing this transcription factor (Suppl. Figure 2A and 2B, respectively) and evaluated whether this could influence the survival upon Doxorubicin treatment. Importantly, ETV7 over-expression exerted a strong protective role against Doxorubicin induced cell death in both cell lines (Figure 2A-B). Interestingly, this effect was also visible in non-breast cancer cells as shown for the osteosarcoma U2OS cells stably over-expressing ETV7 (Suppl. Figure 2C-D). To better understand the mechanism of resistance, we monitored the nuclear efflux of Doxorubicin exploiting its light emission property in the ETV7 over-expressing MDA-MB-231 cells relative to their empty-vector counterpart. By measuring the ratio of nuclear to cytoplasmic Doxorubicin and the area of Doxorubicin efflux from the nuclei, we found a statistically significant decrease of nuclear Doxorubicin in the MDA-MB-231 cells over-expressing ETV7 that corresponded to an increased nuclear efflux of Doxorubicin (Figure 2C-D and Suppl. Figure 2E, showing details regarding the selection of nuclear and cytoplasmic regions). This indicates that ETV7 might influence the expression of ABC transporters such as ABCB1/PgP, ABCC1/MRP1, and ABCB4/MDR2 thereby leading to an increased survival. In particular, we were able to demonstrate that ABCB1 was up-regulated upon ETV7 over-expression in MCF7 and MDA-MB-231 cells (Suppl. Figure 2F and 2G, respectively).

DNAJC15 is a good target for ETV7-mediated drug resistance

To further understand how ETV7, as a transcriptional repressor, could influence drug resistance, we searched for its putative targets by restricting the analysis to genes whose silencing is already known to be involved in Doxorubicin resistance in breast cancer cells. In particular, we considered a list of six genes (*BRCA1, ESR1, DNAJC15, CDH1, RAB6C and SULF2)* whose hyper-methylation correlates with Doxorubicin resistance in breast cancer (Table 1 from Boettcher *et al.*, 2010 [33] and available at the Archive of Functional Genomics Data, accession number #E-MEXP-2698, using the ArrayExpress tool). To restrict the search to the most promising ETV7 targets, we analyzed the expression of this group of genes in microarray data that we previously described with Doxorubicin treated MCF7 cells available (GSE24065, Gene Expression Omnibus, GEO, NCBI [20, 34]). Given that Doxorubicin potently activated ETV7 expression, we expected to observe

significant down-regulation of its targets upon the same treatment condition. Out of the six genes, three of them -DNAJC15, BRCA1 and ESR1- displayed a strong down-regulation pattern upon Doxorubicin treatment (Suppl. Figure 3A). No significant effects were observed for *CDH1* and *RAB6C*, while SULF2 was induced after Doxorubicin treatment. Moreover, most DNAJC family members were repressed upon Doxorubicin in MCF7 cells, based on the previously mentioned microarray data (Suppl. Figure 3B). Therefore, we validated some of the highly down-regulated members of DNAJC family with RT-qPCR experiments in Doxorubicin-treated MCF7 cells and confirmed the repression of DNAJC2, C7, C14, C15 and C17 in response to Doxorubicin treatment (Figure 3A). Furthermore, DNAJC15 has already been reported to be involved in the negative regulation of ABCB1 transcription, thereby potentially explaining the ETV7-mediated ABCB1 up-regulation and, at least partially, the drug resistance mechanism associated with ETV7 [29]. We decided to focus our attention on DNAJC15 as putative mediator of the ETV7-dependent Doxorubicin resistance. We extended the analysis of DNAJC15 repression to other DNA damaging agents in MCF7, MDA-MB-231 cells and in lymphocytes (Figures 3B, 3C and 3D, respectively), and verified DNAJC15 down-regulation in response to most of these agents.

ETV7 transcriptionally regulates DNAJC15 expression

Since we observed that ETV7 and DNAJC15 expression were inversely correlated in response to several stimuli and given the presence of two putative ETV7 binding sites in the *DNAJC15* promoter, we investigated the possibility of direct ETV7 influence on DNAJC15 expression. First, we demonstrated that the modulation of ETV7 expression inversely affected the mRNA levels of DNAJC15. Specifically, ETV7 over-expression led to a small but significant, repression of DNAJC15 both in MCF7 (Figure 4A) and MDA-MB-231 (Suppl. Figure 4A) cells.

In order to assess whether transcriptional repression was associated with ETV7 binding to DNAJC15, we cloned a region of the *DNAJC15* promoter containing two putative binding sites for ETV7 into a pGL4.26 luciferase reporter vector. We found that ETV7 over-expression in MCF7 cells was able to decrease the expression of the luciferase reporter gene under the control of the DNAJC15 promoter (Figure 4B). We then performed site-directed mutagenesis to mutate the most conserved bases within the two putative ETV7-binding sites into the reporter vector in order to

demonstrate the contribution of these two binding sites in DNAJC15 repression. The mutation of the binding site 1 (BS1 – chr.13:43'597'329-43'597'335) did not affect the ETV7-mediated down-regulation of luciferase activity. However, disruption of binding site 2 (BS2 – chr.13:43'597'624-43'597'632) prevented repression of the luciferase reporter induced by ETV7, demonstrating the importance of ETV7 binding to this site in the repression of DNAJC15 (Figure 4B).

Furthermore, we were able to demonstrate with chromatin immunoprecipitation the direct binding of ETV7 to the DNAJC15 promoter region (BS2) in both MCF7 and MDA-MB-231 cells (Figure 4C and Suppl. Figure 4B, respectively). In particular, in MDA-MB-231 cells over-expressing ETV7, the binding to DNAJC15 promoter was markedly stimulated by Doxorubicin treatment. In order to better clarify this effect, we analyzed the distribution of ETV7 protein within the nucleus and found that upon Doxorubicin treatment the ETV7 protein was strongly enriched in the nuclear fraction especially in chromatin-associated structures (Suppl. Figure 4C).

ETV7 represses DNAJC15 expression by DNA methylation

DNAJC15 is recognized to be a methylation-controlled gene, and its methylation-induced down-regulation has been associated with chemoresistance [29]. We investigated whether ETV7-mediated repression was dependent on DNA methylation. The methylation of CpGs in the promoter of DNAJC15 in MCF7 cells following ETV7 over-expression or Doxorubicin treatment was determined by bisulfite-conversion of genomic DNA followed by PCR and direct sequencing. In response to Doxorubicin, the promoter of DNAJC15 showed increased methylation of CpGs, which was even more evident upon ETV7 over-expression, as shown in Figure 5A. Moreover, ETV7-mediated effects on DNAJC15 transcript levels were abolished by treatment with the DNA methyltransferase (DNMT) inhibitor 5-Aza-2'-deoxycytidine (5-Aza) (Figure 5B), demonstrating that ETV7 repression of DNAJC15 expression is indeed methylation dependent.

Given that DNMTs play key roles in Doxorubicin resistance as demonstrated for Adriamycin-resistant MCF7 cells [35], we hypothesized a possible direct interaction between ETV7 and DNMTs mediating the methylation and subsequent repression of the DNAJC15 promoter. Analysis of the expression of the *DNMT1, DNMT3A* and *DNMT3B* genes in our microarray data from Doxorubicin-

treated MCF7 cells (GSE24065 [20, 34]) (Suppl. Figure 5A) and validation by RT-qPCR (Figure 5C), revealed the up-regulation of only DNMT3A among these DNMTs. Conversely, both DNMT1 and DNMT3B were down-regulated in response to the treatment. Moreover, a similar trend could be observed for DNMTs expression in response to ETV7 over-expression in MCF7 cells, even if the only statistically significant alteration in expression was for DNMT1 (Suppl. Figure 5B). To test the putative interaction of ETV7 with DNMT3A as a candidate mediator of DNAJC15 repression, we performed immunoprecipitation of ETV7 and found the direct interaction of ETV7 with DNMT3A in MCF7 cells transiently over-expressing ETV7 (Figure 5D).

DNAJC15 over-expression partially rescues ETV7-mediated drug resistance

To address the idea that ETV7-mediated drug resistance is, at least partially, dependent on the repression of DNAJC15, we over-expressed DNAJC15 in MCF7 and MDA-MB-231 cells stably over-expressing ETV7 and analyzed cellular viability upon Doxorubicin treatment. Cells over-expressing DNAJC15 became more sensitive to Doxorubicin-mediated cell death, thus confirming this pathway as a mechanism exploited by ETV7 for drug resistance (Figure 6A-B). Furthermore, DNAJC15 over-expression was also able to down-regulate ABCB1 expression in MCF7 as well as MDA-MB-231 cells over-expressing ETV7, in accord with its reported negative role on ABCB1 levels (Suppl. Figure 6A-B).

ETV7-DNAJC15 clinical relevance and possible therapeutic strategy

We confirmed a dramatic decrease in DNAJC15 and corresponding increase in ETV7 expression in reported microarray analysis performed with Adriamycin (i.e. Doxorubicin) resistant MCF7 cells (MCF7/ADR, GSE76540, [36]) as shown in Figure 7A. Moreover, this effect was associated with a large increase in ABCB1 expression in MCF7/ADR cells, an observation consistent with what is observed in MCF7 and MDA-MB-231 cells over-expressing ETV7 (Suppl. Figure 2F-G).

To address possible clinical relationships between ETV7, DNAJC15 and Doxorubicin treatment, we evaluated data obtained from 25 chemoresistant samples among 47 neoadjuvant chemotherapy-treated triple negative breast cancer (TNBC) patients (GSE43502, [37]). There is an inverse

correlation between increased ETV7 and strongly decreased DNAJC15 expression in TNBC patients associated with recurrence. These data indicates that ETV7-mediated repression of DNAJC15 could be linked to a worse prognosis in breast cancer patients (Figure 7B).

Given that the over-expression of a particular gene is still a challenging approach for therapeutic purposes, we tried to overcome ETV7-mediated drug resistance using Quercetin, a flavonoid recently shown to both increase therapeutic efficacy of Doxorubicin [38-40] and to reduce its cardiotoxicity [41, 42], and the isoflavone Genistein, which can inhibit topoisomerase II [43] and DNMTs [44] or act as a phytoestrogen [45]. The sensitizing action of flavonoids has not been fully elucidated yet, but it seems to involve the MDR transporter action. Surprisingly, we noticed that both flavonoids Quercetin and Genistein were able to reduce ETV7 expression in MDA-MB-231 cells, thereby suggesting a novel mechanism of sensitization for cancer cells (Figure 7C). Notably, MDA-MB-231 cells that over-express ETV7 were more sensitive to Quercetin relative to the empty counterpart, thereby unveiling a mechanism that could represent a promising target for ETV7-mediated resistance in cancer cells (Figure 7D).

DISCUSSION

ETV7 has been recognized in the literature as an oncoprotein for blood cancers but its role in solid cancers is still poorly studied [10, 17]. In this work we showed that ETV7 is activated in response to different DNA damaging agents in breast cancer cells, but its expression is not affected by other types of anti-cancer treatments such as estrogen antagonists, tyrosine kinase or mTOR inhibitors (Figure 1). We observed that this transcriptional activation is conserved in different cancer cell types and normal cells including lymphocytes obtained from healthy donors, thus highlighting its biological relevance. Moreover, we have demonstrated that ETV7 can directly promote resistance of breast cancer cells to standard-of-care chemotherapy, i.e. Doxorubicin (Figure 2). The ETV7-dependent mechanism of chemoresistance exploited by breast cancer cells involves the direct efflux of Doxorubicin from the nucleus of cells over-expressing ETV7 (Figure 2). This observation led us to hypothesize that the effect can be driven by membrane-associated transporters and, interestingly, we found that cells over-expressing ETV7 showed higher expression levels of ABCB1, a member of the family of ABC transporters (Suppl. Figure 2). Despite being mainly expressed on the plasma membranes, ABCB1 protein has often been detected on nuclear membranes and Golgi compartments [46], possibly mediating the phenomenon of resistance to Doxorubicin observed in breast cancer cells in this study.

As a transcription factor, ETV7 can influence the expression of a complex range of targets that may result in the observed increased survival. Among the various possible ETV7 targets, we proposed DNAJC15, a co-chaperone member of the HSP40 family, reported to affect ABCB1 expression and anti-cancer drug efflux [29] DNAJC15 has already been reported to be frequently hyper-methylated and repressed in breast cancer cells resistant to therapy [27] [28]. However, which direct players were causing its transcriptional repression in breast cancer was not known. We confirmed the DNAJC15 repression triggered by Doxorubicin involves the direct binding of ETV7 on *DNAJC15* promoter. We were also able to identify the precise promoter region that ETV7 uses to reduce the expression of DNAJC15 located at +377 bp from the TSS (Figures 3 and 4). Given reports of DNAJC15 hyper-methylation and decreased expression in cancer [28], we investigated whether ETV7 could modulate DNAJC15 expression through this mechanism. By mapping the CpG islands that are methylated in response to Doxorubicin and ETV7 over-expression in breast cancer cells, we demonstrated that ETV7-dependent DNAJC15 transcriptional repression is methylation-

mediated (Figure 5). We speculate that this may be achieved through the direct recruitment of the DNA methyltransferase DNMT3A on chromatin mediated by ETV7 given our observation of physical interaction between the two proteins (Figure 5).

In Figure 8, we propose a model for the novel mechanism of Doxorubicin resistance in breast cancer cells that includes a pivotal role for ETV7, which is directly activated by this chemotherapeutic drug. The induced ETV7 acts as a direct negative regulator of DNAJC15 expression through the DNA methylation of the promoter region via DNMT3A. DNAJC15 repression leads to the efflux of the drug from the nucleus, a process possibly driven by loss of the DNAJC15-dependent repression of ABCB1.

A better knowledge of the transcriptional repressors that impact DNAJC15 expression could help inform clinical treatment strategies in order to avoid or minimize the activation of one of its direct repressors such as ETV7. A combinatorial treatment could disrupt this resistance circuitry driven by ETV7. Based on our findings, we suggest considering combined treatment of Doxorubicin with Quercetin as a therapeutic strategy, given its protective role against Doxorubicin cardiotoxicity and its negative action on ETV7 expression (Figure 7).

Taken collectively, our results uncovered a novel molecular mechanism that underlies the resistance to a standard-of-care treatment for breast cancer (Doxorubicin), providing insights on the players that take part in this process: ETV7, DNMT3A and DNAJC15 all of which have the potential for pharmacological targeting. Moreover, it is worth noting that our findings provide the first evidence for a role of ETV7 expression and function in the resistance to Doxorubicin in breast cancer cells. We propose that further analyses on additional ETV7 targets could help investigations for novel breast cancer prognostic markers.

In general, given the complex universe beyond chemoresistance in cancer cells, it is of paramount importance to search for downstream master regulators like transcription factors. Despite the difficulties beyond their targeting, understanding how to restrict their activation and activity could provide a more promising therapeutic strategy than simply targeting a specific resistance effector.

CONCLUSIONS

Uncovering pathways and mechanisms involved in drug resistance is an urgent and critical aim for breast cancer research oriented to improve treatment efficacy. Here, we uncovered a novel mechanism of resistance directly activated by Doxorubicin treatment where the transcriptional repressor ETV7 plays a major role. Specifically, we demonstrated that ETV7 can transcriptionally repress DNAJC15 thereby triggering Doxorubicin-resistance. These findings can help to better understand how resistance to conventional chemotherapy can be hindered and possibly tackled pharmacologically.

ABBREVIATIONS

ETV7: Ets Variant Gene 7; ETS: E26 Transformation-Specific; DNAJC15: DNAJ Heat Shock Protein family (Hsp40) member C15; ABCB1: ATP Binding Cassette subfamily B member 1; DNMT3A: DNA Methyl-Transferase 3A; 5-Aza: 5-Aza-2'-deoxycytidine; TNBC: Triple Negative Breast Cancer; ADR: Adriamycin.

DECLARATIONS

ACKNOWLEDGEMENTS

We thank Lia Pinto, Michael Pancher, Dr. Valentina Adami and CIBIO High Throughput Screening Facility for technical assistance. We appreciated Prof. Alberto Inga's group for sharing reagents and helpful discussions. We thank the Clinical Research Unit of NIEHS for providing lymphocytes from healthy donors.

FUNDING

This work was supported by CIBIO Start-up funds (to YC) and by Intramural NIH Research Program NIEHS Z01-ES065079 (to MAR).

AUTHORS' CONTRIBUTIONS

FA, LP, DM, MAR and YC conceived and designed this study. FA, LP and DM performed the experiments. FA, LP and YC conducted the data analyses. All authors read manuscript drafts, contributed edits, and approved the final manuscript.

COMPETING INTERESTS

The authors declare that they have no competing interests.

FIGURE LEGENDS

Figure 1: DNA damaging drugs promote ETV7 transcriptional activation. RT-qPCR analysis of ETV7 expression upon different chemotherapeutics treatment in breast cancer-derived MCF7 **(A)** and MDA-MB-231 cells **(B)**, and in healthy donors-derived lymphocytes **(C)**. Bars represent average Fold Changes relative to the untreated condition and standard deviations of at least three biological replicates. * = p-value < 0.01.

Figure 2: ETV7 can trigger breast cancer resistance to Doxorubicin. A-B) MTT Assays for survival analyses upon Doxorubicin treatment in MCF7 **(A)** and in MDA-MB-231 **(B)** cells over-expressing ETV7 with respect to their empty control. **C)** Analysis of the ratio between nuclear and cytoplasmic intensity of Doxorubicin in MDA-MB-231 cells over-expressing ETV7 compared with their empty control, performed through Operetta Perkin Elmer Software. **D)** Analysis of the cytoplasmic area of Doxorubicin efflux in MDA-MB-231 cells over-expressing ETV7 in comparison to their empty counterpart. Images are reporting one representative analyzed by Operetta PerkinElmer Software. Experiments are done in quadruplicate. * = p-value < 0,01.

Figure 3: DNAJC15 expression is repressed by DNA damaging drugs. A) RT-qPCR analysis in MCF7 cells of the expression of a selected group of DNAJC family members repressed upon Doxorubicin treatment according microarray analysis (GSE24065). **B-C)** Expression analysis of DNAJC15 mRNA upon different chemotherapeutics treatment in breast cancer-derived MCF7 **(B)** and MDA-MB-231 cells **(C)**, and in healthy donors-derived lymphocytes **(D)**. Bars represent averages Fold Changes relative to the untreated condition of at least three biological replicates and standard deviations. * = p-value < 0.01.

Figure 4: ETV7 can repress DNAJC15 expression at the transcriptional level. A) RT-qPCR analysis of ETV7 and DNAJC15 expression in MCF7 cells transfected with pCMV6-Entry-Empty or pCMV6-Entry-ETV7 plasmids. **B)** Gene reporter assay of MCF7 cells transiently over-expressing pCMV6-Entry-Empty or pCMV6-Entry-ETV7 along with pGL4.26-DNAJC15 reporter plasmid or the pGL4.26-DNAJC15-BS1 or -BS2 plasmids mutated in the putative ETV7 binding sites. Data are normalized using pRL-SV40 and are shown as fold of induction relative to the empty control. **C)** ChIP-PCR of DNAJC15 and GAPDH (control) promoter regions in MCF7 transfected with pCMV6-ETV7. Shown is the percentage enrichment of EVT7 or control (IgG) bound to DNAJC15 promoter region in respect to INPUT DNA. For all the panels, bars represent averages and standard deviations of at least three biological replicates. * = p-value < 0.01.

Figure 5: **ETV7 can regulate DNAJC15 expression in a methylation-dependent manner**. **A)** Methylation status of CpGs within DNAJC15 promoter analyzed by bisulfite conversion followed by PCR and direct sequencing in MCF7 untreated, treated with Doxorubicin for 16 hours or

transfected with pCMV6-Entry-Empty or pCMV6-Entry-ETV7 plasmids. Methylated CpGs are shown as black dots, whereas unmethylated CpGs as white dots. **B)** RT-qPCR analysis of DNAJC15 expression in MCF7 transfected with pCMV6-Entry-Empty or pCMV6-Entry-ETV7 and treated with DMSO or 5-Aza-2'-deoxycytidine for 48 hours. **C)** RT-qPCR analysis of DNMT1, DNMT3A and DNMT3B expression in MCF7 treated with Doxorubicin for 16 hours. **D)** Western blot of DNMT3A and ETV7 on the immunoprecipitation with an antibody against ETV7 or normal IgG as control and on INPUT lysates in MCF7 transfected with pCMV6-Entry-ETV7 plasmid. * = p-value < 0.01.

Figure 6: **DNAJC15 over-expression can rescue Doxorubicin sensitivity**. MTT Assay of ETV7-over-expressing MCF7 **(A)** and MDA-MB-231 **(B)** cells transiently transfected with pCMV6-Entry-Empty or pCMV6-Entry-DNAJC15 plasmids and treated with Doxorubicin 1,5 μM or 3 μM for 72 hours. Experiments are done in quadruplicate. * = p-value < 0.01.

Figure 7: ETV7 and DNAJC15 levels inversely correlate with clinical status of breast cancer patients and ETV7 can be exploited pharmacologically. A) ETV7, DNAJC15 and ABCB1 expression levels from microarray data (GSE76540) of MCF7 cells resistant to Adriamycin -MCF7/ADR- (e.g. Doxorubicin). Presented are the averages and standard deviations of at least three biological replicates. **B)** ETV7 and DNAJC15 expression levels from microarray data of Triple Negative Breast Cancer patients treated with neoadjuvant chemotherapy who were showing recurrence or not for the disease (GSE43502). **C)** ETV7 expression levels measured by RT-qPCR from MDA-MB-231 cells untreated (Mock) or treated with Quercetin 50μM or Genistein 30μM for 16 hours. Bars represent averages and standard deviations of at least three biological replicates. **D)** MTT assay in MDA-MB-231 cells over-expressing ETV7 or its empty vector and treated with increasing concentration of Quercetin. Experiments are done in quadruplicate. * = p-value < 0.01.

Figure 8: Model for ETV7 leading to Doxorubicin resistance in breast cancer cells through the methylation-dependent repression of DNAJC15. A graphical description of the novel model for ETV7-dependent Doxorubicin resistance is presented. In normal conditions ETV7 and DNMT3A are maintained at basal levels (particularly low in case of ETV7) and DNAJC15 can be regularly expressed. In response to Doxorubicin treatment, ETV7 levels get elevated and DNMT3A slightly increases as well. Induced ETV7 can then accumulate into the nucleus and specifically to chromatin-enriched regions. In the nucleus, ETV7 recruits DNMT3A (through direct interactions

with putative additional cofactors) on target DNA (DNAJC15 promoter in this case) that in turn it is responsible for the methylation of CpGs. This will result in DNAJC15 repression and ultimately will lead to chemoresistance, partly through exclusion of the drug from the nucleus. EBS: ETV7 Binding Site. Methylated CpGs are shown as filled circles, whereas unmethylated CpGs as empty circles.

Additional file 1: SUPPLEMENTARY MATERIALS

Suppl. Figure 1: A) Western Blot analysis of nuclear and cytoplasmic extracts of Doxorubicin-treated MCF7 cells. Alpha-Actinin serves as loading control while Histone 3 is used as a control for nuclear fractionation. **B)** RT-qPCR analysis of ETV7 expression upon Doxorubicin treatment in cancer cell lines A375M, A549, U2OS and non-cancerous cell lines MCF10a and BJ1. Bars represent average Fold Changes relative to the untreated condition and standard deviations of at least three biological replicates. * = p-value < 0.01.

Suppl. Figure 2: A-B) Western Blot analysis of ETV7 over-expressing clones, relative to MCF7 **(A)**, MDA-MB-231 **(B)** and U2OS **(C)** cells stably transfected with the Empty vector**. D)** MTT Assay for survival analysis upon Doxorubicin treatment in U2OS cells over-expressing ETV7 with respect to their empty control. **E)** Doxorubicin nuclear efflux analysis using Operetta Imaging System, based on the detection of nuclear and cytoplasmic regions; the recognition of Doxorubicin efflux is done by calculating the fluorescence positive spots area (green spots in the panels on the left). This analysis was performed in MDA-MB-231 cells over-expressing ETV7 compared with their empty control cells. **F-G)** RT-qPCR analysis of ABCB1 expression in ETV7 over-expressing clones, MCF7-based **(F)** and MDA-MB-231-based **(G)**. * = p-value < 0.01.

Suppl. Figure 3: A-B) Expression values from microarray data previously obtained by our group from MCF7 cells treated with Doxorubicin (GSE24065) of **(A)** the gene list the Boettcher group had obtained ([33] as hypermethylated genes upon resistance to Doxorubicin) and of **(B)** the DNAJC family members. Results are presented as logarithm of Fold Change from Doxorubicin-treated samples calculated over Mock condition.

Suppl. Figure 4: A) RT-qPCR analysis of ETV7 and DNAJC15 expression in MDA-MB-231 over-expressing pCMV6-Entry-Empty or pCMV6-Entry-ETV7 plasmids. **B)** ChIP-PCR of DNAJC15 and

GTF2H5 (control) promoter regions in MDA-MB-231 stably over-expressing ETV7 untreated or treated with Doxorubicin for 16 hours. **C)** Western Blot of chromatin and nuclear fractions of MDA-MB-231 over-expressing ETV7 upon treatment with Doxorubicin. Alpha-Actinin serves as loading control while Histone 3 is used as a control for chromatin-enriched nuclear fractions. * = p-value < 0.01.

Suppl. Figure 5: **A)** Expression of DNMT1, DNMT3A and DNMT3B from microarray analysis, measured in MCF7 cells treated with Doxorubicin (GSE24065). **B)** RT-qPCR analysis of DNMT1, DNMT3A and DNMT3B expression in MCF7 transfected with pCMV6-Entry-Empty or pCMV6-Etry-ETV7 plasmids. * = p-value < 0.05.

Suppl. Figure 6: RT-qPCR analysis of DNAJC15 and ABCB1 expression in ETV7-over-expressing MCF7 **(A)** and MDA-MB-231 **(B)** cells transiently transfected with pCMV6-Entry-Empty or pCMV6-Entry-DNAJC15 plasmids. Bars represent averages and standard deviations of at least three biological replicates. * = p-value < 0.01.

Suppl. Table 1: Sequences of the primers used for qPCR measurements (mRNA expression and promoter occupancy after ChIP assays).

REFERENCES

1. Cagel M, Grotz E, Bernabeu E, Moretton MA, Chiappetta DA: **Doxorubicin: nanotechnological overviews from bench to bedside**. *Drug discovery today* 2016.
2. Bodley A, Liu LF, Israel M, Seshadri R, Koseki Y, Giuliani FC, Kirschenbaum S, Silber R, Potmesil M: **DNA topoisomerase II-mediated interaction of doxorubicin and daunorubicin congeners with DNA**. *Cancer Res* 1989, **49**(21):5969-5978.
3. De Angelis A, Urbanek K, Cappetta D, Piegari E, Ciuffreda LP, Rivellino A, Russo R, Esposito G, Rossi F, Berrino L: **Doxorubicin cardiotoxicity and target cells: a broader perspective**. *Cardio-Oncology* 2016, **2**(2).
4. Bottero V, Busuttil V, Loubat A, Magne N, Fischel JL, Milano G, Peyron JF: **Activation of nuclear factor kappaB through the IKK complex by the topoisomerase poisons SN38 and doxorubicin: a brake to apoptosis in HeLa human carcinoma cells**. *Cancer Res* 2001, **61**(21):7785-7791.
5. Wang CY, Mayo MW, Baldwin AS, Jr.: **TNF- and cancer therapy-induced apoptosis: potentiation by inhibition of NF-kappaB**. *Science* 1996, **274**(5288):784-787.
6. Koo CY, Muir KW, Lam EW: **FOXM1: From cancer initiation to progression and treatment**. *Biochim Biophys Acta* 2012, **1819**(1):28-37.
7. Zona S, Bella L, Burton MJ, Nestal de Moraes G, Lam EW: **FOXM1: an emerging master regulator of DNA damage response and genotoxic agent resistance**. *Biochim Biophys Acta* 2014, **1839**(11):1316-1322.
8. Kim B, Stephen SL, Hanby AM, Horgan K, Perry SL, Richardson J, Roundhill EA, Valleley EM, Verghese ET, Williams BJ *et al*: **Chemotherapy induces Notch1-dependent MRP1 up-regulation, inhibition of which sensitizes breast cancer cells to chemotherapy**. *BMC cancer* 2015, **15**:634.
9. Bezler M, Hengstler JG, Ullrich A: **Inhibition of doxorubicin-induced HER3-PI3K-AKT signalling enhances apoptosis of ovarian cancer cells**. *Molecular oncology* 2012, **6**(5):516-529.
10. Carella C, Potter M, Bonten J, Rehg JE, Neale G, Grosveld GC: **The ETS factor TEL2 is a hematopoietic oncoprotein**. *Blood* 2006, **107**(3):1124-1132.
11. Graves BJ, Petersen JM: **Specificity within the ets family of transcription factors**. *Adv Cancer Res* 1998, **75**:1-55.
12. Kim CA, Phillips ML, Kim W, Gingery M, Tran HH, Robinson MA, Faham S, Bowie JU: **Polymerization of the SAM domain of TEL in leukemogenesis and transcriptional repression**. *EMBO J* 2001, **20**(15):4173-4182.
13. Potter MD, Buijs A, Kreider B, van Rompaey L, Grosveld GC: **Identification and characterization of a new human ETS-family transcription factor, TEL2, that is expressed in hematopoietic tissues and can associate with TEL1/ETV6**. *Blood* 2000, **95**(11):3341-3348.
14. Kawagoe H, Potter M, Ellis J, Grosveld GC: **TEL2, an ETS factor expressed in human leukemia, regulates monocytic differentiation of U937 Cells and blocks the inhibitory effect of TEL1 on ras-induced cellular transformation**. *Cancer Res* 2004, **64**(17):6091-6100.
15. Matos JM, Witzmann FA, Cummings OW, Schmidt CM: **A pilot study of proteomic profiles of human hepatocellular carcinoma in the United States**. *The Journal of surgical research* 2009, **155**(2):237-243.
16. Quintana AM, Picchione F, Klein Geltink RI, Taylor MR, Grosveld GC: **Zebrafish ETV7 regulates red blood cell development through the cholesterol synthesis pathway**. *Disease models & mechanisms* 2014, **7**(2):265-270.

17. Cardone M, Kandilci A, Carella C, Nilsson JA, Brennan JA, Sirma S, Ozbek U, Boyd K, Cleveland JL, Grosveld GC: **The novel ETS factor TEL2 cooperates with Myc in B lymphomagenesis**. *Mol Cell Biol* 2005, **25**(6):2395-2405.
18. Sang Y, Chen MY, Luo D, Zhang RH, Wang L, Li M, Luo R, Qian CN, Shao JY, Zeng YX *et al*: **TEL2 suppresses metastasis by down-regulating SERPINE1 in nasopharyngeal carcinoma**. *Oncotarget* 2015, **6**(30):29240-29253.
19. Maeda O, Ando T, Ohmiya N, Ishiguro K, Watanabe O, Miyahara R, Hibi Y, Nagai T, Yamada K, Goto H: **Alteration of gene expression and DNA methylation in drug-resistant gastric cancer**. *Oncology reports* 2014, **31**(4):1883-1890.
20. Bisio A, Zamborszky J, Zaccara S, Lion M, Tebaldi T, Sharma V, Raimondi I, Alessandrini F, Ciribilli Y, Inga A: **Cooperative interactions between p53 and NFkappaB enhance cell plasticity**. *Oncotarget* 2014, **5**(23):12111-12125.
21. Navasa N, Martin I, Iglesias-Pedraz JM, Beraza N, Atondo E, Izadi H, Ayaz F, Fernandez-Alvarez S, Hatle K, Som A *et al*: **Regulation of oxidative stress by methylation-controlled J protein controls macrophage responses to inflammatory insults**. *The Journal of infectious diseases* 2015, **211**(1):135-145.
22. Kuang YQ, Charette N, Frazer J, Holland PJ, Attwood KM, Dellaire G, Dupre DJ: **Dopamine receptor-interacting protein 78 acts as a molecular chaperone for CCR5 chemokine receptor signaling complex organization**. *PLoS One* 2012, **7**(7):e40522.
23. Mitra A, Shevde LA, Samant RS: **Multi-faceted role of HSP40 in cancer**. *Clinical & experimental metastasis* 2009, **26**(6):559-567.
24. Lindsey JC, Lusher ME, Strathdee G, Brown R, Gilbertson RJ, Bailey S, Ellison DW, Clifford SC: **Epigenetic inactivation of MCJ (DNAJD1) in malignant paediatric brain tumours**. *Int J Cancer* 2006, **118**(2):346-352.
25. Lau DT, Hesson LB, Norris MD, Marshall GM, Haber M, Ashton LJ: **Prognostic significance of promoter DNA methylation in patients with childhood neuroblastoma**. *Clin Cancer Res* 2012, **18**(20):5690-5700.
26. Schusdziarra C, Blamowska M, Azem A, Hell K: **Methylation-controlled J-protein MCJ acts in the import of proteins into human mitochondria**. *Hum Mol Genet* 2013, **22**(7):1348-1357.
27. Witham J, Vidot S, Agarwal R, Kaye SB, Richardson A: **Transient ectopic expression as a method to detect genes conferring drug resistance**. *Int J Cancer* 2008, **122**(11):2641-2645.
28. Fernandez-Cabezudo MJ, Faour I, Jones K, Champagne DP, Jaloudi MA, Mohamed YA, Bashir G, Almarzooqi S, Albawardi A, Hashim MJ *et al*: **Deficiency of mitochondrial modulator MCJ promotes chemoresistance in breast cancer**. *JCI insight* 2016, **1**(7).
29. Hatle KM, Neveu W, Dienz O, Rymarchyk S, Barrantes R, Hale S, Farley N, Lounsbury KM, Bond JP, Taatjes D *et al*: **Methylation-controlled J protein promotes c-Jun degradation to prevent ABCB1 transporter expression**. *Mol Cell Biol* 2007, **27**(8):2952-2966.
30. Hatle KM, Gummadidala P, Navasa N, Bernardo E, Dodge J, Silverstrim B, Fortner K, Burg E, Suratt BT, Hammer J *et al*: **MCJ/DnaJC15, an endogenous mitochondrial repressor of the respiratory chain that controls metabolic alterations**. *Mol Cell Biol* 2013, **33**(11):2302-2314.
31. Sinha D, Srivastava S, Krishna L, D'Silva P: **Unraveling the intricate organization of mammalian mitochondrial presequence translocases: existence of multiple translocases for maintenance of mitochondrial function**. *Mol Cell Biol* 2014, **34**(10):1757-1775.

32. Vassilev LT, Vu BT, Graves B, Carvajal D, Podlaski F, Filipovic Z, Kong N, Kammlott U, Lukacs C, Klein C *et al*: **In vivo activation of the p53 pathway by small-molecule antagonists of MDM2**. *Science* 2004, **303**(5659):844-848.
33. Boettcher M, Kischkel F, Hoheisel JD: **High-definition DNA methylation profiles from breast and ovarian carcinoma cell lines with differing doxorubicin resistance**. *PLoS One* 2010, **5**(6):e11002.
34. Lion M, Bisio A, Tebaldi T, De Sanctis V, Menendez D, Resnick MA, Ciribilli Y, Inga A: **Interaction between p53 and estradiol pathways in transcriptional responses to chemotherapeutics**. *Cell Cycle* 2013, **12**(8).
35. Segura-Pacheco B, Perez-Cardenas E, Taja-Chayeb L, Chavez-Blanco A, Revilla-Vazquez A, Benitez-Bribiesca L, Duenas-Gonzalez A: **Global DNA hypermethylation-associated cancer chemotherapy resistance and its reversion with the demethylating agent hydralazine**. *Journal of translational medicine* 2006, **4**:32.
36. Wang C, Jin H, Wang N, Fan S, Wang Y, Zhang Y, Wei L, Tao X, Gu D, Zhao F *et al*: **Gas6/Axl Axis Contributes to Chemoresistance and Metastasis in Breast Cancer through Akt/GSK-3beta/beta-catenin Signaling**. *Theranostics* 2016, **6**(8):1205-1219.
37. Yu KD, Zhu R, Zhan M, Rodriguez AA, Yang W, Wong S, Makris A, Lehmann BD, Chen X, Mayer I *et al*: **Identification of prognosis-relevant subgroups in patients with chemoresistant triple-negative breast cancer**. *Clin Cancer Res* 2013, **19**(10):2723-2733.
38. Liu Z, Balasubramanian V, Bhat C, Vahermo M, Makila E, Kemell M, Fontana F, Janoniene A, Petrikaite V, Salonen J *et al*: **Quercetin-Based Modified Porous Silicon Nanoparticles for Enhanced Inhibition of Doxorubicin-Resistant Cancer Cells**. *Advanced healthcare materials* 2017, **6**(3).
39. Lv L, Liu C, Chen C, Yu X, Chen G, Shi Y, Qin F, Ou J, Qiu K, Li G: **Quercetin and doxorubicin co-encapsulated biotin receptor-targeting nanoparticles for minimizing drug resistance in breast cancer**. *Oncotarget* 2016, **7**(22):32184-32199.
40. Minaei A, Sabzichi M, Ramezani F, Hamishehkar H, Samadi N: **Co-delivery with nano-quercetin enhances doxorubicin-mediated cytotoxicity against MCF-7 cells**. *Molecular biology reports* 2016, **43**(2):99-105.
41. Dong Q, Chen L, Lu Q, Sharma S, Li L, Morimoto S, Wang G: **Quercetin attenuates doxorubicin cardiotoxicity by modulating Bmi-1 expression**. *British journal of pharmacology* 2014, **171**(19):4440-4454.
42. Cote B, Carlson LJ, Rao DA, Alani AW: **Combinatorial resveratrol and quercetin polymeric micelles mitigate doxorubicin induced cardiotoxicity in vitro and in vivo**. *Journal of controlled release : official journal of the Controlled Release Society* 2015, **213**:128-133.
43. Lopez-Lazaro M, Willmore E, Austin CA: **Cells lacking DNA topoisomerase II beta are resistant to genistein**. *Journal of natural products* 2007, **70**(5):763-767.
44. Fang M, Chen D, Yang CS: **Dietary polyphenols may affect DNA methylation**. *The Journal of nutrition* 2007, **137**(1 Suppl):223S-228S.
45. Ciribilli Y, Andreotti V, Menendez D, Langen JS, Schoenfelder G, Resnick MA, Inga A: **The coordinated p53 and estrogen receptor cis-regulation at an FLT1 promoter SNP is specific to genotoxic stress and estrogenic compound**. *PLoS One* 2010, **5**(4):e10236.
46. Molinari A, Calcabrini A, Meschini S, Stringaro A, Crateri P, Toccacieli L, Marra M, Colone M, Cianfriglia M, Arancia G: **Subcellular detection and localization of the drug transporter P-glycoprotein in cultured tumor cells**. *Current protein & peptide science* 2002, **3**(6):653-670.

47. Menendez D, Shatz M, Azzam K, Garantziotis S, Fessler MB, Resnick MA: **The Toll-like receptor gene family is integrated into human DNA damage and p53 networks**. *PLoS Genet* 2011, **7**(3):e1001360.
48. Ciribilli Y, Monti P, Bisio A, Nguyen HT, Ethayathulla AS, Ramos A, Foggetti G, Menichini P, Menendez D, Resnick MA *et al*: **Transactivation specificity is conserved among p53 family proteins and depends on a response element sequence code**. *Nucleic Acids Res* 2013, **41**(18):8637-8653.
49. Monti P, Ciribilli Y, Russo D, Bisio A, Perfumo C, Andreotti V, Menichini P, Inga A, Huang X, Gold B *et al*: **Rev1 and Polzeta influence toxicity and mutagenicity of Me-lex, a sequence selective N3-adenine methylating agent**. *DNA Repair (Amst)* 2008, **7**(3):431-438.
50. Monti P, Ciribilli Y, Bisio A, Foggetti G, Raimondi I, Campomenosi P, Menichini P, Fronza G, Inga A: **N-P63alpha and TA-P63alpha exhibit intrinsic differences in transactivation specificities that depend on distinct features of DNA target sites**. *Oncotarget* 2014, **5**(8):2116-2130.
51. Monti P, Perfumo C, Bisio A, Ciribilli Y, Menichini P, Russo D, Umbach DM, Resnick MA, Inga A, Fronza G: **Dominant-negative features of mutant TP53 in germline carriers have limited impact on cancer outcomes**. *Mol Cancer Res* 2011, **9**(3):271-279.
52. Ciribilli Y, Singh P, Inga A, Borlak J: **c-Myc targeted regulators of cell metabolism in a transgenic mouse model of papillary lung adenocarcinoma**. *Oncotarget* 2016, **7**(40):65514-65539.

Figure 1

Click here to download Figure Figure 1.eps

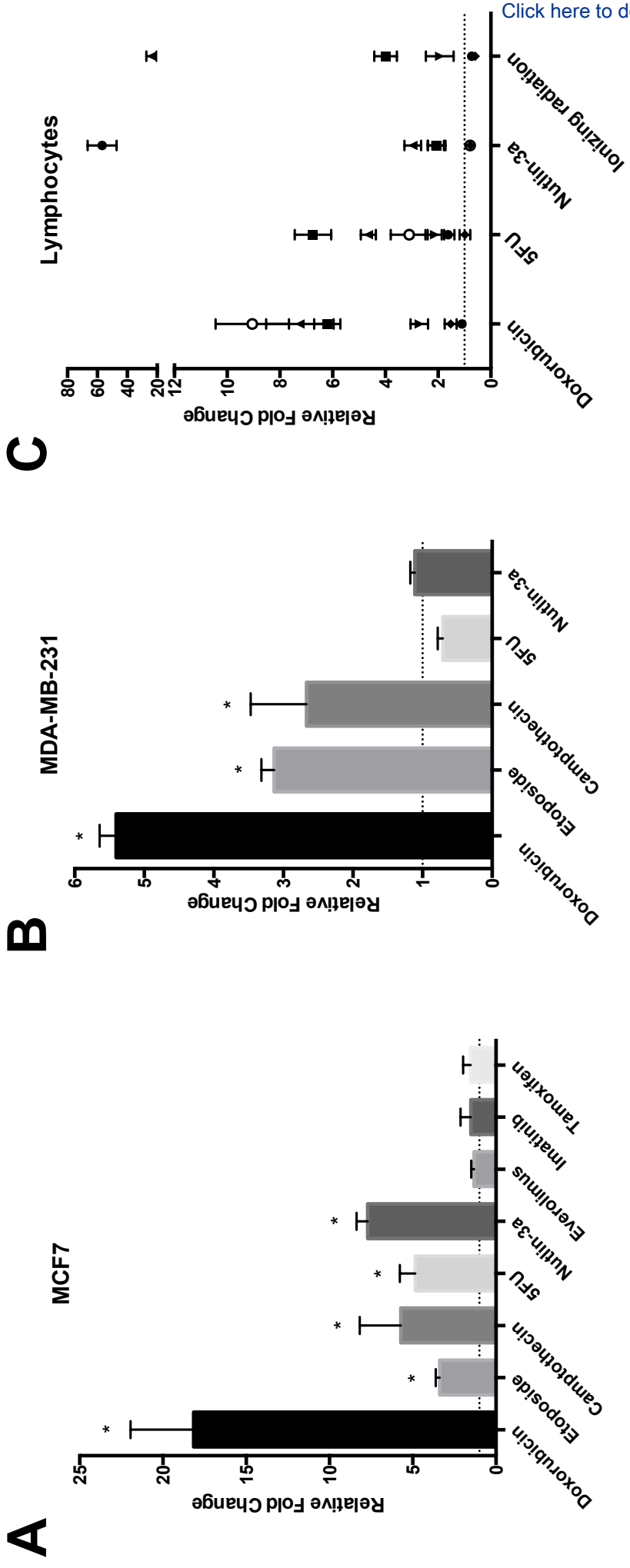

Figure 2

Click here to download Figure Figure 2.eps

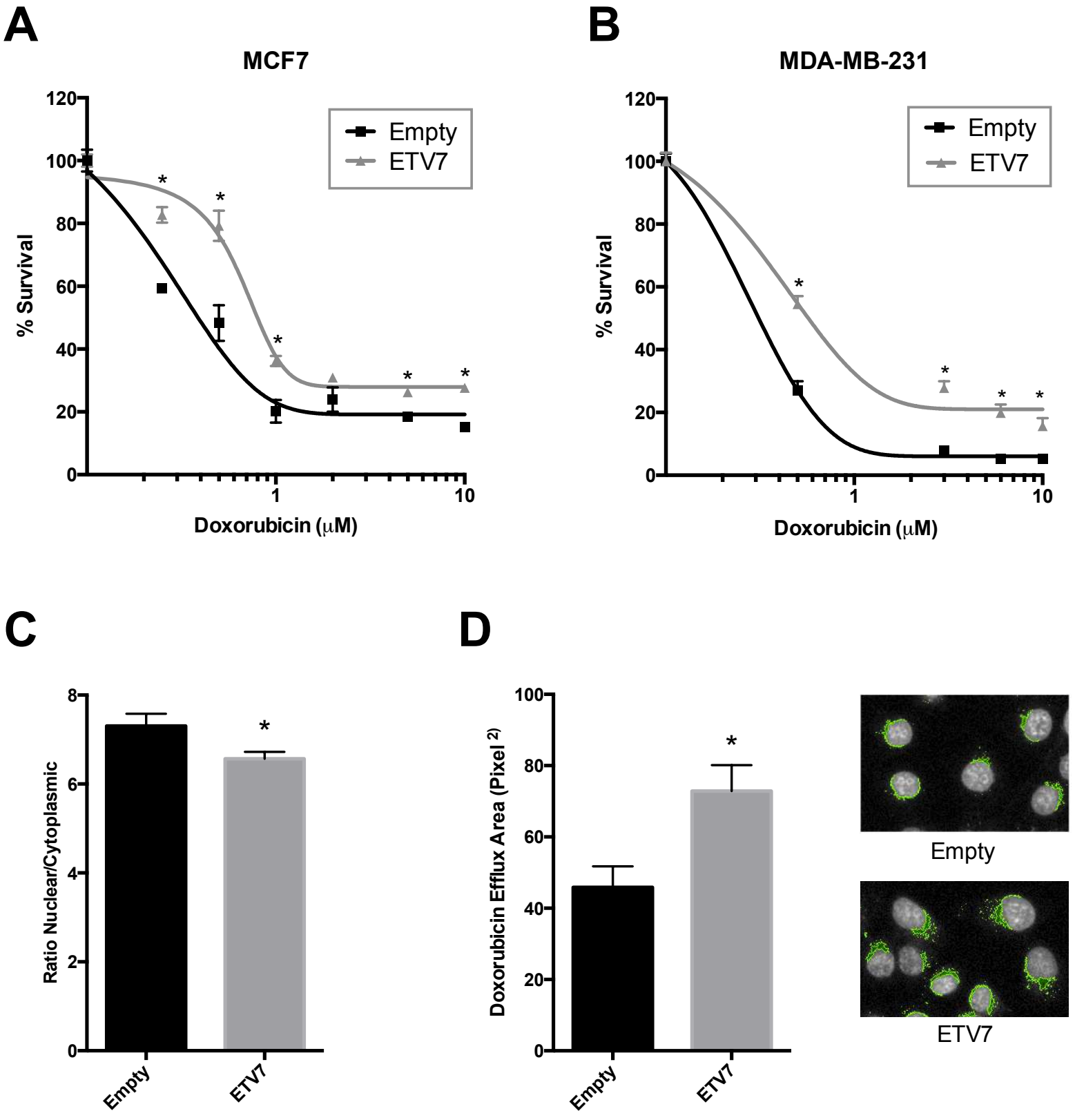

Figure 3

Click here to download Figure Figure 3.eps

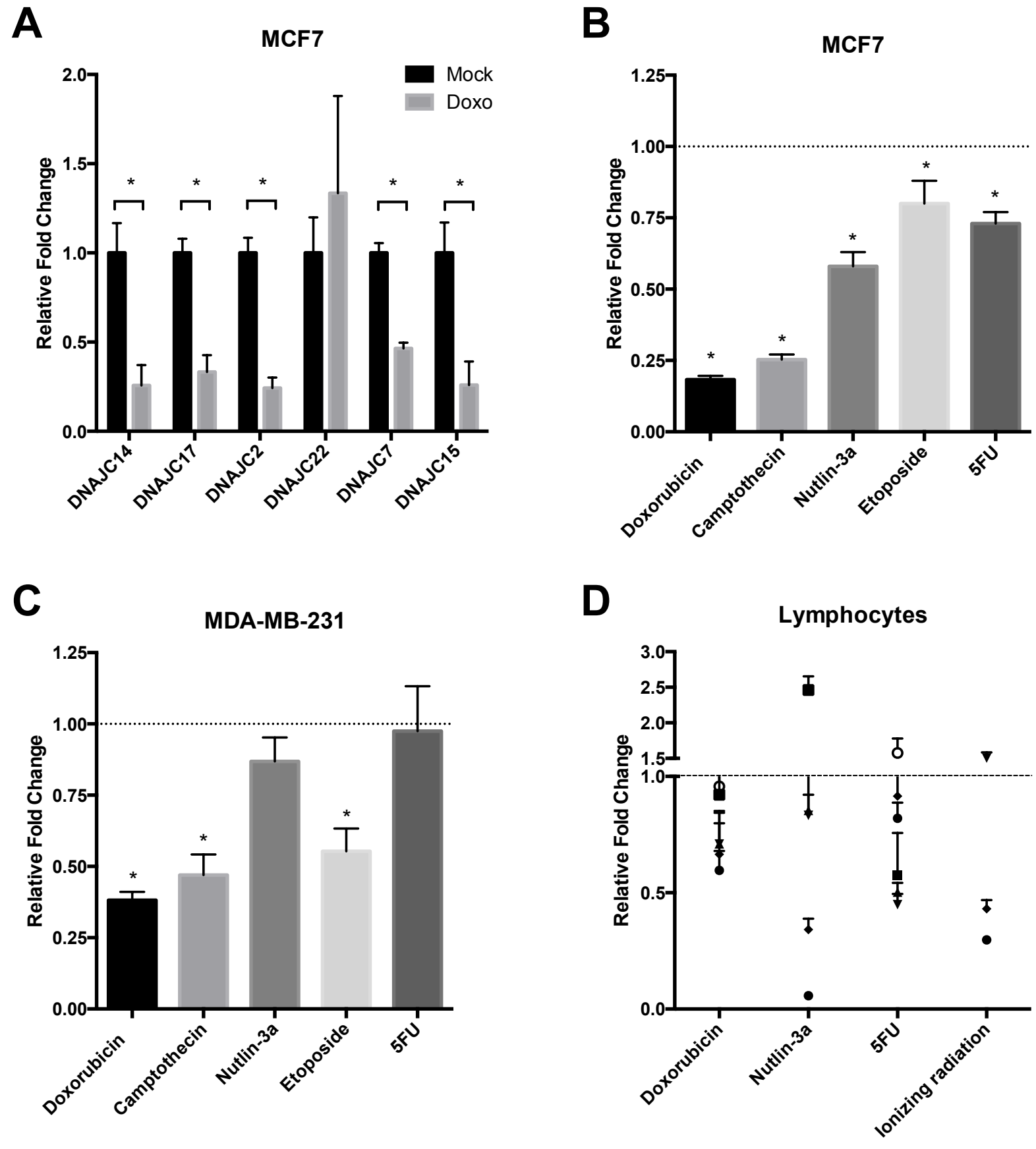

Figure 4

Click here to download Figure Figure 4.eps

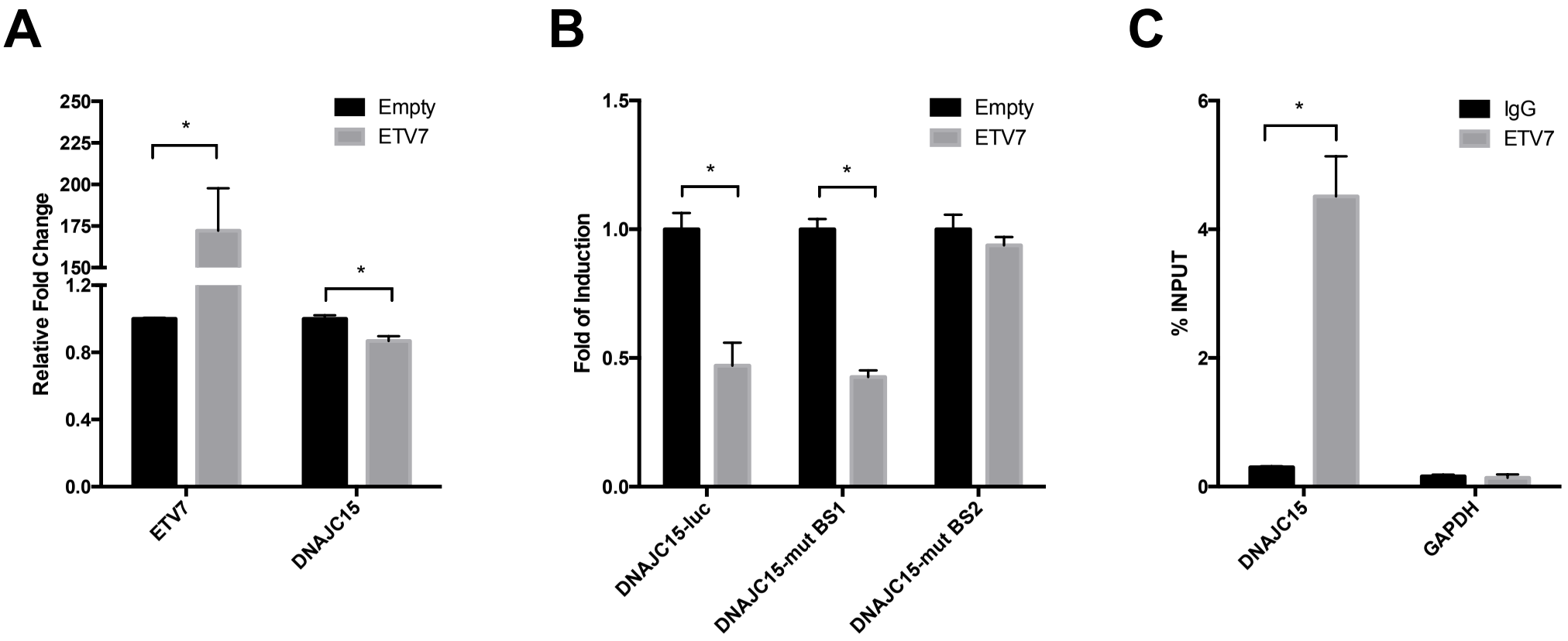

Figure 5

Click here to download Figure Figure 5.eps

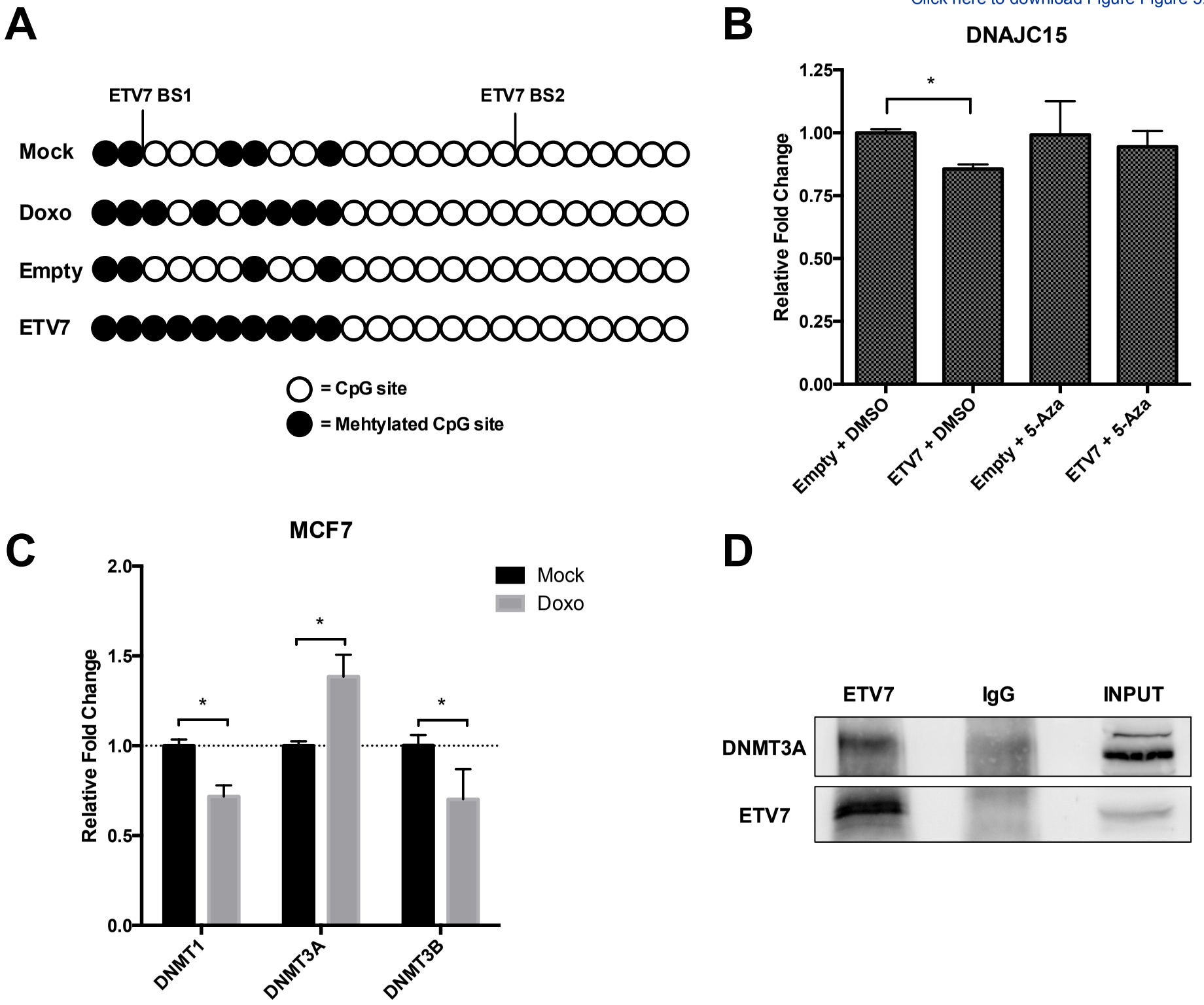

Figure 6

Click here to download Figure Figure 6.eps

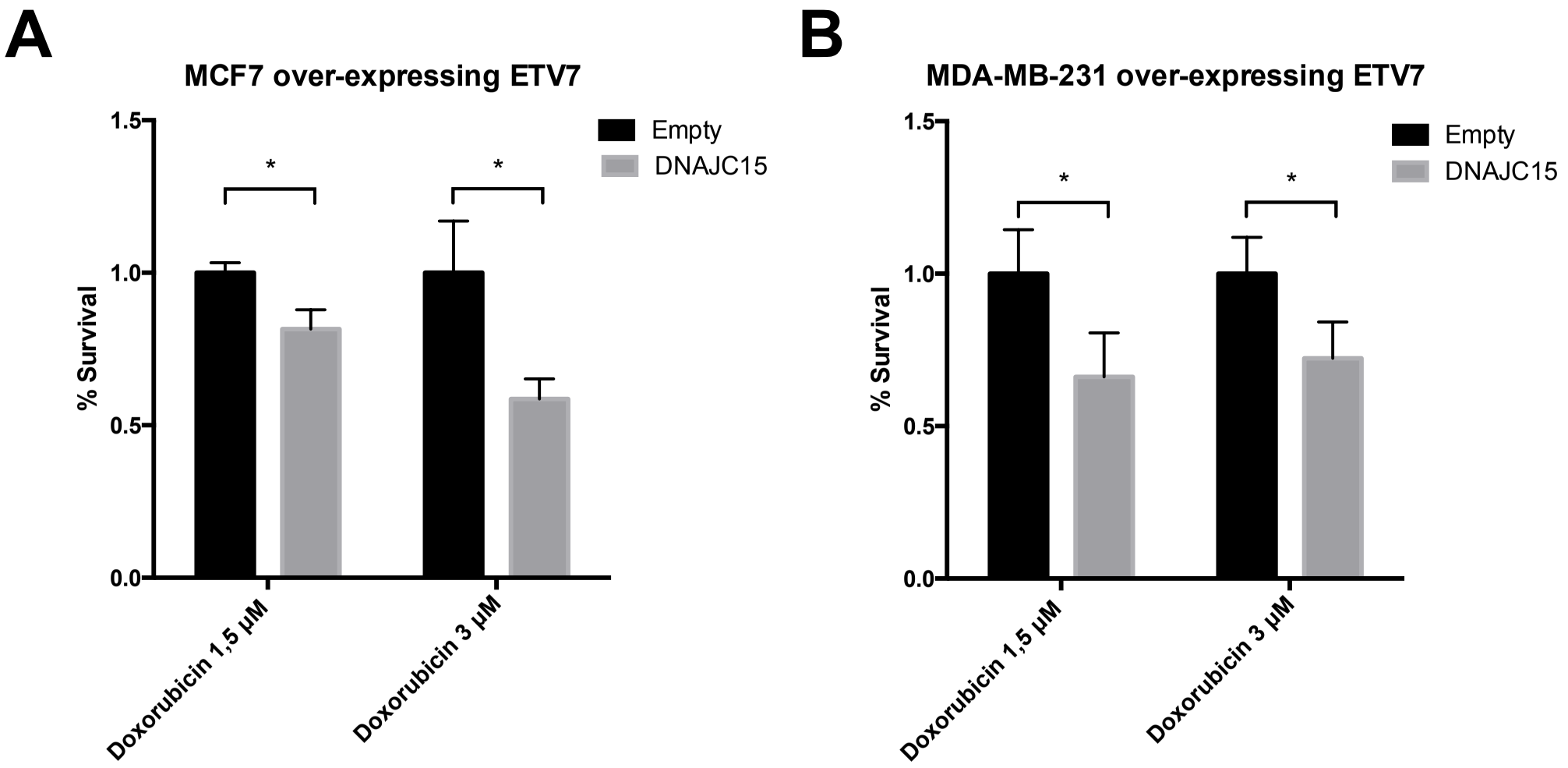

Figure 7

Click here to download Figure FIGURE7.eps

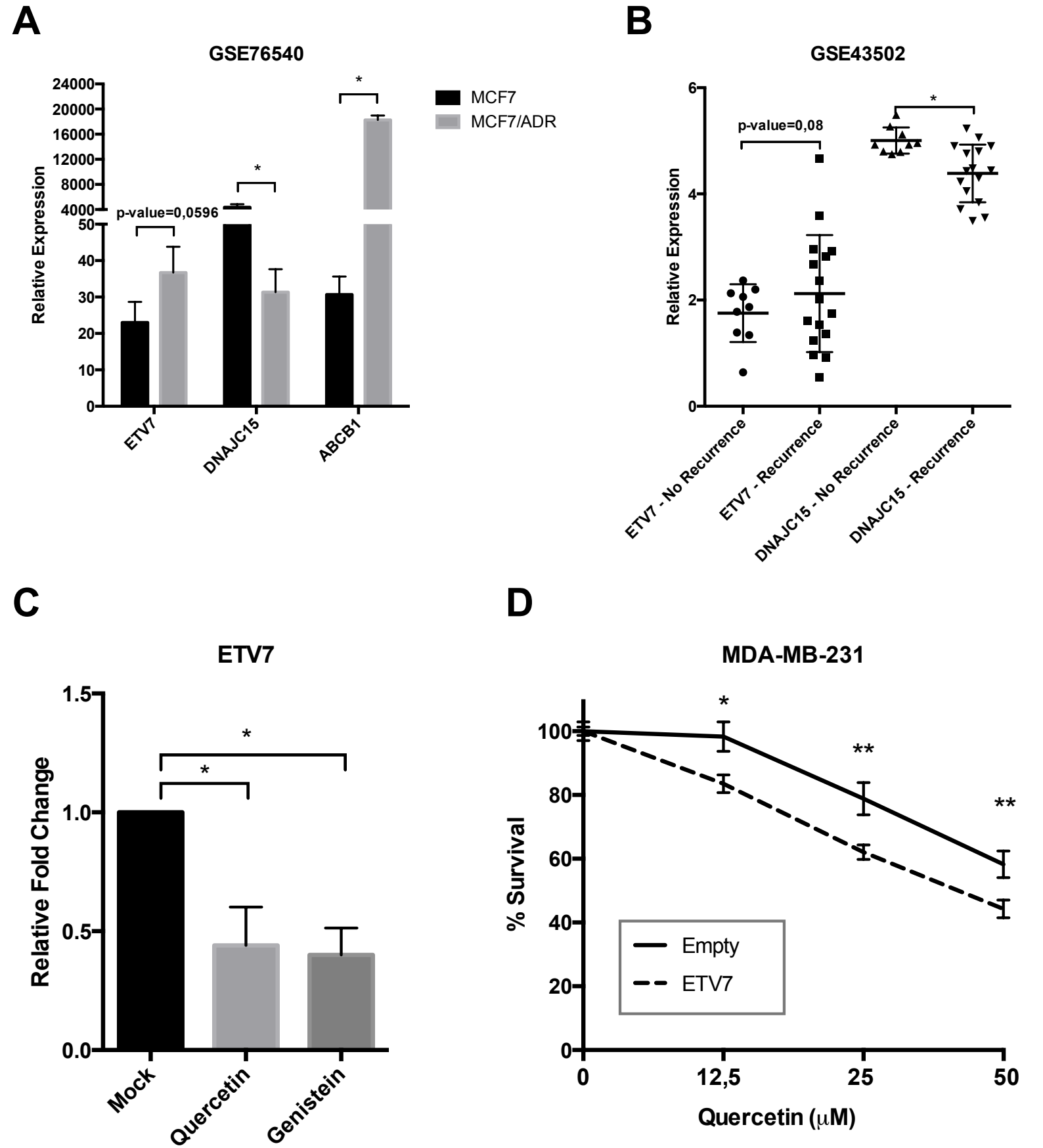

Figure 8

Click here to download Figure Figure 8.eps

UNIVERSITÀ DEGLI STUDI DI TRENTO

CIBIO

CIBIO - Centre for Integrative Biology

Yari Ciribilli
Lab. of Molecular Cancer Genetics
CIBIO, University of Trento, Italy

Breast Cancer Research,
Editor-in-chief, Associate Editors

Trento, May 23nd 2017

Dear Editors,

We wish to submit to "Breast Cancer Research" the manuscript entitled: "*ETV7-mediated DNAJC15 repression leads to Doxorubicin resistance in breast cancer cells"* by Alessandrini F., Pezzè L., Menendez D., Resnick M.A., Ciribilli Y.
Below we bring to the attention of the Editors the key points and the strengths of our manuscript along with the reasons and the novelty of the study.

All authors are aware of and agreed to submit this manuscript and they have all contributed to the work described, sufficiently to be named as authors. Any other person or body with an interest in the manuscript, such as our employer is aware of the submission and agrees to it. On behalf of all the authors I hereby declare that there aren't any competing financial interests or other conflicts of interest and we have provided a sentence within the manuscript declaring that.

We would like to propose your journal an intriguing study regarding chemoresistance in breast cancer. In particular, we have uncovered a new mechanism of resistance to standard chemotherapy (i.e. Doxorubicin) exploited by breast cancer cells. The main player in this regulatory system is ETV7, a poorly characterized transcription factor that we showed is strongly activated in response to different DNA damaging agents in breast cancer cells.
The premise of the study has been the fact that we previously published a story where the combined treatment with Doxorubicin and TNFalpha in MCF7 breast cancer-derived cells can lead to the activation of specific gene expression programs that may impact on cancer phenotypes and potentially modify the efficacy of cancer therapy (Bisio et al., 2014). Among the genes that we found synergistically up-regulated, we identified ETV7 as a potential tumor promoting factor.

In the present study we were able to demonstrate that over-expression of ETV7 can lead to resistance to Doxorubicin in two different cellular models of breast cancer. The ETV7 increased expression lead to the down-regulation of DNAJC15, a co-chaperone protein whose low expression was previously associated with drug resistance in breast and ovarian cancer. We have identified the binding site for ETV7 within the promoter of DNAJC15 and we have also found that DNA methylation contributes to ETV-mediated transcriptional repression at the DNAJC15 promoter. These findings of an inverse

correlation between ETV7 and DNAJC15 expression in MCF7 cells in terms of Doxorubicin resistance, correlates well with treatment responses of breast cancer patients with recurrent disease, based on our analyses of reported genome-wide expression arrays. In addition, we have demonstrated that ETV7-mediated Doxorubicin resistance involves increased Doxorubicin efflux via nuclear pumps, which could be rescued in part by DNAJC15 up-regulation.

In summary, with this work we provide a model for the novel mechanism of Doxorubicin resistance in breast cancer cells that includes a pivotal role for ETV7, which is directly activated by this chemotherapeutic drug (a figure within the manuscript depicts this new molecular mechanism). The activated ETV7 acts as a direct negative regulator of DNAJC15 expression through the DNA methylation of the promoter region via DNMT3A. DNAJC15 repression leads to the efflux of the drug from the nucleus, a process possibly driven by loss of the DNAJC15-dependent repression of ABCB1.
These findings can help to better understand how resistance to conventional chemotherapy can be hindered and possibly tackled pharmacologically.

We believe our manuscript will deliver insights to the reader on a relatively new and compelling topic, emphasizing the role of ETV7 as responsible of resistance to Doxorubicin in breast cancer cells, a gene that has only recently been associated with cancer progression and aggressiveness.

Bisio A., Zámborszky J., Zaccara S., Lion M., Tebaldi T., Sharma V., Raimondi I., Alessandrini F., **Ciribilli Y.***, Inga A.*. Cooperative interactions between p53 and NFκB enhance cell plasticity. *Oncotarget.* 2014 Dec 15;5(23):12111-25.
* = corresponding authors

Dr. Yari Ciribilli, PhD, Assistant Professor
Laboratory of Molecular Cancer Genetics
CIBIO, University of Trento
Via Sommarive 9, 38123, Povo (TN), Italy
+39 461 283173, yari.ciribilli@unitn.it

Below is a list of experts in the study of ETS functions or, more generally speaking, in the breast cancer field, particularly in transcriptional regulation, analysis of response elements and of gene expression, we suggest to be considered as potential reviewers.

Prof. Anne-Lise Børresen-Dale
Department of Genetics, Institute for Cancer Research, Oslo University Hospital The Norwegian Radiumhospital
a.l.borresen-dale@medisin.uio.no

Prof. Giannino Del Sal
Molecular Oncology Unit, Laboratorio Nazionale CIB (LNCIB), Area Science Park,
Department of Life Sciences, University of Trieste, Italy
delsal@lncib.it

Dr. Giuseppina M. Carbone
Tumor Biology and Experimental Therapeutics Program, Institute of Oncology Research (IOR), Bellinzona, Switzerland
pina.carbone@ior.iosi.ch

Prof. Galina Selivanova
Department of Microbiology, Tumor and Cell Biology, Karolinska Institutet, Stockholm, Sweden
Galina.Selivanova@ki.se

ANNEX 2.4

Manuscript Details

Manuscript number	YSONC_2017_24
Title	LAMPs: shedding light on cancer biology
Article type	Review Article

Abstract

Lysosomes are important cytoplasmic organelles whose critical functions into the cells have only relatively recently been acknowledged. In particular, despite the long-standing accepted concept about the role of lysosomes as cellular machineries solely assigned to degradation, it has been demonstrated that they play active roles in homeostasis and even in cancer biology. Indeed, it is now well documented that during the process of cellular transformation and cancer progression lysosomes are changing localization, composition and volume and, through the release of their enzymes, lysosomes can also enhance cancer aggressiveness. LAMPs, Lysosome Associated Membrane Proteins, represent a family of glycosylated proteins present predominantly on the membrane of lysosomes whose expression can vary among different tissues, suggesting a separation of functions. In this review we focus on the functions and roles of the different LAMP family members with a particular emphasis on cancer progression and metastatic spread. LAMP proteins are involved in many different aspects of cell biology and can influence cellular processes such as phagocytosis, autophagy, lipid transport and aging. Interestingly, for all the five members identified so far, LAMP1, LAMP2, LAMP3, CD68 and BAD-LAMP, it has been suggested a role in cancer. While this is well documented for LAMP1 and LAMP2, the involvement of the other three proteins in cancer progression and aggressiveness has recently been proposed and remains to be elucidated. Here we present different examples about how LAMP proteins can influence and support tumor growth and metastatic spread, emphasizing the impact of each single member of the family.

Keywords	LAMPs; lysosomes; cancer; metastasis
Taxonomy	Oncology, Molecular Oncology

Corresponding Author	YARI CIRIBILLI
Corresponding Author's Institution	University of Trento
Order of Authors	Federica Alessandrini, Laura Pezzè, YARI CIRIBILLI

Suggested reviewers	Glenda Halliday, Rajiv D. Kalraiya, Eeva-Liisa Eskelinen

Submission Files Included in this PDF

File Name [File Type]

Cover Letter SinO_Alessandrini_Pezzè 2017.pdf [Cover Letter]

Point-by-point response to reviewers_SiO_2017.pdf [Response to Reviewers]

HIGHLIGHTS_Alessandrini_Pezzè2017.docx [Highlights]

LAMPs review_Alessandrini_Pezzè_revised_June 7.pdf [Manuscript File]

LAMPs Table 1.docx [Figure]

LAMPs Table 2.docx [Figure]

LAMPs Table 3.docx [Figure]

LAMPs Table 4.docx [Figure]

LAMP Table 5.docx [Figure]

Fig1_2017.eps [Figure]

LAMP1-2 cancer cells_Figure 2.pdf [Figure]

LAMP1-2 immune_figure 3.eps [Figure]

LAMP3_Figure 4.eps [Figure]

CD68_Figure 5.eps [Figure]

Figure 6_2017.eps [Figure]

Conflict of Interest_Alessandrini_Pezzè2017.docx [Conflict of Interest]

To view all the submission files, including those not included in the PDF, click on the manuscript title on your EVISE Homepage, then click 'Download zip file'.

UNIVERSITÀ DEGLI STUDI
DI TRENTO

CIBIO

CIBIO - Centre for Integrative Biology

Yari Ciribilli
Lab. of Molecular Cancer Genetics
CIBIO, University of Trento, Italy

Seminars in Oncology,
Editor-in-chief, Review Editor

Trento, March 28th 2017

Dear Editors,

We wish to submit to "Seminars in Oncology" the manuscript entitled: "*LAMPs: shedding light on cancer biology"* by Alessandrini F., Pezzè L. and Ciribilli Y.

All authors are aware of and agreed to submit this manuscript and they have all contributed to the work described, sufficiently to be named as authors. Any other person or body with an interest in the manuscript, such as our employer is aware of the submission and agrees to it. On behalf of all the authors I hereby declare that there aren't any competing financial interests or other conflicts of interest.

We would like to propose a review on a topic that is relatively novel in the cancer field. In this review we focus on the role of lysosomes in cancer, a topic that only more recently has become very interesting in oncology. Specifically, we concentrate on the functions and the impact of the different LAMP (Lysosome-Associated Membrane Proteins) family members with a particular emphasis on cancer progression and metastatic spread. LAMP proteins are involved in many different aspects of cell biology and can influence cellular processes such as phagocytosis, autophagy, lipid transport and aging. Interestingly, for all the five members identified so far, LAMP1, LAMP2, LAMP3, CD68 and BAD-LAMP, it has been suggested a role in cancer. While this is well documented for LAMP1 and LAMP2, for the other three proteins an involvement in cancer progression and aggressiveness has been proposed only recently.
Here we present different examples about how LAMP proteins can influence and support tumor growth and metastatic spread, emphasizing the impact of each single member of the family.

Below we bring to the attention of the Editors the key points and the strengths of our manuscript along with the reasons and the novelty of the proposed review.

Brief explanation of the proposed review
The amount of research material reporting the role of lysosomes in cancer is rapidly increasing in the last decade. Along with the research material also the number of reviews focusing on the general role of lysosomes in cancer is increasing. However, a review collecting all the data regarding role in cancer of lysosome-associated proteins is still

missing. Our motivation to sum up literature regarding this family of proteins is pushed by direct evidences observed in our laboratory specifically related to a member of this family. We have recently published a study to investigate a possible crosstalk between p53 and NFκB driven by chemotherapy-induced responses in the context of an inflammatory microenvironment (Bisio et al., 2014). In that work we propose that the crosstalk between p53 and NFκB can lead to the activation of specific gene expression programs that may impact on cancer phenotypes and potentially modify the efficacy of cancer therapy. Among the genes that were included, LAMP3 showed a nice correlation to tumor aggressiveness that we are further investigating through the generation of breast cancer cells able to over-express or silenced for LAMP3 gene.

In the proposed review we would like to focus on the LAMP family of lysosomal proteins, given the recent evidences on its involvement in cancer. In particular, in this work we will highlight the role and impact of those proteins in cancer aggressiveness and metastatic spread.
The proposed review will be organized with an introduction to contextualize the LAMP proteins and the lysosomes, illustrating the state of the art in the field. Then, we will focus on the LAMP family of proteins, describing the functions of each member with a particular emphasis on cancer. We will provide two figures, the first one to structurally visualize the 5 members of the family and the second one to better explain the role of LAMPs in cancer biology. We will also provide a table listing for each LAMP protein the type of cancer it was involved, its role (pro- or anti-tumorigenic) and finally the relative references. A conclusions-section will close the manuscript.

We believe our review will deliver insights to the reader on a relatively new and compelling topic, summarizing the role of this family of proteins that have been associated only recently to cancer progression and aggressiveness.

Bisio A., Zámborszky J., Zaccara S., Lion M., Tebaldi T., Sharma V., Raimondi I., Alessandrini F., **Ciribilli Y.***, Inga A.*. Cooperative interactions between p53 and NFκB enhance cell plasticity. *Oncotarget.* 2014 Dec 15;5(23):12111-25.

* = corresponding authors

Dr. Yari Ciribilli, PhD, Assistant Professor
Laboratory of Molecular Cancer Genetics
CIBIO, University of Trento
Via Sommarive 9, 38123, Povo (TN), Italy
+39 461 283173, yari.ciribilli@unitn.it

UNIVERSITÀ DEGLI STUDI
DI TRENTO

CIBIO

CIBIO - Centre for Integrative Biology

Yari Ciribilli
Lab. of Molecular Cancer Genetics
CIBIO, University of Trento, Italy

Seminars in Oncology,
Editor-in-chief, Review Editor

Trento, June 09th 2017

Dear Editors,

We wish to submit to "Seminars in Oncology" a revised version of the manuscript we have recently submitted entitled: "*LAMPs: shedding light on cancer biology"* by Alessandrini F., Pezzè L. and Ciribilli Y.

We appreciated the comments and suggestions provided by the Editor, and we have produced a modified version of the manuscript taking into account his specific requests.
Specifically, all the concerns were addressed as outlined in the point-by-point response below. All the changes to the main text are in "track-change" mode.
We hope that in its present form the manuscript can be considered acceptable for publication in Seminars in Oncology.

Yours sincerely,

Dr. Yari Ciribilli, PhD, Assistant Professor
Laboratory of Molecular Cancer Genetics
CIBIO, University of Trento
Via Sommarive 9, 38123, Povo (TN), Italy
+39 461 283173, yari.ciribilli@unitn.it

Author's response to reviewers:

1. The reviewer stated, we quote his words*:*
We are explicitly looking for manuscripts that convey the information to readers in a very comprehensive manner and often the best way to do this is to summarize data in Tables. I would expect a separate table for each LAMP summarizing the data you cite for a pro-tumorigenic roles.

In the revised version of the manuscript, we have produced five new tables that substitute the original one. In this new version, a specific table for each member of the LAMP family is generated summarizing the role in cancer that has been associated with each of them.

2. The reviewer suggested a way to organize the tables; we cite his words again:
The last column critically looks at the data. As you know a lot of the literature is comprised of examples of one study in one model and the value of that is uncertain, indeed it is often of no value. Thus I would question whether LAMP-1 can have all of the "pro-tumorigenic roles" you ascribe to it. Quite frankly I do not think it can have all of the roles you describe.
The newly generated tables are now organized as suggested by the reviewer. We have also included a column where the strengths and weaknesses of the cited references were analyzed, and the reports were criticized accordingly.
Regarding LAMP1 functions, in Table 1 each observation mentioned has been explained and analyzed for possible criticisms.

3. Lastly, the reviewer requested additional figures, as stated*:*
I would also ask you to consider adding another figure or two to better convey to the readers more information about LAMPs other than 1 and 2.
In the original manuscript, we presented three figures, two general and one for the specific roles of LAMP1 and LAMP2 in cancer and immune cells. Following the suggestion of the reviewer, we have now added two new figures, and we have split Figure 2A-B in two separate figures (Figure 2 and 3) to make them uniform with the other figures.
In the current version there are six figures:

1. Organization of LAMP family of proteins;
2. – 5. Localization and functions of LAMP1, LAMP2, DC-LAMP, CD68 in cancer and immune cells;

6. Schematic summary of the roles in cancer carried out by LAMP proteins.

HIGHLIGHTS

- Lysosomes play active roles in homeostasis and even in cancer biology.
- LAMP family members can influence various processes of cancer progression.
- The role of each single member of the family in cancer is emphasized.

LAMPs: shedding light on cancer biology

Federica Alessandrini*, Laura Pezzè*, Yari Ciribilli§

Laboratory of Molecular Cancer Genetics, Centre for Integrative Biology (CIBIO), University of Trento, Via Sommarive 9, 38123, Povo (TN), Italy

* = These authors contributed equally to this work

§ = To whom correspondence should be addressed. Email: yari.ciribilli@unitn.it

Abbreviations:

LAMP	Lysosomal Associated Membrane Protein
DCs	Dendritic cells
TAMs	Tumor Associated Macrophages
ECM	Extra Cellular Matrix

Keywords:
LAMPs, lysosomes, cancer, metastasis

ABSTRACT

Lysosomes are important cytoplasmic organelles whose critical functions into the cells have only relatively recently been acknowledged. In particular, despite the long-standing accepted concept about the role of lysosomes as cellular machineries solely assigned to degradation, it has been demonstrated that they play active roles in homeostasis and even in cancer biology. Indeed, it is now well documented that during the process of cellular transformation and cancer progression lysosomes are changing localization, composition and volume and, through the release of their enzymes, lysosomes can also enhance cancer aggressiveness. LAMPs, Lysosome Associated Membrane Proteins, represent a family of glycosylated proteins present predominantly on the membrane of lysosomes whose expression can vary among different tissues, suggesting a separation of functions. In this review we focus on the functions and roles of the different LAMP family members with a particular emphasis on cancer progression and metastatic spread. LAMP proteins are involved in many different aspects of cell biology and can influence cellular processes such as phagocytosis, autophagy, lipid transport and aging. Interestingly, for all the five members identified so far, LAMP1, LAMP2, LAMP3, CD68 and BAD-LAMP, it has been suggested a role in cancer. While this is well documented for LAMP1 and LAMP2, the involvement of the other three proteins in cancer progression and aggressiveness has recently been proposed and remains to be elucidated. Here we present different examples about how LAMP proteins can influence and support tumor growth and metastatic spread, emphasizing the impact of each single member of the family.

CHARACTERISTICS AND FUNCTIONS OF LYSOSOMES

Lysosomes are eukaryotic acidic organelles originally thought to be exclusively involved in the degradation of intracellular and extracellular macromolecules into building blocks available for the cells. Lysosomes have only recently been recognized as crucial regulators of cell homeostasis and there is accumulating evidence of their involvement in different diseases such as neurodegenerative disorders, cardiovascular diseases and cancer (1, 2). Lysosomes are single membrane cytoplasmic organelles present in almost all eukaryotic cells. They exert several functions in the regulation of cell homeostasis including lysosomal exocytosis, cholesterol homeostasis and, possibly more importantly, the degradation of macromolecules, such as lipids, nucleic acids and proteins. This is achieved through the action of several hydrolases (more than 50 different lysosomal hydrolases have been described so far), among which cathepsins (proteases targeting either cysteine or aspartic residues) occupy a prominent place (3, 4). In particular, degradation of intracellular material is generally obtained via different forms of autophagy, whereas degradation of exogenous material occurs via endocytosis (1).

In the mid-twentieth century, de Duve referred to lysosomes as “suicide bags” because of the important role of these organelles in cell death signaling (5). Indeed, lysosomes are implicated in three main distinct pathways of cell death: apoptosis, necrosis and autophagy (6). However, the recognition of autophagy as a cell death mechanism is still controversial, being a process aimed at survival during stress conditions that can also result is cell death (7). Specifically, the autophagic process (sometimes reported as type II programmed cell death) represents an evolutionarily well-conserved pathway where entire organelles or part of cytoplasm are recycled as a response to starvation or to remove damaged organelles. This multi-step process is mediated through the formation of the so-called autophagosome, a double-membrane vesicle that subsequently will fuse with the lysosomes forming the autolysosome for the final degradation step (8). Lysosomes are the most critical components for a proper clearance of matured autophagosomes, which for instance can cause neurodegenerative disorders in case they accumulate as a result of not being properly digested. Alternatively, the phenomenon of lysosomal permeabilization and the consequent release of proteolytic enzymes into the cytosol has been globally recognized as “lysosomal pathway for apoptosis”. In this process lysosomes are not just passive bystanders, but rather play an active role that is tightly regulated. The factor considered a key determinant in the sort of cell death triggered by lysosomal enzymes, and precisely apoptosis vs. necrosis, is believed to be represented by the magnitude of lysosomal permeabilization, namely the amount of proteolytic enzymes released into the cytosol (9). A complete collapse of the organelle itself with the release of high levels of lysosomal enzymes triggers unregulated necrosis, while selective lysosomes permeabilization results in the induction of apoptosis (10, 11). As soon as lysosomal hydrolases are poured within the cytosol, they can take part in the execution of the apoptotic cascade by acting either in concert with the canonical caspases pathway or directly to actively cleave key cellular substrates (12, 13). However, the precise mechanisms by which lysosomes are involved in apoptosis are still largely unknown and currently under intense investigation.

Relatively recently, the Sabatini’s group has identified the lysosomal surface as the subcellular site where mTORC1 (mammalian Target Of Rapamycin Complex 1) activation in response to amino acids occurs (14). mTOR, the main catalytic component of mTORC1, is an atypical serine/threonine kinase reported as master regulator of cell growth, energy production and protein synthesis (15); its functions are often deregulated in different diseases and in particular in cancer (16). These researchers have demonstrated that amino acids trigger the translocation of mTORC1 complex to the lysosomes where it gets activated through the interaction with Rag GTPases, and Ragulator and Rheb, two proteins that are anchored to the lysosomes’ membrane (14). Active mTORC1 is responsible for the phosphorylation and the subsequent accumulation in the cytosol of TFEB, a nuclear transcription factor responsible for lysosomal biogenesis, thereby integrating signals from the lysosomes to the nucleus (17).

ROLE OF LYSOSOMES IN CANCER

During transformation and cancer progression lysosomes are changing localization, volume and composition and by releasing their enzymes they can increase cancer aggressiveness (4, 18). For instance, several lysosomal enzymes, including cathepsins, are over-expressed in different cancer types, such as breast, prostate and colon cancers (19, 20), and their expression levels can be endowed with clinical significance(11). Different reports have suggested that an increased production and subsequent secretion of these proteases via exocytosis can foster proliferation and invasion ability of cancer cells (19, 21, 22). Therefore, this can enhance cancer progression and metastasis formation by promoting the degradation of the extracellular matrix and increasing the angiogenesis potential (23). Indeed, inhibition of cathepsin B by synthetic cysteine protease inhibitors has been shown to effectively reduce the invasiveness of glioblastoma (24) and breast cancer cells (25). At the same time cancer cells are strongly dependent on lysosome function and are very sensitive to lysosome mediated cell death (1, 26).

Lastly, it has been demonstrated that lysosomal dysfunction can promote the inclusion of lysosomal materials (e.g. proteins) to exosome cargo in order to simplify their elimination from cells (i.e. neurons affected by Alzheimer Disease) (27). Exosomes are small vesicles (30-100 nm in diameter)

derived from the endosomal system that can be released from the cells and represent critical structures for different types of cellular communication (immune responses for instance)(28). Initially it was thought that the fusion of exosomes with lysosomes would serve exclusively for the removal of unnecessary exosomal materials (29), however, since exosome materials can be shuttled to neighboring or even distant cells, secretion of unwanted material to the extracellular environment within exosomes may have either positive or negative effects on surrounding cells. Therefore, also the interplay between exosomes and lysosomes may represent a novel layer of exploration for different pathologies including cancer.

This review focuses on the role of a specific family of highly glycosylated membrane proteins usually found within lysosomal membranes known as lysosomal associated membrane proteins (LAMPs) and their involvement in cancer.

LAMP FAMILY OF LYSOSOMAL PROTEINS

LAMP family is characterized by an evolutionary conserved membrane-proximal LAMP domain, composed by around 200 amino acids and containing several conserved cysteine residues, which allow for the formation of two critical disulfide bonds (30). Other common features in the family are represented by i) a specific proline and two glycine residues in their single transmembrane region (30), ii) the presence of several N-linked glycosylation sites within their luminal domain (31) and iii) a short cytoplasmic tail harboring an endosomal and lysosomal sorting signal (32) (Figure 1).

LAMP family is composed of 5 known members: LAMP1/CD107a, LAMP2/CD107b, LAMP3/DC-LAMP, LAMP4/Macrosialin/CD68 and LAMP5/BAD-LAMP. LAMP1 and LAMP2 are ubiquitously expressed in human tissues and cell lines, whereas LAMP3, CD68 and BAD-LAMP are cell-type specific proteins. LAMPs are involved in a variety of cellular processes including phagocytosis, autophagy, lipid transport and aging (30); moreover, growing evidence suggests an important role for LAMP family members in cancer (Tables 1-5 and Figure 5).

LAMP1 AND LAMP2

LAMP1 and LAMP2 represent the major constituents of the lysosomal membrane, are classified as type I transmembrane proteins, share similar length and 37% amino acid sequence homology (30, 33). Their structure is characterized by a highly glycosylated luminal region forming a glycoprotein layer in the lysosomal lumen, a transmembrane region and a C-terminal short cytosolic domain (Figure 1). LAMP1 has only one transcript, whereas LAMP2 presents three different splicing isoforms: LAMP2A, LAMP2B and LAMP2C (30, 33). LAMP2 isoforms are expressed in a tissue specific manner and can exert opposing functions (34, 35). Specifically, the LAMP-2A isoform is recognized to be responsible for chaperone-mediated autophagy (CMA), a process that targets specific proteins to degradation into the lysosomes via recognition of a definite motif within their amino acids sequence, and its loss is associated with the formation of α-synuclein-positive aggregates in Parkinson's disease (36). The LAMP-2B isoform is not involved in CMA, but mutations in its specific exon (exon 9) have been found in patients bearing a defective fusion process between lysosomes and autophagosomes, thus suggesting a function for this isoform in macroautophagy (37). Conversely, LAMP-2C has been demonstrated to act as an inhibitor of chaperone-mediated autophagy particularly in B cells and to be capable of mediating nucleic acids autophagy by binding to RNA and DNA (38, 39). Many different mutations have been found in LAMP2 gene and are causative of Danon disease, a severe condition characterized by skeletal and cardiac myopathy and cognitive impairment (40-42). Recently, it has been found that specifically the loss of the LAMP-2B isoform could represent the phenotypic leading cause of Danon disease, probably given its putative role in macroautophagy (43). A similar phenotype to Danon disease is recapped in LAMP2 knockout mice, whereas LAMP1 single knockout mice are viable and fertile and double LAMP1 and LAMP2 knockout mice show embryonic lethality, suggesting that these two proteins play key and partially overlapping functions in cellular homeostasis (30). Recently, LAMP2 deficiency has been also associated to pancreatitis, thereby strengthening the importance of a correct lysosomal/autophagic compartment and its associated proteins for cell homeostasis (44).

Growing evidence of a role for lysosomes in different diseases has raised the interest in deciphering the role of LAMP1 and LAMP2 in cancer progression (examples for the roles of LAMP1 and LAMP2 in cancer are presented in Tables 1 and 2 and in Figures 2, 6). LAMP1 and LAMP2 reported roles as pro-invasive and pro-metastatic factors refer to their abnormal localization to the plasma membrane of cancer cells, mainly in metastasizing human melanoma A2058 cells, human colon carcinoma CaCo-2 cells and human fibrosarcoma HT1080 cells (45). There is still no clear explanation on the way LAMP1 and LAMP2 translocate to plasma membrane but, possibly, this could be the result of a plasma membrane damage leading to lysosome fusion and exocytosis as a membrane repair mechanism (46). It has been proposed that Rab3a-dependent complex or the tumor protein D52 could possibly mediate the LAMP1 and LAMP2 trafficking to the plasma membrane (47, 48). It was shown *in vitro* that the translocation of LAMP2 could be driven by an acidic microenvironment, which possibly support the idea of the plasma membrane damage recruiting lysosomes and lysosomal associated membrane proteins to the plasma membrane (49). Specifically, in the early phases of in situ breast carcinoma progression, glycolytic metabolism and the absence of vascularization are generating an acidic microenvironment, which results in an increased expression of LAMP2 on the plasma membrane serving as protective shield (49). In addition to protection, LAMP1 and LAMP2 expression on the plasma membrane provide binding to E-selectin through sialyl-Le^X residues and binding to galectin-3 through poly-N-acetyl-lactosamine (polyLacNAc)-substituted β1,6 branched N-glycans. Thereby, LAMP1 and LAMP2 are promoting both the adhesion of cancer cells to extracellular matrix, basement membrane and endothelium and the migratory potential of cells during metastasis (45, 50). Both LAMP1 and LAMP2 can also be modified by the alpha1,2-fucosyltransferases enzyme FUT1, which works by adding a fucose molecule to N-acetylglucosamine via α1,3-linkage and generates Lewis Y (LeY) antigens. The presence of these modified LeY termini on LAMP1 is increased in breast cancer cells with respect to the normal mammary counterpart and it has been associated with breast cancer cell migration (51, 52). The presence of this modification on both LAMP1 and LAMP2 is able to influence the localization of lysosomes and the autophagic flux, since FUT1 down-regulation has been demonstrated to lead to an accumulation of lysosomes to perinuclear regions and to correlate with increased autophagy and decreased mTORC1 activity (52).

Despite the high expression of both LAMP1 and LAMP2 on the surface of some types of invasive cancer cells, it has been demonstrated that only the surface translocation of LAMP1, but not LAMP2, is correlating with the metastatic potential of melanoma, non-small cell lung cancer (NSCLC) and laryngeal squamous cell carcinoma (LSCC) (50, 53). One well described mechanism responsible for the LAMP1-mediated invasion in melanoma cells is caused by the high expression of polyLacNAc bound to LAMP1 which activates ERK and p38 pathway, thus leading to the secretion of matrix-metallo-protease-9 (MMP-9) and the consequent ECM remodeling (54). In other types of cancer, specifically glioblastoma, pancreatic and ovarian cancer, LAMP1 expression on the cell surface plays a role during early phases of cancer progression rather than in the metastatic process, thus suggesting different LAMP1 functions depending on the cancer type (55-57). In these cases, the exact mechanism for LAMP1 tumor promoting role is still poorly studied, but there are data reporting a regulation of EGF pathway in some serous ovarian malignancies (56). Probably, LAMP1 when expressed on the plasma membrane can shape growth factor signaling, thereby modulating cancer development at various stages.

LAMP1 expression on the cell surface is commonly found also in some types of immune cells, such as natural killer cells (NK cells) and T cells, where is commonly used as a marker for degranulation and active cytotoxicity (Figure 3) (58-63). In particular, in NK cells LAMP1 is necessary for an efficient expression of perforin in lytic granules, and at the same time to protect NK cells from damages during the cytotoxic granules exocytosis (60, 61). LAMP1 expression on cancer cells could possibly recapitulate the role carried out in immune cells, thus protecting cancer cells from lytic granules and the immune mediated destruction. Similarly, both LAMP1 and LAMP2 expression has been associated to the ability of leukocytes to adhere to endothelium and migrate, therefore favoring the migration of cancer cells too (64).

LAMP1 over-expression can also influence cancer progression from its normal localization inside the lysosomal membrane. In particular, increased expression of LAMP1 can influence lysosomal biogenesis and cancer cell viability: its knockdown in acute myeloid leukemia (AML) cells leads to diminished cancer cell viability through lysosome disruption(65). LAMP1 abnormal expression in the lysosomal membrane can also promote drug resistance by increasing lysosomal size and lysosomal exocytosis in rhabdomyosarcoma, soft tissue sarcomas, renal and colorectal cancers. This ultimately leads to drug sequestration into lysosomes and drug release via exocytosis, thereby causing drug resistance (66, 67). An increased lysosomal exocytosis is also responsible for an increased invasiveness of aggressive soft tissue sarcomas (68). However, a reduced expression of LAMP1 and LAMP2 have been reported in ovarian carcinoma cells resistant to cisplatin, suggesting that their role in drug resistance could either be drug specific or cancer cell type specific (69). Tissue and type specificity effect of LAMP1, could also explain some conflicting evidence regarding the tumor suppressing role of LAMP1 reported in pancreatic carcinoma and ovarian carcinoma cells exposed to ascites. Indeed, LAMP1 expression correlates with prolonged survival in pancreatic carcinoma, whereas ascites-mediated up-regulation of LAMP1 expression in ovarian carcinoma cells is responsible for a decreased cancer cell migration (70, 71).

LAMP1 increased expression could be driven by the activation of specific cancer signaling pathways (such as STAT3, ETS1 and p65) or could be a result of a genetic amplification like in chronic lymphocytic leukemia and in a number of p53 null and basal-like breast cancers (ENCODE database (72, 73)). In the latter case, LAMP1 was seen to be over-expressed compared to normal mammary epithelium as a result of gene amplification, but this phenomenon was not correlating with patient survival (72, 73). Differently, a homozygous deletion within LAMP1 gene has been found in some cases of gastric carcinoma, thereby confirming again the opposing roles of LAMP1 in cancer progression (74).

LAMP1 is also commonly found expressed on the membrane of exosomes secreted by different types of tumors (28, 75). The exact role for LAMP1 expression on secreted exosomes is still unknown, however it could be involved in the different effects of exosomes on immune system by either promoting cancer antigens recognition or inducing immune tolerance to cancer cells (75, 76).

LAMP2 has fewer reports on its involvement in cancer progression respect to LAMP1, but similarly to it, some contradictory functions are also reported. LAMP2 may regulate migration of ovarian

clear cell adenocarcinoma possibly through ANXA4 (Annexin A4), whose knockout in OVISE cell line resulted in a reduced expression of LAMP2 and it was associated with a loss of migration and invasion capability (77). LAMP2 is also highly expressed in poorly differentiated human gastric adenocarcinoma, hepatocellular carcinoma, salivary adenoid cystic carcinoma compared to normal tissues and in broncho-alveolar lavage fluid of patients with lung adenocarcinoma, representing one novel molecular marker for these cancer types (78, 79). It may be involved in the pathogenesis of multiple myeloma patients positive for a specific translocation BCL1/JH t(11;14)(q13;q32) and, therefore, used as a prognostic markers or therapeutic target (80).

The specific LAMP2A isoform showed an increased expression in breast tumor tissues and a prognostic value in non-small cell lung cancer; indeed, LAMP2A inhibition or genetic knockdown resulted in the sensitization of tumor cells to doxorubicin and radiation therapy (81-83). Another important role reported for LAMP2A isoform in cancer refers to its involvement in immunogenic cell death, a type of apoptosis that stimulates anti-cancer immune response (84). In particular, LAMP2A isoform can induce the expression of calreticulin and the secretion of ATP upon mitoxantrone and hypericin-based photodynamic therapy, thus leading to immunogenic cell death, thereby suggesting opposing roles for this isoform in cancer (84).

Another reported tumor suppressor role for LAMP2 stands on its ability to induce cell death upon depletion of the VEGF-NRP2 axis in prostate cancer cells. The up-regulation of LAMP2 and WDFY1 resulting from autophagy blockade caused by VEGF-NRP2 axis inhibition leads to increased cell death (85). Similar oncosuppressive effects have been observed in neuroblastoma cells cultured under hyperoxia, which causes up-regulation of LAMP2 and LC3-II, macro-autophagy and ultimately induces apoptosis (86). A protective role of LAMP2 in drug resistance has been reported in lung cancer, where it is directly targeted by miR-487b-5p, a microRNA often found over-expressed in Temozolomide resistant lung cancer cells(87).

LAMP2 is often found expressed on the membrane of exosomes secreted from immune cells but its role is still largely unknown; however, there could be a possible role for both LAMP1 and LAMP2 exosomal expression in shaping immune system response (Figure 3) (28).

LAMP3/DC-LAMP

Lysosomal-associated membrane protein 3 (LAMP3) is a 44 kDa protein and, unlike LAMP1 and LAMP2, which are ubiquitously expressed, LAMP3 is expressed only in specific conditions and tissues. To avoid ambiguity, it is worth noting that LAMP3 gene/protein name can be also wrongly referred to CD63, which, despite being a protein enriched in late endosomal and lysosomal compartment, belongs to the tetraspanin family (88). In this review, we always refer to LAMP3 as the member of the LAMP family.

LAMP3 is also called DC-LAMP, because it was firstly shown to be induced progressively upon maturation of human dendritic cells (DCs), where it transiently co-localizes with MHC class II molecules at the limiting membrane of specific intracellular compartments (i.e. MHC class II compartment, MIIC), and is thus considered as a marker of mature DCs in humans(89).

In the same year of this observation, Ozaki and coworkers independently characterized LAMP3 as a gene specifically expressed in lung tissue, designated as TSC403 transcript(90). Indeed, LAMP3 is also highly expressed in another specific cell-type in mammals, normal and transformed type II pneumocytes (PnIIs)(91), which are pulmonary specialized cells important for the repopulation of lung tissue during normal homeostasis and injury, and responsible for surfactant synthesis, secretion and recycling (92, 93).

The trend of LAMP3 expression in time and space is significantly different between human DCs and type II pneumocytes. Indeed, LAMP3 is transiently expressed in the MIIC compartment (responsible for the exposure of MHC class II/peptide complexes on the plasma membrane) during DCs' maturation and then it accumulates in perinuclear lysosomes without localizing to the plasma membrane (89). Conversely, LAMP3 is constitutively expressed at the limiting membrane of PnII lamellar bodies (responsible for secretion of surfactant proteins, and also containing MHC class II molecules), and low levels of the protein could also be detected at the cell surface membrane in these cells (91). Functional similarity between MIIC in DCs and lamellar bodies in PnIIs suggests a possible role for LAMP3 in the regulation of the exocytosis of these lysosomes, and particularly in MHC class II-restricted antigen presentation, which is a characteristic of both mature DCs and PnIIs (94).

LAMP3 expression is induced by the unfolded protein response (UPR) activated by hypoxia condition (95) and this induction is mediated by the PERK/eIF2α arm of UPR (96). Further, proteasome inhibition induces LAMP3 expression in an ATF4 (a UPR transcription factor)-dependent manner. Increased expression of LAMP3 is able to trigger autophagy, whereas preventing LAMP3 induction enhanced apoptotic cell death, thereby demonstrating that LAMP3 regulation is important for proteasomal degradation and cell survival during proteasome dysfunction (97). Furthermore, a recent meta-analysis of genome-wide association studies in Parkinson disease has identified MCCC1/LAMP3 genetic locus associated with Parkinson disease risk (98, 99)

LAMP3 expression is also driven by IFN-α during dendritic cells maturation(100), and it has been shown to regulate the expression of antiviral genes in cervical cancer (101). LAMP3 expression is also induced in an interferon-dependent way upon influenza A and hepatitis C virus infection and may play a role in the regulation of virus replication and infection at the post-entry stages (102, 103).

Growing evidence has shown that LAMP3 is over-expressed in various human tumors, where it correlates with poor prognosis (LAMP3 functions in cancer are summarized in Table 3 and Figures 4, 6) (104, 105). Some recent studies revealed that LAMP3 might be important in tumor metastasis and resistance to therapies, suggesting LAMP3 as a molecular marker for the prognosis of various cancers (106, 107). Indeed, LAMP3 has been shown to be expressed at higher levels in several primary cancers compared to normal tissues, including cancers of the esophagus, colon, fallopian tube, ovary, uterus breast, and liver (90, 108). Moreover, the region 3q27, where LAMP3 gene is located, is often amplified in various types of cancers, in particular squamous cell carcinomas and penile carcinomas (109).

LAMP3 over-expression into uterine cervical cancer cell lines is able to promote metastasis *in vitro* and *in vivo* (106), and its expression has been associated with lymph node metastasis (104), (110) and increased migration in breast cancer cells (95), suggesting a role for LAMP3 in the metastatic process (106). The mechanism employed by cancer cells to favor metastasis has not yet been completely elucidated; however, similarly to LAMP1 and LAMP2, its exposure on the plasma membrane could allow cancer cells to interact with endothelial cells. Nevertheless, LAMP3 expression on the cellular plasma membrane could be detected only in specific circumstances on cancer cells, such as upon Influenza A virus infections in HeLa cells (102), whereas it could not be detected on the plasma membrane of other cancer cell lines, as MDA-MB-231 (95). Another possible mechanism by which LAMP3 expression can increase the metastatic potential of cancer cells is through the modulation of the autophagic flux, which is known to play key roles in cancer metastasis (111). Particularly, the cytoplasmic tail of LAMP3 seems to be required for the fusion of the autophagosome with the lysosome (i.e. maturation step), a process inhibited in LAMP3 knockdown cancer cells (112).

LAMP3 expression was also correlated with poor overall survival in head and neck squamous cell carcinomas (107, 108), uterine cervical cancer (106), gastric and colorectal cancers (105), whereas its expression levels, together with other pneumocyte-specific genes expression, has been associated with increased survival in the adenocarcinoma subgroup of non-small cell lung cancer (NSCLC) cohorts (113). These conflicting data could be due to the high levels of LAMP3 expression in lung normal tissue, where LAMP3 could play a specific role that could be compromised during cancer development.

LAMP3 has also been implicated in drug resistance; in particular, up-regulation of LAMP3 has been associated with resistance to chemotherapy and radiotherapy in breast cancer (112, 114), and its down-regulation could increase cisplatin sensitivity in prostate cancer cells (115). LAMP3 expression could decrease the sensitivity of cancer cells to chemotherapy by modulating autophagy, whose ability to influence drug resistance has been extensively studied (116). LAMP3-mediated radiotherapy resistance was conversely attributed to its ability to positively regulate the DNA damage repair signaling response (114).

Furthermore, Bisio A. and colleagues observed the synergistic induction of LAMP3, among a subset of genes, upon combined treatment with the chemotherapeutic drug Doxorubicin and the inflammatory cytokine TNF-α in breast cancer cells, suggesting a possible involvement of LAMP3 in cancer related inflammation (117).

Given that LAMP3 is highly expressed in DCs, it is essential to distinguish between its contribution to cancer when expressed by cancer cells or by dendritic cells infiltrating the tumor. For example, it has been observed that infiltration of LAMP3$^+$ DCs in the sentinel lymph nodes of melanoma patients was correlated with the absence of metastasis in downstream lymph nodes (118).

CD68/Macrosialin/LAMP4

CD68, the human homologue to murine Macrosialin, is a heavily glycosylated transmembrane glycoprotein mainly localized in the endosomal/lysosomal compartment of macrophages showing a distinctive structure corresponding to the LAMP signature, with highest homology to LAMP3 (119, 120). Similarly to LAMP3, CD68 contains only a single LAMP-like domain and a mucin-like domain (Figure 1) (119); but, unlike LAMP3, which is mainly located within lysosomes, CD68 is rather found in endosomes and can rapidly shuttle to the plasma membrane (121).

CD68 has been extensively used as a histological marker of macrophage lineage cells, since it is preferentially expressed by resident macrophages of multiple tissues, including macroglia in the brain, Kupffer cells in the liver and bone marrow macrophages (122-124). Although initially classified as a group D scavenger receptor due to its ability to bind oxidized low density lipoproteins (OxLDL) (125), CD68 silencing and knock-out experiments failed to affect OxLDL binding and uptake to macrophages (126, 127). Beyond the use of CD68 as histological marker to identify macrophages, the apparent specificity of the expression of CD68 has proposed the use of CD68 transcriptional regulatory sequences to specifically drive *in vitro* and *in vivo* transgene expression, as well as for gene therapy approaches (89, 128, 129). However, recent studies show that a high expression of CD68 is not limited to macrophage cell lineage, but is observed also in other hematopoietic and non-hematopoietic cells (130, 131); therefore, CD68 should be considered

a non-specific marker of macrophages.

Though it is unknown a role for CD68 in antigen processing, Song and colleagues observed that $CD68^{-/-}$ mononuclear phagocytes showed enhanced capacity of antigen presentation to $CD4^+$ T cells, proposing that CD68 may have negative regulatory functions in MHC class II trafficking or antigen uptake and loading (127). Interestingly, CD68 is expressed also in immature dendritic cells, and its expression progressively disappears during maturation at the same time as LAMP3 accumulates in the lysosomes (89) suggesting a putative competing role in the antigen presentation process.

Immunohistochemical staining of bone specimens has identified CD68 expression in osteoclasts (124), which are multi-nucleated cells responsible for bone reabsorption during normal bone remodeling or pathological conditions (132), and genetic ablation of CD68 resulted in morphological alteration and functional defects in osteoclasts and increased bone in mice (133).

Importantly, infiltration of CD68-positive cells is a marker for both inflammation and tumor progression (presented in Table 4 and Figures 5, 6) (134, 135). A population-based cohort study of malignant uveal melanoma observed diffuse infiltration of CD68-positive macrophages in 83% of analyzed tumors and the number of macrophages has been associated with largest basal tumor diameter (LBD), presence of epithelioid cells and high microvessel density (MVD) in areas of high vascularization (135), which represent independent high-risk indicators for metastasis in uveal melanoma (135, 136 1996).

Tumor-associated macrophages (TAMs), for which CD68 represents one of the most recognized marker (137), are one of the most abundant population of normal cells in the tumor microenvironment and there is accumulating evidence for TAMs' pivotal role in driving pro-tumorigenic phenotype. Indeed, density of $CD68^+$ TAMs is increased in poorly differentiated thyroid cancers (PDTCs), and high density of these cells correlates with invasion and decreased cancer-related survival in these advanced thyroid cancers (138). Furthermore, increased expression of $CD68^+$ macrophages in the tumor stroma of triple-negative breast cancer (TNBC) patients after surgery and of patients with classic Hodgkin's lymphoma correlates with poor prognosis (139, 140). In contrast, high $CD68^+$ macrophages density correlates with increased overall survival in non-small cell lung cancer and esophageal squamous cell carcinoma (141, 142). However, this discrepancy in the predictive power of CD68 for tumor prognosis could be due to several factors, including technical variability, specificity of the antibodies, and difference in the case series (143). We have reported here few evidence of the role of $CD68^+$ macrophages in tumorigenic processes and we refer to other recent reviews for a comprehensive description of the role of TAMs in cancer (144-147).

Importantly, CD68 association to cancer is not only related to its expression in TAMs, but also in tumor cells (131). For example, CD68 was found to be highly expressed in human gliomas by both microglia and tumor cells; its expression was associated with malignancy in these tumors, and was suggested as prognostic marker of reduced survival in human gliomas (148). This observation is in agreement with the fact that malignant tumor cells often express immune cells-markers to evade the immune system during the metastatic process, and, most frequently, it has been observed the expression of macrophage antigens, such as CD68, CD47, CD163 and DAP12 (149-151). The mechanism explaining the expression of macrophage antigens by tumor cells is still debated, and it seems to be mediated by genetic exchange either directed by direct macrophage-cancer cell fusion (152), or by exosome-mediated transfer (149). CD68 was found to be expressed in mouse macrophages-derived exosomes (153), thereby supporting the hypothesis that exosomes can mediate a genetic exchange between macrophages and cancer cells and, ultimately, it could also explain the CD68 expression in cancer cells.

Although CD68 is widely used as diagnostic and prognostic marker for several malignancies, the role of this protein in cancer is still to be explained and further studies investigating its mechanism of actions are needed.

BAD-LAMP/LAMP5

The latest characterized LAMP protein is the *C. elegans* ortholog of UNC-46, BAD-LAMP (Brain and Dendritic Cell associated LAMP-like molecule), also known as LAMP5 or C20orf103. Unlike other LAMP family members, BAD-LAMP does not localize to late endosomes or lysosomes and, similarly to LAMP3 and CD68, its expression is limited to specific tissues. BAD-LAMP is a 280 aa protein with a transmembrane domain and a cytoplasmic tail containing a YKHM sequence, corresponding to a classic YXXΦ internalization and endosomal targeting signal. It also contains several N-glycosylation sites, as well as four cysteine residues separated by a fixed number of amino acids, allowing for the formation of the disulfide bonds required for the "LAMP-fold" (Figure 1) (32).

David and co-workers first identified BAD-LAMP as a new LAMP family member in mice, where it is mainly expressed in specific subtypes of cortical projecting neurons. In these cells, BAD-LAMP expression considerably increased after birth, suggesting its involvement in the late steps of neuronal differentiation. BAD-LAMP can be endocytosed and directed to uncharacterized vesicles clustered in the growth cone of developing axons or in defined dendritic domains, identified as a specific class of early neuronal endosomes(32). In *C. elegans*, BAD-LAMP ortholog UNC-46 mutations cause defects in most GABA-mediated behaviors, and it has been proposed as a sorting factor able to address the GABA transporter (UNC-47) to the synaptic vesicles(154). In humans, like in mice, BAD-LAMP is expressed at higher levels in the brain, but, among blood cells, it is also specifically expressed in the type I IFN-producing primary plasmacytoid dendritic cells (pDCs) and transformed pDCs (blastic plasmacytoid dendritic cell neoplasms or BPDCNs), for which it represents a relevant biomarker (155). In these cells, BAD-LAMP is principally localized in the ER-Golgi intermediate compartment (ERGIC) and its expression is lost upon pDC activation by Toll-like Receptor (TLR) ligands (155).

A second observation for an association between this poorly studied protein and cancer comes from the analysis of the expression of a set of genes, including BAD-LAMP, which has been shown to be correlated with a poor prognosis in stage II gastric cancer patients treated with chemo-radiotherapy (Table 5 and Figure 6) (156); however, it is not clear whether BAD-LAMP expression observed in the analyzed tissues is determined by pDCs infiltration within the tumor or by a higher expression of the protein in cancer cells. Further studies are required to establish the putative role of BAD-LAMP in cancer.

CONCLUSIONS

A correct functioning of the lysosomal compartment represents a guarantor for an efficient cell homeostasis and a critical protection against various diseases, among them cancer. Differential expression of proteins associated with the lysosomal membrane, categorized as LAMP family members, can substantially influence various processes of cancer progression. This review inspected the various LAMP proteins and their reported roles in oncogenic processes, with conflicting evidence for some of the members.

LAMP1 represents the most studied member of the family and together with LAMP2 is involved in various oncogenic processes, such as local cancer progression, ECM adhesion and remodeling, migration, drug resistance and metastasis. The strong potential of LAMP1 in cancer therapy encouraged the Sanofi S.A. pharmaceutical company to patent anti-LAMP1 antibodies and immunoconjugates for detection and treatment (patent number: WO2014102299). Furthermore, LAMP1 and LAMP2 expression on cancer cell plasma membrane renders them optimal targets for immunotherapy approaches. Nevertheless, LAMP1 has important reported roles in immune system, thus when planning its targeting by immunotherapies, its crucial to bear in mind the importance of specifically target LAMP1 and LAMP2 expressed on cancer cells. A decreased expression of LAMP1 in NK cells would reduce their perforin-mediated cytotoxicity, which represents the most efficacious NK-mediated cell death (157), thereby potently decreasing the anti-cancer immune responses. Furthermore, a better understanding of LAMP1 role in cancer-derived exosomes and its effects on immune system is of paramount importance, also for future applications of exosomes in cancer immunotherapy.

The other members of LAMP family are not extensively studied yet, but there is growing evidence supporting their pro-tumorigenic potential. For instance, LAMP3 and CD68, which are activated by various stimuli often present during cancer development and therapy, and are closely connected with inflammation, represent additional promising targets for cancer therapy. The mechanisms by which LAMP3 and CD68 expression can affect tumor progression is still to be elucidated, however, a possible explanation could be inferred from its role in the trafficking of MHC class II/peptide complexes (158), which is critical for antitumor immune response (159).

Interestingly, LAMP3, CD68 and BAD-LAMP are highly expressed in immune cells and have shown to be associated with various types of tumors, either when expressed on immune or cancer cells. Therefore, it would be intriguing to investigate their role at the interplay between cancer and the immune system and to elucidate whether they could play a direct role in the immune response to cancer.

In conclusion, a better knowledge of LAMP family and lysosomal role in cancer progression could represent a fruitful approach in cancer research.

ACKNOWLEDGEMENT

We thank Prof. Alberto Inga, Dott. Alessandra Bisio, Dott. Sara Zaccara and Francesca Precazzini for helpful discussions. This work was partially supported by CIBIO Start up funds, University of Trento (Y.C.).

FIGURE LEGENDS

Figure 1. Structural organization of LAMP family members. Sequential boxes stand for domains, small flags indicates glycosylation residues and protein length is also provided for each depicted member. SP: signal peptide; LAMP: LAMP domain; H: hinge region; TM: transmembrane domain; C: cytoplasmic domain.

Figure 2. LAMP1-LAMP2 subcellular localization and thier roles in cancer. LAMP1 and LAMP2 can influence cancer biology in different ways depending on their localization: on the plasma membrane they promote adhesion to endothelium and extracellular membrane (ECM), migration and metastasis; whereas on the lysosomal membrane they promote drug resistance by increasing lysosomal drug sequestration and lysosomal exocytosis. LAMP1 expression on the plasma membrane can also play a role in ECM remodeling and invasion, whereas LAMP2 can act as a protective shield. LAMP1 is often found expressed in tumor-derived exosomes but its role in exosome biology it is still unknown.

Figure 3. LAMP1-LAMP2 subcellular localization and their roles in immune cells. LAMP1 and LAMP2 in immune cells are acting as activation markers when expressed on the plasma membrane and they can promote adhesion to endothelium and migration. LAMP1 specifically has a crucial role in the degranulation process, whereas LAMP2 is expressed in immune cancer cells-derived exosomes.

Figure 4. LAMP3 subcellular localization and its roles in cancer and immune cells. LAMP3 can localize to different cell compartments and therefore exert different functions. LAMP3 can be bound to the lysosomal membrane or to the plasma membrane and regulate migration, metastasis, and drug resistance in cancer cells. Moreover, its cytoplasmic tail plays a role in the process of fusion of the lysosome with the autophagosome, thereby modulating the autophagic process, which can also mediate its pro-tumorigenic functions. LAMP3 is also a marker for mature dendritic cells, in which it is progressively expressed during maturation. During this process LAMP3 co-localizes with MHC class II molecules (MHCII) within MHC class II compartment (MIIC), suggesting a possible role for LAMP3 in antigen presentation process.

Figure 5. CD68 subcellular localization and its roles in cancer and immune cells. CD68 represents a marker for tumor-associated macrophages, where it can rapidly shuttle between the endosomal compartment and the plasma membrane. Recent observations suggest that CD68 may also have a negative role in the antigen presentation process. CD68 has recently been found to be also expressed by some cancer cells, where it is associated with increased malignancy, possibly caused by immune evasion mechanisms. Expression of this immune-cell marker by cancer cells could be explained by genetic exchange between macrophages and cancer cells, which is supported by the recent detection of CD68 in macrophages-derived exosomes.

Figure 6. LAMP family roles in cancer progression. All the LAMP proteins are involved in cancer progression; LAMP1, LAMP2 and LAMP3 are also implicated in migration and stress or drug resistance. LAMP1 and LAMP2 also promote ExtraCellular Matrix (ECM) adhesion or remodeling whereas LAMP1 and LAMP3 can induce metastasis formation. CD68 is often expressed on Tumor Associated Macrophages (TAM).

REFERENCES

1. Appelqvist H, Waster P, Kagedal K, Ollinger K. The lysosome: from waste bag to potential therapeutic target. Journal of molecular cell biology. 2013;5(4):214-26.
2. Schwake M, Schroder B, Saftig P. Lysosomal membrane proteins and their central role in physiology. Traffic. 2013;14(7):739-48.
3. Schroder BA, Wrocklage C, Hasilik A, Saftig P. The proteome of lysosomes. Proteomics. 2010;10(22):4053-76.
4. Piao S, Amaravadi RK. Targeting the lysosome in cancer. Annals of the New York Academy of Sciences. 2016;1371(1):45-54.
5. de Duve C. Lysosomes, a new group of cytoplasmic particles. In: Hayashi T, editor Subcellular Particles. 1959;New York: The Ronald Press Co:128-59.
6. Turk B, Turk V. Lysosomes as "suicide bags" in cell death: myth or reality? J Biol Chem. 2009;284(33):21783-7.
7. Lindqvist LM, Simon AK, Baehrecke EH. Current questions and possible controversies in autophagy. Cell death discovery. 2015;1.
8. Hoyer-Hansen M, Jaattela M. Autophagy: an emerging target for cancer therapy. Autophagy. 2008;4(5):574-80.
9. Li W, Yuan X, Nordgren G, Dalen H, Dubowchik GM, Firestone RA, et al. Induction of cell death by the lysosomotropic detergent MSDH. FEBS Lett. 2000;470(1):35-9.
10. Bursch W. The autophagosomal-lysosomal compartment in programmed cell death. Cell Death Differ. 2001;8(6):569-81.
11. Guicciardi ME, Leist M, Gores GJ. Lysosomes in cell death. Oncogene. 2004;23(16):2881-90.
12. Leist M, Jaattela M. Four deaths and a funeral: from caspases to alternative mechanisms. Nat Rev Mol Cell Biol. 2001;2(8):589-98.
13. Leist M, Jaattela M. Triggering of apoptosis by cathepsins. Cell Death Differ. 2001;8(4):324-6.
14. Sancak Y, Bar-Peled L, Zoncu R, Markhard AL, Nada S, Sabatini DM. Ragulator-Rag complex targets mTORC1 to the lysosomal surface and is necessary for its activation by amino acids. Cell. 2010;141(2):290-303.
15. Laplante M, Sabatini DM. mTOR Signaling in Growth Control and Disease. Cell. 2012;149(2):274-93.
16. Guertin DA, Sabatini DM. Defining the role of mTOR in cancer. Cancer Cell. 2007;12(1):9-22.
17. Settembre C, Zoncu R, Medina DL, Vetrini F, Erdin S, Huynh T, et al. A lysosome-to-nucleus signalling mechanism senses and regulates the lysosome via mTOR and TFEB. EMBO J. 2012;31(5):1095-108.
18. Gocheva V, Zeng W, Ke D, Klimstra D, Reinheckel T, Peters C, et al. Distinct roles for cysteine cathepsin genes in multistage tumorigenesis. Genes Dev. 2006;20(5):543-56.
19. Koblinski JE, Ahram M, Sloane BF. Unraveling the role of proteases in cancer. Clinica chimica acta; international journal of clinical chemistry. 2000;291(2):113-35.
20. Mohamed MM, Sloane BF. Cysteine cathepsins: multifunctional enzymes in cancer. Nat Rev Cancer. 2006;6(10):764-75.
21. Vasiljeva O, Papazoglou A, Kruger A, Brodoefel H, Korovin M, Deussing J, et al. Tumor cell-derived and macrophage-derived cathepsin B promotes progression and lung metastasis of mammary cancer. Cancer Res. 2006;66(10):5242-50.
22. Sevenich L, Werner F, Gajda M, Schurigt U, Sieber C, Muller S, et al. Transgenic expression of human cathepsin B promotes progression and metastasis of polyoma-middle-T-induced breast cancer in mice. Oncogene. 2011;30(1):54-64.
23. Bengsch F, Buck A, Gunther SC, Seiz JR, Tacke M, Pfeifer D, et al. Cell type-dependent pathogenic functions of overexpressed human cathepsin B in murine breast cancer progression. Oncogene. 2014;33(36):4474-84.
24. Demchik LL, Sameni M, Nelson K, Mikkelsen T, Sloane BF. Cathepsin B and glioma invasion. International journal of developmental neuroscience : the official journal of the International Society for Developmental Neuroscience. 1999;17(5-6):483-94.
25. Xing W, Archer TK. Upstream stimulatory factors mediate estrogen receptor activation of the cathepsin D promoter. Molecular endocrinology. 1998;12(9):1310-21.
26. Tu C, Ortega-Cava CF, Chen G, Fernandes ND, Cavallo-Medved D, Sloane BF, et al. Lysosomal cathepsin B participates in the podosome-mediated extracellular matrix degradation and invasion via secreted lysosomes in v-Src fibroblasts. Cancer Res. 2008;68(22):9147-56.
27. Goetzl EJ, Boxer A, Schwartz JB, Abner EL, Petersen RC, Miller BL, et al. Altered lysosomal proteins in neural-derived plasma exosomes in preclinical Alzheimer disease. Neurology. 2015;85(1):40-7.
28. Thery C, Zitvogel L, Amigorena S. Exosomes: composition, biogenesis and function. Nature reviews Immunology. 2002;2(8):569-79.
29. Urbanelli L, Magini A, Buratta S, Brozzi A, Sagini K, Polchi A, et al. Signaling pathways in exosomes biogenesis, secretion and fate. Genes. 2013;4(2):152-70.
30. Wilke S, Krausze J, Bussow K. Crystal structure of the conserved domain of the DC lysosomal associated membrane protein: implications for the lysosomal glycocalyx. BMC biology. 2012;10:62.
31. Fukuda M. Lysosomal membrane glycoproteins. Structure, biosynthesis, and intracellular trafficking. J Biol Chem. 1991;266(32):21327-30.
32. David A, Tiveron MC, Defays A, Beclin C, Camosseto V, Gatti E, et al. BAD-LAMP defines a subset of early endocytic organelles in subpopulations of cortical projection neurons. J Cell Sci. 2007;120(Pt 2):353-65.
33. Eskelinen EL. Roles of LAMP-1 and LAMP-2 in lysosome biogenesis and autophagy. Molecular aspects of medicine. 2006;27(5-6):495-502.
34. Konecki DS, Foetisch K, Zimmer KP, Schlotter M, Lichter-Konecki U. An alternatively spliced form of the human lysosome-associated membrane protein-2 gene is expressed in a tissue-specific manner. Biochem Biophys Res Commun. 1995;215(2):757-67.
35. Lichter-Konecki U, Moter SE, Krawisz BR, Schlotter M, Hipke C, Konecki DS. Expression patterns of murine lysosome-associated membrane protein 2 (Lamp-2) transcripts during morphogenesis. Differentiation; research in biological diversity. 1999;65(1):43-58.
36. Murphy KE, Gysbers AM, Abbott SK, Spiro AS, Furuta A, Cooper A, et al. Lysosomal-associated membrane protein 2 isoforms are differentially affected in early Parkinson's disease. Movement disorders : official journal of the Movement Disorder Society. 2015;30(12):1639-47.
37. Bandyopadhyay U, Kaushik S, Varticovski L, Cuervo AM. The chaperone-mediated autophagy receptor organizes in dynamic protein complexes at the lysosomal membrane. Mol Cell Biol. 2008;28(18):5747-63.
38. Fujiwara Y, Hase K, Wada K, Kabuta T. An RNautophagy/DNautophagy receptor, LAMP2C, possesses an arginine-rich motif that mediates RNA/DNA-binding. Biochem Biophys Res Commun. 2015;460(2):281-6.

39. Perez L, McLetchie S, Gardiner GJ, Deffit SN, Zhou D, Blum JS. LAMP-2C Inhibits MHC Class II Presentation of Cytoplasmic Antigens by Disrupting Chaperone-Mediated Autophagy. J Immunol. 2016;196(6):2457-65.
40. Bottillo I, Giordano C, Cerbelli B, D'Angelantonio D, Lipari M, Polidori T, et al. A novel LAMP2 mutation associated with severe cardiac hypertrophy and microvascular remodeling in a female with Danon disease: a case report and literature review. Cardiovascular pathology : the official journal of the Society for Cardiovascular Pathology. 2016;25(5):423-31.
41. Csanyi B, Popoiu A, Hategan L, Hegedus Z, Nagy V, Racz K, et al. Identification of Two Novel LAMP2 Gene Mutations in Danon Disease. The Canadian journal of cardiology. 2016.
42. Fu L, Luo S, Cai S, Hong W, Guo Y, Wu J, et al. Identification of LAMP2 Mutations in Early-Onset Danon Disease With Hypertrophic Cardiomyopathy by Targeted Next-Generation Sequencing. The American journal of cardiology. 2016;118(6):888-94.
43. Rowland TJ, Sweet ME, Mestroni L, Taylor MR. Danon disease - dysregulation of autophagy in a multisystem disorder with cardiomyopathy. J Cell Sci. 2016;129(11):2135-43.
44. Mareninova OA, Sendler M, Malla SR, Yakubov I, French SW, Tokhtaeva E, et al. Lysosome associated membrane proteins maintain pancreatic acinar cell homeostasis: LAMP-2 deficient mice develop pancreatitis. Cellular and molecular gastroenterology and hepatology. 2015;1(6):678-94.
45. Sarafian V, Jadot M, Foidart JM, Letesson JJ, Van den Brule F, Castronovo V, et al. Expression of Lamp-1 and Lamp-2 and their interactions with galectin-3 in human tumor cells. Int J Cancer. 1998;75(1):105-11.
46. Corrotte M, Castro-Gomes T, Koushik AB, Andrews NW. Approaches for plasma membrane wounding and assessment of lysosome-mediated repair responses. Methods in cell biology. 2015;126:139-58.
47. Encarnacao M, Espada L, Escrevente C, Mateus D, Ramalho J, Michelet X, et al. A Rab3a-dependent complex essential for lysosome positioning and plasma membrane repair. J Cell Biol. 2016;213(6):631-40.
48. Thomas DD, Martin CL, Weng N, Byrne JA, Groblewski GE. Tumor protein D52 expression and Ca2+-dependent phosphorylation modulates lysosomal membrane protein trafficking to the plasma membrane. American journal of physiology Cell physiology. 2010;298(3):C725-39.
49. Damaghi M, Tafreshi NK, Lloyd MC, Sprung R, Estrella V, Wojtkowiak JW, et al. Chronic acidosis in the tumour microenvironment selects for overexpression of LAMP2 in the plasma membrane. Nat Commun. 2015;6:8752.
50. Agarwal AK, Srinivasan N, Godbole R, More SK, Budnar S, Gude RP, et al. Role of tumor cell surface lysosome-associated membrane protein-1 (LAMP1) and its associated carbohydrates in lung metastasis. Journal of cancer research and clinical oncology. 2015;141(9):1563-74.
51. Garrigues J, Anderson J, Hellstrom KE, Hellstrom I. Anti-tumor antibody BR96 blocks cell migration and binds to a lysosomal membrane glycoprotein on cell surface microspikes and ruffled membranes. J Cell Biol. 1994;125(1):129-42.
52. Tan KP, Ho MY, Cho HC, Yu J, Hung JT, Yu AL. Fucosylation of LAMP-1 and LAMP-2 by FUT1 correlates with lysosomal positioning and autophagic flux of breast cancer cells. Cell Death Dis. 2016;7(8):e2347.
53. Krishnan V, Bane SM, Kawle PD, Naresh KN, Kalraiya RD. Altered melanoma cell surface glycosylation mediates organ specific adhesion and metastasis via lectin receptors on the lung vascular endothelium. Clinical & experimental metastasis. 2005;22(1):11-24.
54. Dange MC, Agarwal AK, Kalraiya RD. Extracellular galectin-3 induces MMP9 expression by activating p38 MAPK pathway via lysosome-associated membrane protein-1 (LAMP1). Molecular and cellular biochemistry. 2015;404(1-2):79-86.
55. Jensen SS, Aaberg-Jessen C, Christensen KG, Kristensen B. Expression of the lysosomal-associated membrane protein-1 (LAMP-1) in astrocytomas. International journal of clinical and experimental pathology. 2013;6(7):1294-305.
56. Marzinke MA, Choi CH, Chen L, Shih Ie M, Chan DW, Zhang H. Proteomic analysis of temporally stimulated ovarian cancer cells for biomarker discovery. Molecular & cellular proteomics : MCP. 2013;12(2):356-68.
57. Tian Y, Almaraz RT, Choi CH, Li QK, Saeui C, Li D, et al. Identification of sialylated glycoproteins from metabolically oligosaccharide engineered pancreatic cells. Clinical proteomics. 2015;12(1):11.
58. Valor L, Teijeiro R, Aristimuno C, Faure F, Alonso B, de Andres C, et al. Estradiol-dependent perforin expression by human regulatory T-cells. European journal of clinical investigation. 2011;41(4):357-64.
59. Alitalo K, Carmeliet P. Molecular mechanisms of lymphangiogenesis in health and disease. Cancer Cell. 2002;1(3):219-27.
60. Cohnen A, Chiang SC, Stojanovic A, Schmidt H, Claus M, Saftig P, et al. Surface CD107a/LAMP-1 protects natural killer cells from degranulation-associated damage. Blood. 2013;122(8):1411-8.
61. Krzewski K, Gil-Krzewska A, Nguyen V, Peruzzi G, Coligan JE. LAMP1/CD107a is required for efficient perforin delivery to lytic granules and NK-cell cytotoxicity. Blood. 2013;121(23):4672-83.
62. Naito T, Baba T, Takeda K, Sasaki S, Nakamoto Y, Mukaida N. High-dose cyclophosphamide induces specific tumor immunity with concomitant recruitment of LAMP1/CD107a-expressing CD4-positive T cells into tumor sites. Cancer Lett. 2015;366(1):93-9.
63. Hromadnikova I, Li S, Kotlabova K, Dickinson AM. Influence of In Vitro IL-2 or IL-15 Alone or in Combination with Hsp 70 Derived 14-Mer Peptide (TKD) on the Expression of NK Cell Activatory and Inhibitory Receptors on Peripheral Blood T Cells, B Cells and NKT Cells. PLoS One. 2016;11(3):e0151535.
64. Kannan K, Stewart RM, Bounds W, Carlsson SR, Fukuda M, Betzing KW, et al. Lysosome-associated membrane proteins h-LAMP1 (CD107a) and h-LAMP2 (CD107b) are activation-dependent cell surface glycoproteins in human peripheral blood mononuclear cells which mediate cell adhesion to vascular endothelium. Cellular immunology. 1996;171(1):10-9.
65. Sukhai MA, Prabha S, Hurren R, Rutledge AC, Lee AY, Sriskanthadevan S, et al. Lysosomal disruption preferentially targets acute myeloid leukemia cells and progenitors. J Clin Invest. 2013;123(1):315-28.
66. Williams M, Catchpoole D. Sequestration of AS-DACA into acidic compartments of the membrane trafficking system as a mechanism of drug resistance in rhabdomyosarcoma. International journal of molecular sciences. 2013;14(7):13042-62.
67. Gotink KJ, Rovithi M, de Haas RR, Honeywell RJ, Dekker H, Poel D, et al. Cross-resistance to clinically used tyrosine kinase inhibitors sunitinib, sorafenib and pazopanib. Cellular oncology. 2015;38(2):119-29.
68. Machado E, White-Gilbertson S, van de Vlekkert D, Janke L, Moshiach S, Campos Y, et al. Regulated lysosomal exocytosis mediates cancer progression. Science advances. 2015;1(11):e1500603.
69. Safaei R, Larson BJ, Cheng TC, Gibson MA, Otani S, Naerdemann W, et al. Abnormal lysosomal trafficking and enhanced exosomal export of cisplatin in drug-resistant human ovarian carcinoma cells. Mol Cancer Ther. 2005;4(10):1595-604.
70. Kunzli BM, Berberat PO, Zhu ZW, Martignoni M, Kleeff J, Tempia-Caliera AA, et al. Influences of the lysosomal associated membrane proteins (Lamp-1, Lamp-2) and Mac-2 binding protein (Mac-2-BP) on the prognosis of pancreatic carcinoma. Cancer. 2002;94(1):228-39.
71. Meunier L, Puiffe ML, Le Page C, Filali-Mouhim A, Chevrette M, Tonin PN, et al. Effect of ovarian cancer ascites on cell migration and gene expression in an epithelial ovarian cancer in vitro model. Translational oncology. 2010;3(4):230-8.
72. Abba MC, Fabris VT, Hu Y, Kittrell FS, Cai WW, Donehower LA, et al. Identification of novel amplification gene targets in mouse and human breast cancer at a syntenic cluster mapping to mouse ch8A1 and human ch13q34. Cancer Res. 2007;67(9):4104-12.
73. Sargent R, Jones D, Abruzzo LV, Yao H, Bonderover J, Cisneros M, et al. Customized oligonucleotide array-based comparative genomic hybridization as a clinical assay for genomic profiling of chronic lymphocytic leukemia. The Journal of molecular diagnostics : JMD. 2009;11(1):25-34.
74. Kang JU, Koo SH, Kwon KC, Park JW. AMY2A: a possible tumor-suppressor gene of 1p21.1 loss in gastric carcinoma. Int J Oncol. 2010;36(6):1429-35.
75. Wolfers J, Lozier A, Raposo G, Regnault A, Thery C, Masurier C, et al. Tumor-derived exosomes are a source of shared tumor rejection antigens for CTL cross-priming. Nat Med. 2001;7(3):297-303.
76. Li Y, An J, Huang S, He J, Zhang J. Esophageal cancer-derived microvesicles induce regulatory B cells. Cell biochemistry and function. 2015;33(5):308-13.
77. Mogami T, Yokota N, Asai-Sato M, Yamada R, Koizume S, Sakuma Y, et al. Annexin A4 is involved in proliferation, chemo-resistance and migration and invasion in ovarian clear cell adenocarcinoma cells. PLoS One. 2013;8(11):e80359.
78. Wei SH, Li W, Liu Y, Gao DK, Pan J, Gu CW, et al. Disturbance of autophagy-lysosome signaling molecule expression in human gastric adenocarcinoma. Oncol Lett. 2014;7(3):635-40.
79. Li QK, Shah P, Li Y, Aiyetan PO, Chen J, Yung R, et al. Glycoproteomic analysis of bronchoalveolar lavage (BAL) fluid identifies tumor-associated glycoproteins from lung adenocarcinoma. Journal of proteome research. 2013;12(8):3689-96.
80. Ni IB, Ching NC, Meng CK, Zakaria Z. Translocation t(11;14) (q13;q32) and genomic imbalances in multi-ethnic multiple myeloma patients: a Malaysian study. Hematology reports. 2012;4(3):e19.
81. Saha T. LAMP2A overexpression in breast tumors promotes cancer cell survival via chaperone-mediated autophagy. Autophagy. 2012;8(11):1643-56.
82. Kon M, Kiffin R, Koga H, Chapochnick J, Macian F, Varticovski L, et al. Chaperone-mediated autophagy is required for tumor growth. Science translational medicine. 2011;3(109):109ra17.
83. Koukourakis MI, Kalamida D, Mitrakas A, Pouliliou S, Kalamida S, Sivridis E, et al. Intensified autophagy compromises the efficacy of radiotherapy against prostate cancer. Biochem Biophys Res Commun. 2015;461(2):268-74.
84. Garg AD, Dudek AM, Agostinis P. Calreticulin surface exposure is abrogated in cells lacking, chaperone-mediated autophagy-essential gene, LAMP2A. Cell Death Dis. 2013;4:e826.
85. Stanton MJ, Dutta S, Zhang H, Polavaram NS, Leontovich AA, Honscheid P, et al. Autophagy control by the VEGF-C/NRP-2 axis in cancer and its implication for treatment resistance. Cancer Res. 2013;73(1):160-71.
86. Zheng L, Terman A, Hallbeck M, Dehvari N, Cowburn RF, Benedikz E, et al. Macroautophagy-generated increase of lysosomal amyloid beta-protein mediates oxidant-induced apoptosis of cultured neuroblastoma cells. Autophagy. 2011;7(12):1528-45.
87. Bao L, Lv L, Feng J, Chen Y, Wang X, Han S, et al. miR-487b-5p Regulates Temozolomide Resistance of Lung Cancer Cells Through LAMP2-Medicated Autophagy. DNA and cell biology. 2016;35(8):385-92.
88. Pols MS, Klumperman J. Trafficking and function of the tetraspanin CD63. Experimental cell research. 2009;315(9):1584-92.
89. de Saint-Vis B, Vincent J, Vandenabeele S, Vanbervliet B, Pin JJ, Ait-Yahia S, et al. A novel lysosome-associated membrane glycoprotein, DC-LAMP, induced upon DC maturation, is transiently expressed in MHC class II compartment. Immunity. 1998;9(3):325-36.
90. Ozaki K, Nagata M, Suzuki M, Fujiwara T, Ueda K, Miyoshi Y, et al. Isolation and characterization of a novel human lung-specific gene homologous to lysosomal membrane glycoproteins 1 and 2: significantly increased expression in cancers of various tissues. Cancer Res. 1998;58(16):3499-503.
91. Salaun B, de Saint-Vis B, Pacheco N, Pacheco Y, Riesler A, Isaac S, et al. CD208/dendritic cell-lysosomal associated membrane protein is a marker of normal and transformed type II pneumocytes. The American journal of pathology. 2004;164(3):861-71.
92. Mason RJ, Williams MC. Type II alveolar cell. Defender of the alveolus. The American review of respiratory disease. 1977;115(6 Pt 2):81-91.
93. Fehrenbach H. Alveolar epithelial type II cell: defender of the alveolus revisited. Respiratory research. 2001;2(1):33-46.
94. Cunningham AC, Milne DS, Wilkes J, Dark JH, Tetley TD, Kirby JA. Constitutive expression of MHC and adhesion molecules by alveolar epithelial cells (type II pneumocytes) isolated from human lung and comparison with immunocytochemical findings. J Cell Sci. 1994;107 (Pt 2):443-9.
95. Nagelkerke A, Bussink J, Mujcic H, Wouters BG, Lehmann S, Sweep FC, et al. Hypoxia stimulates migration of breast cancer cells via the PERK/ATF4/LAMP3-arm of the unfolded protein response. Breast cancer research : BCR. 2013;15(1):R2.
96. Mujcic H, Nagelkerke A, Rouschop KM, Chung S, Chaudary N, Span PN, et al. Hypoxic activation of the PERK/eIF2alpha arm of the unfolded protein response promotes metastasis through induction of LAMP3. Clin Cancer Res. 2013;19(22):6126-37.
97. Dominguez-Bautista JA, Klinkenberg M, Brehm N, Subramaniam M, Kern B, Roeper J, et al. Loss of lysosome-associated membrane protein 3 (LAMP3) enhances cellular vulnerability against proteasomal inhibition. European journal of cell biology. 2015;94(3-4):148-61.
98. International Parkinson Disease Genomics C, Nalls MA, Plagnol V, Hernandez DG, Sharma M, Sheerin UM, et al. Imputation of sequence variants for identification of genetic risks for Parkinson's disease: a meta-analysis of genome-wide association studies. Lancet. 2011;377(9766):641-9.
99. Lill CM, Roehr JT, McQueen MB, Kavvoura FK, Bagade S, Schjeide BM, et al. Comprehensive research synopsis and systematic meta-analyses in Parkinson's disease genetics: The PDGene database. PLoS Genet. 2012;8(3):e1002548.
100. Mohty M, Vialle-Castellano A, Nunes JA, Isnardon D, Olive D, Gaugler B. IFN-alpha skews monocyte differentiation into Toll-like receptor 7-expressing dendritic cells with potent functional activities. J Immunol. 2003;171(7):3385-93.
101. Mine KL, Shulzhenko N, Yambartsev A, Rochman M, Sanson GF, Lando M, et al. Gene network reconstruction reveals cell cycle and antiviral genes as major drivers of cervical cancer. Nat Commun. 2013;4:1806.
102. Zhou Z, Xue Q, Wan Y, Yang Y, Wang J, Hung T. Lysosome-associated membrane glycoprotein 3 is involved in influenza A virus replication in human lung epithelial (A549) cells. Virology journal. 2011;8:384.
103. Ignatius Irudayam J, Contreras D, Spurka L, Subramanian A, Allen J, Ren S, et al. Characterization of type I interferon pathway during hepatic differentiation of human pluripotent stem cells and hepatitis C virus infection. Stem cell research. 2015;15(2):354-64.

104. Nagelkerke A, Mujcic H, Bussink J, Wouters BG, van Laarhoven HW, Sweep FC, et al. Hypoxic regulation and prognostic value of LAMP3 expression in breast cancer. Cancer. 2011;117(16):3670-81.
105. Sun R, Wang X, Zhu H, Mei H, Wang W, Zhang S, et al. Prognostic value of LAMP3 and TP53 overexpression in benign and malignant gastrointestinal tissues. Oncotarget. 2014;5(23):12398-409.
106. Kanao H, Enomoto T, Kimura T, Fujita M, Nakashima R, Ueda Y, et al. Overexpression of LAMP3/TSC403/DC-LAMP promotes metastasis in uterine cervical cancer. Cancer Res. 2005;65(19):8640-5.
107. Qiu X, You Y, Huang J, Wang X, Zhu H, Wang Z. LAMP3 and TP53 overexpression predicts poor outcome in laryngeal squamous cell carcinoma. International journal of clinical and experimental pathology. 2015;8(5):5519-27.
108. Liao X, Chen Y, Liu D, Li F, Li X, Jia W. High Expression of LAMP3 Is a Novel Biomarker of Poor Prognosis in Patients with Esophageal Squamous Cell Carcinoma. International journal of molecular sciences. 2015;16(8):17655-67.
109. Racz A, Brass N, Heckel D, Pahl S, Remberger K, Meese E. Expression analysis of genes at 3q26-q27 involved in frequent amplification in squamous cell lung carcinoma. Eur J Cancer. 1999;35(4):641-6.
110. Nagelkerke A, Sweep FC, Stegeman H, Grenman R, Kaanders JH, Bussink J, et al. Hypoxic regulation of the PERK/ATF4/LAMP3-arm of the unfolded protein response in head and neck squamous cell carcinoma. Head & neck. 2015;37(6):896-905.
111. Mowers EE, Sharifi MN, Macleod KF. Autophagy in cancer metastasis. Oncogene. 2016.
112. Nagelkerke A, Sieuwerts AM, Bussink J, Sweep FC, Look MP, Foekens JA, et al. LAMP3 is involved in tamoxifen resistance in breast cancer cells through the modulation of autophagy. Endocrine-related cancer. 2014;21(1):101-12.
113. Lindskog C, Fagerberg L, Hallstrom B, Edlund K, Hellwig B, Rahnenfuhrer J, et al. The lung-specific proteome defined by integration of transcriptomics and antibody-based profiling. FASEB journal : official publication of the Federation of American Societies for Experimental Biology. 2014;28(12):5184-96.
114. Nagelkerke A, Bussink J, van der Kogel AJ, Sweep FC, Span PN. The PERK/ATF4/LAMP3-arm of the unfolded protein response affects radioresistance by interfering with the DNA damage response. Radiotherapy and oncology : journal of the European Society for Therapeutic Radiology and Oncology. 2013;108(3):415-21.
115. Pennati M, Lopergolo A, Profumo V, De Cesare M, Sbarra S, Valdagni R, et al. miR-205 impairs the autophagic flux and enhances cisplatin cytotoxicity in castration-resistant prostate cancer cells. Biochem Pharmacol. 2014;87(4):579-97.
116. Holohan C, Van Schaeybroeck S, Longley DB, Johnston PG. Cancer drug resistance: an evolving paradigm. Nat Rev Cancer. 2013;13(10):714-26.
117. Bisio A, Zamborszky J, Zaccara S, Lion M, Tebaldi T, Sharma V, et al. Cooperative interactions between p53 and NFkappaB enhance cell plasticity. Oncotarget. 2014.
118. Movassagh M, Spatz A, Davoust J, Lebecque S, Romero P, Pittet M, et al. Selective accumulation of mature DC-Lamp+ dendritic cells in tumor sites is associated with efficient T-cell-mediated antitumor response and control of metastatic dissemination in melanoma. Cancer Res. 2004;64(6):2192-8.
119. Holness CL, da Silva RP, Fawcett J, Gordon S, Simmons DL. Macrosialin, a mouse macrophage-restricted glycoprotein, is a member of the lamp/lgp family. J Biol Chem. 1993;268(13):9661-6.
120. Kostich M, Fire A, Fambrough DM. Identification and molecular-genetic characterization of a LAMP/CD68-like protein from Caenorhabditis elegans. J Cell Sci. 2000;113 (Pt 14):2595-606.
121. Kurushima H, Ramprasad M, Kondratenko N, Foster DM, Quehenberger O, Steinberg D. Surface expression and rapid internalization of macrosialin (mouse CD68) on elicited mouse peritoneal macrophages. Journal of leukocyte biology. 2000;67(1):104-8.
122. Graeber MB, Streit WJ, Kiefer R, Schoen SW, Kreutzberg GW. New expression of myelomonocytic antigens by microglia and perivascular cells following lethal motor neuron injury. Journal of neuroimmunology. 1990;27(2-3):121-32.
123. Tomita M, Yamamoto K, Kobashi H, Ohmoto M, Tsuji T. Immunohistochemical phenotyping of liver macrophages in normal and diseased human liver. Hepatology. 1994;20(2):317-25.
124. Athanasou NA, Puddle B, Quinn J, Woods CG. Use of monoclonal antibodies to recognise osteoclasts in routinely processed bone biopsy specimens. Journal of clinical pathology. 1991;44(8):664-6.
125. Ramprasad MP, Fischer W, Witztum JL, Sambrano GR, Quehenberger O, Steinberg D. The 94- to 97-kDa mouse macrophage membrane protein that recognizes oxidized low density lipoprotein and phosphatidylserine-rich liposomes is identical to macrosialin, the mouse homologue of human CD68. Proc Natl Acad Sci U S A. 1995;92(21):9580-4.
126. de Beer MC, Zhao Z, Webb NR, van der Westhuyzen DR, de Villiers WJ. Lack of a direct role for macrosialin in oxidized LDL metabolism. Journal of lipid research. 2003;44(4):674-85.
127. Song L, Lee C, Schindler C. Deletion of the murine scavenger receptor CD68. Journal of lipid research. 2011;52(8):1542-50.
128. Gough PJ, Gordon S, Greaves DR. The use of human CD68 transcriptional regulatory sequences to direct high-level expression of class A scavenger receptor in macrophages in vitro and in vivo. Immunology. 2001;103(3):351-61.
129. Gough PJ, Raines EW. Gene therapy of apolipoprotein E-deficient mice using a novel macrophage-specific retroviral vector. Blood. 2003;101(2):485-91.
130. Kunisch E, Fuhrmann R, Roth A, Winter R, Lungershausen W, Kinne RW. Macrophage specificity of three anti-CD68 monoclonal antibodies (KP1, EBM11, and PGM1) widely used for immunohistochemistry and flow cytometry. Annals of the rheumatic diseases. 2004;63(7):774-84.
131. Gottfried E, Kunz-Schughart LA, Weber A, Rehli M, Peuker A, Muller A, et al. Expression of CD68 in non-myeloid cell types. Scandinavian journal of immunology. 2008;67(5):453-63.
132. Boyce BF, Yao Z, Xing L. Osteoclasts have multiple roles in bone in addition to bone resorption. Critical reviews in eukaryotic gene expression. 2009;19(3):171-80.
133. Ashley JW, Shi Z, Zhao H, Li X, Kesterson RA, Feng X. Genetic ablation of CD68 results in mice with increased bone and dysfunctional osteoclasts. PLoS One. 2011;6(10):e25838.
134. Liu C, Tao Q, Sun M, Wu JZ, Yang W, Jian P, et al. Kupffer cells are associated with apoptosis, inflammation and fibrotic effects in hepatic fibrosis in rats. Laboratory investigation; a journal of technical methods and pathology. 2010;90(12):1805-16.
135. Makitie T, Summanen P, Tarkkanen A, Kivela T. Tumor-infiltrating macrophages (CD68(+) cells) and prognosis in malignant uveal melanoma. Investigative ophthalmology & visual science. 2001;42(7):1414-21.
136. Foss AJ, Alexander RA, Jefferies LW, Hungerford JL, Harris AL, Lightman S. Microvessel count predicts survival in uveal melanoma. Cancer Res. 1996;56(13):2900-3.
137. Sanchez-Espiridion B, Martin-Moreno AM, Montalban C, Medeiros LJ, Vega F, Younes A, et al. Immunohistochemical markers for tumor associated macrophages and survival in advanced classical Hodgkin's lymphoma. Haematologica. 2012;97(7):1080-4.
138. Ryder M, Ghossein RA, Ricarte-Filho JC, Knauf JA, Fagin JA. Increased density of tumor-associated macrophages is associated with decreased survival in advanced thyroid cancer. Endocrine-related cancer. 2008;15(4):1069-74.
139. Wang J, Chen H, Chen X, Lin H. Expression of Tumor-Related Macrophages and Cytokines After Surgery of Triple-Negative Breast Cancer Patients and its Implications. Medical science monitor : international medical journal of experimental and clinical research. 2016;22:115-20.
140. Steidl C, Lee T, Shah SP, Farinha P, Han G, Nayar T, et al. Tumor-associated macrophages and survival in classic Hodgkin's lymphoma. N Engl J Med. 2010;362(10):875-85.
141. Kim DW, Min HS, Lee KH, Kim YJ, Oh DY, Jeon YK, et al. High tumour islet macrophage infiltration correlates with improved patient survival but not with EGFR mutations, gene copy number or protein expression in resected non-small cell lung cancer. Br J Cancer. 2008;98(6):1118-24.
142. Li J, Zhang BZ, Qin YR, Bi J, Liu HB, Li Y, et al. CD68 and interleukin 13, prospective immune markers for esophageal squamous cell carcinoma prognosis prediction. Oncotarget. 2016.
143. Chistiakov DA, Killingsworth MC, Myasoedova VA, Orekhov AN, Bobryshev YV. CD68/macrosialin: not just a histochemical marker. Laboratory investigation; a journal of technical methods and pathology. 2017;97(1):4-13.
144. Pollard JW. Tumour-educated macrophages promote tumour progression and metastasis. Nat Rev Cancer. 2004;4(1):71-8.
145. Allavena P, Mantovani A. Immunology in the clinic review series; focus on cancer: tumour-associated macrophages: undisputed stars of the inflammatory tumour microenvironment. Clinical and experimental immunology. 2012;167(2):195-205.
146. Noy R, Pollard JW. Tumor-associated macrophages: from mechanisms to therapy. Immunity. 2014;41(1):49-61.
147. Takeya M, Komohara Y. Role of tumor-associated macrophages in human malignancies: friend or foe? Pathology international. 2016;66(9):491-505.
148. Strojnik T, Kavalar R, Zajc I, Diamandis EP, Oikonomopoulou K, Lah TT. Prognostic impact of CD68 and kallikrein 6 in human glioma. Anticancer research. 2009;29(8):3269-79.
149. Shabo I, Svanvik J. Expression of macrophage antigens by tumor cells. Advances in experimental medicine and biology. 2011;714:141-50.
150. Maniecki MB, Etzerodt A, Ulhoi BP, Steiniche T, Borre M, Dyrskjot L, et al. Tumor-promoting macrophages induce the expression of the macrophage-specific receptor CD163 in malignant cells. Int J Cancer. 2012;131(10):2320-31.
151. Steinert G, Scholch S, Niemietz T, Iwata N, Garcia SA, Behrens B, et al. Immune escape and survival mechanisms in circulating tumor cells of colorectal cancer. Cancer Res. 2014;74(6):1694-704.
152. Shabo I, Midtbo K, Andersson H, Akerlund E, Olsson H, Wegman P, et al. Macrophage traits in cancer cells are induced by macrophage-cancer cell fusion and cannot be explained by cellular interaction. BMC cancer. 2015;15:922.
153. Hassani K, Olivier M. Immunomodulatory impact of leishmania-induced macrophage exosomes: a comparative proteomic and functional analysis. PLoS neglected tropical diseases. 2013;7(5):e2185.
154. Schuske K, Palfreyman MT, Watanabe S, Jorgensen EM. UNC-46 is required for trafficking of the vesicular GABA transporter. Nature neuroscience. 2007;10(7):846-53.
155. Defays A, David A, de Gassart A, De Angelis Rigotti F, Wenger T, Camossetto V, et al. BAD-LAMP is a novel biomarker of nonactivated human plasmacytoid dendritic cells. Blood. 2011;118(3):609-17.
156. Lee J, Sohn I, Do IG, Kim KM, Park SH, Park JO, et al. Nanostring-based multigene assay to predict recurrence for gastric cancer patients after surgery. PLoS One. 2014;9(3):e90133.
157. Brodbeck T, Nehmann N, Bethge A, Wedemann G, Schumacher U. Perforin-dependent direct cytotoxicity in natural killer cells induces considerable knockdown of spontaneous lung metastases and computer modelling-proven tumor cell dormancy in a HT29 human colon cancer xenograft mouse model. Molecular cancer. 2014;13:244.
158. Barois N, de Saint-Vis B, Lebecque S, Geuze HJ, Kleijmeer MJ. MHC class II compartments in human dendritic cells undergo profound structural changes upon activation. Traffic. 2002;3(12):894-905.
159. Thibodeau J, Bourgeois-Daigneault MC, Lapointe R. Targeting the MHC Class II antigen presentation pathway in cancer immunotherapy. Oncoimmunology. 2012;1(6):908-16.

Table 1: Summary of cancer-associated functions for LAMP1 [Lysosome Associated Membrane Protein-1]

Pro-tumorigenic roles	Evidence	Strength / Weakness of the Evidence
Early cancer progression (56)	In OVCAR3 cells, LAMP1 was significantly up-regulated 1.84-fold 24 h post-EGF treatment and significantly down-regulated 48 h post-EGF exposure (normalized ratio, 0.41) relative to vehicle-treated cells. Tissue microarray analysis for LAMP1 demonstrated protein staining in 35% of ovarian serous adenocarcinoma core biopsies.	Although studies confirming the findings have not been reported, the observations were confirmed by GESA analysis performed using the TCGA database to assess the association of LAMP1 with EGFR-mediated signaling cascades and it revealed that LAMP1 is positively associated with EGFR-modulated molecular pathways (p <0.0060).
Cancer cell survival (65)	Screening identified the anti-malarial agent mefloquine as a compound that selectively kills AML cells and AML stem cells. A yeast genome-wide functional screen for mefloquine sensitizers, identified genes associated with the yeast vacuole, the homolog of the mammalian lysosome and demonstrated that mefloquine disrupts lysosomes, by permeabilizing the lysosome membrane, and releasing cathepsins into the cytosol.	Knock-down of LAMP1 and LAMP2 reduced AML cell viability, as did the treatment with lysosome disruptor, suggesting that lysosomal disruption preferentially targets AML cells and AML progenitor cells, thus providing a rationale for therapy. In support of this observation, artemisinins, artesunate (ART), and dihydroartemisinin (DHA), have been shown to be toxic to AML cells.
Local tumor progression (55)	In glioblastomas, LAMP1 was detected in the cytoplasm of tumor cells, and in blood vessels. The percentage of LAMP1$^+$ tumor cells and staining intensities increased with tumor grade. LAMP1 and CD133, a marker for stemness, were co-expressed suggesting that cancer stem cells contain LAMP1 positive lysosomes.	Data provided did not fully support the presence of higher number of lysosomes in cancer stem cells of glioblastomas. Moreover, despite the increase in LAMP1$^+$ tumor cells with tumor grade, an association between LAMP1 expression and OS could not be found.
Cancer development (57)	LAMP1 was identified as a sialylated glycoprotein from metabolically oligosaccharide engineered pancreatic cells. Immunohistochemistry, showed preferential expression of LAMP1 in tumor cells but not in paired non-tumor pancreatic ductal cells.	At odds with previous studies showing longer survival after resection for patients whose pancreatic tumors expression high levels of LAMP1 mRNA. Furthermore, transfection of CAPAN-1 cells with LAMP1 showed decreased cell growth compared with the non-transfected cells. Hence, the role for LAMP1 in cancer development remains uncertain.
Adhesion of cancer cells to ECM, basement membrane and endothelium (45); ECM remodelling (54)	Flow cytometry experiments showed LAMP1 expression on the cell surface of A2058, HT1080 (human fibrosarcoma) and CaCo-2 (human colon adenocarcinoma) cells, further increasing upon 2 mM sodium butyrate treatment for 24 and 48 hr. FACS analysis proved interaction between LAMP1 expressing cells A2052 and Galectin-3 (45). LAMP1 down-regulation by shRNA in murine melanoma cells B16F10, decreases the induction of the expression of MMP9 by p38 MAPK signaling, activated by Galectin-3 binding to the polyLacNAc present on LAMP1 (54).	Data are supported by previous studies showing increased expression of LAMP1 on the plasma membrane of highly metastatic cells compared to the poorly metastatic ones, associated with increased expression of carriers for polyLacNAc, that can represent ligand structures to cell-adhesion molecules. However, LAMP1 role in adhesion to ECM and ECM remodeling is indirect, since it uses Galectin-3 as mediator, giving more importance to LAMP1 role as a carrier of polyLacNAc rather than the protein itself. Other proteins can also be carrier of these modifications such as β1 integrin, rendering LAMP1 role in ECM regulation not exclusive (45; 54).
Metastasis (50; 53)	Anti-LAMP1 antibodies proved to reduce lung metastasis of murine melanoma cells B16F10 cells in 4 mice.	Data are supported by previous studies showing increased LAMP1 expression correlating with metastatic potential of human colon carcinoma and melanoma cells, and by silencing experiments linking LAMP1 expression with metastatic potential. Nevertheless, the absence of a direct involvement diminishes the possible therapeutic potential of LAMP1 targeting.
Cancer cell migration (51; 52)	LAMP1 was found as a BR96 antigen and expressed on the cell surfaces domains responsible for locomotion (51). FUT1 was reported to be able to fucosylate LAMP1, thereby influencing lysosomes localization and promoting cell migration (52).	The link between LAMP1 expression and migration is not direct, but controlled by LAMP1 polylactosamine modifications and fucosylation, responsible for the binding to key antigens for migration such as BR96 (51-52).
Drug resistance (66; 67; 68)	Increased protein LAMP1 expression was shown in RMS cells resistant to AS-DACA (66) and in renal and colorectal cancer cells resistant to TKIs (67). Higher LAMP1 expression was found in human sarcomas associated with relapse, and its direct role in increasing lysosomal exocytosis was found to be responsible for promoting invasion and Doxorubicin-resistance in human sarcomas.	Increased LAMP1 protein expression was used as a proxy for the increased lysosomal capacity, without clearly stating the molecular mechanism involved in this process (66-67). In contrast, a detailed analysis of the role played by LAMP1 in lysosomal exocytosis is clearly stated by this paper (68).

Abbreviations: EGF, Epidermal Growth Factor; EGFR, Epidermal Growth Factor Receptor; GESA, Gene-set Enrichment Analysis; TCGA, The Cancer Genome Atlas; AML, Acute Myeloid Leukemia; OS, Overall Survival; polyLacNAc, poly-N-AcetylLactosamines; RMS, RhabdoMyoSarcoma; AS-DACA, N-[2-(Dimethylamino)ethyl]Acridine-4-CarboxAmide; TKIs, Tyrosine Kinase Inhibitors.

Table 2: Summary of cancer-associated functions for LAMP2 [Lysosome Associated Membrane Protein-2]

Pro-tumorigenic roles	Evidence	Strength / Weakness of the Evidence
Cancer pathogenesis (78; 80)	Increased LAMP2 protein expression was reported in poorly differentiated human gastric adenocarcinoma with respect to adjacent gastric mucosal tissues (78). *LAMP2* gene is located in a region involved in BCL1/JH t(11;14)(q13;q32) translocation found in multiple myeloma patients (80).	LAMP2 protein expression increase was used as a proxy for autophagy-lysosome signaling with no clear indications on its specific role in the signaling. There are conflicting data regarding the role of autophagy-lysosome circuitry in cancer pathogenesis (78). Functional studies supporting the pathogenic significance of LAMP2 in multiple myeloma are still missing (80).
Cancer cell migration (52; 77)	LAMP2 modification by FUT1 was reported to be able to control localization of lysosomes, which often shift from perinuclear to peripheral compartment in invasive cancer (52). LAMP2 protein expression was highly expressed in the invasive OVISE human ovarian clear cell adenocarcinoma cells, and ANXA4 knock-out decreased LAMP2 protein expression and migration (77).	LAMP2 is not directly involved in the regulation of migration, but rather its modification by FUT1 plays a more important role (52). A direct LAMP2 knock-out experiment is needed to confirm its possible direct involvement in ovarian cancer cells migration (77).
Support early cancer growth (49)	LAMP2 expression on the plasma membrane supported early breast cancer progression by acting as a protective shield against the acidic extracellular microenvironment.	The relevance for a LAMP2 role in survival within an acidic microenvironment was supported by strong data from both breast cancer cell lines and patients. The exact molecular mechanisms involved in LAMP2 protective action were not addressed in the reported study and are not discovered yet.
Adhesion of cancer cells to ECM, basement membrane and endothelium (45)	LAMP2 was observed by flow cytometry on the cell surface of A2058, HT1080 (human fibrosarcoma) and CaCo-2 (human colon adenocarcinoma) cells and their interaction with Galectin-3 was reported.	Data are supported by previous studies but the fact that modifications of LAMP2 rather than their expression are reported as causal link with ECM adhesion diminishes the therapeutic potential of their targeting.
Drug resistance (67)	Increased protein expression of LAMP2 was reported in renal and colorectal cancer cells resistant to TKIs (67).	This study didn't a provide data regarding the mechanisms involved in the lysosomal control exerted by LAMP2 and how this could lead to increased drug secretion.
CMA activation (81; 82)	Ectopic expression of LAMP2A isoform, through its key action on CMA, was able to support cell survival upon oxidative stress; conversely, its inhibition was promoting apoptosis and Doxorubicin-resistance in breast cancer cells (81). The inhibition of LAMP2A blocked the constitutive activation of CMA and led to the reduction of cell proliferation, the growth of preexisting tumors and promoted the metastatic potential of lung cancer cells (82).	LAMP2A key role in cancer was supported by its high expression in patients-derived invasive carcinoma compared with adjacent tissues and in several cancer cell lines. Given its direct control on CMA, LAMP2A inhibition could represent a very promising strategy for sensitizing cancer cells to chemotherapy (81; 82).

Abbreviations: ECM, ExtraCellular Matrix; CMA, Chaperone-Mediated Autophagy; TKIs, Tyrosine Kinase Inhibitors.

Table 3: Summary of cancer-associated function for LAMP3 [Lysosome Associated Membrane Protein-3], DC-LAMP

Pro-tumorigenic roles	Evidence	Strength / Weakness of the Evidence
Metastasis induction (106; 95; 112)	Researchers demonstrated that upon ectopic over-expression of LAMP3 in a uterine cervical cancer cell line (TCS), cancer cells acquired a higher migratory potential (106). Moreover, in SCID mice 82% (9/11) of injected LAMP3 over-expressing TSC cells efficiently generated metastases (prevalently to liver and lung) compared to 9% (1/11) of controls (106). LAMP3 detection by RT-qPCR and IHC in lymph node metastases from cervical carcinoma patients revealed that distant metastasis formation was associated with a higher expression of LAMP3 higher levels (106). In another study (95), an increased migration potential of breast cancer-derived cells correlated with higher basal LAMP3 expression levels. Furthermore, LAMP3 knock-down resulted in a decreased migration potential of MDA-MB-231 cells after exposure to 1% O_2. Moreover, MDA-MB-231-derived spheroids showed reduced migratory properties and a lower invasion into collagen when depleted of LAMP3 (95). Lastly, breast cancer patients with soft tissue metastases showed higher LAMP3 mRNA expression compared with ones with non-soft tissue or bone metastases (p=0.034) (112).	Results obtained *in vitro* are also supported by *in vivo* experiments. However, these results were based on over-expression experiments and therefore rely on excessive expression levels; thus they need to be further validated. Consequently, data were also confirmed by analyses on human patient samples (106). A stronger migration potential of LAMP3 expressing cells was also found in breast cancer-derived cell lines and spheroids, structures that represent a more physiologic model of the disease (95).
Lymph node metastasis (104; 110)	Despite the variability among samples, high level of LAMP3 mRNA was found in lymph node-positive breast cancer patients (n=183; p=0.019) and ER/PR-negative tumors (p<0.001) (104). Notably, loco-regional recurrences were found more frequently in breast cancer patients with high LAMP3 mRNA levels (p=0.032 log-rank) that underwent lumpectomy and treated with radiotherapy (p=0.009) (104). Another report showed that by IHC staining from HNSCC patient biopsies, high expression of LAMP3 was restricted to normoxic regions of tumors and correlated with the occurrence of lymph node metastasis (110). Moreover, a worse metastasis-free survival was observed in patients showing higher levels of LAMP3 (110).	These data underline the relevant role of LAMP3 in tumor progression and metastatic spread processes, also in patient-derived samples both from breast cancers (104) and HNSCC (110). Surprisingly, the same group reported the controversial observation that while LAMP3 expression is associated with hypoxic regions in breast cancer tumors (104), it is limited to normoxic regions in HNSCC (110).
Poor overall survival of patients (105; 106; 107; 108)	Through IHC on TMA from gastric (n=750) and colorectal (n=479) cancer patients, LAMP3 expression was found significantly higher in cancer tissues in respect to normal or benign tissues. In both cancer types, there was a significant association between high LAMP3 levels and tumor stage and a poorer overall survival, respectively with a remarkable HR of 2.8 and 2.9, also confirmed with multivariate analysis (HR=2.8 and 2.6). In a second study conducted on patients with stage I or stage II uterine cervical cancers, who underwent radical hysterectomy (n=24), high LAMP3 mRNA levels were associated with a poorer prognosis and higher mortality. In another work, IHC analysis using TMA from LSCC patients (n=117) showed that a stronger LAMP3 signal was associated with worse tumor stage (p=0.029), bigger size (p=0.012) and poorer prognosis (HR=5.706). According to the last report on a cohort of 157 ESCC patients and 50 uninvolved normal tissues (measuring LAMP3 mRNA levels) and 46 paired normal and cancerous tissues (to detect LAMP3 protein by IHC), elevated LAMP3 levels were correlated with OS (HR = 1.90) and DFS (HR = 1.80). Interestingly, increased expression of LAMP3 in cancer tissues correlated well with DNA Copy Number Amplification (observed in 35/50 cases).	The association between high LAMP3 levels and clinical features and OS of gastric as well as colorectal cancer patients is remarkable. The relevance of the results from the second study is limited by the reduced number of patients. A significant correlation between LAMP3 and TP53 expression was shown in LSCC, even if the authors considered LAMP3 and TP53 as independent prognostic markers for LSCC. Taken collectively, all these studies, while relevant, reported retrospective analyses on human samples and the conclusions drawn might not apply to the general population. Moreover, there was not a direct impact on the therapeutic strategy used and the OS.
Resistance to hormonal therapy (112)	Researchers showed that in MCF7 breast cancer-derived cells the silencing of LAMP3 increased the sensitivity to hormonal therapy (tamoxifen). This observation was linked to the activation of autophagy, a process that was associated with tamoxifen resistance. Indeed, tamoxifen was able to induce LAMP3 mRNA levels, thus leading to breast cancer cells resistance. Interestingly, tamoxifen-resistant MCF7 cells showed LAMP3 mRNA levels 7-fold higher than tamoxifen-sensitive counterparts. Remarkably, high LAMP3 expression was found in advanced breast cancer patients with shorter progression-free survival (p=0.003) and post-relapse overall survival (p=0.040) that were treated with tamoxifen.	Notably, the inhibition of autophagic process by silencing of associated genes such as MAP1LC3B, ATG5, and BECN1 resulted in an enhanced sensitivity to tamoxifen, suggesting that the impact of LAMP3 in autophagy is the crucial step to achieve tamoxifen resistance. LAMP3 inhibition may be clinically relevant to hinder tamoxifen resistance in breast cancer.
Resistance to radiation therapy (114)	Silencing of LAMP3 (along with PERK and ATF4, other two members of the UPR during hypoxia) revealed to be able to sensitize MDA-MB-231 breast cancer cells to radiation therapy. This result seemed to be related to an attenuated DNA damage response during irradiation when LAMP3 was down-regulated by siRNA (measured by the quantification of γ-H2AX foci). Therefore, resistance to radiotherapy can be driven by up-regulation of LAMP3 (and PERK and ATF4) through UPR pathway and relies on an increase of DNA repair process. The effect was more evident with MDA-MB-231 cells compared to MCF7 cells, another breast cancer-derived model that express wild-type p53. This could suggest that the presence of functional p53 may reduce the effectiveness of LAMP3 knock-down.	The specific mechanism underlying the LAMP3-dependent radio-resistance was not completely elucidated and can rely on autophagy as shown for resistance to hormonal therapy. There are other pieces of evidence that MDA-MB-231 cells (but not others such as HCT116) can be sensitized by the treatment with the autophagy inhibitor chloroquine. Thus, these effects may be cancer type-dependent.
Resistance to chemotherapy (115)	Researchers proposed LAMP3 as a direct target of miR-205, a miRNA down-regulated during the EMT process in prostate cancer. miR-205 impaired autophagy through levels reduction of the lysosome-associated proteins LAMP3 and RAB27A, thus enhancing the cytotoxic effects of cisplatin in prostate cancer cells. Similar effects were seen with the silencing of LAMP3 with synthetic oligonucleotides, confirming the putative role of LAMP3 expression in the resistance to cisplatin.	The researchers based the effects on LAMP3 via *in silico* predictions and indirect measurements, but they did not provide any direct evidence of miR-205 binding to LAMP3 mRNA. Furthermore, while it is well established that miR-205 is repressed or lost in prostate cancer patients, the expression of LAMP3 in the same patients has not been evaluated.

Abbreviations: LSCC, Laryngeal Squamous Cell Carcinoma; ER, Estrogen Receptor; PR, Progesteron Receptor; IHC, ImmunoHistoChemistry; HNSCC, Head and Neck Squamous Cell Carcinoma; TMA, Tissue MicroArray; HR, Hazard Ratio; ESCC, Esophageal Squamous Cell Carcinoma; OS, Overall Survival; Disease-Free Survival; UPR, Unfolded Protein Response; EMT, Epithelial-to-Mesenchymal Transition.

Table 4: Summary of cancer-associated functions for CD68, Macrosialin, LAMP4 [Lysosome Associated Membrane Protein-4]

Pro-tumorigenic roles	Evidence	Strength / Weakness of the Evidence
Marker for pro-tumorigenic in malignant uveal melanoma (135)	CD68$^+$ tumor infiltrating macrophages were identified in 83% of malignant uveal melanoma patients (n=167). The abundance of CD68$^+$ TAMs was found associated with parameters of known poorer prognosis, such as LBD (tumor dimension), heavy pigmentation and high MVD (presence of capillaries). Moreover, melanoma-specific mortality rate at 10 years from diagnosis was enhanced in patients with higher number of CD68$^+$ macrophages.	The evidence regarding the enrichment of CD68$^+$ macrophages in uveal melanoma and its association with aggressiveness is pretty strong. However, as expected from the functions identified so far for CD68 protein, there is not a direct role for CD68 in cancer cells, rather it is relevant its impact on TAMs, where it represents one of the most used markers.
Associated with TAMs in Hodgkin's lymphoma (137; 140)	CD68 expression in TAMs was analyzed by IHC on tissue microarrays from lymph-node of classical Hodgkin's lymphoma (cHL) patients (n=168), including 79 that showed treatment failure. CD68$^+$ TAMs-enriched patients showed an at least 8-times lower progression-free survival compared to patients with very low levels of CD68$^+$ TAMs (<5%) (137). Moreover, CD68 revealed to be more effective with respect to the conventional IPS value used for cHL samples (137). In another study on 2 series of advanced cHL patients (n=266 and n=103), CD68 was used as macrophage marker in IHC staining along with CD163, LYZ and STAT1 (140). CD68 resulted to be the only marker associated with clinical features (140).	At least two different studies from three independent patients' cohorts proved the prognostic value of CD68 positivity within tumor tissues of cHL patients, suggesting the effectiveness and the value of this measurement. The relevant drawback of the first observation is represented by the reduced number of cHL cases with very low levels of CD68$^+$ TAMs and low risk patients (137). Interestingly, the fact that only CD68 staining (among TAM markers) was significantly associated with clinical parameters, underlies the possibility that CD68 could be also expressed by cancer cells (see below).
Marker for TAMs in advanced thyroid cancer (138)	CD68 was used as a marker for TAMs in studying thyroid cancers. Using tissue microarrays associated with IHC it was observed that TAMs density increased with the growing aggressiveness of thyroid cancer; specifically, from 27% in WDTC (n=33), to 54% in PDTC (n=37) and 95% in ATC (n=20).	The correlation between CD68 positivity and tumor progression (increased grade, invasion property and decreased survival) in thyroid cancers is remarkable.
Marker for TAMs in TNBCs (139)	CD68-positive TAMs were found in 71.45% of TNBC-derived samples. The increased presence of TAMs correlated with poorer prognosis and it was associated with enhanced expression of IL-6 and CCL-5 diffusible factors.	Another report supporting the association of high infiltration of TAMs (measured as CD68 positive cells) with cancer progression and poorer prognosis also in TNBCs.
Associated to poor prognosis (148)	CD68 immunostaining was detected from histological sections of 51 primary astrocytic tumors (11 benign astrocytomas, 40 malignant tumors) and 8 relapses. CD68 signal was significantly higher in malignant tumors compared to benign ones (p=0.036). Moreover, a higher staining score for CD68 was associated with a poorer prognosis of OS for all the tumors analyzed (p<0.01), with a remarkable enrichment for anaplastic astrocytomas (p=0.021).	CD68 can also be considered a marker for microglia and in gliomas the infiltration of macrophages and microglia has been established. This is in line with the characteristics mentioned above. Notably, here the authors show the presence of CD68 also on the surface of cancer cells as well as in U87 glioblastoma-derived cell line.

Abbreviations: TAMs, Tumor-Associated Macrophages; LBD, Largest Basal Diameter; MVD, MicroVascular Density; IPS, International Prognostic Score; IHC, ImmunoHistoChemistry; WDTC, Well-Differentiated Thyroid Cancer; PDTC, Poorly Differentiated Thyroid Cancer; ATC, Anaplastic Thyroid Cancer; TNBCs, Triple Negative Breast Cancers; OS, Overall Survival.

Table 5: Summary of cancer-associated functions for BAD-LAMP, LAMP5 [Lysosome Associated Membrane Protein-5], C20orf103

Pro-tumorigenic roles	Evidence	Strength / Weakness of the Evidence
Associated with poor prognosis (156)	BAD-LAMP has been identified (through gene expression profiling with microarrays on FFPE samples) along with other 7 genes (part of the so called "Gastric Cancer Prognostic Score", GCPS) as high-risk gene for recurrence in 3 different cohorts of stage II gastric cancer patients who underwent adjuvant chemo-radiotherapy. A higher expression of BAD-LAMP was associated with poorer prognosis.	The GCPS was validated in more than 700 stage II GC patients and proposed for the routine usage in the clinic. The increased BAD-LAMP expression was however significantly higher in stromal cells rather than in cancer cells, highlighting a more important role for BAD-LAMP in the tumor microenvironment.

Abbreviations: FFPE, Formalin-Fixed Paraffin-Embedded; GC, Gastric Cancer.

Figure 1

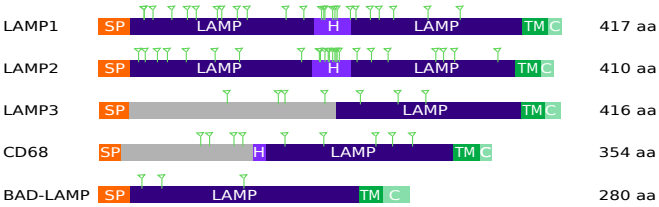

Figure 2

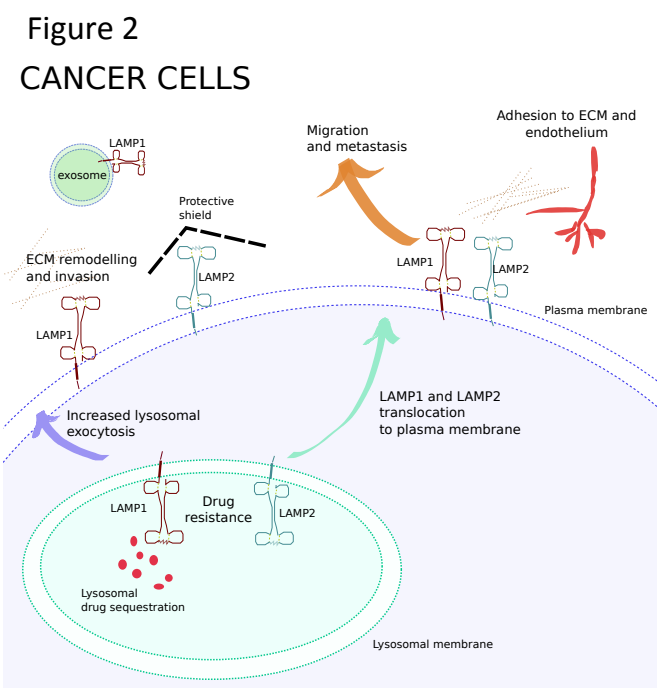

Figure 3

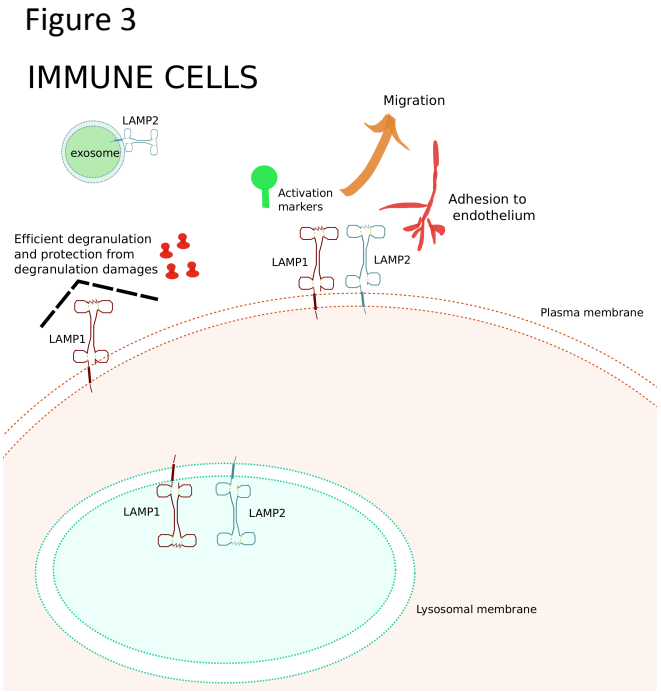

Figure 4

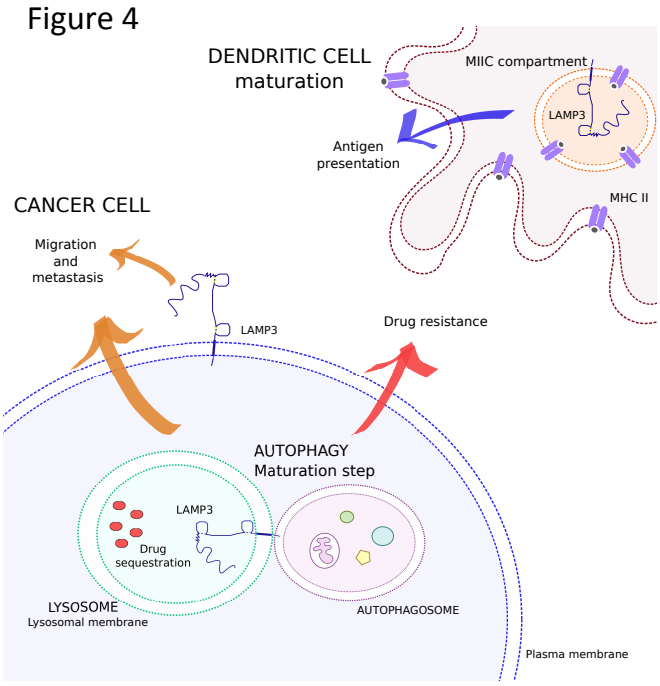

Figure 5

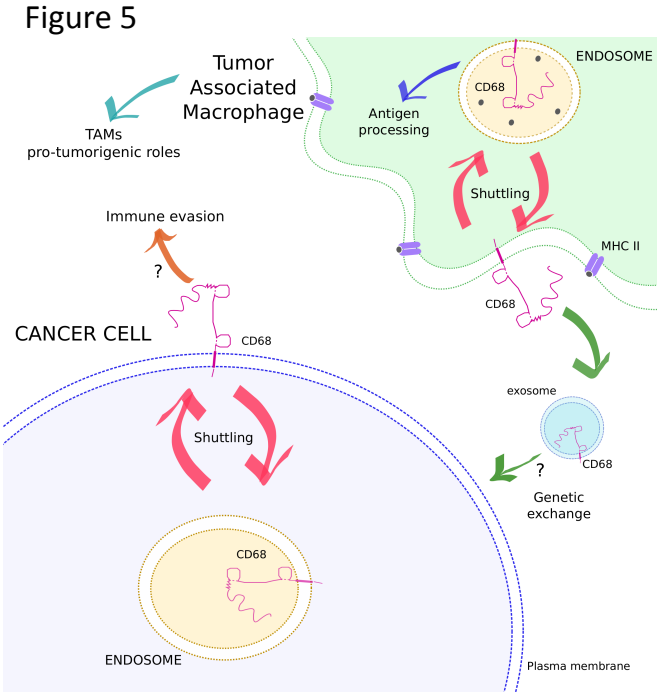

Figure 6